



HAL
open science

In vitro toxicity of titanium dioxide nanoparticles on human lung cells - impact of the physicochemical features

Ozge Kose

► **To cite this version:**

Ozge Kose. In vitro toxicity of titanium dioxide nanoparticles on human lung cells - impact of the physicochemical features. Chemical and Process Engineering. Université de Lyon, 2020. English. NNT : 2020LYSEM022 . tel-03888106

HAL Id: tel-03888106

<https://theses.hal.science/tel-03888106>

Submitted on 7 Dec 2022

HAL is a multi-disciplinary open access archive for the deposit and dissemination of scientific research documents, whether they are published or not. The documents may come from teaching and research institutions in France or abroad, or from public or private research centers.

L'archive ouverte pluridisciplinaire **HAL**, est destinée au dépôt et à la diffusion de documents scientifiques de niveau recherche, publiés ou non, émanant des établissements d'enseignement et de recherche français ou étrangers, des laboratoires publics ou privés.



N°d'ordre NNT : 2020LYSEM022

THESE de DOCTORAT DE L'UNIVERSITE DE LYON
opérée au sein de
l'Ecole des Mines de Saint-Etienne

Ecole Doctorale N° 488
Sciences, Ingénierie, Santé

Spécialité de doctorat :
Discipline : Génie des Procédés

Soutenue publiquement le 27/11/2020, par :
Özge KÖSE

Toxicité *in vitro* de nanoparticules de dioxyde de titane sur des cellules pulmonaires humaines - impact des caractéristiques physicochimiques

Devant le jury composé de:

Hochepped, Jean-François	Maître de recherches	MINES ParisTech	Président
Carrière, Marie	Professeure	Commissariat à l'énergie atomique et aux énergies alternatives (CEA)	Rapporteure
Bencsik, Anna	Professeure	Agence nationale de sécurité sanitaire de l'alimentation, de l'environnement et du travail (ANSES)	Rapporteure
Turci, Francesco	Professeur	Université de Turin	Examineur
Forest, Valérie	Professeure	Ecole des Mines de Saint-Etienne	Directrice de thèse
Pourchez, Jérémie	Professeur	Ecole des Mines de Saint-Etienne	Co-directeur de thèse

ACKNOWLEDGMENTS

I would like to express my sincere gratitude to my advisor Prof. Valérie Forest and to my co-advisor Prof. Jérémie Pourchez for their continuous support of my PhD study and related research, for their patience, motivation, and immense knowledge.

Besides my advisors, I would like to thank my thesis jury: Prof. Marie Carrière, Prof. Anna Bencsik, Prof. Jean-François Hochepped, and Prof. Francesco Turci.

I will forever be thankful to Prof. Marie Carrière, who has supported me and was a reference for me when I applied to this PhD project. From the very beginning to the end of my thesis, I am very grateful for her advice and suggestions.

My sincere thanks also go to Naila-Besma Belblidia and Prof Jean-François Hochepped for their support and help since they assisted in the synthesis and characterization of nanoparticles forming the base of my research. They always very helpful and supportive.

A special group from the University of Turin, Chemistry Department is not mentioned yet, because they deserve their own part. I praise the enormous amount of help by Prof. Francesco Turci and Prof. Maura Tomatis throughout my mobility at their department. Without their precious support, it would not be possible to improve this research. During the 3 months I spent there, I learned a lot from them, had a great time, and I was always greeted with so much smile and positivity.

I thank the BioPI team, especially to Dr. Lara Leclerc a wonderful person who always supports and helps in many ways, and to my great office mate Yoann Mountigaud.

I took part of many other activities, with countless people teaching and helping me every step. Thank you to everyone from CIS, especially Françoise Bresson stands out notoriously as an amazing source of support and to my best friend Cyriac Azefack, your friendship was irreplaceable and has always been very precious. There are no words to convey how much I enjoyed the time we spent. He has been a true and great friend.

I also would like to thank Prof. Bedri Kurtulus for the precious support he gave me throughout my life.

I would like to thank my family: my parents, my brother, and my sister who are by my side with their love and support at every stage of my life.

List of Publications

1. **Kose, O.**; Tomatis, M.; Leclerc, L.; Belblidia, N.-B.; Hochepped, J.-F.; Turci, F.; Pourchez, J.; Forest, V. Impact of the physicochemical features of TiO₂ nanoparticles on their *in vitro* toxicity. Chem. Res. Toxicol. August 10, 2020. <https://doi.org/10.1021/acs.chemrestox.0c00106>
2. **Kose, O.**; Stalet, M.; Leclerc, L.; Forest, V. Influence of the physicochemical features of TiO₂ nanoparticles on the formation of a protein corona and impact on cytotoxicity. RSC Adv. 10, 43950, 2020. <https://doi.org/10.1039/d0ra08429h/rsc.li/rsc-advances>
3. **Kose, O.**; Tomatis, M.; Turci, F.; Belblidia, N.-B.; Hochepped, J.-F.; Pourchez, J.; Forest, V. Short pre-irradiation of TiO₂ Nanoparticles increases cytotoxicity on human lung coculture system. Chem. Res. Toxicol.. In revision.
4. Chapple, R.; **Kose, O.**; Kandola, B.; Ferry, L.; Lopez-Cuesta, J.M.; Chivas-Joly, C.; Forest, V. Effect of impact and fire on the physicochemical features of advanced aerospace and automotive nanocomposites and consequences on their toxicological profile. In preparation.
5. Bernal, K.; **Kose, O.**; Mirallès, K.; Leclerc, L.; Porrás Yaruro, JP.; Vergnon, JM.; Pourchez, J.; Forest, V. *In vitro* toxicity of NPs isolated from patients' broncho-alveolar lavages. In preparation.

List of Presentations

1. **Kose, O.**; Tomatis, M.; Leclerc, L.; Belblidia, N.-B.; Hochepped, J.-F.; Turci, F.; Pourchez, J.; Forest, V. Impact of the physicochemical features of TiO₂ nanoparticles on their *in vitro* toxicity. IRC 2020 XIV. International Conference on Nanotoxicology and Toxicity of Nanomaterials, ICNTN 2020: XIV. Amsterdam, Netherlands, 20-21 January 2020 (oral presentation).
2. **Kose, O.**; Tomatis, M.; Turci, F.; Belblidia, N.-B.; Hochepped, J.-F.; Pourchez, J.; Forest, V. Influence of the Pre-irradiated TiO₂ Nanoparticles on their *in vitro* toxicity. Seminar, University Of Torino - Department of Chemistry, Turin Italy, 19 November 2019 (oral presentation).
3. **Kose, O.**; Leclerc, L.; Belblidia, N.-B.; Hochepped, J.-F.; Pourchez, J.; Forest, V. *In Vitro* Toxicity of TiO₂ Nanoparticles with different physicochemical properties. Seminar, University Of Torino - Department of Chemistry, Turin Italy, 14 October 2019 (oral presentation).
4. **Kose, O.**; Leclerc, L.; Belblidia, N.-B.; Hochepped, J.-F.; Pourchez, J.; Forest, V. *In Vitro* Toxicity of TiO₂ Nanoparticles on human lung cells. IMT Symposium Healthcare 4.0- New advances in health engineering, Saint Etienne, France, 15 October 2019 (poster).
5. **Kose, O.**; Leclerc, L.; Belblidia, N.-B.; Hochepped, J.-F.; Pourchez, J.; Forest, V. *In Vitro* Toxicity of TiO₂ Nanoparticles on human lung cells. Journée de la Recherche de l'Ecole Doctorale Sciences Ingénierie Santé, Saint Etienne, France, 13 June 2019 (poster).

Awards

1. **Best Presentation Award**, ICNTN 2020: XIV. International Conference on Nanotoxicology and Toxicity of Nanomaterials Amsterdam, Netherlands, 20-21 January 2020.
2. **Third Best Poster Award**, Journée de la Recherche de l'Ecole Doctorale Sciences Ingénierie Santé, Saint Etienne, France, 13 June 2019.

CONTENTS

ACKNOWLEDGMENTS	i
List of Publications	ii
List of Presentations	ii
Awards	ii
FIGURES	v
TABLES	vii
ABBREVIATIONS	viii
INTRODUCTION	1
BIBLIOGRAPHY	5
1. Nanomaterials	5
1.1. Nanomaterial properties and applications.....	5
1.2. Titanium dioxide nanoparticles and their applications.....	7
1.3. Titanium dioxide nanoparticles environmental release	10
1.4. Titanium dioxide nanoparticles exposure routes	12
2. Adverse effects of inhaled nanoparticles	13
2.1. General anatomy of the respiratory system and nanoparticle interaction	13
2.2. Cellular organization of the respiratory system and nanoparticle interaction	16
3. Mechanisms of nanoparticle toxicity	20
3.1. Oxidative stress.....	20
3.2. Pro-inflammation	21
3.3. Role of physicochemical features in nanoparticle toxicity	22
4. <i>In vivo</i> and <i>in vitro</i> titanium dioxide toxicity	27
4.1. <i>In vivo</i> studies.....	27
4.2. <i>In vitro</i> studies.....	30
5. Conclusion and Objectives of the Work	32
EXPERIMENTAL PART	35
Chapter 1 Development and Validation of the <i>In vitro</i> Biological Models ...	35
1. The THP-1 Cell Line and the Identification of Macrophage Differentiation in PMA-stimulated THP-1 Cells	39
1.1. Optimal PMA exposure time and cell density determination after exposure to various PMA concentrations	40
1.2. Optimal PMA concentration determination by immunocytochemistry staining (Protocol 4)	46
2. Conclusion	47
Chapter 2 Impact of the Physicochemical Features of TiO₂ Nanoparticles on their <i>In vitro</i> Toxicity	49
Article 1. Impact of the Physicochemical Features of TiO₂ Nanoparticles on Their In Vitro Toxicity	51
1. Complementary Data	65
1.1. Cell membrane integrity-Lactate dehydrogenase release	65
1.2. Cell viability-MTT assay	67
1.3. Pro-inflammatory response	70
1.4. Oxidative stress.....	72
2. Conclusion	73
Chapter 3 Short Pre-irradiation of TiO₂ Nanoparticles Increases Cytotoxicity on Human Lung Coculture System	75
Article 2. Short pre-irradiation of TiO₂ nanoparticles increases cytotoxicity on human lung coculture system	77
1. Complementary Data	107

1.1. Electron spin resonance method for detection of HO [•] and CO ₂ ^{•-} radicals from UV-irradiated TiO ₂ nanoparticles	107
1.2. HO [•] and CO ₂ ^{•-} radicals generation	108
2. Conclusion	110
Chapter 4 Impact of the Physicochemical Features of Titanium Dioxide Nanoparticles on The Protein Corona Formation.....	113
Article 3. Influence of the physicochemical features of TiO₂ nanoparticles on the formation of a protein corona and impact on cytotoxicity	115
1. Complementary Data	125
1.1. Protein concentration of UV irradiated titanium dioxide nanoparticles	125
1.2. Profile of proteins adsorbed at the surface of the 30 min UV irradiated nanoparticles by gel electrophoresis	126
2. Conclusion	127
Chapter 5	129
Exploratory studies.....	129
1. Titanium dioxide nanoparticles interaction with lactate dehydrogenase (cell free condition)	131
2. Titanium dioxide nanoparticle interaction with MTT (cell free condition)	132
3. Conclusion	136
CONCLUSIONS AND PERSPECTIVES.....	137
REFERENCES	147
Abstract :	165
Résumé :	166

FIGURES

Figure	Page
Figure 1. Examples of nanoparticle shapes.	5
Figure 2. Crystalline forms of TiO ₂ [19].	8
Figure 3. Brief overview of TiO ₂ photocatalyst activity.	9
Figure 4. Main industrial applications of TiO ₂ (adapted from [30]).	9
Figure 5. Upper and lower respiratory system.	14
Figure 6. Nanoparticle translocation in human body.	15
Figure 7. Cell organization of the respiratory system.	16
Figure 8. Scheme of the mucociliary clearance.	17
Figure 9. Schematic illustration of the phagocytosis.	18
Figure 10. Protein corona formation.	19
Figure 11. Interaction of NPs with cells and possible biologic effects.	26
Figure 12. 72 h DMSO treated THP-1 cell viability. DMSO solutions were prepared in culture media (RPMI) in indicated concentrations.	41
Figure 13. Microscopic images of THP-1 cells (7.5 x 10 ⁶ cells/ T25 cm ² flask) exposed to 5; 30; 50; 100 ng/mL PMA for 24 h and 48 h. Control represents THP-1 cells without PMA treatment (20 x magnification).	43
Figure 14. THP-1 cell adhesion after treatment with the indicated PMA concentrations for 24 h and 48 h. Independent experiments were conducted three times in triplicate. Statistically different from control (****) $P < 0.0001$. Statistical analyses were conducted using one-way Anova analyses, followed by Dunnett's test.	44
Figure 15. Absorbance values of 30, 50, 100 ng/mL PMA treated cells at the indicated cell densities as determined by MTT assay.	45
Figure 16. Immunocytochemistry staining of CD11b (marker of macrophage activation) in THP-1-derived macrophages. The detection of protein expression was performed by fluorescence microscopy (magnification 25 X).	46
Figure 17. Principle of LDH release assay.	65
Figure 18. LDH release 24 h after cell exposure to TiO ₂ NPs. Control (C-) represents unexposed cells. Lysed cells were used as positive control (C+). Values are the mean ± SEM of three independent experiments. Statistically different from control (****) $P < 0.0001$. Statistical analyses were conducted using one-way Anova analyses, followed by Dunnett's test.	66
Figure 19. MTT reduction into purple formazan by mitochondrial dehydrogenase in viable cells.	67
Figure 20. Cell viability after 24 h exposure to TiO ₂ NPs assessed by MTT. Control (C) represents unexposed cells. Values are the mean ± SEM of three independent experiments. Statistically different from control (*) $P < 0.05$, (**) $P < 0.01$, (***) $P < 0.0001$, (****) $P < 0.0001$. Statistical analyses were conducted using one-way Anova analyses, followed by Dunnett's test.	69
Figure 21. TNF-α production after a 24 h exposure of differentiated THP-1 to TiO ₂ NPs. Control (C) represents unexposed cells. Values are the mean ± SEM of three independent experiments. Statistically different from control (*) $P < 0.05$ (****) $P < 0.0001$. Statistical analyses were conducted using one-way Anova analyses, followed by Dunnett's test.	71
Figure 22. ROS production after 90 min and 24 hours exposure to the indicated concentrations of TiO ₂ NPs in differentiated THP-1. Control (C-) represents unexposed	

cells, positive control (C+) cells incubated with H ₂ O ₂ . Statistically different from control (****) <i>P</i> < 0.0001. Statistical analyses were conducted using one-way Anova analyses, followed by Dunnett's test.....	72
Figure 23. Detection of DMPO-HO• and the DMPO-CO ₂ •- from UV-irradiated TiO ₂ samples by ESR method (a), example of ESR spectrum of the DMPO-HO• and the DMPO-CO ₂ •- radical adducts (b).	107
Figure 24. Generation of HO• radicals from 5, 10, 20, and 30 min UV irradiated TiO ₂ NPs and 30 min UV irradiated negative control (NC-without TiO ₂ NPs).....	108
Figure 25. Generation of CO ₂ •- radicals from 5, 10, 20, and 30 min UV irradiated TiO ₂ NPs and 30 min UV irradiated negative control (NC-without TiO ₂ particles).	109
Figure 26. Concentrations of proteins eluted from the protein corona of pristine and 30 min UV irradiated NPs after incubation in cDMEM. Control is cDMEM. Results are means of 3 independent experiments, standard deviation is also indicated. Statistically different from P25 (****) <i>P</i> < 0.0001. Statistical differences between S2 and S4 (§§§§) <i>P</i> < 0.0001. Statistical analyses were conducted using one-way Anova analyses followed by Tukey's multiple comparison test.....	125
Figure 27. Electrophoresis gels for pristine and UV irradiated S1, S2, S4 and P25 NPs incubated in cDMEM. As controls, the complete biological media were also run (last lane).	126
Figure 28. Absorbance at 450 nm of TiO ₂ NPs (120 µg/mL) and LDH (0.16 U/µL) mixture and LDH (0.16 U/µL) alone (cell free condition). Absorbances are the mean ± SD of three independent experiments. Statistically different from 0.16 U/µL LDH standard (**) <i>P</i> < 0.01, (***) <i>P</i> < 0.001, (****) <i>P</i> < 0.0001. Statistical analyses were conducted using one-way Anova analyses, followed by Dunnett's test, compared with the value of LDH standard.	131
Figure 29. Absorbance measured during incubation of TiO ₂ NPs with MTT. DMEM was used as a control. The absorbances were measured during 3 hours incubation at 10; 30; 60; 180 min.....	133
Figure 30. Corrected cell viability of A549. Control (C) represents unexposed cells. Values are the mean ± SEM. Statistically different from control (*) <i>P</i> < 0.05, (**) <i>P</i> < 0.01, (***) <i>P</i> < 0.0001, (****) <i>P</i> < 0.0001. Statistical analyses were conducted using one-way Anova analyses, followed by Dunnett's test.....	135
Figure 31. Corrected cell viability of cocultured cells. Control (C) represents unexposed cells. Values are the mean ± SEM. Statistically different from control (*) <i>P</i> < 0.05, (**) <i>P</i> < 0.01, (***) <i>P</i> < 0.0001, (****) <i>P</i> < 0.0001. Statistical analyses were conducted using one-way Anova analyses, followed by Dunnett's test.....	135

TABLES

Table	Page
Table 1. Physical and chemical properties of different nanoparticles (Adapted from [16]).	6
Table 2. Workplace measurements in TiO ₂ depending on the activity types [35–37].	10
Table 3. <i>In vitro</i> studies in literature related to NPs size impact on its toxicity.	23
Table 4. Protocols for determining optimal conditions for THP-1 differentiation	39
Table 5. Percentage values of differentiated THP-1 cell viability monitored by flow cytometry after treatment with PMA (50, 100, 150 and 200 ng/mL PMA) for 72 h + 5 days resting (without PMA).	41

ABBREVIATIONS

16HBE	Human bronchial epithelial cell line
A172	Human glioblastoma cells
AECs I	Type I Alveolar Epithelial Cells
AECs II	Type II Alveolar Epithelial Cells
Al ₂ O ₃	Aluminium oxide
ANSES	National Agency for Food, Environmental and Occupational Health Safety
APTES	Aminopropyltriethoxysilane
ATP	Adenosine triphosphate
BET	Brunauer, Emmett and Teller Method
BioPI	Biomaterials and Inhaled Particles Engineering Department
Caco-2	Human epithelial colorectal adenocarcinoma cells
CD11b	Cluster of differentiation molecule 11b
CF	Cystic fibrosis
CHO-K1	Chinese hamster ovary cell line
CNT	Carbon Nano Tubes
CO ₂ • ⁻	Carbon dioxide radical anion
COPD	Chronic obstructive pulmonary disease
DCF	2,7-dichlorodihydrofluorescein
DCFH	2,7-dichlorohydrofluorescein
DCFH-DA	2,7-dichlorodihydrofluorescein diacetate
DLS	Dynamic Light Scattering
DMEM	Dulbecco's modified Eagle's medium
DMSO	Dimethyl sulfoxide
DP-MFA	Dynamic probabilistic material flow model
ELS	Electrophoretic Light Scattering
ESR	Electron Spin Resonance spectroscopy
EU	European Union

FADH ₂	Flavin adenine dinucleotide
FBS	Fetal bovine serum
Fe ₂ O ₃	Iron (III) oxide
FeTiO ₃	Ilmenite
H ₂ O•	Hydroperoxyl radical
H ₂ O ₂	Hydrogen peroxide
HEK 293	Human embryonic kidney cell line
HeLa	Cervical cancer cell line
HepG2	Human liver cancer cell line
IC ₅₀	The half maximal inhibitory concentration
IARC	International Agency for Research on Cancer
ICC	Immunocytochemistry
ICP-MS	Inductively Coupled Plasma Mass Spectrometry
IL	Interleukin
J774 A1	Mouse monocyte macrophage cells
L-02	Human fetal hepatocyte
LAL	Limulus ameobocyte lysate
LDH	Lactate dehydrogenase
MCF-7	Breast cancer cell line
MTT	3-(4,5-Dimethylthiazol-2-yl)-2,5-Diphenyltetrazolium Bromide
N9	Murine microglia
NADH	Nicotinamide adenine dinucleotide
NCI-H292	Human pulmonary carcinoma cells
NMs	Nanomaterials
NFκB	Nuclear factor-kappa B
NPs	Nanoparticles
O ₂ • ⁻	Superoxide radical
OH•	Hydroxyl radicals

PBS	Phosphate-Buffered Saline
PC12	Cell line derived from adrenal pheochromocytoma
PMA	Phorbol Myristate Acetate
RAW 264.7	Murine macrophage cell line
ROS	Reactive oxygen species
RPMI-1640	Roswell Park Memorial Institute Medium
SEM	Scanning Electron Microscopy
SH- SY5Y	Neuroblastoma cells
SSA	Specific surface area
TEM	Transmission Electron Microscopy
TiO ₂	Titanium dioxide
TNF- α	Tumor necrosis factor alpha
XRD	X-ray Diffraction
ZnO	Zinc oxide

INTRODUCTION

Nanoparticles, an increasingly important product of nanotechnology, are defined as objects with at least one dimension measuring less than 100 nanometers (nm) [1].

Metallic and poorly soluble nanoparticles such as titanium dioxide (TiO₂) are among the most widely used nanoparticles in the world [2]. In addition to its unique physicochemical properties such as small particle size, TiO₂ has received much attention due to its chemical stability, high refractive index and photocatalytic activity [3,4]. TiO₂ nanoparticles are used in many consumer products such as paints, antiseptic and antimicrobial compositions, deodorization (purifying/deodorizing indoor air), inks, toothpastes, ceramics, anti-reflective coating in silicon solar cells and many thin film optical devices [4]. The abundance of these products has raised concerns about human exposure and health consequences.

The main route of exposure to TiO₂ nanoparticles is by inhalation. It mainly concerns the worker, the consumer being more probably concerned by the oral route. The environmental and occupational atmospheres are not well characterized for nanoparticles, which may explain the lack of epidemiological studies on the relationship between human exposure to nanoparticles and its adverse effects. Despite this, to show associations between exposure to fine and ultrafine particles in the atmosphere and their adverse health effects, their potential toxicity has been investigated in animal and cellular models. Two important chronic inhalation studies reported elevated risk of lung cancer after exposure to fine [5] or ultrafine [6] TiO₂ in rats and the International Agency for Research on Cancer (IARC) has classified TiO₂ as a possible human carcinogen (Group 2B) [7]. This classification applies to all forms of TiO₂ without considering the size criterion and therefore the nanometric forms. However, given their specificities, the nanometric structure could give rise to more concern regarding health and safety.

still specific, between the different physicochemical characteristics of exposure to TiO₂ NPs and their impact on human health

Due to the reported adverse effects of nano TiO₂, its use in food products in the form of the additive E171 has been suspended for one year in France since January 1, 2020 [8]. Consequently, the French government has sought to reduce the exposure of workers, consumers and the environment to TiO₂ NPs following the notice published

by the French National Agency for Food, Environmental and Occupational Health Safety (ANSES) [9]. As a result, the French government sought to reduce exposure to nano-TiO₂ to workers, consumers and the environment.

With regard to safety, it is important to know what property makes a nanomaterial more or less safe, especially when producing and designing nanomaterials (NMs) according to a "safer by design" approach [10]. Therefore, it is necessary to evaluate the toxic effects of TiO₂ nanoparticles and to study how the physical and chemical properties of these nanoparticles determine their biological effects.

Depending on their physicochemical properties, TiO₂ nanoparticles can cross the biological membranes, circulate in the human body, and interact with biomolecules once inhaled. Due to their interaction with biomolecules, their toxicity usually results in damaged organelle structures, DNA/RNA break, membrane structure destruction, mitochondrial dysfunction, oxidative stress, or inflammation [11]. All these toxic manifestations induce many respiratory diseases such as chronic bronchitis, asthma, chronic obstructive pulmonary disease, or cystic fibrosis [12–14] and even cause injuries in other tissues.

The objective of this thesis work was to systematically study the *in vitro* toxicity of TiO₂ nanoparticles in relation to their different physicochemical properties. As one of the main routes of exposure to these nanoparticles is inhalation, their toxic potential was evaluated on human lung cell lines. This thesis was carried out within the Biomaterials and Inhaled Particles Engineering Department (BioPI) of the Engineering and Health Center of the Ecole des Mines de Saint-Etienne, within the framework of the research unit U1059 Inserm Sainbiose.

INTRODUCTION

Les nanoparticules (NP), produits de plus en plus importants de la nanotechnologie, se définissent comme des objets dont au moins une dimension mesure moins de 100 nanomètres (nm)[1].

Les NPs métalliques et faiblement solubles comme les NPs de dioxyde de titane (TiO_2) sont parmi les nanomatériaux (NMs) les plus utilisés au monde [2]. Outre ses propriétés physicochimiques uniques telles que la taille des particules, le TiO_2 est un nanomatériau très répandu en raison de sa stabilité chimique, de son indice de réfraction élevé et de son activité photocatalytique [3,4]. Les NPs de TiO_2 sont utilisées dans de nombreux produits de consommation comme les peintures, les compositions antiseptiques et antimicrobiennes, la désodorisation (purifier/désodoriser l'air intérieur), les encres, les dentifrices, les céramiques, le revêtement anti-reflet dans les cellules solaires en silicium et de nombreux dispositifs optiques à couches minces [4]. L'abondance de ces produits a soulevé des inquiétudes concernant l'exposition humaine et les conséquences sur la santé.

La principale voie d'exposition aux NPs de TiO_2 est l'inhalation. Elle concerne essentiellement le travailleur, le consommateur moyen étant lui plus probablement concerné par la voie alimentaire. Cependant, les atmosphères environnementales et professionnelles ne sont pas bien caractérisées pour les NPs, ce qui peut expliquer le manque d'études épidémiologiques sur la relation entre l'exposition humaine aux NPs et leurs effets négatifs. Malgré cela, pour montrer les associations entre l'exposition aux particules fines et ultrafines présentes dans l'atmosphère et les effets indésirables sur la santé, leur toxicité potentielle a été étudiée sur des modèles animaux et cellulaires. Deux études sur l'inhalation chronique ont signalé un risque de cancer du poumon élevé après exposition à du TiO_2 fin [5] ou ultrafin [6] chez le rat. Par conséquent, le Centre international de recherche sur le cancer (CIRC) a classé le TiO_2 comme cancérigène possible pour l'homme (groupe 2B) [7]. Cette classification s'applique à toutes les formes de TiO_2 sans tenir compte du critère de taille et donc des formes nanométriques. Cependant, compte tenu de leurs spécificités, la structure nanométrique pourrait susciter davantage de préoccupations en matière de santé et de sécurité.

En raison des effets adverses observés pour certaines formes de nano TiO_2 , son usage dans les produits alimentaires sous la forme de l'additif E171 a été suspendue pour un

an en France depuis le 1er janvier 2020 [8]. Par conséquent, le gouvernement français a cherché à réduire l'exposition des travailleurs, consommateurs et de l'environnement aux NPs de TiO₂, suite à l'avis publié par l' Agence nationale de sécurité sanitaire de l'alimentation, de l'environnement et du travail (ANSES) [15]. Par conséquent, le gouvernement français a cherché à réduire l'exposition au TiO₂ des travailleurs, des consommateurs et de l'environnement.

En ce qui concerne la sécurité, il est important de savoir quelle propriété rend un nanomatériau plus ou moins sûr, en particulier lors de sa production et de sa conception selon une approche dite *safer by design* [10]. Par conséquent, il est nécessaire d'évaluer les effets toxiques des NPs de TiO₂ et d'étudier comment les propriétés physiques et chimiques de ces NPs déterminent leurs effets biologiques.

Selon leurs propriétés physicochimiques, les nanoparticules de TiO₂ peuvent traverser les membranes biologiques, circuler dans le corps humain et interagir avec les biomolécules une fois inhalées. En raison de leur interaction avec les biomolécules, leur toxicité entraîne généralement des endommagements de la structure des organites, une rupture de l'ADN / ARN, une destruction de la structure membranaire, un dysfonctionnement mitochondrial, un stress oxydatif ou une inflammation [11]. Toutes ces manifestations toxiques induisent de nombreuses maladies respiratoires telles que la bronchite chronique, l'asthme, la bronchopneumopathie chronique obstructive ou la fibrose kystique [12–14] et provoquent même des lésions dans d'autres tissus.

L'objectif de ce travail de thèse était d'étudier systématiquement la toxicité *in vitro* des NPs de TiO₂ en relation avec leurs différentes propriétés physicochimiques. Comme l'une des principales voies d'exposition à ces NPs est l'inhalation, le potentiel toxique de ces NPs a été évalué sur des lignées cellulaires pulmonaires humaines. Cette thèse a été menée au sein du département Ingénierie des biomatériaux et des particules inhalées (BioPI) du Centre Ingénierie et Santé de l'Ecole des Mines de Saint-Etienne, dans le cadre de l'unité de recherche U1059 Inserm Sainbiose.

BIBLIOGRAPHY

1. Nanomaterials

Up to date, there is no universal definition for nanomaterials (NMs). The European Union (EU) adopted a definition of a nanomaterial in 2011 as "A natural, incidental or manufactured material containing particles, in an unbound state or as an aggregate or as an agglomerate and where, for 50% or more of the particles in the number size distribution, one or more external dimensions is in the size range 1 nm - 100 nm" [1].

According to ISO/TS 80004 [16], material with any external dimension in the nanoscale or having an internal structure or surface structure in the nanoscale, with nanoscale defined as the length range approximately from 1 nm to 100 nm is defined as a nanomaterial. This includes both nano-objects, and nanostructured materials, which have internal or surface structure on the nanoscale; a nanomaterial may be a member of both these categories.

1.1. Nanomaterial properties and applications

Due to NMs' unique properties and their atomic sequences which can be changed according to the purpose, they are extremely suitable for both industrial and scientific applications and uses [11].

The physical and chemical properties of the nanoparticles are different from the properties of micro-sized particles. Although nanoparticles consist of the same atoms as microparticles, they have a different formation geometry. The smaller a material, the higher the surface to volume ratio, meaning that equal volumes of nanoparticles have a much greater surface activity than micro-sized materials [4]. The high surface activity gives exceptional properties to nanoparticles or manufactured products containing nanoparticles. In addition to their size and surface area, the other properties of nanoparticles such as surface properties, crystallinity, dispersion status, and shape are among the factors affecting their behavior. Nanoparticles come in varied shapes including spherical, triangular, cubic, prism, oval, rod, nanoshell, helical, tubes and fibers [17] (Figure 1).



Figure 1. Examples of nanoparticle shapes.

Nanoparticles are generally divided into several categories depending on their morphology, size and chemical properties. Carbon-based NMs containing fullerenes and carbon nanotubes (CNTs), metal NMs which are made by purely metal precursors, metal oxide semiconductor materials which possess properties between metals and nonmetals, polymeric and lipid-based nanoparticles are some of the well-known nanoparticle classes [4]. The properties of few common nanoparticles are given in Table 1.

Table 1. Physical and chemical properties of different nanoparticles (Adapted from [18]).

Classification	Material	Properties
Carbon based nanoparticles	Fullerenes	Semiconductor, conductor and superconductor
	Graphene	Extreme strength, thermal, electrical conductivity, light absorption
	Carbon Nano Tubes	High thermal and electrical conductivity, flexible and elastic
	Carbon Nanofiber	High thermal and electrical conductivity
	Carbon Black	High strength and electrical conductivity, resistant to UV degradation
Metal based nanoparticles	Aluminium	High reactivity; sensitive to moisture, heat, and sunlight
	Iron	Reactive and gold interactive with visible light
	Silver	Unstable, absorbs and scatters light, stable, anti-bacterial, disinfectant
	Lead	High toxicity, reactive, highly stable
	Zinc	Antibacterial, anti-corrosive, antifungal, UV filtering
Metal oxide nanoparticles	Titanium dioxide	High refractive index, photoactive, UV filtering
	Cerium oxide	Antioxidant, low reduction potential
	Iron oxide	Reactive and unstable
	Zinc oxide	Antibacterial, anti-corrosive, antifungal and UV filtering
	Aluminium oxide	Reactive, sensitive to moisture, heat, and sunlight

Each nanoparticle in these categories depending on its own physicochemical properties has been used in many applications such as in mechanical, energy, electronic industries, environmental approach, manufacturing materials, and pharmaceuticals [19]. With the help of this type of high-tech industrial applications, many daily products have been produced with nanotechnology in higher quality such as cosmetics, inks, food package, food additives, diet products, antibacterial coated clothes. The nanoparticles used in the industrial consumer products are metal oxide such as titanium dioxide (TiO_2), aluminium oxide (Al_2O_3), zinc oxide (ZnO), and iron (III) oxide (Fe_2O_3) nanoparticles. TiO_2 and ZnO nanoparticles which are present in almost all cosmetic products as a sunscreen and as an ingredient in interior-exterior paints due to their high refractive index and photocatalytic properties. Film coatings consisting of organic nanoparticles are frequently used in dietary products and drug coatings. CNTs are used in textile industry. Ag NPs with antibacterial properties are used to keep all kinds of fabric hygienic [20]. Ceramic nanocomposites, TiO_2 and silica NPs owing color protecting, hydrophobic and durability enhancing properties are used on glass and ceramic surfaces and insulation materials. Nanoparticles are abundant in the products we contact everyday such as health products and medical treatments as well. Products like sunscreen, deodorant, and cosmetics all employ nanoparticles and nanotechnology [11].

1.2. Titanium dioxide nanoparticles and their applications

Titanium dioxide is a metal oxide, white powder with a molecular weight of 79.87 g. It melts at 1855°C , boils at 2750°C and has no smell. It is a cheap and abundant semiconductor and naturally exists in three crystal structures as the two most common tetragonal crystallographic polymorphs rutile and anatase, the rarer orthorhombic third crystal structure is brookite (Figure 2).

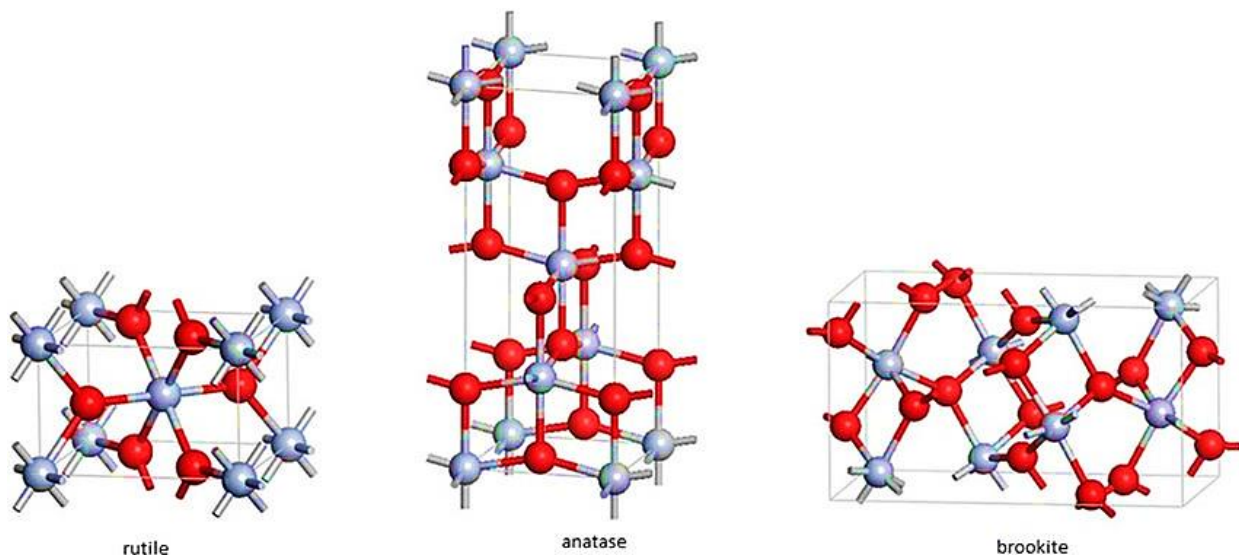


Figure 2. Crystalline forms of TiO_2 [21].

TiO_2 can be extracted from ilmenite (FeTiO_3) by the chloride or sulphate process, which both yield pure rutile titania. Rutile TiO_2 can be transformed by calcination process into anatase or brookite. Due to the lower density of anatase phase (3.894 g/cm^3), it can undergo transition to rutile phase (4.250 g/cm^3) at high temperatures.

In pure TiO_2 for photovoltaic and photocatalytic applications, the anatase phase shows superior catalytic activity with the 3.2 eV energy band gap than rutile (3.02 eV) or brookite phases (2.96 eV) [22]. Also, the increased photoreactivity of the anatase phase is associated with low oxygen adsorption capacity, increased hydroxylation degree and slightly higher Fermi level. The rutile phase also exhibits high refractive index and high optical absorptivity [23].

Upon UV light exposure to TiO_2 nanoparticles, the electrons in the valence bands (VBs) gain energy and therefore are stimulated to the corresponding conduction bands (CBs), thereby produce the electrons (e^-) on the CBs and forming holes (h^+) on these VBs. Formed holes, h^+ , interact with surrounding water and produce hydroxyl radical ($\text{HO}\cdot$) radicals [24–26].

If there is oxygen in the environment, the electron in the CB reduces molecular oxygen to form a superoxide radical ($\text{O}_2\cdot^-$) [27]. The superoxide radical can react with water and produce hydrogen peroxide (H_2O_2). This hydrogen peroxide can either react with light energy ($\text{h}\nu$) or electrons to produce $\text{HO}\cdot$ radicals. The produced $\text{HO}\cdot$ radicals then decompose the organic compounds (R) into water (H_2O) and carbon dioxide (CO_2) (Figure 3) [28].

The formation of such photocatalytic oxidation in organic compounds damages microorganisms in air or in water [29]. Generally, electrons in the TiO₂ structure can switch from the valence band to the conductivity band due to the absorbed beam. During recombination, electrons can return to their old energy levels in a short time such as 10⁻⁶-10⁻¹¹ s [29–31].

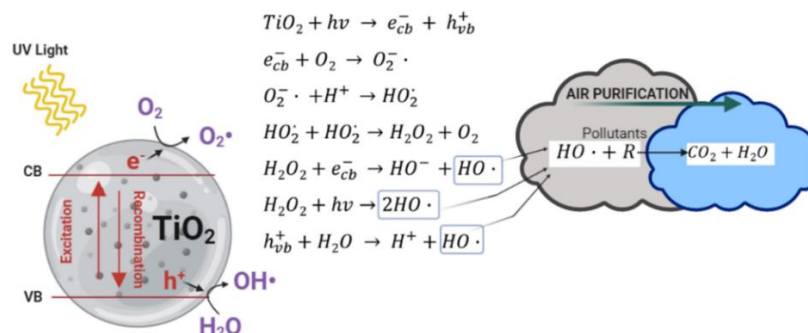


Figure 3. Brief overview of TiO₂ photocatalyst activity.

Due to its photocatalytic activity, TiO₂ nanoparticles are frequently used in air, water purification deodorization and sterilization processes. On the other hand, the extensive use of TiO₂ nanoparticles is attributed to their mechanical durability, high transparency in the visible region, band gap, crystalline quality, size distribution, morphology, porosity, and particle size. The current applications and potential future use of TiO₂ nanoparticles are shown in Figure 4.

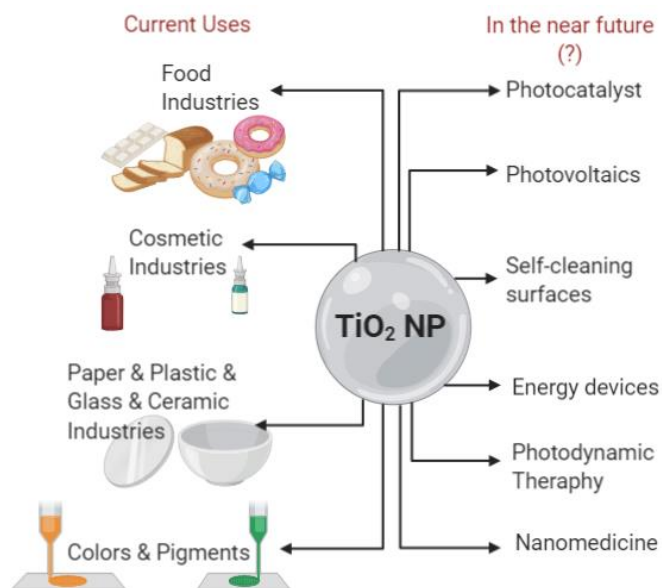


Figure 4. Main industrial applications of TiO₂ (adapted from [32]).

1.3. Titanium dioxide nanoparticles environmental release

The increase in production and use of nanoparticles leads to a potential increase in their release into air, water and/or soil through various processes. Nanoparticles can pass and accumulate into the soil compartments, contaminate water and air during their production, their use and disposal of nanoparticle-containing products (waste handling) [33].

Especially in nanotechnology companies both in producer and user companies, workers are the largest group to have contact with nanoparticles. Work environment can be contaminated during processing of nanoparticle containing products, packaging, cleaning of industrial installations. Regarding their airborne release; the collection and sorting of materials during production are the most frequently described activities, followed by physical and chemical synthesis processes [34,35].

Nanoparticles also spread to the working environment during sonication, weighing, mixing [36,37]. The quantities of nanoparticles emitted, in particular into the ambient air, can be significant and reach hundreds of thousands of particles per cm³ of air and even values approaching the million particles per cm³ in mass concentration. In the absence of collective or individual protection, workers can be potentially exposed in an acute and chronic manner to much greater amounts of NPs than in environmental exposure.

Some studies investigated the release of TiO₂ nanoparticles in workplace area depending on the activities [37–39]. Background concentrations at the workplace were analyzed by a wide-range aerosol spectrometer (range of particle size 5 nm to >32 μm). Measured parameters were particle number concentration as well as particle size distribution. No significant airborne release was observed in comparison to background levels during the production of TiO₂ nanoparticles and cleaning process. Cleaning consists of a pyrolysis system, vacuum cleaning and cleaning-up spilled materials from dumping operations in this study [38]. Twelve facilities were evaluated between December 2005 and January 2008 and an increased release of particles was found during spraying process [37]. Especially flame-spray processes which are used for coating often resulted in very small sizes of highly airborne particles (Table 2) [39].

Table 2. Workplace measurements in TiO₂ depending on the activity types [37–39].

Background p/cm ³ nm	During activity p/cm ³	Sampling size range	Mean size ^a	Agglomeration
------------------------------------	---	------------------------	---------------------------	---------------

Production (flame pyrolysis)	7000-20000	21000	5 nm to >32 μm	2 μm	Agglomerated
Spraying	33500	144800	10-1000 nm	N/A	Agglomerated
Cleaning	7000-20000	22000	5 nm to >32 μm	0.5 - 1 μm	Agglomerated

(p: particle, a: Mean particle size was taken from the mode sizes in number size distributions or estimated from TEM/SEM images).

Another study revealed that TiO_2 aerosols were released in diameters up to 6.0 μm during industrial packaging activities and the higher levels of the respirable particle mass and number concentrations were found to be near the packing site of the pigment TiO_2 production factory [40].

A study [41] using the dynamic probabilistic material flow model (DP-MFA) based on the recently developed method by Bornhöft *et al.* [42], calculated the estimated air concentrations of four NPs in 2020. The predictions were based on the combined estimates of different market research companies and were grounded in the increase in the market in the last years. The predicted (accumulated) concentration of TiO_2 , ZnO, Ag and CNT NPs in the air was found as 5.48, 2.33, 0.03, and 0.05 ng/m^3 , respectively. Among these four nanoparticles, the particle expected to be in the highest concentrations in the environment is TiO_2 .

US National Institute for Occupational Safety and Health, Organisation for Economic Co-operation and Development, International Organization for Standardization, and many other institutions have established the general rules of the protection of workers.

- The recommended exposure limit (REL) for ultrafine and nano TiO_2 is set to 0.3 mg/m^3 (10 h TWA—time weighted average—per day during a 40-h work week) by US NIOSH [43].
- Maximum admissible concentration—the time-weighted average (MAC-TWA) is proposed as 300 $\mu\text{g}/\text{m}^3$ for nano TiO_2 by the Polish Nofer Institute of Occupational Medicine [44].
- Nano reference values (NRV) which is a risk management tool for unknown occupational exposure limits (OELs) of NPs, is defined for particles with a density lower than 6 g/cm^3 NRV like metal oxides (*e.g.* TiO_2 , ZnO, Al_2O_3),

fullerenes, dendrimers, nanoclay, polystyrene, SiO₂, carbon black, etc., NRV is 40,000 particles/cm³ [45].

- Following an in-depth analysis of all the available toxicity data, the ANSES is recommending a chronic TRV by inhalation for the P25 form of TiO₂-NP of 0.12 µg/m³. This reference value will be used when conducting health risk assessments as part of the management of industrial facilities and sites in France. It is also the first TRV developed for a nanomaterial in France [46].

1.4. Titanium dioxide nanoparticles exposure routes

1.4.1. Dermal

Considering the area it covers, the skin can be described as the most exposed organ to the nanoparticles. Therefore, the dermal exposure of nanoparticles should not be neglected, especially for lipophilic and low molecular weight materials. However, in the absence of organic solvents, the interaction with the cells of the skin barrier remains limited because the nanoparticles hardly cross the upper layer of skin known as *Stratum corneum*. It has been shown on healthy volunteers that the TiO₂ nanoparticles present in sunscreens did not cross the *Stratum corneum* [47]. However, it has been shown that NPs can pass through the damaged skin (e.g. eczema) [48,49]. Therefore, special attention should be paid to the safety assessment prior to human use.

1.4.2. Ocular

Ocular exposure is possible after applying cosmetics to the eyes or accumulating aerosolized NMs. However, the research on this route of exposure is limited [49].

1.4.3. Oral

Due to the fact that food products contain nanoparticles, especially when considering Food grade TiO₂ (E171) as an ingredient in many products, such as sweets, candies and chewing gum, the digestive system is also an entry route of NPs of concern. If the route of administration is different, the biokinetic/biodistribution patterns vary significantly.

Titanium dioxide nanoparticles are generally fecally cleared after oral administration. Nanoparticles are absorbed by the gastrointestinal tract and can translocate to tissues and organs such as the liver, spleen, kidneys, and lung tissues, and where they can lead to lung injury, nephrotoxicity and hepatic injury [55].

In addition to consuming foods containing nanoparticles, their oral intake can occur from unintentional hand to mouth transfer of materials for example during handling of materials that contain nanoparticles. Ingestion may also accompany inhalation exposure because particles which enter the organism by the respiratory route can pass to the digestive tract by mucociliary clearance [48].

1.4.4. Inhalation

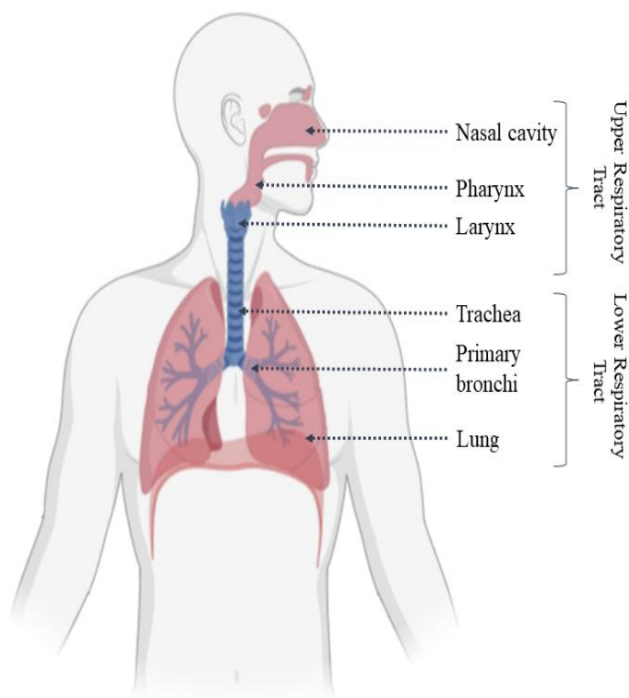
Taking into account the significant nanoparticle concentrations released into the work environment, the most common route of exposure is by inhalation.

Once inhaled, depending on their size, the nanoparticles can penetrate deep into the lungs and can pass into the blood and/or translocate into other organs. The retention time of nanoparticles in the compartments depends on the exposure time. The NMs are cleared with alveolar macrophages slowly in the alveoli and then drained into the lymph nodes [50]. On the other hand, NPs can be rapidly cleared by the mucociliary escalator.

2. Adverse effects of inhaled nanoparticles

2.1. General anatomy of the respiratory system and nanoparticle interaction

The respiratory system is divided into two parts: the upper and lower respiratory tracts. The upper respiratory tract consists of a nasal layer, which trap harmful substances in the air, pharynx and larynx. The inhaled air passes from the larynx to the trachea, reaching the right and left bronchi. The bronchi eventually split into smaller airways called bronchioles. The diameter and length of each airway branch decreases progressively from the trachea to the bronchioles. At the end, the air reaches the alveoli where gas exchange occurs. The lower respiratory tract consists of trachea, bronchi, bronchioles and lungs (including alveoli) (Figure 5) [51].

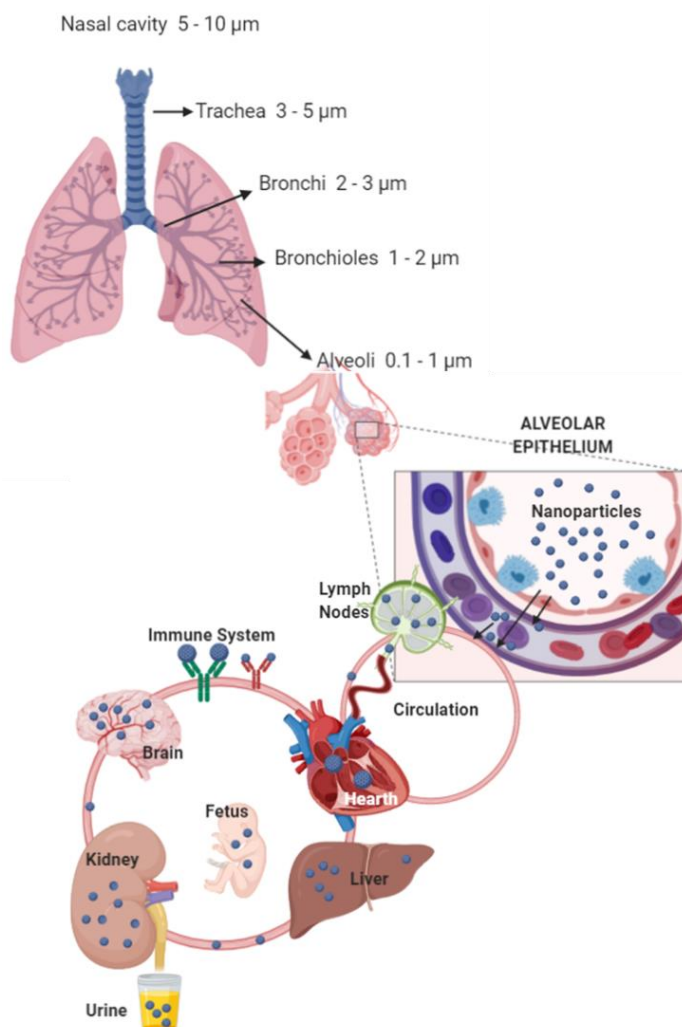


The respiratory tract is a complex anatomical structure and the diameter of the upper airways is relatively large, and the lower airways and alveolar diameters are smaller. The inhaled particles deposit in the entire respiratory tract, from the nasal cavity to alveoli. Therefore, mainly the sizes and surface areas of particles, and their physical state (liquid or solid), density, shape and velocity are important factors in influencing NPs deposition [52].

Figure 5. Upper and lower respiratory system.

Particles inhaled in different sizes show deposits in different regions of the human respiratory system. Ultra-fine particles with a diameter lower than 100 nm were observed in all regions, particles smaller than 10 nm in the tracheobronchial region, and particles from 10 to 20 nm in the alveolar region [53]. It has been shown that 22 nm inhaled TiO_2 NPs deposited in different compartments of lung tissue, capillaries, and on the luminal surface of the airways and alveoli [54]. The relocation of particles from the lung surface to lymphatic drainage might result in entering blood vessels and translocate easily in the circulatory system. Translocation of NPs cause their accumulation in several major organs such as the heart, liver, immune system, liver etc. (Figure 6) [47].

The retention of particles starts with their wetting and displacement from the air into the aqueous phase by surfactant. In general, it has been shown in rodents, that microparticles (0.5 - 10 μm) remain on the epithelial surface in airways and alveoli and are accessible to BAL [55]. The same can be expected for nanoparticles even more efficiently due to their smaller size. The retention time of nanoparticles depends on



the exposure time, the localization of NPs and their size. The retention time is short in conducting airways due to fast mucociliary clearance and cough. The studies show that within 24 hours of aerosol inhalation, nanoparticles in the alveoli can bypass the major clearance mechanisms [56].

The phagocytosed nanoparticles by alveolar macrophages and free particles in alveoli are cleared by the larynx. Approximately 5–20% absorbed/translocated TiO_2 nanoparticles pass through the gut epithelium and then undergo long-term clearance from the lungs via larynx [57,58].

Figure 6. Nanoparticle translocation in human body.

However, clearance can be long in deeper region of lung due to the high mucus velocity. As we discuss in detail in the following section, the interaction of particles with macrophages results in phagocytic uptake that is also a key factor for particle clearance in airways and alveoli.

2.2. Cellular organization of the respiratory system and nanoparticle interaction

The respiratory tract is lined by different epithelial cells. There are thirteen different cells known, eleven of these are epithelial cells and two are mesenchymal cells. Most of the epithelium cells are defined as ciliated and mucus secreted cells (*e.g.* goblet cells). The ciliated, brush, basal, club, pulmonary neuroendocrine (PNEC) cells have been found in airways. The area from the trachea to the bronchi is usually covered with ciliated pseudostratified columnar epithelium. Epithelial cells take more cubic shape as they are directed towards the bronchioles to alveoli, while mesenchymal cells cover the lung tissue [59].

Alveolar epithelium is made up of two cell types, Type I Alveolar Epithelial Cells (AECs I, Type I pneumocytes) and Type II Alveolar Epithelial Cells (AEC2s, Type II pneumocytes). The major epithelial cell types of the gas exchanging region are cuboidal AEC2s that are specialized for surfactant protein production and secretion, Type I cells are characterized by a narrow and extensive cytoplasm and are joined together by tight junctions (Figure 7). These cells allow passive gas diffusion while making the alveolar epithelium fairly impermeable to other substances [60].

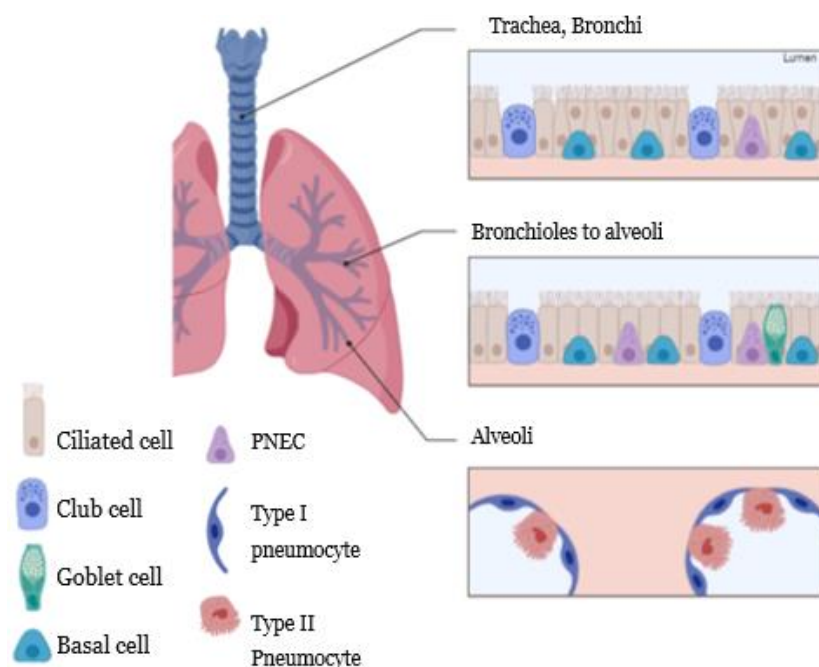


Figure 7. Cell organization of the respiratory system.

Airway epithelium, which plays a critical role in delivering air to the alveoli, also plays a role in defense against inhaled pathogens and particles. Foreign material can be removed in the major bronchi and trachea by coughing. Mucociliary transport allows

removal of unwanted particles from the terminal bronchioles to the trachea. Also, the organization of epithelial cells such as intercellular connections provide an effective mechanical barrier and contribute to the mucociliary clearance function. Mucociliary clearance is the mechanism by which cilia of the bronchial epithelial cells remove particles trapped in mucus from the airways. The particles are transported towards the oral cavity, where they can be swallowed and taken up by the oral route. Mucus secreting cells express mucins. Secretion of salt and water results in the formation of two extracellular fluid layers. The periciliary layer allows the movement of cilia of the ciliary cells. The viscous mucus layer absorbs many particles. Driven by ciliary activity, the mucus layer with the absorbed material is continuously transported to the throat [61]. Epithelial cells recruit inflammatory cells by releasing cytokines and chemokines against the inhaled pathogens or toxic agents (Figure 8).

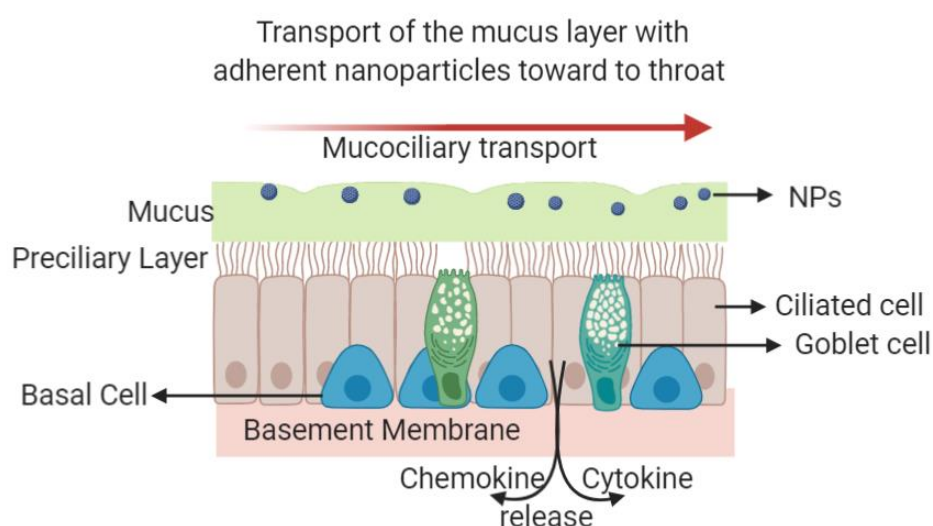


Figure 8. Scheme of the mucociliary clearance.

When nanoparticles come in contact with the outer membrane of a cell, it can interact with the components of the plasma membrane or extracellular matrix. They can enter the cell mainly through endocytosis. Endocytosis leads to ingestion of nanoparticles in membrane invaginations. Endocytosis is classified as phagocytosis, clathrin-mediated endocytosis, caveolin-mediated endocytosis, clathrin/caveola-independent endocytosis and micropinocytosis [62].

The phagocytic activity of macrophages is considered as the primary mechanism for the intake of nanoparticles into the cell. In the biological fluids, proteins adsorb on the surface of the nanoparticles (forming the so-called protein corona, see 2.2.1). Proteins from the corona (especially immunoglobulins or complement proteins) are recognized by cell membrane receptors of macrophages. This initiates a signaling

cascade that can trigger actin assembly, the formation of cell surface extensions, and forming a zipper-like structure and subsequent engulfing and internalization of particles (Figure 9) [63].

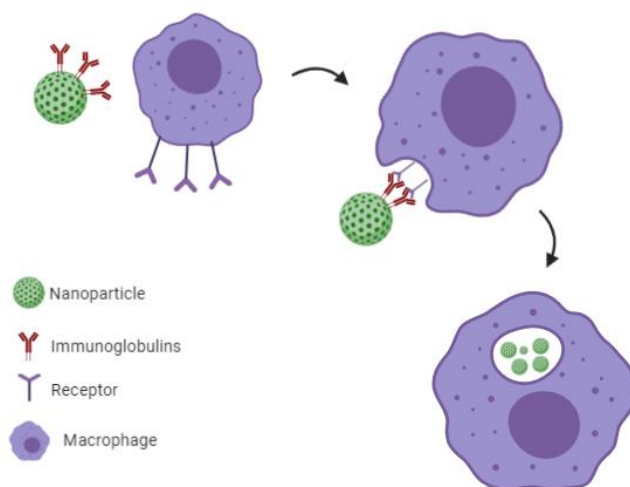


Figure 9. Schematic illustration of the phagocytosis.

In general, reorganization of cytoskeleton occurs in many cell types but especially in certain cells called as professional phagocytes. These cells are: macrophages, neutrophils, dendritic cells, monocytes and include endothelial and secretory epithelial cells in some special cases [63]. During the phagocytosis of NPs by macrophages, inflammatory markers such as cytokines and pro-inflammatory chemokines can be released [64]. The release of such chemokines leads to inflammatory cascades in the alveolar milieu, which are an important part of innate immunity. Chronic inflammation could represent an environment favorable to the development of lung diseases.

2.2.1. Protein corona formation

When nanoparticles interact with the biological environment, proteins in the biological fluids, sugars, lipids, and other macromolecules adsorb to the nanoparticle surface. Since proteins are largely predominant in biological fluids, this nanoparticle-protein structure is called the protein corona [65]. But the understanding of the formation and composition of the protein corona remains poor.

The adsorption of proteins on the surface of the nanoparticles is mainly driven by electrostatic interactions, as well as H-bond, van der Waals interactions, and salt bridge formations. The protein corona is composed of two main layers: the *hard corona*, which is the first and richer layer of proteins, characterized by direct

adsorption, tighter bonds, slow exchange time and high conformational change; and the *soft corona*, which is the second and exterior layer of proteins, characterized by weak bonds (protein-protein interactions), quick exchange time and low conformational change (Figure 10) [66–68].

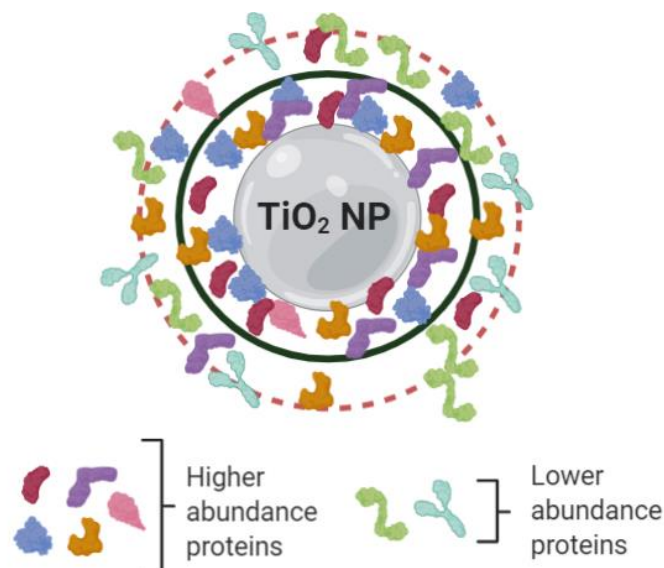


Figure 10. Protein corona composition.

The evolution and dynamics of hard corona formation are relatively well studied [69,70]. The current understanding is that the hard corona proteins—with their long residence time—give the nanoparticles a biological identity by presenting receptor-binding sites for cellular interactions with a biologically relevant timescale. As soft corona proteins by definition have a shorter residence time on nanoparticles than hard corona proteins making them difficult to isolate from free proteins of the mother liquid, their potential biological impacts through specific and/or nonspecific interactions have often been ignored [71].

The protein corona evolves when nanoparticle-adsorbed-protein complexes are moved from one biological environment into another, with some proteins from the original corona being replaced by proteins from the new biological fluid. It is intriguing that while the corona evolves, it retains a fingerprint of its prior history. This may turn out to be an important paradigm, for understanding *in vitro* and *in vivo* transport. Besides this, however, the protein-particle complex may contain a history-dependent set of protein markers or signals that can be elucidated via the protein corona of particles recovered from their final subcellular location [72].

The physicochemical properties of NPs have an impact on the formation and composition of the protein corona [73]. The size and surface area of the NPs are the

main factors that affect the amount of proteins that can adsorb to its surface. The surface charge, surface chemistry, shape of NPs also have a great effect on the composition of the corona. The protein interaction can also alter the physicochemical properties of NPs. Proteins adsorbed on the nanoparticle surface may change their conformation, agglomeration status and surface charge [67].

All these are parameters can affect the contact of nanoparticles with the cells. The proteins on the nanoparticle surface can be recognized by the receptors on the cell membrane and the nanoparticle-cell membrane interaction begins. After this point, nanoparticles can be taken up into the cell and their fate is determined [74].

3. Mechanisms of nanoparticle toxicity

Following the uptake of nanoparticles into the cell, the next important consideration is the determination of their cellular outcomes. Nanoparticles show their toxicity mainly by inducing oxidative stress or by causing inflammation.

3.1. Oxidative stress

Aerobic organisms use the mitochondria organelle as the main energy producer to perform vital functions [75]. Mitochondria produce adenosine triphosphate (ATP) through oxidation and reduction reactions, and the produced ATP goes through to the tricarboxylic acid cycle by the electron transport chain [75]. This situation occurs by oxidation of food produced in different metabolic pathways such as glycolysis, B oxidation and Krebs cycle, and nicotinamide adenine dinucleotide (NADH) or flavin adenine dinucleotide (FADH₂) reduction-oxidation [76].

However, these reactions lead to the production of extremely highly reactive oxygen species (ROS), which are unstable due to their unpaired electrons. ROS try to stabilize their unpaired electrons by attacking nucleic acids, proteins, carbohydrates and the consequence is an alteration of the functions of these biomolecules. A complex antioxidant defense system often balances this attack. However, in some cases, this balance may be disrupted. Oxidative stress is a physiological response to a cellular stress or aggression, it becomes deleterous when it is uncontrolled [77].

The transport chain of the mitochondrial electron is the main source of the endogenous ROS; molecular oxygen is gradually reduced to a number of intermediate types: hydroperoxyl radical, superoxide radical anion, hydrogen peroxide (H₂O₂), hydroxide ion and hydroxyl radical. Gradual molecular oxygen reduction is shown as follows [78].

1. $O_2 + e^- \rightarrow O_2^{\bullet-}$ Superoxide radical
2. $O_2^{\bullet-} + H_2O \rightarrow H_2O^{\bullet}$ Hydroperoxyl radical
3. $H_2O^{\bullet} + e^- + H^+ \rightarrow H_2O_2$ Hydrogen peroxide
4. $H_2O_2 + e^- \rightarrow OH^- + OH^{\bullet}$ Hydroxyl radical

The oxidative stress induced by NPs can be caused by the active redox cycle on the surface of metal-based NPs, and the interaction of NPs with the cell. Reduced particle size causes structural defects and alteration of electronic properties on the particle surface, forming reactive groups on the NP surface [79,80]. Within these reactive regions, electron donor or acceptor active sites interact with molecular O_2 to form $O_2^{\bullet-}$ which can generate additional ROS via Fenton-type reactions [80]. ROS can be produced by photocatalytic NPs such as TiO_2 . As electrons migrate from the valence band to the conduction band, during their stimulation with light, they can react with molecular O_2 and H_2O to form hydroxyl radicals (see Figure 3) [81].

Besides being oxidative by themselves, NPs can induce cellular ROS production by interacting with cells, affecting NADPH-like enzyme systems and mitochondrial mechanism. In particular, they can affect the cellular redox systems of alveolar macrophages and neutrophils. Professional phagocytic cells including neutrophils and alveolar macrophages of the immune system induce substantial ROS upon internalization of NPs via the NADPH oxidase enzyme system [82].

3.2. Pro-inflammation

The immune system works with blood and lymphatic circulatory systems that interact and communicate via chemical conductors to regulate an immune response against a particular stimulus. T and B lymphocytes, natural killer cells and phagocytic cells are the main cells of the immune system. Macrophages are essential parts of the immune system that function as cleansers or antigen presenting cells. Phagocytic cells are found in many tissues. Monocytes and neutrophils circulate throughout the body through blood, therefore they can detect pathogens, remove them and synthesize and release the cytokines necessary for the immune system [83].

Many cytokines, such as interleukin 1 (IL-1), IL-6, IL-8 and tumor necrosis factor alpha $TNF-\alpha$, activate inflammatory cells during inflammatory responses. While $TNF-\alpha$ is stimulated by endothelial cells, IL-8 is a chemokine that stimulates the activation of neutrophils. Many cytokines act together to initiate and regulate the inflammation process [84].

When the NPs enter the systemic circulation, the immune system can detect many components of the NPs (*e.g.* shell, core, surface-decorating moieties) as foreign entities which stimulate the immune system through a complex process [85].

3.3. Role of physicochemical features in nanoparticle toxicity

Cellular internalization of nanoparticles depends on their physicochemical properties, especially nanoparticle size, surface area, shape, surface charge. Therefore, it is clear that nanoparticle physicochemical properties determine their toxicity. The toxicity-inducing abilities of certain physicochemical properties are discussed below.

3.3.1. Effect of size and surface area

Particle size and surface area are important in the interaction of nanoparticles with biological systems. When the particle size decreases and the surface area increases, the nanomaterial surface becomes more reactive in the biological environment.

In general, the toxicity of the NPs can be attributed to the ability to enter biological systems, to pass through the cell membrane more easily, and then to change the structure of various biomolecules, thereby interfering with critical biological functions [17]. Therefore, in nanoparticle toxicity, their cellular internalization is the major step. In that case nanoparticle size has an important impact on its cellular internalization [86].

The fact is that small NPs can pass through the cell membrane more easily than large particles. In studies supporting this idea, a size-dependent internalization in different cell lines was observed for Au [87–90], mesoporous silica [91], polystyrene [92] and iron oxide NPs [93]. On the other hand, some studies reported that larger nanoparticles exhibited higher cellular uptake or no any size related internalization in various cell lines [94,95].

The maximum intracellular uptake size range was observed as 30-50 nm [93]. The internalization of <200 nm size nanoparticles is mediated by clathrine-dependent endocytosis, however bigger than 200 nm size nanoparticle internalization is found evident in caveolae-mediated endocytosis [96]. However, it should be noted that this process is highly dependent on the cell type. Because internalization requires compatible formation of NP-receptor interactions. Small NPs have less ligand-receptor interactions than large NPs; therefore, many small NPs are expected to interact with nearby receptors simultaneously, in order to trigger the membrane

wrapping. A study showed that thermodynamically 50-60 nm NP has the capacity to have enough receptors to successfully trigger internalization [97].

Overall, the nanoparticle internalization highly depends on the cell type, and nanoparticle characteristics. Also most of the uptake studies involving living cells are carried out in a cell culture medium supplemented with protein mixtures of different compositions, it is not surprising that in some cases the apparently "identical" studies give contradictory results.

Following the internalization, smaller sized nanoparticles showed greater cytotoxicity than larger ones in several studies but there are also conflicting results (Table 3).

Table 3. *In vitro* studies in literature related to NPs size impact on its toxicity.

NPs	Size (nm)	Cell lines	Evaluation techniques	Main conclusions	Ref
TiO₂	14–196	Osteoblasts, Human fetal hepatocyte (L-02), Human embryonic kidney (HEK 293)	Alkaline phosphatase and zymography evaluation	Size-dependent cytotoxicity, 100 nm critical size	[98]
QDs	2.2, 5.2	The adrenal phaeochromocytoma (PC12), Murine microglia (N9)	MTT assays	Smaller NPs more toxic	[99]
Au	5, 15	Mouse embryo (Balb/3 T3)	Colony forming efficiency, Trypan Blue assays	5 nm, cytotoxic; 15 nm non-cytotoxic Autophagosomes observed after AuNPs 5 nm exposed cells	[100]
Au Ag	3–38 3–25	Mouse monocyte macrophage cell (J774 A1)	Sizing and counting of cells	Au NPs, increased toxicity for smaller NPs Smaller Au NPs up-regulate the expressions of pro-inflammatory genes Ag NPs, no size-dependent toxicity	[101]
SiO₂	32, 83	Human colorectal adenocarcinoma cells (Caco-2)	WST-1 assays, comet assays	No cytotoxicity observed for either size	[102]

The critical size of many NPs is defined as 30 nm for toxicity. Surface reactions increase the likelihood of toxicity as nanoparticle surface energy increases at sizes lower than 30 nm. The results of one study showed that Ag NPs with smaller

dimensions (4 nm) stimulated the production of ROS in human myeloid leukaemia cell line (U937) and caused more severe pulmonary inflammation than Ag NPs with larger dimensions (20 nm and 70 nm) [103]. Another study showed that 1.4 nm gold NPs caused more severe toxicity in connective tissue, fibroblasts, epithelial cells, macrophages and melanoma cells than the smaller (0.8 nm and 1.2 nm) or larger (1.8 nm and 15 nm) particles [104].

Overall, there is no definitive conclusion about the effect of particle size on toxicity. Toxic effect of TiO₂ NPs may be related to their structural characteristics as suggested by Zhang *et al.* [105].

3.3.2. Effect of particle shape

Shape-related toxicity is mainly associated with the membrane's ability to wrap particles during endocytosis [106]. For example, studies showed that the cellular uptake of spherical gold nanoparticles by murine macrophages was higher than that of rod gold nanoparticles [107,108]. The reason might be associated with membrane wrapping time which is longer for the larger rod-shaped nanoparticles due to the varying number of receptor localization [109].

On the other hand, it was observed that the fiber-shaped TiO₂ NPs were more cytotoxic than the spherical-shaped ones [110]. Due to the unusual aerodynamics of fiber materials such as asbestos fibers or carbon nanotubes, long fibers penetrate and accumulate beyond the ciliated airways. Short fibers could be completely covered by cell membrane and can be cleared with phagocytosis. Longer fibers, on the other hand, cannot be enclosed. Therefore it leads to 'frustrated phagocytosis' which can cause chronic inflammation, oxidative stress, direct cell damage, and chromosomal abnormalities [111].

In a study, among the rods (39×18 nm), stars (215 nm) and spheres (6 nm) gold nanoparticles, spherical caused less cytotoxicity than others [112]. However, it should be considered that the examined nanoparticles had a wide variety of dimensions.

3.3.3. Effect of surface charge

The surface charge of nanoparticles, which is of great importance in interacting with biological systems, plays an important role in toxicity.

Positively charged particles show significant cellular uptake compared to negatively charged and neutral NPs due to their increased opsonization by plasma proteins [113]. Considering that the surface charge of the cell membrane is negative, positively

charged particles may pass through the membrane easily. However, studies in our laboratory in the previous years showed the positively charged nanoparticles were more uptaken by cells than neutral or negatively charged nanoparticles [66,114]. Therefore, nanoparticles with different surface charge may cause different toxic manifestations. In a study using molecular simulation [115], the electrostatic attraction effect between cationic nanoparticles and the cell membrane was investigated. Charged nanoparticles showed a more favorable thermo-dynamic interaction than their uncharged counterparts. In another molecular dynamic simulation study, the interaction of cationic, hydrophobic and anionic Au nanoparticles with the cell membrane was investigated [116]. They showed that the internalization increased with increasing charge density. They also reported membrane disruptions with higher nanoparticle charge density.

3.3.4. Effect of agglomeration

The aggregation status of NPs also influences their toxicity. Generally, the aggregation status of nanoparticles depends on size, surface charge, and chemical composition among others.

3.3.5. Conclusion

Once nanoparticle are uptaken into human body by inhalation, ingestion or dermal route, they can circulate in the bloodstream. Nanoparticles can interact with cells, tissues and organs, and depending on their physico-chemical properties they can internalize through the cell membrane, interacting with macromolecules and altering their structure and function [117–120]. The typical changes in cell functions and structures play an important role in the pathogenesis of many respiratory diseases such as chronic bronchitis, asthma, chronic obstructive pulmonary disease (COPD) or cystic fibrosis (CF), and such natural and engineered particles, fibrous materials and inhaled chemicals can be caused by exposure to daily lung inhalants (Figure 11) [12,13].

Therefore, the NP toxicity strongly depends on their physical and chemical properties, such as the size, shape, surface charge, chemical composition, etc. It also should be noted that, the physicochemical properties of nanoparticles has an impact on protein corona formation since it is known that the protein corona has an impact on the internalization of NPs by cells and thus potentially on the cytotoxicity.

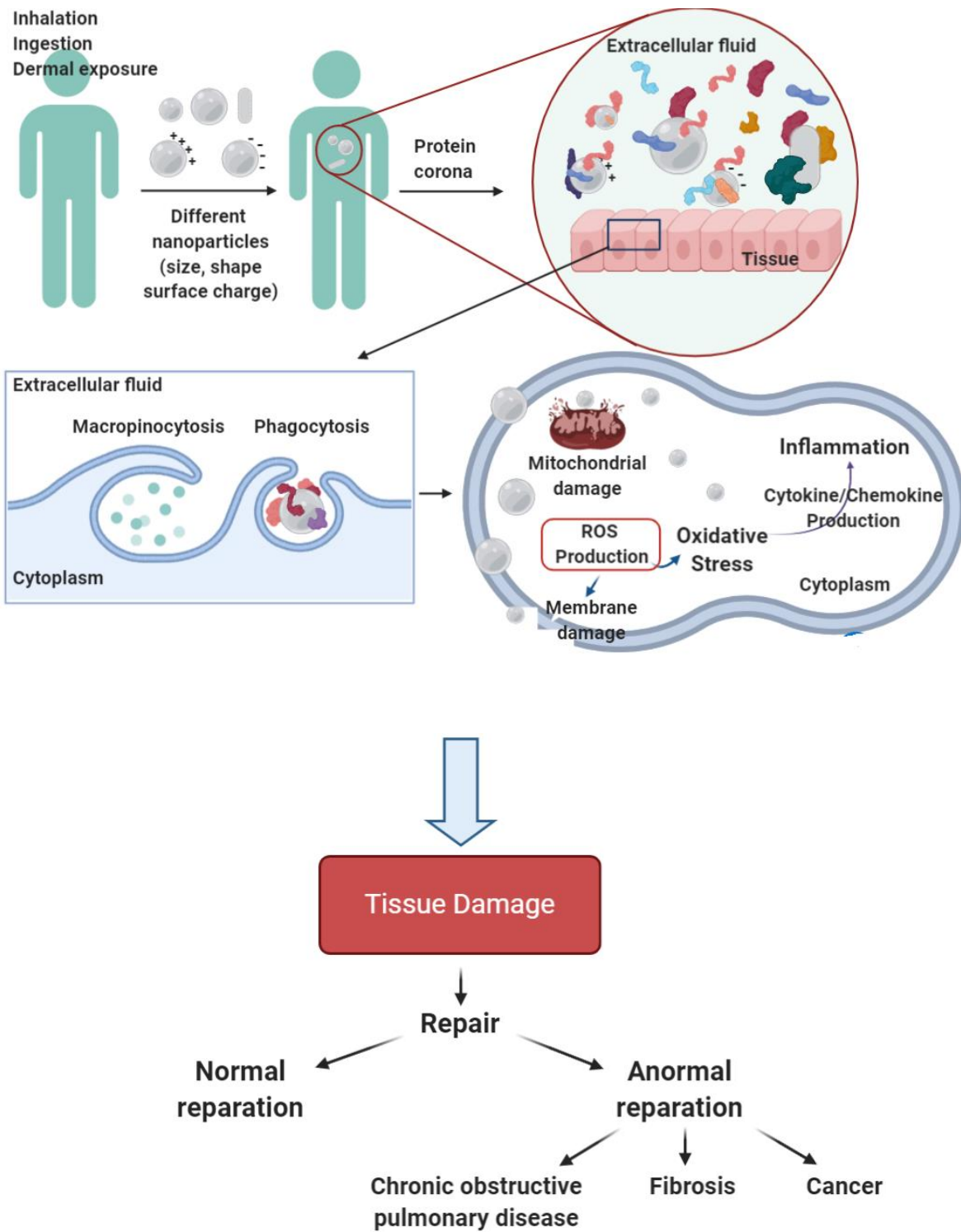


Figure 11. Interaction of NPs with cells and possible biologic effects.

4. *In vivo* and *in vitro* titanium dioxide toxicity

4.1. *In vivo* studies

In vivo studies have shown that after inhalation or after instillation of TiO₂ NPs, undesirable effects might occur at high doses, generally higher than 0.5 mg/kg in rats and mice [121–123].

In particular, a rapid inflammatory response characterized by a significant increase in the number of phagocytes in the broncho-alveolar lavage fluids as well as by an increase in pro-inflammatory cytokines production, oxidative stress cytotoxicity, and lung tissue structural damage have been demonstrated in several studies [121,122]. After chronic exposure to large doses of TiO₂, genotoxic and carcinogenic effects have been demonstrated [122,124]. Some studies are categorized depending on their exposure duration.

Acute studies

According to Noël et al. [125], bronchoalveolar lavage fluid indicated large aerosols (>100 nm) caused an acute inflammatory response, as shown by the significantly enhanced number of neutrophils, while small aerosols (5, 10–30 or 50 nm) produced significant oxidative stress damages and cytotoxicity in the lungs of male rats exposed to TiO₂ NPs at 20 mg/m³ for 6 h. In both aerosols, the 10–30 nm TiO₂ NPs induced the significant pro-inflammatory effects in comparison to the controls. Noël et al. (2012) also showed that an acute (6 hours) inhalation of 5 nm TiO₂ (anatase) with two distinct agglomeration states, smaller or larger than 100 nm, induced mild pulmonary effects at 7 mg/m³ [126].

Sub-acute studies

Oberdorster et al. [127] found a marked increase in pulmonary inflammation due to 20 nm TiO₂ NPs in rats and mice, expressed by the increase of total protein in BALF, and LDH activity. Li et al. [128] studied the effects of intratracheally instilled 3-nm-sized TiO₂ NPs once a week for 28 days in mice after a total dose of 13.2 mg/kg body weight. Lung damage and change in the permeability of the alveolar-capillary barrier were observed. A 12-week inhalation experiment in rats resulted in a similar mass deposition of the two particle types in the lower respiratory tract. The ultrafine particles elicited a persistently high inflammatory reaction in the lungs of the animals compared to the larger-sized particles [129].

Sub-chronic studies

Warheit et al. [130] compared several types of TiO₂ fine particles and nanoparticles with different sizes, surface areas and crystal structures by intratracheal instillation of TiO₂ NPs with the size of 25 or 100 nm and dose of 1 and 5 mg/kg body weight for 24 h, 1 week and 3 months into rats. In the comparison between these particles, even though the surface areas differed as large as 30-fold, the lung inflammation observed was almost similar for the two particle sizes. Therefore, they concluded that toxicity of TiO₂ particles is not dependent on the particle size or surface area through lung instillation. Moreover, the same research group suggested that toxicity depends upon particle surface properties instead of surface areas. When mice were intratracheally instilled with single fixed doses (5, 50 and 500 µg) of TiO₂ fine as well as rutile nanoparticles, Roursgaard et al. [131] found an increase in interleukin-6 and total protein in BALF as well as airway inflammation at the highest doses in the acute phase by both fine as well as nanoparticles. Another sub-chronic inhalation study (13 weeks) showed that clearance was strongly impacted in rats and mice, more particularly at the highest concentration in aerosol (10 mg/m³), but not in the hamster. More pronounced inflammatory effects were observed in the rat than in the mouse, with the consequence of greater tissue damage [132]. Nanoparticles, compared to fine particles made of the same chemical substance, are less efficiently cleared. This participates to the different potential of toxicity of nanoparticles compared to fine particles of the same chemical composition. It might be related to the fact that most of inhaled TiO₂ particles are eliminated from the lungs in a size dependent manner [133].

Chronic studies

In the longer term, tissue damage may appear (fibrosis for example), due to the slow clearance of NPs [124,134]. Indeed, the presence of tissue damage is even more important for chronic or subchronic exposures, due to persistent inflammation. The exposure of mice to various shapes of anatase TiO₂ (nanospheres, short belts of 1–5 µm, and long nanobelts of 4–12 µm) resulted in the lung deposition of 135 µg for the animals exposed to both nanospheres and long nanobelts. At 112 days after exposure, the lung burden was significantly lower in nanosphere-exposed mice than in nanobelt-exposed mice [39].

TiO₂ has been classified by the IARC as a possible carcinogen for humans (Group 2B) by inhalation due to sufficient evidence from chronic animal studies in 2010 [135]. This classification is not specific to the nano forms of TiO₂.

NIOSH also declined inhaled ultrafine TiO₂ is a potential occupational carcinogen [43,44]. This statement needs to be reviewed. On the other hand, what is important to clarify is that the NIOSH proposes exposure limit values which were established from (and therefore are strictly applicable only for) P25. NIOSH recommends airborne exposure limits of 2.4 mg/m³ for fine TiO₂ and 0.3 mg/m³ for ultrafine (including engineered nanoscale) TiO₂, as time-weighted average (TWA) concentrations for up to 10 hr/day during a 40-hour work week. These recommendations represent levels that over a working lifetime are estimated to reduce risks of lung cancer to below 1 in 1,000. The recommendations are based on using chronic inhalation studies in rats to predict lung tumor risks in humans. The hazard assessment of inhaled TiO₂ NPs should be performed in consideration of the significant role of this route of exposure for both the general and occupational populations.

Several studies reported a greater inflammatory response against TiO₂ NPs with comparison to its fine counterparts in acute or chronic exposure [136,137]. Some studies have shown no correlation between nanoparticle agglomeration and pulmonary inflammation [138,139]. Size-related impact studies revealed that smaller particles have a greater impact on inflammation than bigger nanoparticles [140,141].

Crystal structure (anatase or rutile) may influence TiO₂ NPs reactivity in *in vivo* as shown by *in vitro* studies [142]. But until now there is no *in vivo* studies that would provide sufficient evidence to demonstrate which crystallinity could be the most toxic and to what extent. In order to evaluate the effect of surface chemistry on biocompatibility, there are a few studies investigating APTES modified NPs *in vivo* toxicity. To assess lung inflammation, C57BL/6 mice were administered bare or amine-functionalized silica NPs via intra-tracheal instillation. Two doses (0.1 and 0.5 mg NPs/mouse) were tested using the *in vivo* model. At the higher dose used, bare silica NPs elicited a significantly higher inflammatory response, as evidence by increased neutrophils and total protein in bronchoalveolar lavage fluid compared to amine-functionalized NPs. From this study, they conclude that functionalization of nonporous silica NPs with APTES molecules reduces murine lung inflammation and improves the overall biocompatibility of the nanomaterial [143].

The differences in species, application methods and physicochemical properties of the applied nanoparticles lead to contradictory results. There is still limited number of *in vivo* studies regarding TiO₂ toxicity to draw a conclusion, additional researches seem highly necessary.

4.2. *In vitro* studies

It has been shown in *in vitro* studies that TiO₂ nanoparticles can induce a pro-inflammatory response, oxidative stress, cytotoxicity, and genotoxicity on lung cells [124,144].

The size impact on toxicity was investigated in number of studies. Generally smaller TiO₂ nanoparticles caused cytotoxicity [145–149], however other studies showed contradictory results. For example, an interesting finding was that 25 nm anatase particles induced more cell death, higher LDH release, and ROS activities than 5 and 100 nm anatase particles [105]. Similar to this results, Braydich-Stolle *et al.* (2009) showed that 50 nm TiO₂ NPs had a higher toxicity than TiO₂ NPs of 6.3, 10, and 100 nm [150]. Therefore, there is no unanimous conclusion about the effect of particles size on toxicity.

The effects of TiO₂ NP phase on the toxicity were investigated on A549 cells among amorphous, anatase and anatase/rutile phases (18-53 nm) [110]. The toxicity order of NPs was amorphous >anatase >anatase-rutile TiO₂. The amorphous and anatase NPs induced greater IL-8 pro-inflammatory response than anatase-rutile phase P25. Although the anatase and P25 NPs had a similar surface area, size, and shape, they exhibited different toxicity responses, confirming that the phase of a TiO₂ NP affects its cytotoxicity. Similarly, Sayes *et al.* [151] also found that the anatase TiO₂ was 100 times more toxic than an equivalent sample of rutile TiO₂.

In another study [152], custom-made 9 nm rutile (R9, 270 m²/g), 5 nm rutile (R5, 11 m²/g) and 14 nm anatase (A14, 300 m²/g) NPs and commercial 60 nm anatase (A60, 40 m²/g) and 21 nm P25 (50 m²/g) were used to compare their cytotoxic potential on 16HBE cells, and human lung epithelial cell lines (A549 and BEAS-2B). None of the TiO₂ NPs were found to have significant effect on cell viability in 16HBE, BEAS-2B and A549 cells. Whereas, a significant concentration-dependent increase in IL-8 release in all three-cell types was observed for P25, and it was more important compared to other particles. In A549 cells, P25 caused concentration-dependent ROS production whereas A14 particles did not cause significant ROS production. A60 and R9 also induced the ROS response. The researchers emphasized that the toxicity of NPs varies depending on the cell type and the physicochemical properties of NPs [152]. Discussing the phase effect alone on toxicity is very difficult due to the different NP sizes used. However, this study shows that TiO₂ NPs are able to induce ROS and IL-8 production without causing cell viability loss. Similar to this result, a study showed that TiO₂ NPs caused a toxicity by triggering other pathways than decrease of

cell viability. TiO₂ (200 nm, 0-800 µg/mL) were exposed to alveolar macrophage-like THP-1, A549 and Human Pulmonary Microvascular Endothelial (HPMEC-ST1.6R) cells. Concentration-dependent ROS formation was observed in all cell lines at a 24-hour exposure. However, the increase in ROS in A549 and HPMEC-ST1.6R cell lines was more pronounced at 4-hour exposures [153]

There are also studies showing that TiO₂ toxicity depends on concentration and exposure time [152]. A549 cell viability decreased in a concentration dependent manner when cells were exposed to 0.75-75 mg/L TiO₂ NPs (<150 nm, anatase/rutile 80/20) for 24 hours [154]. In a recent study published in 2020 is reported that 25, 50, 100 and 200 µg/mL TiO₂ inhibited A549 cell proliferation depending on time and concentration [155]. In subsequent studies, where only 48 hours of exposure were applied, DNA damage increased depending on the concentration. The mRNA levels of caspase-3 and caspase-9 genes increased significantly only in cells treated with high doses (100 and 200 µg/mL) of TiO₂ NPs [155]. These studies have shown the potential to cause a negative biological response in two cell lines related to the respiratory system.

However, there are also contradictory findings. In a study, the toxicity of TiO₂ NPs (Evonik P25) on A549 was investigated. TiO₂ NPs did not cause statistically significant cytotoxic effect even up to their highest tested concentration of 250 µg/mL as determined by WST-1 (cell metabolism) and LDH assay [154]. In another study THP-1 differentiated macrophages were exposed for 24 hours to TiO₂ (spherical/ellipsoidal 10 m²/g) at an average size of 190 nm at 1, 10, 25, 50 and 100 µg/mL concentrations. Even at the highest concentrations, TiO₂ NPs showed no significant reduction in THP-1 cell viability as determined by MTS method. TEM analyzes confirmed the cell internalization of NPs. Regarding the cytokine production, no changes were observed in the IL-1b, IL-8 and TNF-α production compared to the control group for all tested concentrations. In addition, intracellular ROS formation was not detected [156]. Differentiated THP-1 cells were exposed to 30-40 nm TiO₂ at 0.1, 1, 10, 30 and 100 µg/mL concentrations for 24 h. MTT assay showed that TiO₂ NPs exposure did not change THP-1 viability compared to the control group. Moreover, no IL-1b and TNF-α cytokine expressions were detected [157].

Overall, like in *in vivo* studies, it is hard to draw a conclusion on TiO₂ nanoparticle *in vitro* toxicity due to the number of varieties in studies such as cell type, nanoparticle exposure time, concentration, NP preparation conditions (handling, sonication, suspension preparation) and variable NPs physicochemical properties.

5. Conclusion and Objectives of the Work

Due to the widespread use of TiO₂ nanoparticles in the industry, concerns about their potential harmful effects on human health have increased. After exposure to TiO₂ nanoparticles, they reach the target organs through inhalation or other routes described, where they can exert their toxic effects. TiO₂ nanoparticle cytotoxicity can be summarized as follows;

- As a semi-conductor material, TiO₂ nanoparticles can induce ROS production following the induction of electron–hole pairs under light.
- Cell membrane damage and cell membrane lipid peroxidation might occur due to the cell-nanoparticle interaction.
- Nanoparticles can interact with cellular organelles and disrupt their functions.
- TiO₂ nanoparticles depending on their properties can lead to ROS production and induce up-regulation of stress related genes, as well as inflammation related genes [158].

Their biological effects are related to some basic physicochemical properties, namely particle size, charge, crystallinity, shape and agglomeration state. However, understanding the effect of these properties on TiO₂ NPs toxicity is rather limited and although there is growing scientific evidence about TiO₂ NPs toxicological properties, controversial data are still reported.

In the light of the information described in this bibliography part, the aim of this thesis was to evaluate the toxic effects of five types of TiO₂ NPs with different and well-controlled physicochemical properties on three *in vitro* human lung cell systems: A549 cell line, macrophages differentiated from THP-1 cells and coculture of A549 and macrophages. In addition to commercial P25 NPs, used as a reference, four types of TiO₂ NPs samples differing in size, shape, agglomeration state and surface functionalization/charge were synthesized at MINES Paris Tech. All samples were characterized before toxicity experiments regarding their size, hydrodynamic size, surface charge, shape, crystallinity, and they were tested regarding possible endotoxin contamination.

The characterization and validation of accurate cell differentiation are initial steps to ensure the reliable and reproducible results before conducting *in vitro* toxicity experiments. Therefore, THP-1 cell differentiation into the macrophages were studied extensively and the optimal conditions necessary for THP-1 differentiation into the

macrophages were determined. The THP-1 cell differentiation processes are reported in **Chapter 1**.

Once cell lines were well established and ready to toxicological experiments, the cell membrane integrity, cell viability, pro-inflammatory response and cellular oxidative responses were assessed after exposure to TiO₂ nanoparticles and reported in **Chapter 2** and in the associated article entitled “**Impact of the physicochemical features of TiO₂ nanoparticles on their *in vitro* toxicity**”.

As TiO₂ is photo-activated with either UV light, visible light or combination of both, TiO₂ nanoparticles in the environment are expected to become photoactive in the UV spectrum. After the toxicity results we obtained in Chapter 2, we evaluated if a short time exposure of TiO₂ NPs to UV light induced changes in their physicochemical properties and eventually affected the toxicity they induced on a human lung coculture system. These results are reported in **Chapter 3** and in the associated paper entitled “**Short pre-irradiation of TiO₂ nanoparticles increases cytotoxicity on human lung coculture system**”.

Then, the protein corona formation, which is another factor affecting toxicity, was compared in the five TiO₂ NP types in different cell culture media. This is the topic of **Chapter 4** and the article entitled “**Influence of the physicochemical features of TiO₂ nanoparticles on the formation of a protein corona and impact on cytotoxicity**”.

Finally, in **Chapter 5** some exploratory studies are reported on TiO₂ NPs interactions with LDH and MTT assay components in cell free conditions.

The findings obtained through this thesis provide a wide perspective in toxicity potentials depending on the physicochemical properties of TiO₂ nanoparticles by the systematic evaluation of their adverse effects on human lung cell lines. In addition, it provides a comparative evaluation of pristine TiO₂ nanoparticles and their UV-irradiated counterparts. The thesis results indicate health concerns that might be due to inhalation of different properties of pristine TiO₂ nanoparticles and photo-activated TiO₂, and it improves our understanding of the hazards and risks that TiO₂ NPs could pose to public health. It can serve as a basis for a safer by design approach to mitigate the toxicity of this material and for preventive actions to limit human exposure.

EXPERIMENTAL PART

Chapter 1

Development and Validation of the *In vitro* Biological Models

Considering that the lungs are the target organs in the exposure to inhaled NPs and inhalation is the main route of the entrance of NPs in the body, in this study, the toxicity of TiO₂ NPs was evaluated on *in vitro* human lung cell lines: widely used adenocarcinomic human alveolar basal epithelial cells (A549 cell line), differentiated THP-1 macrophages from THP-1 monocytes and coculture of both cell lines.

Since primary tissue macrophages cannot be easily expanded *ex vivo* and are difficult to grow *in vitro*, THP-1 monocyte cell lines are widely used in obtaining macrophages. Due to their metabolic and morphological similarities, human monocytic THP-1 cell line can be differentiated into macrophages by Phorbol-12-myristate-13-acetate (PMA) or 1,25-dihydroxyvitamin D₃ (VD₃). However, their differentiation state may not always accurately predict the behavior of differentiated tissue macrophages depending on the experimental conditions. Thus it may lead to misinterpretation of biological responses in toxicity tests. Therefore the characterization and validation of accurate cell differentiation are important and initial steps to ensure reliable and reproducible results, before conducting toxicity experiments.

Once large, round single-cell morphology and suspension THP-1 cells differentiate into macrophages, they result in a more mature phenotype with a lower rate of proliferation, higher levels of adhesion, enhanced granularity, increased expression of specific surface markers associated with macrophage differentiation such as cluster of differentiation molecule 11b (CD11b) and CD14. Therefore, the THP-1 differentiation can be verified by the simple checking of cell adhesion, morphology, and by examining the expression of macrophage specific surface markers.

Since THP-1 macrophages are used as target cells in TiO₂ NP toxicity in this thesis, this chapter presents the general features of THP-1 cells and the various protocols used for optimization and validation of their differentiation into macrophages, and the results of these protocols. At the end of the studies carried out in this chapter, the most suitable conditions for THP-1 differentiation were determined. The findings in this section are the fundamental results of the optimal cell differentiation conditions required to perform toxicity studies.

Chapitre 1

Développement et validation des modèles biologiques *in vitro*

Considérant que les poumons sont les organes cibles de l'exposition aux NP inhalées et que l'inhalation est la principale voie d'entrée des NP dans le corps, dans cette étude, la toxicité des NPs de TiO_2 a été évaluée *in vitro* sur des lignées cellulaires pulmonaires humaines: cellules épithéliales basales alvéolaires issues d'un adénocarcinome humain (lignée A549, largement décrite et utilisée dans la littérature), des macrophages THP-1 différenciés à partir des monocytes de la lignée THP-1 et une coculture de ces deux lignées cellulaires.

Étant donné que les macrophages tissulaires primaires ne peuvent pas être facilement multipliés *ex vivo* et sont difficiles à cultiver *in vitro*, les lignées cellulaires de monocytes THP-1 sont largement utilisées pour obtenir des macrophages. En raison de leurs similitudes métaboliques et morphologiques, la lignée cellulaire monocyttaire humaine THP-1 peut être différenciée en macrophages par le Phorbol-12-myristate-13-acétate (PMA) ou la 1,25-dihydroxyvitamine D₃ (VD₃). Cependant, leur état de différenciation peut ne pas toujours prédire avec précision le comportement des macrophages tissulaires différenciés en fonction des conditions expérimentales. Ainsi, cela peut conduire à une mauvaise interprétation des réponses biologiques dans les tests de toxicité. Par conséquent, la caractérisation et la validation d'une différenciation cellulaire précise sont des étapes importantes et initiales pour garantir des résultats fiables et reproductibles, avant de mener des expériences de toxicité.

Une fois que les cellules THP-1 en suspension sont différenciées en macrophages, elles donnent un phénotype plus mature avec un taux de prolifération plus faible, des niveaux d'adhérence plus élevés, une granularité accrue, une expression de marqueurs de surface spécifiques des macrophages accrue tels que le groupe de molécule de différenciation 11b (CD11b) et CD14. Par conséquent, la différenciation THP-1 peut être vérifiée par la simple vérification de l'adhérence cellulaire, de la

morphologie et en examinant l'expression des marqueurs de surface spécifiques des macrophages.

Étant donné que les macrophages THP-1 sont utilisés comme cellules cibles dans la toxicité des NP de TiO₂ dans cette thèse, ce chapitre présente les caractéristiques générales des cellules THP-1 et les différents protocoles utilisés pour l'optimisation et la validation de leur différenciation en macrophages, et les résultats de ces protocoles. A l'issue des études réalisées dans ce chapitre, les conditions les plus adaptées à la différenciation THP-1 ont été déterminées. Les résultats de cette section sont les résultats fondamentaux des conditions optimales de différenciation cellulaire requises pour effectuer des études de toxicité.

1. The THP-1 Cell Line and the Identification of Macrophage Differentiation in PMA-stimulated THP-1 Cells

The THP-1 cell line which is a human monocytic leukaemia cell line was initiated in 1980 by Tsuchiya *et al.* [159] from the blood of a patient with acute monocytic leukaemia. THP-1 cells were cultured in Roswell Park Memorial Institute Medium (RPMI-1640, Gibco, Life Technologies, France) containing 10% FBS and 1% penicillin-streptomycin.

Optimal conditions required for accurate THP-1 differentiation into macrophages were investigated by applying different protocols as summarized in Table 4. First of all, PMA was chosen as differentiation agent. Stock solution of PMA (1 mg/mL) was prepared in dimethyl sulfoxide (DMSO). Fresh dilutions of PMA were prepared in culture medium at 5, 30, 50, 100, 150, and 200 ng/mL to determine the minimum PMA concentration required for the macrophage differentiation. These concentrations of PMA were applied to different density of cells at different exposure times. Afterwards, cell adhesion, morphology, and expression of macrophage surface marker CD11b were evaluated by various protocols (Table 4).

Table 4. Protocols for determining optimal conditions for THP-1 differentiation

^aAfter removing the PMA-containing medium then incubating the cells in fresh culture medium, ICC Immunocytochemistry

	Protocol	Cell density	PMA concentration	PMA exposure time	Method	Parameter	Ref.
determination	Protocol 1	5 x 10 ⁶ cells per T25 cm ² Flask	50, 100, 150, 200 ng/mL PMA	72 hours PMA exposure + 5 days resting*	Flow Cytometry	Cell Adhesion Cell Morphology	[160, 161]
Exposure time	Protocol 2	5 x 10 ⁶ cells per T25 Flask 7,5 x 10 ⁶ cells per T25 Flask 10 x 10 ⁶ cells per T25 Flask	5, 30, 50, 100 ng/mL PMA	24 and 48 hours	Trypan Blue assay	Cell adhesion Cell Morphology	[162]

Table 4. Continue Protocols for determining optimal conditions for THP-1 differentiation

^aAfter removing the PMA-containing medium then incubating the cells in fresh culture medium, ICC Immunocytochemistry

	Protocol	Cell density	PMA concentration	PMA exposure time	Method	Parameter	Ref.
Cell density determination	Protocol 3	6.5 x 10 ⁴ cells, 10 x 10 ⁴ cells, 13 x 10 ⁴ cells per well (96 well plate)	30, 50, 100 ng/mL PMA	24 hours	MTT assay	Metabolic Activity	-
Concentration determination	Protocol 4	2 x 10 ⁵ cells per 8 Well Chamber Slide	30, 50, 100 ng/mL PMA	24 hours	ICC	CD11b expression	[144, 153, 163]

1.1. Optimal PMA exposure time and cell density determination after exposure to various PMA concentrations

1.1.1. Protocol 1 (72 hours PMA exposure + 5 days resting)

5 x 10⁶ THP-1 cells were treated with 0, 50, 100, 150, 200 ng/mL PMA for 72 hours. At the end of incubation PMA containing-medium was discarded and cells rested in PMA-free culture medium for 5 days. Medium being refreshed every 2 days for a period of 5 days resting. Cell adhesion was evaluated by optical microscopy (Leica ICC50 HD, Leica Microsystems) at the end of a total 8 days.

Adherent cells were detached from culture flask enzymatically and the morphological changes in terms of cell granularity were determined by an increase in side scatter (SSC) on flow cytometry which allows the discrimination between differentiated THP-1 and THP-1 monocytes. The cell size (FSC) and granularity (SSC) of cells and viability were analyzed by flow cytometry using a BD FACSCalibur instrument (Becton Dickinson Biosciences, Le Pont-de-Claix, France) equipped with an air-cooled argon laser (488-nm emission; 20 mW).

The cell adhesion, the first indicator of macrophage differentiation, was detected by microscope observation in all of the applied PMA concentrations.

However, decreases in cell viability were observed when the cells were enzymatically separated from the culture flask and collected for flow cytometry analysis, as reported in Table 5. Due to this low cell viability, it was not possible to get a fully efficient result from flow cytometry regarding increasing cell size and granularity. The cells were then collected by scrabing rather than enzymatic separation. However, similar results were obtained although the experiments were repeated at least twice.

Table 5. Percentage values of differentiated THP-1 cell viability monitored by flow cytometry after treatment with PMA (50, 100, 150 and 200 ng/mL PMA) for 72 h + 5 days resting (without PMA).

	50 ng/mL PMA	100 ng/mL PMA	150 ng/mL PMA	200 ng/mL PMA
Cell Viability	59.6%	60.4%	60.1%	75.1%

Afterwards, it has been investigated whether this low cell viability was due to the DMSO in which PMA stock solution was prepared. Therefore, DMSO content of 50, 100, 150, 200 ng/mL PMA concentrations in culture media were calculated as 0.0005%, 0.005%, 0.01%, 0.015% and 0.02%, respectively. These concentrations of DMSO were prepared in culture medium and applied to the cells for 72 hours. Cell viability was determined by the trypan blue method as shown in Figure 12.

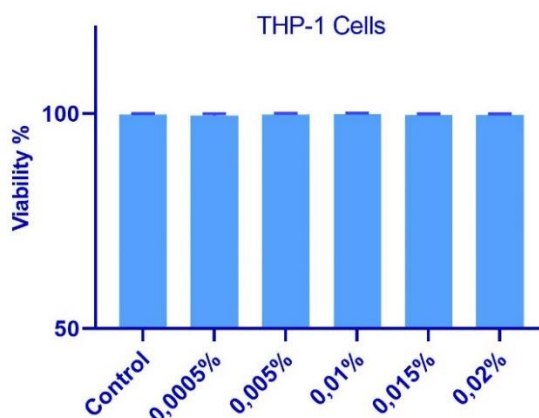


Figure 12. 72 h DMSO treated THP-1 cell viability. DMSO solutions were prepared in culture media (RPMI) in indicated concentrations.

As the DMSO in the applied concentrations did not cause a decrease in cell viability, it was concluded that the low cell viability obtained from flow cytometry results was not due to the DMSO content in PMA working solutions.

Although there are studies that show successful results with flow cytometry analysis, some researchers [164] reported an excessive cell death occurring upon scraping the differentiated THP-1 cells, like our observations. They also indicated that during the activation process PMA induced strong responses in THP-1 cells, resulting in severe clumping of the THP-1 cells [164].

In consequence of the results described above, it was determined that investigation of size and granularity of cells by flow cytometry was not an ideal method because it requires the cell collection enzymatically or by scrubbing technique. It was also suspected that 72 hours of PMA exposure with 5 days of resting phase was not appropriate in our study although this length of exposure to PMA is commonly used in the literature [160,161,165,166]. However, there is currently no standard protocol for differentiating THP-1 monocytes into macrophages using PMA. For this reason, to find the best conditions in our study further experiments were carried out by applying 24 and 48 hours PMA exposure without resting phase.

1.1.2. Protocol 2 and 3

5×10^6 , 7.5×10^6 , 10×10^6 cells were treated with 0, 5, 30, 50, 100 ng/mL PMA for 24 and 48 h in T25 cm² flask.

Cell morphology and adhesion were observed using optical microscopy and pictures were captured at 20 x magnification. The microscopic images of THP-1 after treatment with PMA are shown in Figure 13.

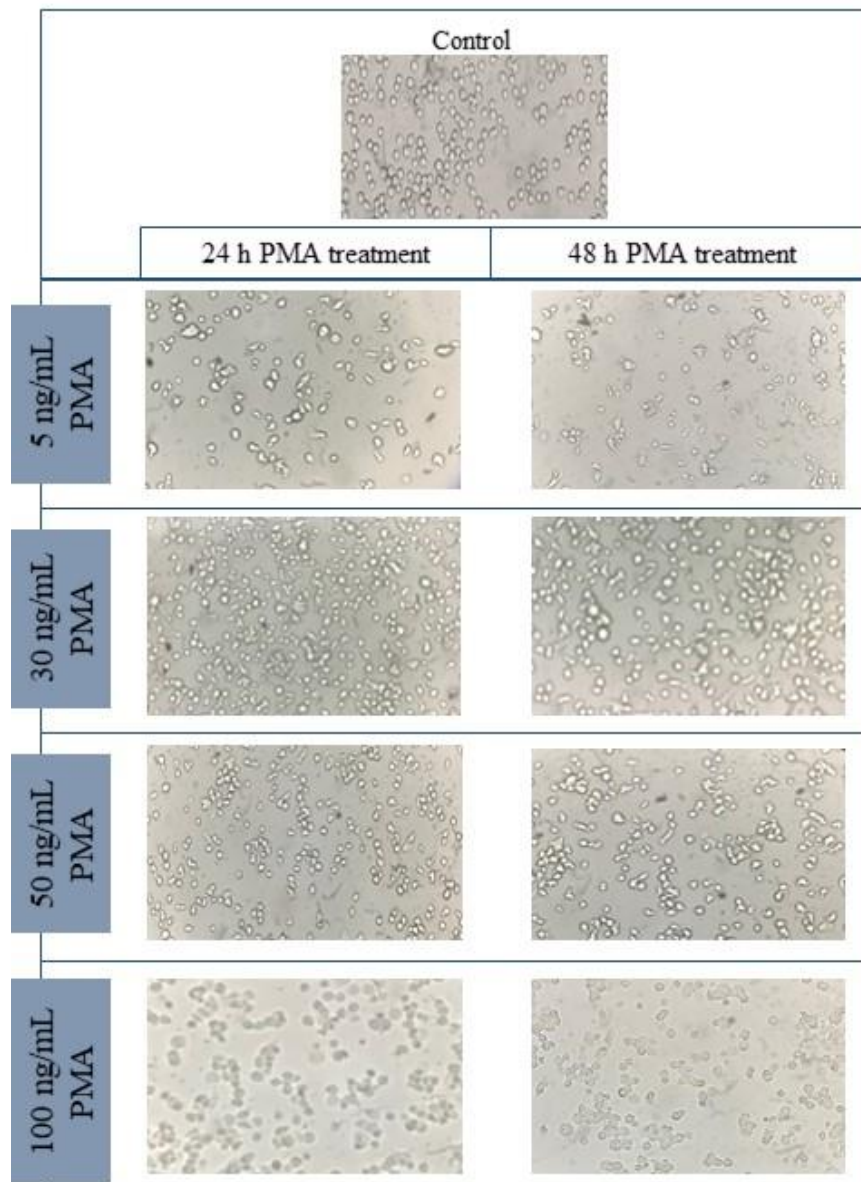


Figure 13. Microscopic images of THP-1 cells (7.5×10^6 cells/ T25 cm² flask) exposed to 5; 30; 50; 100 ng/mL PMA for 24 h and 48 h. Control represents THP-1 cells without PMA treatment (20 x magnification).

It is observed that the adhesion rate of THP-1 cells varies depending on the PMA concentration and exposure time (Figure 13). 48 hours incubation of 5 ng/ml PMA showed less cell adhesion compared to other concentrations and incubation time. Thus, the percentage of cell adhesion was determined by counting unattached THP-1 cells and subtracting them from the initial/total cell amount. Results were expressed as percentage of cell adhesion in Figure 14.

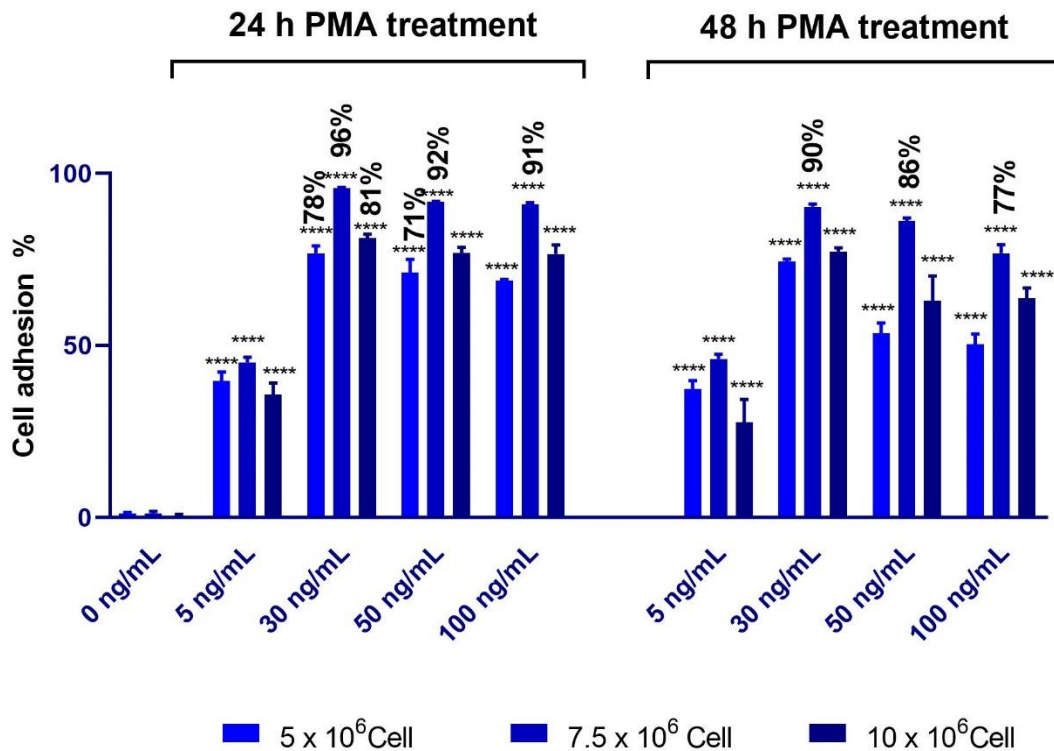


Figure 14. THP-1 cell adhesion after treatment with the indicated PMA concentrations for 24 h and 48 h. Independent experiments were conducted three times in triplicate. Statistically different from control (****) $P < 0.0001$. Statistical analyses were conducted using one-way Anova analyses, followed by Dunnett's test.

As shown in Figure 13, 24 hours PMA treatment showed slightly more cell adherence than 48 hours treatment for all tested PMA concentrations. Cell attachment was found unstable at 5 ng/mL PMA concentration for both treatment time showing that 5 ng/mL PMA was not enough to differentiate the THP-1 cells as confirmed by the microscope images (Figure 13). Similar to our results, Park *et al.* [162] showed the increased cell adhesion at 48 h after 10-100 ng/mL PMA treatment (10^6 cells/60 mm dish qsp. 1.2×10^6 cells/25cm² flask). 30 ng/mL PMA for 24 hours treatment to 7.5×10^6 cells showed the highest THP-1 cell adhesion (96%). When these results and microscope images were evaluated together, PMA incubation time was selected as 24 hours.

The appropriate cell density was then determined by measuring the cell metabolic activity after PMA treatment by MTT method.

Corresponding to the cell density used in T25 cm² flask in 96-well plate 6.5×10^4 cells, 9×10^4 cells, and 13×10^4 cells were seeded and treated with 0, 30, 50 and 100 ng/mL of PMA for only 24 hours. After, cell surface was washed with DPBS and 200 μ L MTT solution (5 mg/mL in DMEM) were added in each well. Plates were incubated for 3 hours. After, MTT was removed and 200 μ L DMSO were added in each well. Plates were placed on orbital shaker for 20 min. Optical density was read on a microplate reader at 570 nm (Multiskan RC; Thermolabsystems, Helsinki, Finland). An increase in number of living cells results in an increase in the total metabolic activity. This increase directly correlates to the amount of purple formazan crystals formed, as monitored by the absorbance. The condition that gives an absorbance between 0.8-1.0 was preferred. With the evaluation of all results obtained from these protocols, optimal incubation time and cell density were determined.

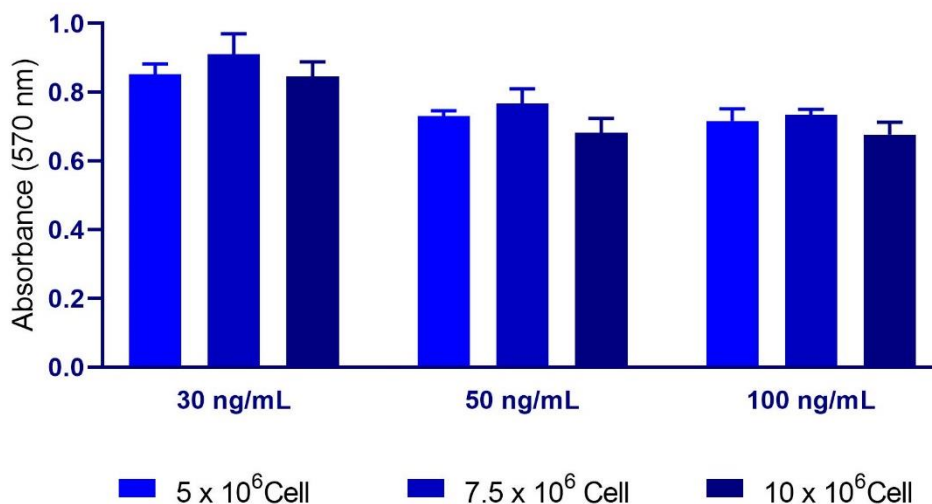


Figure 15. Absorbance values of 30, 50, 100 ng/mL PMA treated cells at the indicated cell densities as determined by MTT assay.

The absorbance range for all cell densities were found between 0.68-0.90 O.D. units. 7.5×10^6 cells showed higher absorbance of all tested concentrations. Among the tested concentrations 30 ng/mL showed higher absorbance thus high metabolic activity at 7.5×10^6 cell density.

When all the results above were evaluated, it was decided to apply a **24-hour PMA exposure** to **7.5×10^6 cells** in T25 cm² flask (corresponding to **10^5 cells** per well in **96-well plate**).

1.2. Optimal PMA concentration determination by immunocytochemistry staining (Protocol 4)

CD11b expression was determined by the ICC method, since cells do not need to be separated from the culture flask surface in this method.

2×10^5 cells/well were differentiated in 8 Well Chamber Slide (corresponding to 1×10^5 cells per well in 96-well plate) for 24 hours with 0, 30, 50, 100 ng/mL PMA. After, cells were fixed in 4% paraformaldehyde for 10 min. At the end of fixation, cells were permeabilized in 0.2% Triton X-100 for 10 min and incubated with 2% BSA for 30 min. Cells were incubated for 60 min with a primary antibody directed against human CD11b coupled to FITC (fluorescein isothiocyanate) (2% BSA-FPS). After the cells were washed with PBS and stained with DAPI dye. Cells were examined under the fluorescence microscope IX81 (Olympus, Tokyo, Japan) equipped with the Cell[^]P imaging software (Soft Imaging System GmbH, Munster, Germany).

ICC analysis of CD11b expression in THP-1 treated with 0, 30, 50, 100 ng/mL PMA for 24 h is shown in Figure 16.

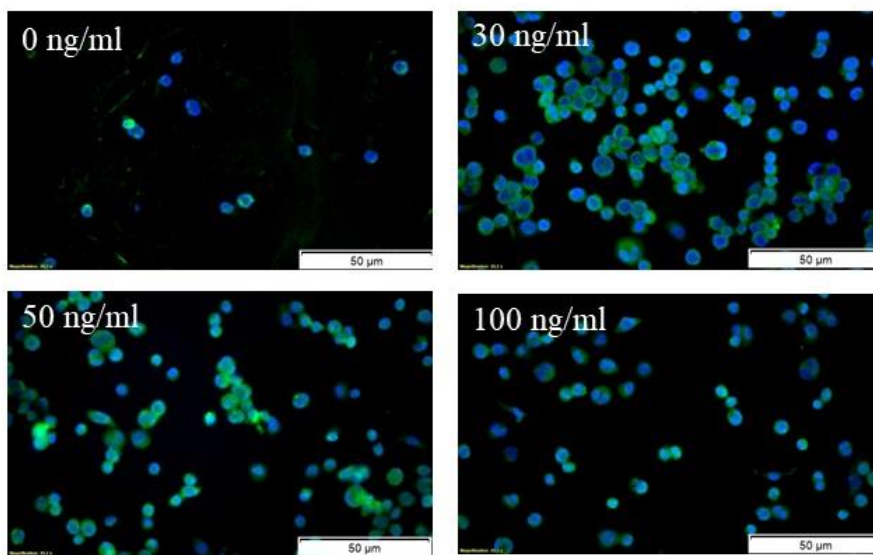


Figure 16. Immunocytochemistry staining of CD11b (marker of macrophage activation) in THP-1-derived macrophages. The detection of protein expression was performed by fluorescence microscopy (magnification 25 X).

As observed by ICC analysis, the stimulation with PMA induced cell adhesion and the expression of CD11b (macrophage marker) in differentiated THP-1 was detected. This is in good agreement with other studies [167,168] which showed the increased CD11b

surface levels by flow cytometry and ICC. Starr *et al.* [167] detected the increased levels of CD11b in 2 and 3 days 20 ng/mL of PMA treated cells. Among tested concentrations, 30 and 50 ng/mL PMA showed more pronounced CD11b expression, supporting their differentiation into macrophages.

When all the results were evaluated, and as the studies recommending that PMA and THP-1 differentiation should be optimized to reduce the possibility of masking the effect caused by excessive PMA use [161,162], **30 ng/mL** was chosen as the optimal concentration, since 30 ng/mL PMA treated cells showed higher cell adhesion and metabolic activity than 50 ng/mL PMA treated cells.

2. Conclusion

We determined the optimal conditions for THP-1 cell differentiation into macrophages: **10⁵ cells** (per well in 96-well plate) exposed to **30 ng/mL PMA** for **24 hours**.

We validated the differentiation of THP-1 cells into macrophages by the determination of the expression of CD11b, one of the main surface marker of macrophages.

Nous avons déterminé les conditions optimales pour la différenciation des cellules THP-1 en macrophages: **10⁵ cellules** (par puits, en plaque 96 puits) exposées à **30 ng/mL** de PMA pendant **24 heures**.

Nous avons validé la différenciation des cellules THP-1 en macrophages par la détermination de l'expression de CD11b, l'un des principaux marqueurs de surface des macrophages.

Chapter 2

Impact of the Physicochemical Features of TiO₂ Nanoparticles on their *In vitro* Toxicity

Once our biological models were validated, we were able to accurately assess the toxicity of TiO₂ NPs with 5 different physicochemical properties. This was the topic of the following paper published in Chemical Research in Toxicology.

Chapitre 2

Impact des Caractéristiques Physicochimiques des Nanoparticules de TiO₂ sur leur Toxicité *In vitro*

Une fois nos modèles biologiques validés, nous avons pu évaluer avec précision la toxicité des NPs de TiO₂ avec 5 propriétés physicochimiques différentes. Cette étude a fait l'objet de l'article suivant publié dans *Chemical Research in Toxicology*.

Impact of the Physicochemical Features of TiO₂ Nanoparticles on Their *In Vitro* Toxicity

Ozge Kose, Maura Tomatis, Lara Leclerc, Naila-Besma Belblidia, Jean-François Hochepped, Francesco Turci, Jérémie Pourchez, and Valérie Forest*



Cite This: *Chem. Res. Toxicol.* 2020, 33, 2324–2337



Read Online

ACCESS |



Metrics & More



Article Recommendations



Supporting Information



ABSTRACT: The concern about titanium dioxide nanoparticles (TiO₂-NPs) toxicity and their possible harmful effects on human health has increased. Their biological impact is related to some key physicochemical properties, that is, particle size, charge, crystallinity, shape, and agglomeration state. However, the understanding of the influence of such features on TiO₂-NP toxicity remains quite limited. In this study, cytotoxicity, proinflammatory response, and oxidative stress caused by five types of TiO₂-NPs with different physicochemical properties were investigated on A549 cells used either as monoculture or in co-culture with macrophages differentiated from the human monocytic THP-1 cells. We tailored bulk and surface TiO₂ physicochemical properties and differentiated NPs for size/specific surface area, shape, agglomeration state, and surface functionalization/charge (aminopropyltriethoxysilane). An impact on the cytotoxicity and to a lesser extent on the proinflammatory responses depending on cell type was observed, namely, smaller, large-agglomerated TiO₂-NPs were shown to be less toxic than P25, whereas rod-shaped TiO₂-NPs were found to be more toxic. Besides, the positively charged particle was slightly more toxic than the negatively charged one. Contrarily, TiO₂-NPs, whatever their physicochemical properties, did not induce significant ROS production in both cell systems compared to nontreated control groups. These results may contribute to a better understanding of TiO₂-NPs toxicity in relation with their physicochemical features.

1. INTRODUCTION

Titanium dioxide (TiO₂) is an inorganic compound, which is widely used in a large range of industrial applications mainly due to its high refractive index or photocatalytic properties.^{1,2} World production of TiO₂ nanoparticles (TiO₂-NPs) in 2014 was estimated to exceed 9 million metric tons³ to be used in many consumer products such as paints (e.g., UV resistant and antibacterial self-cleaning paints), antiseptic-antimicrobial compositions, deodorization (purify/deodorize indoor air), inks, papers, plastics, UV-sunscreen, toothpastes, ceramics, and food products.^{3–5} This makes TiO₂-NPs one of the most abundantly produced nanomaterials (NMs) showing various forms of shape, crystalline phases, and nano size ranges. As it is the second most used NM in consumer products,⁶ the concern about TiO₂-NPs toxicity and their possible harmful effects on human health has increased.^{7–9}

The toxicity of NPs is greatly related to their interaction with biological systems. This interaction is associated with the physicochemical properties of the NPs.¹⁰ Generally, cellular uptake of NPs is determined by their size, surface area, shape, surface charge, chemical composition, crystallographic phases, and surface modifications.¹¹ The internalization of NPs through cell membrane might lead to potential hazards by interaction with intracellular biological macromolecules. It might cause an imbalance between cellular antioxidants and

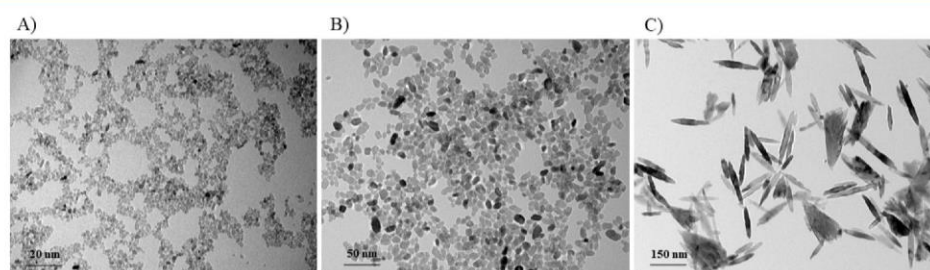
Received: March 21, 2020

Published: August 10, 2020



Table 1. TiO₂-NPs Used in This Study with Their Specific Characteristics

S1	S2	S3	S4	P25
custom-made for size/SSA	custom-made for agglomeration	custom-made for shape	custom-made for functionalization/charge	commercial/used as a reference

Figure 1. TEM images of TiO₂-NPs (A) S1, (B) S2, and (C) S3.Table 2. Particle Primary Size, SSA, Shape, Average Hydrodynamic Size, Polydispersity Index, and ζ Potential in Culture Media (in DMEM) and in Deionized Water (DI H₂O) after Dispersion of TiO₂-NPs (120 μ g/mL)^a

	primary size (nm)	SSA (m ² /g)	shape	DI H ₂ O			DMEM + 10% FBS		
				average hydrodynamic size ^b (nm)	PDI ^c	ζ potential (mV) pH 7.5	average hydrodynamic size ^b (nm)	PDI ^c	ζ potential (mV) pH 7.5
S1	15	146	spherical	211.4 \pm 2.3	0.145 \pm 0.01	-13.2 \pm 4.2	226 \pm 9.1	0.282 \pm 0.01	-33.8 \pm 1.8
S2	30	61	spherical	969.3 \pm 39.5	0.266 \pm 0.01	-13.8 \pm 4.4	1094 \pm 46.4	0.364 \pm 0.04	-32.6 \pm 1.7
S3	20 ^d -250 ^e	41	rod	1419 \pm 16.6	0.405 \pm 0.08	-15.8 \pm 4.0	1275 \pm 66.6	0.179 \pm 0.02	-33.7 \pm 3.5
S4	30	61	spherical	1049 \pm 146.3	0.823 \pm 0.13	12.3 \pm 0.5	1398 \pm 54.9	0.475 \pm 0.01	-36.4 \pm 3.5
P25	21	55	spherical	256.4 \pm 136.6	0.272 \pm 0.02	-15.2 \pm 5.3	325 \pm 4.1	0.260 \pm 0.01	-33.1 \pm 1.7

^aAll data are presented as mean of three independent characterizations \pm SD. ^bDLS measurements are the mean of at least 3 runs each containing 20 submeasurements. ^cPolydispersity index (PDI); SSA: specific surface area; and FBS: fetal bovine serum. ^dMinimum Feret diameter. ^eMaximum Feret diameter.

oxidants, in the favor of oxidants. As a result, the high accumulation of reactive oxygen species (ROS) causes the oxidative stress. Oxidative stress responses are crucial for further pathological effects including genotoxicity, inflammation, and fibrosis. Previous studies have shown that relatively large surface areas/particle size have a critical role in increased incidence of lung injury and pulmonary inflammation.^{12,13} Specifically, aerodynamic diameter of inhaled particles strongly influences particles deposition to occur in different regions of the human respiratory tract¹⁴ and can cause different biological effects depending on the anatomic target of the human respiratory tract (alveolar or tracheobronchial area) where they accumulate.¹⁵ Studies have also reported that the NP shape could affect toxicity during endocytosis or phagocytosis, for example, the endocytosis of spherical NPs is a more favorable process than that of rod-shaped NPs.^{16,17} Nonetheless, spherical NPs are usually less toxic than rod-shaped NPs.¹⁸⁻²⁰

Although there is growing scientific evidence about TiO₂-NPs toxicological and even pathological properties,²¹ the question of how the physicochemical features of TiO₂-NPs impact their *in vitro* toxicity has not yet been fully addressed, especially to foster a safer-by-design approach to NP production. Indeed, a safer-by-design approach aims at developing functional as well as safe NMs from their conception, while current NMs are regarded as intrinsically unsafe. The main objective of this approach is to know what property makes a NM or nanoparticle more or less safe.²² Subsequent steps involve the application of this knowledge to industrial innovation processes, and as a result, NPs that are

safer to human and environment are produced. The key factor in this regard is the comprehensive study of the toxicological effects of the physicochemical properties of NPs.²³

As TiO₂-NPs could be hazardous, for NP safety and for defining an adequate risk assessment, in particular to protect exposed workers and general population subjects, it is necessary to study how the physical and chemical properties of TiO₂-NPs determine their biological effects.^{24,25}

As one of the main exposure routes to these NPs is inhalation, in this study we aimed to determine the impact of physicochemical properties of TiO₂-NPs on their *in vitro* toxicity on human lung cell lines. The A549 carcinoma epithelial cell line was used as a monoculture system. A co-culture system consisting of A549 and macrophages (differentiated from the human monocytic THP-1 cell line) was also used as an extended approach to reflect the interactions between different cell types in the lung after exposure to NPs. To that purpose, we thoroughly characterized five types of TiO₂-NPs with different and well-controlled physicochemical properties: a commercially available P25 sample and four custom-made TiO₂ samples. After exposure, the cell response was assessed in terms of cell viability, proinflammatory response, and oxidative stress status.

2. MATERIAL AND METHODS

2.1. Physicochemical Characterization of TiO₂ Nanoparticles. In this study, we used five types of TiO₂-NPs with different and well-controlled physicochemical properties. In addition to P25 NPs (Evonik P25 CAS: 1317-70-0, Sigma-Aldrich, Saint-Quentin-

Fallavier, France), used as a reference, four types of TiO₂-NPs samples differing in size, shape, agglomeration state, and surface functionalization/charge were synthesized and were named S1–S4 as shown in Table 1.

TiO₂-NPs were synthesized using Chen *et al.*²⁶ method. Basically, titanium(IV) butoxide (CAS: 5593-70-4 reagent grade 97%, Sigma-Aldrich, Saint-Quentin-Fallavier, France) was mixed with triethanolamine (CAS: 102-71-6, analytical reagent 97%, VWR International, Fontenay-sous-Bois, France) in 1:2 molar ratio. The mixture was put in a Teflon-lined sealed autoclave and then heated at 150 °C during 24 h. The pH values of the synthesis medium were adjusted using HCl or NH₄OH to tune particle size and morphology. Finally, the solutions were washed by three centrifugations using deionized water, and the resulting products were dried in an oven at 40 °C. Surface functionalization of S2 NPs was generated by aminopropyltriethoxysilane (APTES) using Zhao *et al.*²⁷ method. Briefly, 0.25 g of S2 nanopowder was dispersed in 25 mL of deionized water by ultrasonication for 10 min. Then, the silane coupling agents APTES were added in the dispersion (molar ratio of 1:1). The mixture was sonicated until a clear solution was obtained and then refluxed at 80 °C for 4h. After that, dispersed particles were separated from solvent by centrifugation (10 min at 1200 g) followed by washing with water at least 2 times. The final functionalized samples were then prepared in deionized water and labeled as S4. The features of NPs are reported in Figure 1 and Table 2.

Stock suspensions of all NPs (1600 µg/mL) were prepared in deionized water (Milli-Q systems, Millipore, Bedford, MA, USA) and sonicated with Branson Sonifier S-450 for 10 min at 89% amplitude. Before each physicochemical measurement and toxicity experiment, stock suspensions were sonicated for 15 min in a bath sonicator and vortexed vigorously, and fresh dilutions were prepared in low light conditions (*i.e.*, 1 µW/cm² irradiation intensity) by using Dulbecco's modified Eagle medium (DMEM) to achieve the following final concentrations: 15, 30, 60, and 120 µg/mL. The pH of solutions was measured using a Metrohm digital pH meter of model 827.

The morphology and size distribution of NPs were analyzed by transmission electron microscopy (TEM) using a FEI TECNAI 20FST operating at 200 kV and scanning electron microscopy (SEM) at 2–3 kV on a Zeiss Sigma 300 microscope using a secondary electron (SE) detector. After each TEM image of each sample were chosen, the size distribution and the mean diameter were measured by ImageJ software. The hydrodynamic size and the agglomeration status of TiO₂-NPs (120 µg/mL) in deionized water and in DMEM were determined by using dynamic light scattering (DLS, Zetasizer Nano ZS Malvern Instruments, Worcestershire, UK) measurements. Surface charge of the NPs was monitored using electrophoretic light scattering (ELS, Zetasizer Nano ZS Malvern Instruments, Worcestershire, UK). Specific surface areas (SSA) were measured by linearizing the physisorption isotherm of N₂ at 77 K with the classical method of Brunauer, Emmett, and Teller (BET) (Volumetric Adsorption ASAP 2020, Micrometrics, USA).²⁸

Raman spectroscopy (Horiba Jobin–Yvon Xplora spectrometer) and X-ray diffraction (XRD, Miniflex, Rigaku, Japan) techniques were used for the structural identification of the crystalline phases of NPs. Raman spectra were recorded on a system equipped with a confocal microscope and a nitrogen-cooled CCD detector. The high-resolution XRD patterns were measured in the continuous scan mode using a step width of 0.05° (2θ). The scan range was 20–80°. Further parameters of the diffractometer were: Ni filtered K-β radiation; voltage 40 kV; tube current 15 mA; scan speed 4° min⁻¹.

The spin trapping technique (5-5'-dimethyl-1-pyrroline-N-oxide, DMPO, as trapping agent) associated to the electron spin resonance (ESR) spectroscopy (Miniscope 100 ESR spectrometer, Magnetech, Germany) was used to assess whether TiO₂-NPs have the potential to generate free radicals (hydroxyl and carboxyl radical) under the same laboratory light conditions used for administration to cells. TiO₂ samples (120 µg/mL) were suspended in a buffered solution (potassium phosphate buffer 0.25 M, pH 7.4) containing 0.04 M DMPO or 0.04 M DMPO and 1 M sodium formate to detect hydroxyl and carboxyl radicals, respectively. The reaction mixtures

were prepared under laboratory light conditions and then kept in the dark at 37 °C. ESR spectra were recorded on aliquots (50 µL) withdrawn after 5, 10, 20, and 30 min of incubation. The instrument settings were as follows: microwave power 10 mW; modulation 1000 mG; scan range 120 G; center of field 3345 G. Blanks were performed with the same reaction mixtures without TiO₂. A suspension of P25, irradiated with a UV lamp for 30 min (100 W, 365 nm UV light, Cole-Parmer, Paris, France), was used as positive control. The irradiation intensity was 1 mW/cm² as measured by a radiometer (Model PCE-UV34, PCE Instruments UK Ltd., Southampton, UK). All experiments were repeated at least twice.

The presence of Al, Sb, Hg, Pb, Fe, Zn, As, and Cd impurities in TiO₂ samples was determined by Agilent 7800 inductively coupled plasma mass spectrometry (ICP-MS) as recommended by national and international standards (European Commission Directive 95/45/EC, Food and Drug Administration (FDA) Regulation 21-CFR, European Pharmacopoeia, Pharmacopoeia of the USA, *etc.*) that have set limiting values for the contents of these eight element impurities in TiO₂ samples.²⁹

2.2. Limulus Amebocyte Lysate Assay: Endotoxin Contamination Assessment. The amount of endotoxin present in the NP solutions was determined by the chromogenic method with a ToxinSensor Chromogenic Limulus Amebocyte Lysate (LAL) Endotoxin Assay kit (Genscript, Piscataway, Associates of Cape Cod Inc., Falmouth, MA, USA) according to the manufacturer's instructions. All samples were prepared in endotoxin-free vials. The optical density was read at 545 nm. The amount of endotoxin in samples was calculated by comparison with a standard curve of endotoxin. Endotoxin concentrations were expressed as endotoxin units per milligram (EU/mg) of NPs.

2.3. Cell Culture. The A549 human carcinoma epithelial cell line was supplied by the American Type Culture Collection (ATCC, CCL-185). The THP-1 human monocytic leukemia monocyte cell line (ATCC, TIB-202) was a generous gift from Dr Ghislaine Lacroix from French National Institute for Industrial Environment and Risks (INERIS). A549 cells were used either as a monoculture or co-culture with macrophages differentiated from THP-1 cells (10 A549:1 differentiated-THP-1 ratio).

A549 cells were grown in DMEM supplemented with 10% (v/v) fetal bovine serum (FBS, S1810; Biowest, Nuaillé, France) and 1% penicillin-streptomycin (VWR International, Fontenay-sous-Bois, France). A549 cells were grown in flasks, and after reaching 80% confluency, cells were trypsinized, washed with sterile phosphate-buffered saline (PBS), and centrifuged at 1500 g for 10 min and subcultured. The flasks were stored at 37 °C in a humidified atmosphere with 5% CO₂.

THP-1 was cultured in Roswell Park Memorial Institute (RPMI) 1640 (Gibco, Life Technologies, Cergy-Pontoise, France) containing 10% FBS and 1% penicillin-streptomycin. THP-1 cells were counted with Trypan blue regularly and subcultured usually twice a week. Subcultures were started with a cell concentration of 2 × 10⁵ to 4 × 10⁵ viable cells/mL, and cells were maintained at a concentration between 10⁵ and 10⁶ cells/mL in suspension. THP-1 cells were maintained in a humidified atmosphere containing 5% CO₂ at 37 °C.

For the co-culture, THP-1 cells were differentiated into mature macrophage-like cells in 96-well plate with 30 ng/mL of phorbol myristate acetate (PMA) (P1585, Sigma-Aldrich, Saint-Quentin-Fallavier, France) in RPMI for 24 h. After the incubation, cell surface was rinsed two times with DPBS. Then A549 cells were added on top of the differentiated THP-1, and the system was further cultivated for 24 h at a ratio of one differentiated THP-1 cell to 10 A549 cells with direct cell-to-cell contact in DMEM supplemented with 10% (v/v) FBS and 1% penicillin-streptomycin.

2.4. Cell Morphology. A549 cells and co-culture cells were seeded on 96 well plates (1 × 10⁵ cells/well in 50 µL of medium) and were allowed to adhere for 24 h. After 24 h exposure to the highest dose (120 µg/mL) of TiO₂ samples, supernatant was discarded, and cell surfaces were washed with PBS. After, cells were observed using optical microscopy (Leica ICC50 HD, Leica Microsystems, Nanterre, France) at 20× magnification, and pictures were captured.

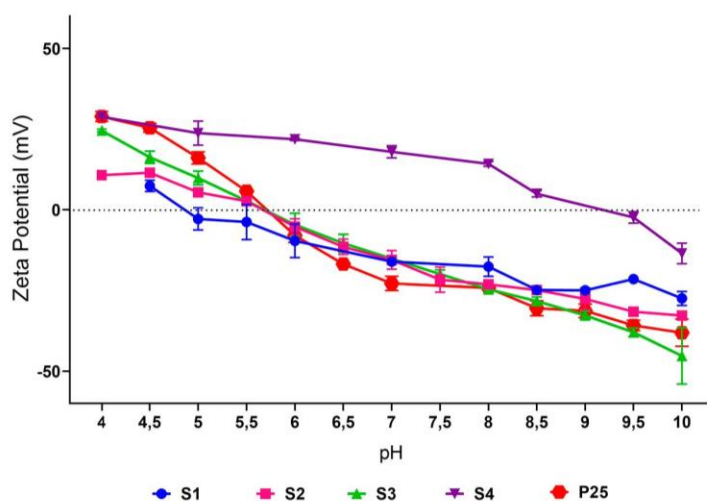


Figure 2. The ζ potential vs pH curves of TiO_2 -NPs in 1 mM sodium nitrate (NaNO_3) solution. Values are the mean \pm SEM of three independent experiments.

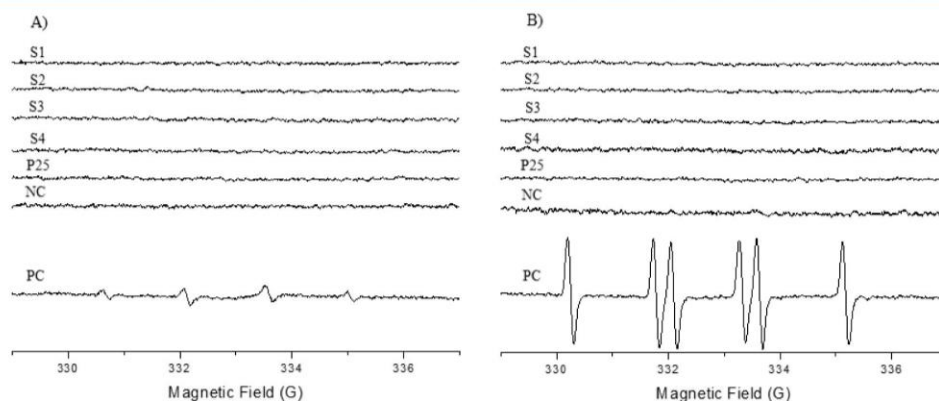


Figure 3. Generation of HO^\bullet (A) and $\text{CO}_2^{\bullet-}$ (B) radicals. Negative control (NC) corresponds to buffer solution without particles. Positive control (PC) corresponds to UV-irradiated P25. The number of radicals produced is proportional to the intensity of the ESR signal.

2.5. Determination of Cell Viability. Cell viability was determined by Trypan blue exclusion since TiO_2 -NPs have been reported to have interactions with MTT, XTT, and LDH viability assays.^{30,31} Trypan blue is a cell membrane-impermeable azo dye that live cells exclude, whereas dead cells do not. 1.5×10^6 cells/well were plated onto 6-well microtiter plates in 1000 μL culture medium with or without TiO_2 -NPs. After incubation for 24 h at 37 $^\circ\text{C}$ in a humidified incubator, the culture medium was removed, and cells were washed with PBS and trypsinized. Twenty μL cell suspensions were mixed with 80 μL Trypan blue dye to obtain 1:5 dilution, and cells were counted under a microscope using Thoma cell counting chamber. Results are expressed as the mean of three independent experiments and relative to control (unexposed) cells.

2.6. Proinflammatory Response. A549 cells and co-culture cells were seeded in 96-well-plates (1×10^5 cells/well in 50 μL of medium) and were allowed to adhere for 24 h. NPs were diluted in DMEM cell culture medium to reach the following final concentrations: 15, 30, 60, and 120 $\mu\text{g}/\text{mL}$. After 24 h cell exposure to TiO_2 -NPs, the production of tumor necrosis factor alpha (TNF- α) was evaluated in a co-culture using a commercial ELISA Kit (Quantikine Human TNF- α Immunoassay; R&D Systems, Lille, France) according to the manufacturer's instructions. Interleukin-8 (IL-8) production was assessed in the two cell systems (A549 cells and A549/differentiated-THP-1 co-culture) after exposure to TiO_2 -NPs for 24 h by a

commercially available ELISA kit (Quantikine Human IL-8 Immunoassay; R&D Systems, Lille, France) according to the manufacturer's instructions. The optical density of each sample was determined using a microplate reader (Multiskan RC; Thermo LabSystems, Helsinki, Finland) set to 450 nm. Three independent experiments were performed, and the production of TNF- α and IL-8 was reported to that of control (unexposed) cells.

2.7. Determination of Reactive Oxygen Species Production. A549 cells and co-culture cells were seeded in 96-well black polystyrene microplates (1×10^5 cells/well in 50 μL of medium) and were allowed to adhere for 24 h before assay. After 90 min and 24 h exposure to 15, 30, 60, and 120 $\mu\text{g}/\text{mL}$ TiO_2 -NPs, the level of ROS was determined using the OxiSelect kit from Cell Bio Laboratories (San Diego, CA, USA) according to the manufacturer's instructions. Fluorescence was detected using a Fluoroskan Ascent fluorometer (excitation: 480 nm, emission: 530 nm, Thermo LabSystems), and the generation of ROS was reported to that of control (unexposed) cells.

2.8. Statistical Analyses. Statistical analyses were performed using GraphPad Prism (version 8.0, GraphPad Software, San Diego, CA, USA). All data were presented as mean \pm standard error of the mean (SEM). Differences were considered to be statistically significant when P value was <0.05 . One-way Anova Tukey test analysis was performed for comparison between control and experimental groups and among experimental groups.

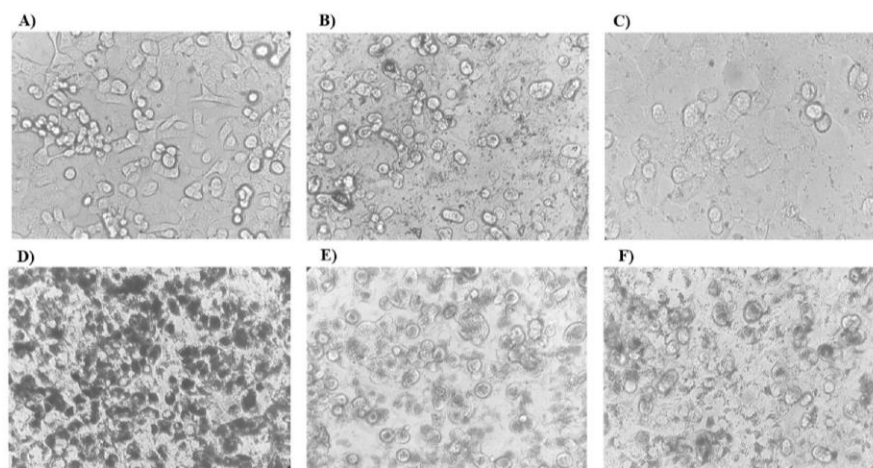


Figure 4. Microscopic images of A549 cells exposed to 120 $\mu\text{g}/\text{mL}$ TiO_2 -NPs for 24 h (20 \times magnification). (A) Control cells (unexposed to NPs), (B) S1, (C) S2, (D) S3, (E) S4, and (F) P25.

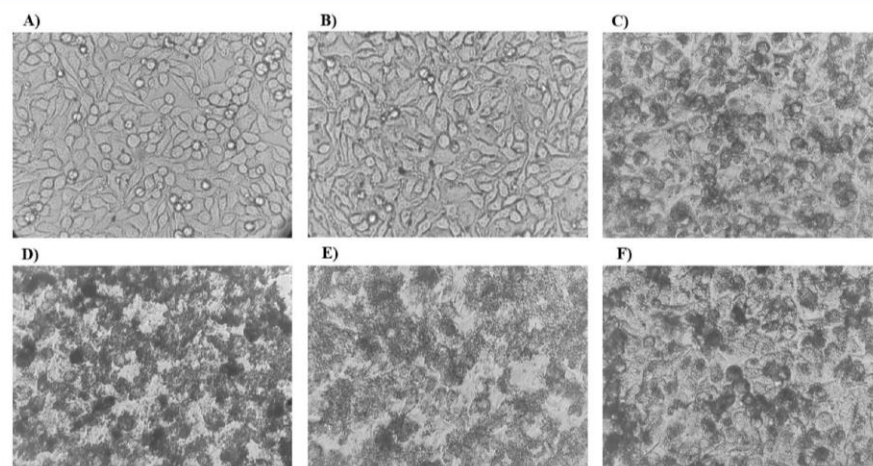


Figure 5. Microscopic images of co-culture cells exposed to 120 $\mu\text{g}/\text{mL}$ TiO_2 -NPs for 24 h (20 \times magnification). (A) Control cells (unexposed to NPs), (B) S1, (C) S2, (D) S3, (E) S4, and (F) P25.

3. RESULTS

3.1. Physicochemical Features of TiO_2 Nanoparticles.

The physicochemical characterization of five different TiO_2 -NPs was performed using TEM, SEM, DLS, BET, ζ -potential, Raman spectroscopy, XRD, and ICP-MS to provide clear insight into their primary size, hydrodynamic size, shape, specific surface area, surface charge, crystallinity, and chemical composition. The key toxicity-relevant features of the TiO_2 -NPs are listed in Table 2 with corresponding TEM images shown in Figure 1.

Please note that TEM images were shown to illustrate the NP shape, and as surface functionalization is not expected to alter the NP shape, we consider that a TEM picture of S2 is representative of that of S4.

All samples exhibited a negative surface charge up to $\text{pH} < 5.5$, while the S4 surface was positively charged in almost all pH values investigated ($\text{pH} < 9.5$) (Figure 2). S4 differentiated from the other samples also in DI H_2O at $\text{pH} 7.5$, exhibiting a remarkably positive surface charge (Table 2) which is due to

the presence of amine groups ($-\text{NH}_2$) on the surface of the NPs after APTES modification. In the culture medium ($\text{pH} 7.5$), all samples, including S4, exhibited a negative surface charge. The opposite sign of the surface charge of S4 in DI H_2O and DMEM may be due to the different adsorption and affinity of protons on the surface of the particle in the culture medium.

Raman spectra and XRD pattern (Supporting Information) of TiO_2 -NPs confirmed the anatase phase of S1–S4 and anatase-rutile mixed phase (*ca.* 90:10) of P25.

The free radical generation of TiO_2 -NPs is shown in Figure 3. No ESR spectra of the $\text{DMPO}\cdot\text{HO}^\bullet$ and of the $\text{DMPO}\cdot\text{CO}_2^{\bullet-}$ adducts were observed for the TiO_2 samples under the same light conditions used in the cellular tests, thus suggesting that the photocatalytic activity of TiO_2 -NPs is not a parameter that may affect toxicity results in this study.

The trace toxic impurities of Cd, Hg, As, Pb, Sb, and Zn in the tested samples met purity requirements of typical maximum tolerable limits of 0.5, 0.5, 3, 10, 50, and 50 mg/kg , respectively. Moreover, all particle samples were tested by

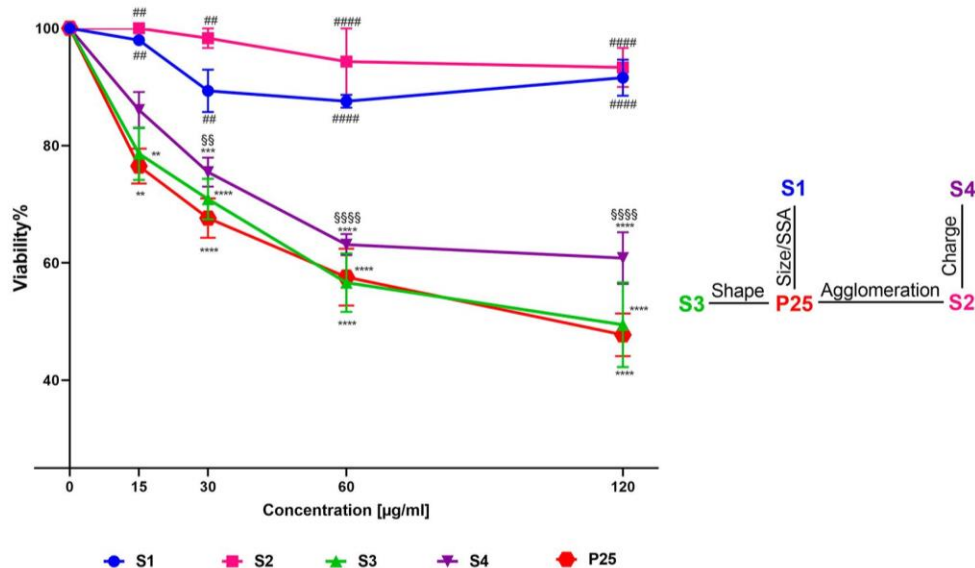


Figure 6. Cell viability assessed by Trypan blue assay 24 h after A549 cells were exposed to TiO₂-NPs at the indicated concentrations. Values are the mean \pm SEM of three independent experiments. Statistically different from control (***) $P < 0.0001$. Statistically different from P25 (###) $P < 0.01$, (####) $P < 0.0001$. Statistical difference between S2 and S4 (§§) $P < 0.01$, (§§§§) $P < 0.0001$. Statistical analyses were conducted using one-way Anova analyses, followed by Tukey's multiple comparison test.

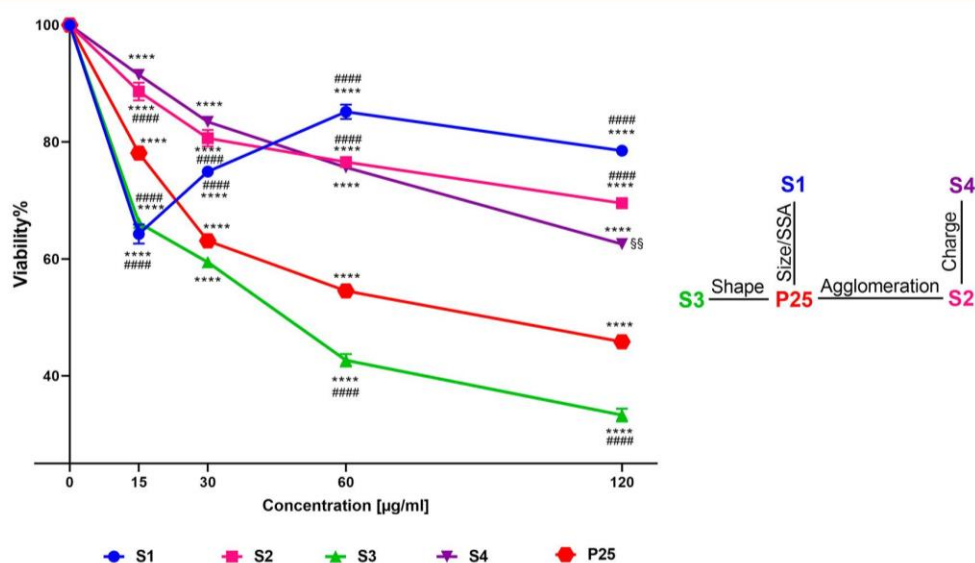


Figure 7. Cell viability assessed by Trypan blue assay 24 h after co-culture cells were exposed to TiO₂-NPs at the indicated concentrations. Values are the mean \pm SEM of three independent experiments. Samples statistically different from control (****) $P < 0.0001$. Statistically different from P25 (#####) $P < 0.0001$. Statistical difference between S2 and S4 (§§) $P < 0.01$. Statistical analyses were conducted using one-way Anova analyses, followed by Tukey's multiple comparison test.

endotoxin assay for the possible presence of endotoxin. Endotoxin content was found to be below the detection limit for all the samples. Since the tested NPs did not contain toxic elements and endotoxins, it could be claimed that the possible toxic effects after NP exposure are only caused by TiO₂-NPs themselves.

3.2. Cell Morphology. Figures 4 and 5 illustrate the morphology of A549 cells and A549/differentiated-THP-1 co-

cultured cells after 24 h exposure to the highest dose of TiO₂-NPs (120 $\mu\text{g}/\text{mL}$), respectively.

Please note that we chose the highest NP concentration (120 $\mu\text{g}/\text{mL}$) to illustrate the cell morphological changes induced as they were more pronounced in this condition. However, cell morphology alterations were not the same depending on the NP concentration and type. For instance, with the smallest NP concentration, cell morphology was similar to that of control cells. Although such changes should

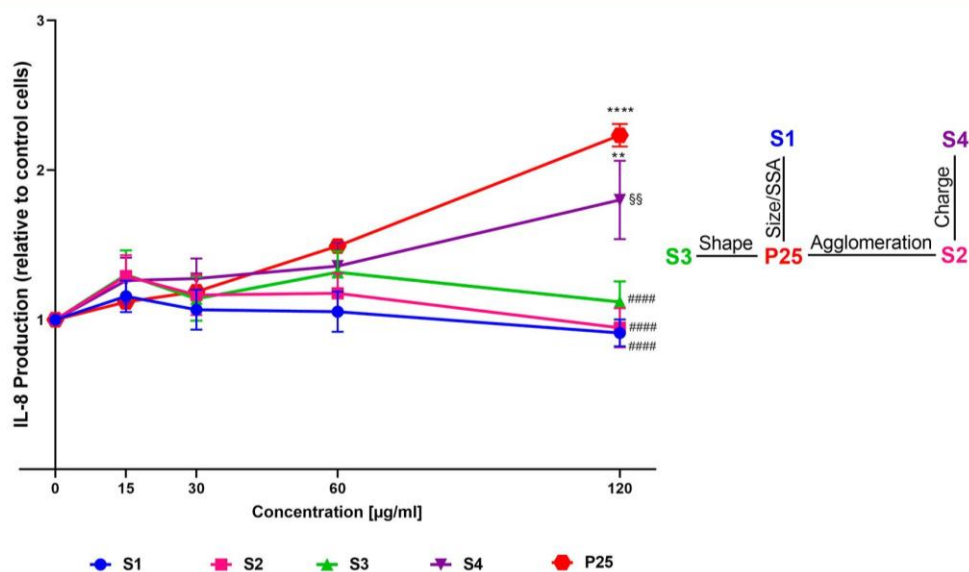


Figure 8. IL-8 production after 24 h exposure to the indicated concentrations of TiO₂-NPs in A549 cells. Values are the mean \pm SEM of three independent experiments. Statistically different from control (***) $P < 0.01$ and (****) $P < 0.0001$. Statistically different from P25 (####) $P < 0.0001$. Statistical difference between S2 and S4 (§§) $P < 0.01$. Statistical analyses were conducted using one-way Anova analyses, followed by Tukey's multiple comparison test.

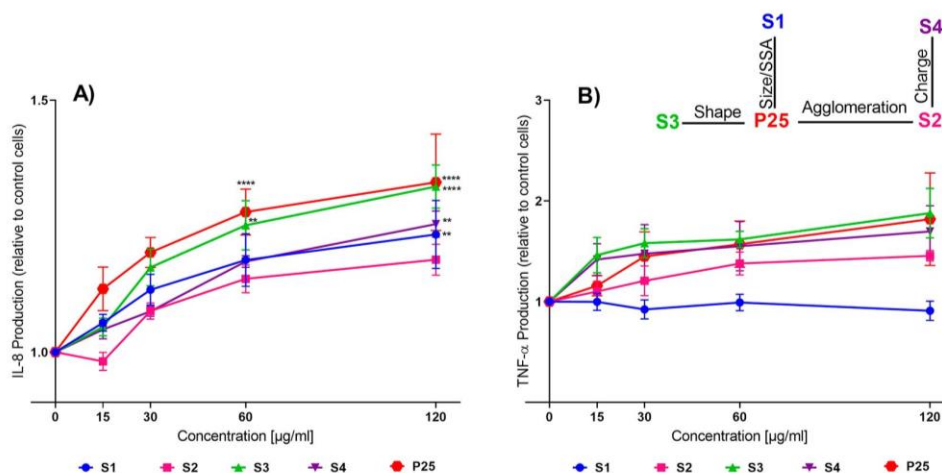


Figure 9. IL-8 (A) and TNF- α (B) production after 24 h of exposure to the indicated concentrations of TiO₂-NPs in co-culture cells. Values are the mean \pm SEM of three independent experiments. Statistically different from control (***) $P < 0.01$ and (****) $P < 0.0001$. Statistical analyses were conducted using one-way Anova analyses, followed by Tukey's multiple comparison test.

deserve further investigation, here our primary goal was to verify that the cell viability assessment was consistent with cell morphology observations.

3.3. Cell Viability. Cell viability, assessed by Trypan blue, after exposure to TiO₂-NPs of A549 cells and A549/differentiated-THP-1 co-culture is reported in Figures 6 and 7, respectively.

In general, a decrease in cell viability was observed after incubating A549 cells with all TiO₂-NPs, although not statistically significant for S1 and S2. Statistically significant differences were found between P25 and S1, P25 and S2, and S2 and S4.

The co-culture system is considered a more sensitive model than monocultures and better reflect the real tissue environ-

ment.^{32–34} In co-culture, the tested NPs caused slightly more cell loss than in the A549 cell monoculture. The cell viability decreased in a dose-dependent manner in all samples except S1 (Figure 7). The drastic drop of cell viability at the lowest S1 concentration is quite peculiar. We assume it might be due to experimental artifacts. Direct interaction between NPs and test reagents might cause artifacts; however, there is no evidence that Trypan blue interacts with TiO₂, unlike MTT and LDH viability tests. Furthermore, artifacts may be a result of unacknowledged impurity (e.g., metal) or endotoxin contamination leading to an overestimation of NP toxicity; however, we assessed toxic element impurity and endotoxin levels and did not observe any contamination. Other possible causes for artifacts include unexpected changes to 15 μ g/mL S1 NPs

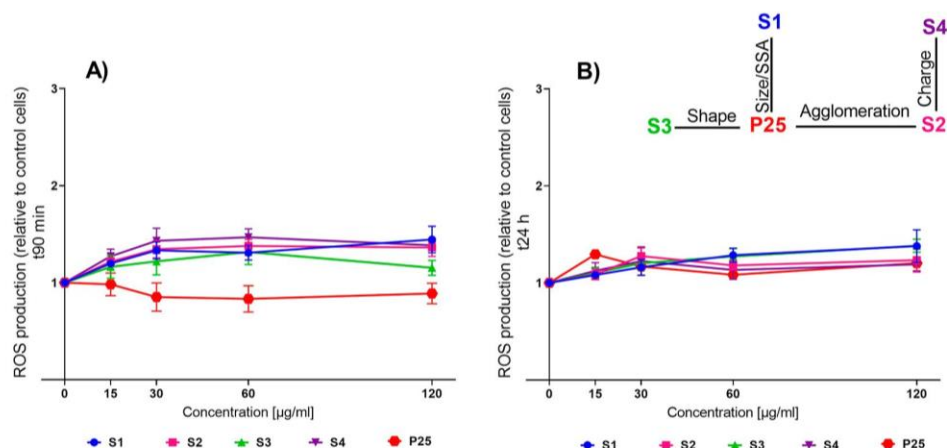


Figure 10. ROS production after 90 min (A) and 24 h (B) exposure to the indicated concentrations of TiO₂-NPs in A549 cells. Statistical analyses were conducted using one-way Anova analyses, followed by Tukey's multiple comparison test.

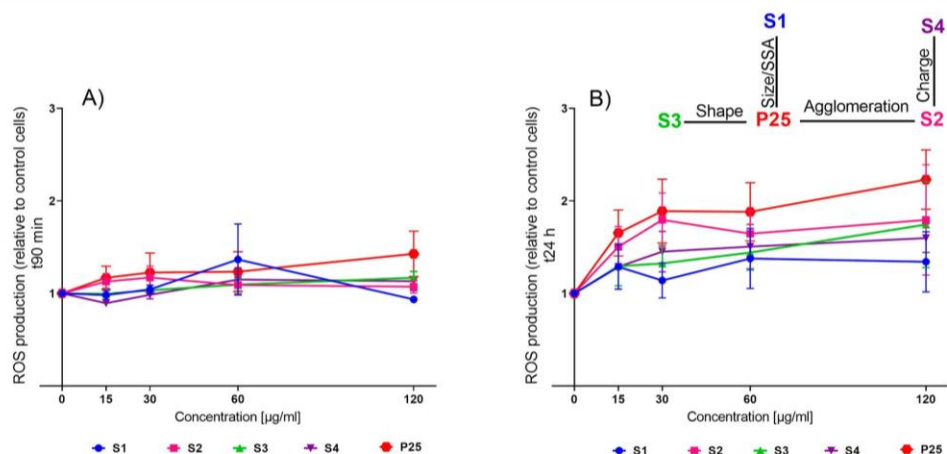


Figure 11. ROS production after 90 min (A) and 24 h (B) exposure to the indicated concentrations of TiO₂-NPs in co-culture. Statistical analyses were conducted using one-way Anova analyses, followed by Tukey's multiple comparison test.

(dissolution, agglomeration, oxidation, *etc.*) during sample preparation (ultrasonication may cause multiple undesirable and hard to quantify changes) or during testing (settling, dissolution, agglomeration, *etc.*), leading to inaccurate dosing. It is hard to definitively determine the sources of artifacts, and further testing with regard to this aspect is necessary.

The exposure to S3 and P25 induced a higher cell viability loss than S1, S2, and S4. The maximal cell loss was observed for S3. Statistically significant differences were observed when comparing P25 to S1, P25 to S2, and P25 to S3 ($P < 0.0001$, all). When comparing S2 to S4, a statistically significant difference was observed only at the highest dose (120 $\mu\text{g}/\text{mL}$, $P < 0.01$).

3.4. Proinflammatory Response. As IL-8 is a major proinflammatory mediator in A549 cells and TNF- α is a proinflammatory cytokine secreted from monocytes/macrophages, IL-8 was assessed for A549, and IL-8 and TNF- α were assessed for the co-cultures. Results are reported in Figures 8 and 9.

In A549 cells, S4 and P25 samples caused a dose-dependent increase in IL-8 production compared to the control group and

showed a statistically significant difference at the highest concentration (S4, $P < 0.01$; P25, $P < 0.0001$). When comparing P25 to S1, S2, and S3, only the highest NP concentration (120 $\mu\text{g}/\text{mL}$) induced significant productions of IL-8 ($P < 0.0001$, all). When comparing S2 to S4, a statistically significant difference was observed only at the highest dose (120 $\mu\text{g}/\text{mL}$, $P < 0.01$).

In the co-cultures, all samples caused a dose-dependent increase in IL-8 production compared to the control group, although not statistically significant for S2. When the IL-8 production was compared between P25 and the other samples, no statistically significant difference was found.

Except S1, all groups showed a concentration-dependent increase in TNF- α production, although not statistically significant. When compared with P25, no statistically significant difference was found.

3.5. Reactive Oxygen Species Production. Figures 10 and 11 report a ROS production after exposure to the different TiO₂-NPs of A549 cells and A549/differentiated-THP-1 co-culture, respectively.

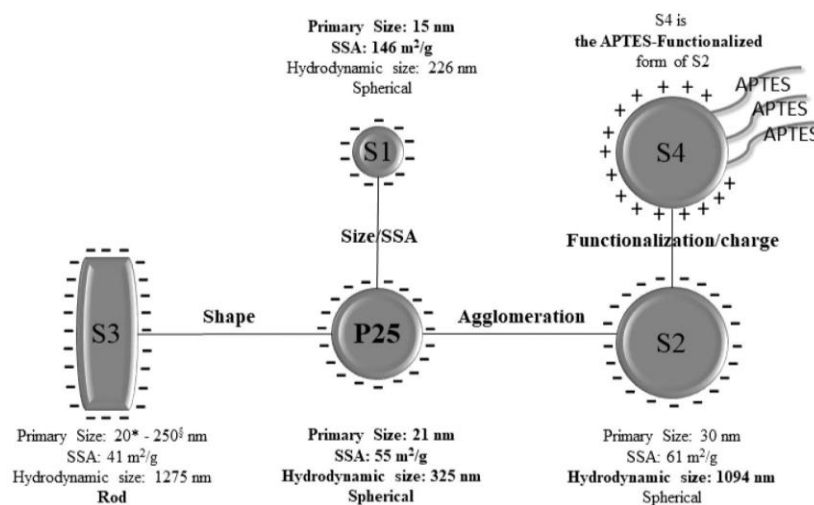


Figure 12. A comparison of NPs with regard to their primary size/SSA, shape, agglomeration state, and surface functionalization/charge (APTES). Particle properties that differ from P25 TiO₂ are reported in bold. (–) Indicates negative surface charge, (+) indicates positive surface charge, * minimum Feret diameter, and [§] maximum Feret diameter.

Table 3. Impact of TiO₂-NPs Size and SSA, Shape, Agglomeration State, and Functionalization on their Cytotoxicity^a

impact of the indicated physicochemical features on cytotoxicity as evaluated by comparison between the indicated samples		cell viability		proinflammatory effect		oxidative stress	
		A549	A549/differentiated THP-1	A549	A549/differentiated THP-1	A549	A549/differentiated THP-1
		size and SSA	P25 vs S1	+	+	+ ^b	–
shape	P25 vs S3	–	+	+ ^b	–	–	–
agglomeration	P25 vs S2	+	+	+ ^b	–	–	–
surface charge	S2 vs S4	+	+ ^b	–	–	–	–

^aThe + and – indicate an impact or no impact of the physicochemical features on the cytotoxicity respectively. ^bOnly at the highest dose.

TiO₂-NPs did not induce significant ROS production neither in A549 cells nor in co-culture compared to the control group (unexposed to TiO₂-NPs), whatever the time of analysis (90 min or 24 h).

4. DISCUSSION

As it is commonly acknowledged that the physicochemical properties of NPs (*e.g.*, size, shape, solubility, aggregation, *etc.*) strongly influence their toxicity, we aimed to determine the impact of such features on TiO₂-NPs toxicity on human lung cell lines. As illustrated by Figure 12 and based on the physicochemical features of the different NPs, by comparing P25 and S1, we were able to highlight the impact of size and SSA on TiO₂-NPs cytotoxicity. We compared S2 and P25 to investigate the effect of agglomeration on toxicity, as this feature was different between these samples, whereas their primary size, specific surface area, surface charge, and shape were all similar. The influence of particle shape was investigated by comparing rod-shaped S3 with isometric P25 that share similar specific surface areas. Lastly, the surface charge impact on cell response was compared between S2 and S4. It is important to state that the crystalline phases of synthesized NPs and P25 are different from each other in this study. P25 is a mixture of anatase and rutile (approximately 90% anatase and 10% rutile), while other samples have a pure anatase structure. Several studies have shown that anatase is

more toxic than similarly sized rutile TiO₂-NPs.^{35–37} Therefore, we can confidently affirm that the anatase phase might be more responsible than the rutile phase for the toxic manifestations that P25 may create. A summary of our observations is reported in Table 3.

As highlighted in the Introduction, a safer-by-design approach cannot be achieved without knowing the impact of physicochemical properties of NPs on their toxicity. In the R&D phase of the safer-by-design approach, the assessment of the hazard profile of NPs exhibiting different physicochemical properties is the first step for avoiding their adverse effects.³⁸ The results obtained in this study (as summarized in Table 3 and further discussed below) provide data for the design and development of safer TiO₂-NPs.

4.1. Size and Surface Area Effects. To determine the effects of the size and surface area of the TiO₂-NPs on their cytotoxicity, we compared S1 and P25 NPs, whose agglomeration states in the culture medium were very similar.

Generally, P25 (21 nm) caused more cell death than smaller sized S1 (15 nm). This finding is consistent with observations at the microscope of cell morphology. Cells were more affected when incubated with P25. P25 also induced a higher IL-8 production in A549 than S1 at the highest NP concentration. Finally, ROS production was similar between P25 and S1. These findings suggest a NP size and surface area impact on cell viability and proinflammatory response, but only at the

highest NP concentration. Our findings are consistent with studies showing that size and surface area of NPs might contribute to cytotoxicity.^{39,40} In agreement with our finding that larger particles caused more toxicity, Park *et al.*¹⁸ showed that 1 μm TiO₂-Degussa microparticles caused more pronounced morphological changes than smaller 30 nm TiO₂-NPs in A549 cells. Another study⁴¹ reported that mouse neuroblastoma (Neuro-2A) cells showed a much lower cell viability when incubated with 150 nm nickel ferrite NPs than with 10 nm particles. Pan *et al.*⁴² reported that 1.4 nm-sized gold NPs caused more cytotoxicity than 1.2 and 0.8 nm gold NPs on the HeLa cervix carcinoma epithelial cells, SK-Mel-28 melanoma cells, L929 mouse fibroblasts, and mouse monocyte/macrophage cells (J774A1).

However, conflicting results have been reported. For example, exposure to 5 nm TiO₂-NPs inhibited A549 cell proliferation and led to apoptosis and intracellular ROS production.⁴³ In another study, 25 nm TiO₂-NPs showed greater toxicity than 60 nm TiO₂-NPs in A549 and 16HBE cells.⁴⁴ In addition, Simon-Deckers *et al.* as well as Zhu *et al.* reported that smaller TiO₂-NPs caused a higher toxicity than bigger ones.^{45,46} Therefore, there is no definitive conclusion about the effect of particle size on toxicity. Another example is that 50 nm TiO₂-NPs caused a greater toxicity than the 6.3, 10, and 100 nm TiO₂-NPs.⁴⁷ Similarly, an interesting finding was that 25 nm TiO₂-NPs induced more cell death, higher LDH release, and ROS production than 5 and 100 nm TiO₂-NPs in mouse macrophages.⁴⁸ Therefore, toxic effects of TiO₂-NPs may be related to their structural characteristics as suggested by Zhang *et al.*⁴⁸ More mechanistic studies are needed to clarify the NP size impact on cytotoxicity.

Regarding the production of ROS, Jiang *et al.*⁴⁹ reported an S-shaped curve for ROS generation per unit surface area within a certain size range (4–195 nm) of TiO₂-NPs. Also, TiO₂-NPs below 10 nm or above 30 nm produced similar levels of ROS per surface area, while a sharp increase was observed from 10 to 30 nm. ROS production was clearly observed in A549 cells in two studies^{45,50} whatever the size, crystal phase, and shape of TiO₂-NPs, which were studied in conditions very similar to ours (same cellular model: A549 cells exposed to various types of TiO₂-NPs, for 24 h at 100 $\mu\text{g}/\text{mL}$). Especially, intracellular ROS production started as early as after 15 min of exposure to P25.⁵⁰ However, in our study, TiO₂-NPs did not trigger the production of ROS whatever the size and surface area. This must be confirmed by a comprehensive study of the oxidative stress also including the assessment of antioxidant systems induction.

4.2. Shape Effects. When comparing rod-shaped S3 and spherical P25 NPs, we observed that S3 NPs caused more cell death than P25 in co-cultures, suggesting an impact of NP shape on cell viability. However, NP shape had no impact on ROS production and did not seem to influence the proinflammatory response as in co-cultures P25 and S3 induced similar IL-8 and TNF- α productions. Only in A549 cells, P25 caused more IL-8 production than S3 but at the highest NP concentration.

A limited number of studies have considered how the shape of NPs impacts on their toxicity,^{20,51,52} and only few papers reported about a specific shape effect of TiO₂-NPs.^{53,54} Gea *et al.*⁵³ investigated the cytotoxicity of TiO₂-NPs of three different shapes (bipyramids, rods, platelets) on human bronchial epithelial cells (BEAS-2B) in the presence or absence of light. They observed that in the presence of light,

rod-shaped TiO₂ were more cytotoxic than bipyramids and platelets; the latter showing a similar profile of toxicity. However, in the absence of light, platelets induced a higher cytotoxicity than bipyramids and rods. In an *in vivo* study,⁵⁴ male Sprague–Dawley rats were exposed to sphere anatase/rutile P25, sphere pure anatase TiO₂, and nanobelts pure anatase TiO₂ by intratracheal instillation. Only nanobelts were able to induce inflammation *in vivo*. Studies using other NP types could be mentioned to illustrate the NP shape influence on cytotoxicity. For example, rod-shaped Fe₂O₃ NPs were found to produce much higher levels of lactate dehydrogenase (LDH) leakage, inflammatory response, and ROS production than sphere Fe₂O₃ NPs in RAW 264.7.⁵² On the contrary, Forest *et al.*²⁰ reported that rod-shaped CeO₂ NPs produced more toxic effects in terms of LDH release and TNF- α production than octahedron or cubic CeO₂ NPs in RAW 264.7 cells.

On the other hand, some studies did not report any effect of NP shape on their cytotoxicity. For instance, Zhao *et al.*⁵⁵ did not find a significant difference in the toxicity of rod and sphere mesoporous silica NPs on human colorectal adenocarcinoma (Caco-2) cells.

The discrepancies described above can be explained by the fact that besides the shape of the NPs, NPs' interaction forces which are different for each type of particle may also affect biological responses, for example, interparticle van der Waals forces of rod-shaped NPs are larger than those of spherical ones.^{56,57} These forces define the ability of NP's cell internalization *via* phagocytosis.^{17,58} Meng *et al.*⁵⁹ reported that the internalization of rod-shaped silica particles in A549 cells was much higher than that of spherical particles. This may explain why rod-shaped particles caused more cell death in our study. Moreover, when having different attractive forces (van der Waals and others), the tendency to agglomerate in the suspension may also be different.⁶⁰ Therefore, it is also difficult to distinguish the shape effect from the agglomeration effect, since agglomeration always occurs in an aqueous system. Finally, due to different cell types, cell sensitivity, and phagocytic activity, it is difficult to compare studies from the literature.

4.3. Agglomeration Effects. We compared the responses induced by S2 and P25 to determine the effect of agglomeration on toxicity because primary size, surface area, surface charge, and shape of the two particles were all similar, and only their agglomeration state differed. When considering cell viability, highly agglomerated S2 NPs caused less cell death than less agglomerated P25 in both cell systems. Furthermore, IL-8 production was enhanced in the presence of less agglomerated NPs compared to that induced by highly agglomerated NPs in A549 but only at the highest NP concentration. In addition, agglomeration did not affect IL-8 and TNF- α production in co-cultures and had no impact on ROS production.

Magdolenova *et al.*⁶¹ reported that the highly agglomerated TiO₂-NPs decreased the proliferation activity in Cos-1 monkey kidney fibroblast-like cell line and EUE human embryonic epithelial cells compared to well-dispersed NPs. Large agglomerates of TiO₂-NPs caused DNA damage, whereas small agglomerates did not. Another study reported that⁶² in comparison to large A14 TiO₂-NP agglomerates, P25 and A60 TiO₂-NPs that exhibit small and soft agglomerates were more efficiently taken up by the A549 cells, generated more intracellular oxidative stress, and induced a more potent

interleukin-8 (IL-8) and monocyte chemoattractant protein 1 (MCP-1) proinflammatory response.

There are few *in vivo* studies in the literature which investigated the agglomeration impact of NPs on lung diseases. Noël *et al.*⁶³ exposed male CDF (F344)/CrIBR rats to aerosolized nano-TiO₂. In groups exposed to large agglomerates (>100 nm), an increase in the number of neutrophils, an indicator of lung inflammation, was observed. However, no increase in other inflammation markers (IL-1 α , IL-6, and TNF- α production) was observed. Exposure to small agglomerates (<100 nm) caused more cell death and ROS production than large agglomerates. Although these results are in agreement with ours, at least regarding cell viability, it is difficult to compare *in vivo* and *in vitro* studies because of a different agglomeration status of NPs that can occur *in vitro* (in culture medium) and *in vivo* in lung fluids. The protein corona forming around the NPs may also have a strong impact on agglomeration and on the subsequent cell/NP interactions.⁶⁴

4.4. Surface Charge Effects. When the impact of NP surface charge on cell viability was examined, it was observed that positively charged S4 NPs (APTES-functionalized) caused slightly more cell loss than S2, their nonfunctionalized, negatively charged counterparts. However, they exhibited a similar profile of proinflammatory response and oxidative stress, suggesting no impact of this functionalization on proinflammatory response and oxidative stress. Since it is well documented that positively charged NPs have a high affinity for negatively charged cell membrane protein,⁶⁵ it is more likely to have a destructive effect on cell membranes.

In a study,⁶⁶ TiO₂-NPs bearing -OH, -NH₂, or -COOH surface groups were evaluated for their effect on several cancer cells and control cell cytotoxicity. Specifically, -NH₂ and -OH groups exhibited a significantly higher toxicity than -COOH on Lewis lung carcinoma and on a prostate cancer cell line isolated from Copenhagen rats. In some studies on other APTES-functionalized NPs, for instance, the cytotoxicity of APTES-functionalized mesoporous and nonporous silica NPs was investigated on RAW 264.7 macrophages.⁶⁷ They both induced very low levels of toxicity. Also, these particles did not cause any ROS production, similar to our results. Chavez *et al.*⁶⁸ reported that APTES-functionalized luminescent upconversion NPs were found noncytotoxic to HeLa and DLD-1 human colorectal adenocarcinoma cells. Petushov *et al.*⁶⁹ showed that 30 nm APTES-functionalized silicalite NPs did not significantly change LDH release activity in HEK293 embryonic kidney cells and in RAW264.7 cells.

Besides the observation of the impact of the NPs physicochemical properties on their toxicity, another main finding of this study was that the co-culture model seemed more sensitive to the adverse effects of TiO₂-NPs than the monoculture model. It may be due to different uptake levels of NPs in monoculture and co-culture cells. Co-culture cells may show a stronger barrier compared to monoculture due to intercellular bonds and interactions. In a tetra-culture model consisting of A549 + THP-1 + HMC-1 + EAhy926 cells, only phagocytic THP-1 cells have been shown to internalize 50 nm silica particles.⁷⁰ Due to cell interaction through cytokines and chemokines, the uptake in one cell type may affect the reaction of the other cell types in the same culture. This can lead to differences in the uptake mechanisms of NPs compared to monoculture. However, in our study, further investigations are needed to support this hypothesis. On the other hand, the fact that co-culture is more sensitive to the toxic effects of NPs may

result from different behaviors of cells in the co-culture. Data showed that when co-cultured with A549 cells, THP-1-derived macrophages (M0) differentiated toward the M1- and M2-macrophage phenotype. Therefore, the co-culture of THP-1-derived macrophages with A549 leads to the release of higher levels of proinflammatory cytokines compared to levels observed in the medium of THP1-derived macrophages.⁷¹ In this case, a strong protection of A549 cells provided by THP-1 cells against toxic agents in co-culture has been reported. However, in order to mimic aerosol accumulation in the air space of the lung, direct cell culture may have some limitations given the weak interactions of the cells.⁷² Also, different proliferation rates of the co-cultured cells may present a problem and limit the use of co-cultures. The multiple cell cultures represent an improvement compared with single cell cultures and more closely resemble the *in vivo* situation, yet they are still limited to the cells investigated. Thus, co-culture cell model may be considered as essential for developing a predictive *in vitro* model of the lung.

5. CONCLUSION

As reported in Table 3, the main effects observed in this study were an impact of TiO₂-NP size/SSA, shape, agglomeration state, and surface functionalization/charge (APTES) on cell viability in co-cultures. This model seems more sensitive than the A549 monocultures. The same features seemed to have an impact on the proinflammatory response, but only in A549 cells cultivated alone and only at the highest NP concentration. No impact was observed on ROS production. The effect on toxicity was higher in bigger sized, less agglomerated particles and rod-shaped and positively charged particles. Although further investigations are needed, the present study contributes to a better characterization of TiO₂-NP toxicity by the systematic evaluation of their adverse effects on human lung cell lines in relation to their physicochemical properties. Moreover, such results could open promising perspectives, especially in the context of a safer-by-design approach.

■ ASSOCIATED CONTENT

Supporting Information

The Supporting Information is available free of charge at <https://pubs.acs.org/doi/10.1021/acs.chemrestox.0c00106>.

XRD pattern of the TiO₂-NPs (PDF)

■ AUTHOR INFORMATION

Corresponding Author

Valérie Forest – Mines Saint-Etienne, Université Lyon, Université Jean Monnet, INSERM, U1059 Sainbiose, Centre CIS, F-42023 Saint-Etienne, France; orcid.org/0000-0003-3124-0413; Email: vforest@emse.fr

Authors

Ozge Kose – Mines Saint-Etienne, Université Lyon, Université Jean Monnet, INSERM, U1059 Sainbiose, Centre CIS, F-42023 Saint-Etienne, France

Maura Tomatis – Dipartimento di Chimica and G. Scansetti Interdepartmental Center for Studies on Asbestos and other Toxic Particulates, Università degli Studi di Torino, 10125 Torino, Italy

Lara Leclerc – Mines Saint-Etienne, Université Lyon, Université Jean Monnet, INSERM, U1059 Sainbiose, Centre CIS, F-42023 Saint-Etienne, France

Naila-Besma Belblidia – Mines ParisTech, PSL Research University, MAT - Centre des matériaux, CNRS UMR 7633, 91003 Evry, France; ENSTA ParisTech UCP, Institut Polytechnique Paris, 91762 Palaiseau, France

Jean-François Hochepped – Mines ParisTech, PSL Research University, MAT - Centre des matériaux, CNRS UMR 7633, 91003 Evry, France; ENSTA ParisTech UCP, Institut Polytechnique Paris, 91762 Palaiseau, France

Francesco Turci – Dipartimento di Chimica and G. Scansetti Interdepartmental Center for Studies on Asbestos and other Toxic Particulates, Università degli Studi di Torino, 10125 Torino, Italy; orcid.org/0000-0002-5806-829X

Jérémy Pourchez – Mines Saint-Etienne, Université Lyon, Université Jean Monnet, INSERM, U1059 Sainbiose, Centre CIS, F-42023 Saint-Etienne, France

Complete contact information is available at:

<https://pubs.acs.org/10.1021/acs.chemrestox.0c00106>

Funding

This research did not receive any specific grant from funding agencies in the public, commercial, or not-for-profit sectors.

Notes

The authors declare no competing financial interest.

REFERENCES

- (1) Fujishima, A., Rao, T. N., and Tryk, D. A. (2000) Titanium Dioxide Photocatalysis. *J. Photochem. Photobiol., C* 1 (1), 1–21.
- (2) Chen, X., and Selloni, A. (2014) Introduction: Titanium Dioxide (TiO₂) Nanomaterials. *Chem. Rev.* 114 (19), 9281–9282.
- (3) (2015) *Mineral Commodity Summaries*, p 196, U.S. Geological Survey, Reston, VA.
- (4) Weir, A., Westerhoff, P., Fabricius, L., Hristovski, K., and Von Goetz, N. (2012) Titanium Dioxide Nanoparticles in Food and Personal Care Products. *Environ. Sci. Technol.* 46 (4), 2242–2250.
- (5) Wang, Y., He, Y., Lai, Q., and Fan, M. (2014) Review of the Progress in Preparing Nano TiO₂: An Important Environmental Engineering Material. *J. Environ. Sci. (Beijing, China)* 26, 2139–2177.
- (6) Piccinno, F., Gottschalk, F., Seeger, S., and Nowack, B. (2012) Industrial Production Quantities and Uses of Ten Engineered Nanomaterials in Europe and the World. *J. Nanopart. Res.* 14 (9), 1109.
- (7) Shi, H., Magaye, R., Castranova, V., and Zhao, J. (2013) Titanium Dioxide Nanoparticles: A Review of Current Toxicological Data. *Part. Fibre Toxicol.* 10 (1), 15.
- (8) Grande, F., and Tucci, P. (2016) Titanium Dioxide Nanoparticles: A Risk for Human Health? *Mini-Rev. Med. Chem.* 16 (9), 762–769.
- (9) Baranowska-Wójcik, E., Szwajgier, D., Oleszczuk, P., and Winiarska-Mieczan, A. (2020) Effects of Titanium Dioxide Nanoparticles Exposure on Human Health—a Review. *Biol. Trace Elem. Res.* 193 (1), 118–129.
- (10) Albanese, A., Tang, P. S., and Chan, W. C. W. (2012) The Effect of Nanoparticle Size, Shape, and Surface Chemistry on Biological Systems. *Annu. Rev. Biomed. Eng.* 14 (1), 1–16.
- (11) Oberdörster, G., Oberdörster, E., and Oberdörster, J. (2005) Nanotoxicology: An Emerging Discipline Evolving from Studies of Ultrafine Particles. *Environ. Health Perspect.* 113 (7), 823–839.
- (12) Oberdörster, G., Ferin, J., and Lehnert, B. E. (1994) Correlation between Particle Size, in Vivo Particle Persistence, and Lung Injury. *Environ. Health Perspect.* 102, 173–179.
- (13) Braakhuis, H. M., Gosens, I., Krystek, P., Boere, J. A., Cassee, F. R., Fokkens, P. H., Post, J. A., van Loveren, H., and Park, M. V. (2014) Particle Size Dependent Deposition and Pulmonary Inflammation after Short-Term Inhalation of Silver Nanoparticles. *Part. Fibre Toxicol.* 11 (1), 49.
- (14) Kuehl, P. J., Anderson, T. L., Candelaria, G., Gershman, B., Harlin, K., Hesterman, J. Y., Holmes, T., Hoppin, J., Lackas, C., Norenberg, J. P., Yu, H., and McDonald, J. D. (2012) Regional Particle Size Dependent Deposition of Inhaled Aerosols in Rats and Mice. *Inhalation Toxicol.* 24 (1), 27–35.
- (15) Asgharian, B., and Price, O. T. (2007) Deposition of Ultrafine (NANO) Particles in the Human Lung. *Inhalation Toxicol.* 19 (13), 1045–1054.
- (16) Verma, A., and Stellacci, F. (2010) Effect of Surface Properties on Nanoparticle–Cell Interactions. *Small* 6 (1), 12–21.
- (17) Champion, J. A., and Mitragotri, S. (2006) Role of Target Geometry in Phagocytosis. *Proc. Natl. Acad. Sci. U. S. A.* 103 (13), 4930–4934.
- (18) Park, S., Lee, Y. K., Jung, M., Kim, K. H., Chung, N., Ahn, E.-K., Lim, Y., and Lee, K.-H. (2007) Cellular Toxicity of Various Inhalable Metal Nanoparticles on Human Alveolar Epithelial Cells. *Inhalation Toxicol.* 19 (sup1), 59–65.
- (19) Hsiao, I.-L., and Huang, Y.-J. (2011) Effects of Various Physicochemical Characteristics on the Toxicities of ZnO and TiO₂ Nanoparticles toward Human Lung Epithelial Cells. *Sci. Total Environ.* 409 (7), 1219–1228.
- (20) Forest, V., Leclerc, L., Hochepped, J.-F., Trouvé, A., Sarry, G., and Pourchez, J. (2017) Impact of Cerium Oxide Nanoparticles Shape on Their in Vitro Cellular Toxicity. *Toxicol. In Vitro* 38, 136–141.
- (21) (2006) *IARC Monographs on the Evaluation of Carcinogenic Risks to Humans Carbon Black, Titanium Dioxide, and Talc*, Vol. 93, pp 193–412, International Agency for Research on Cancer, Lyon, France.
- (22) Fadeel, B. (2013) Nanosafety: Towards Safer Design of Nanomedicines. *J. Intern. Med.* 274 (6), 578–580.
- (23) Geraci, C., Heidel, D., Sayes, C., Hodson, L., Schulte, P., Eastlake, A., and Brenner, S. (2015) Perspectives on the Design of Safer Nanomaterials and Manufacturing Processes. *J. Nanopart. Res.* 17 (9), 1–13.
- (24) Shin, S. W., Song, I. H., and Um, S. H. (2015) Role of Physicochemical Properties in Nanoparticle Toxicity. *Nanomaterials* 5 (3), 1351–1365.
- (25) Iavicoli, I., Leso, V., and Bergamaschi, A. (2012) Toxicological Effects of Titanium Dioxide Nanoparticles: A Review of in Vivo Studies. *J. Nanomater.* 2012, 1.
- (26) Chen, D. W., Shi, J. E., Yan, J. C., Wang, Y. H., Yan, F. C., Shang, S. X., and Xue, J. (2008) Controllable Synthesis of Titania Nanocrystals with Different Morphologies and Application to the Degradation of Phenol. *Chem. Res. Chin. Univ.* 24 (3), 362–366.
- (27) Zhao, J., Milanova, M., Warmoeskerken, M. M. C. G., and Dutschk, V. (2012) Surface Modification of TiO₂ Nanoparticles with Silane Coupling Agents. *Colloids Surf., A* 413, 273–279.
- (28) Brunauer, S., Emmett, P. H., and Teller, E. (1938) Adsorption of Gases in Multimolecular Layers. *J. Am. Chem. Soc.* 60 (2), 309–319.
- (29) Wang, Z., Ni, Z., Qiu, D., Chen, T., Tao, G., and Yang, P. (2004) Determination of Metal Impurities in Titanium Dioxide Using Slurry Sample Introduction by Axial Viewing Inductively Coupled Plasma Optical Emission Spectrometry. *J. Anal. At. Spectrom.* 19 (2), 273.
- (30) Wang, S., Yu, H., and Wickliffe, J. K. (2011) Limitation of the MTT and XTT Assays for Measuring Cell Viability Due to Superoxide Formation Induced by Nano-Scale TiO₂. *Toxicol. In Vitro* 25 (8), 2147–2151.
- (31) Holder, A. L., Goth-Goldstein, R., Lucas, D., and Koshland, C. P. (2012) Particle-Induced Artifacts in the MTT and LDH Viability Assays. *Chem. Res. Toxicol.* 25, 1885.
- (32) Drumm, K., Attia, D. I., Kannt, S., Micic, P., Buhl, R., and Kienast, K. (2000) Soot-Exposed Mononuclear Cells Increase Inflammatory Cytokine mRNA Expression and Protein Secretion in Cocultured Bronchial Epithelial Cells. *Respiration* 67 (3), 291–297.
- (33) Holownia, A., Wielgat, P., Kwolek, A., Jackowski, K., and Braszko, J. J. (2015) Crosstalk between Co-Cultured A549 Cells and

Thp1 Cells Exposed to Cigarette Smoke. *Adv. Exp. Med. Biol.* 858, 47–55.

(34) Dehai, C., Bo, P., Qiang, T., Lihua, S., Fang, L., Shi, J., Jingyan, C., Yan, Y., Guangbin, W., and Zhenjun, Y. (2014) Enhanced Invasion of Lung Adenocarcinoma Cells after Co-Culture with THP-1-Derived Macrophages via the Induction of EMT by IL-6. *Immunol. Lett.* 160 (1), 1–10.

(35) Uboldi, C., Urbán, P., Gilliland, D., Bajak, E., Valsami-Jones, E., Ponti, J., and Rossi, F. (2016) Role of the Crystalline Form of Titanium Dioxide Nanoparticles: Rutile, and Not Anatase, Induces Toxic Effects in Balb/3T3 Mouse Fibroblasts. *Toxicol. In Vitro* 31, 137–145.

(36) Gerloff, K., Fenoglio, I., Carella, E., Kolling, J., Albrecht, C., Boots, A. W., Förster, I., and Schins, R. P. F. (2012) Distinctive Toxicity of TiO₂ Rutile/Anatase Mixed Phase Nanoparticles on Caco-2 Cells. *Chem. Res. Toxicol.* 25 (3), 646–655.

(37) Sayes, C. M., Wahj, R., Kurian, P. A., Liu, Y., West, J. L., Ausman, K. D., Warheit, D. B., and Colvin, V. L. (2006) Correlating Nanoscale Titania Structure with Toxicity: A Cytotoxicity and Inflammatory Response Study with Human Dermal Fibroblasts and Human Lung Epithelial Cells. *Toxicol. Sci.* 92 (1), 174–185.

(38) Kraegeloh, A., Suarez-Merino, B., Sluijters, T., and Micheletti, C. (2018) Implementation of Safe-by-Design for Nanomaterial Development and Safe Innovation: Why We Need a Comprehensive Approach. *Nanomaterials* 8 (4), 239.

(39) Zhang, S., Gao, H., and Bao, G. (2015) Physical Principles of Nanoparticle Cellular Endocytosis. *ACS Nano* 9 (9), 8655–8671.

(40) Hoshyar, N., Gray, S., Han, H., and Bao, G. (2016) The Effect of Nanoparticle Size on *in Vivo* Pharmacokinetics and Cellular Interaction. *Nanomedicine* 11 (6), 673–692.

(41) Yin, H., Too, H. P., and Chow, G. M. (2005) The Effects of Particle Size and Surface Coating on the Cytotoxicity of Nickel Ferrite. *Biomaterials* 26 (29), 5818–5826.

(42) Pan, Y., Neuss, S., Leifert, A., Fischler, M., Wen, F., Simon, U., Schmid, G., Brandau, W., and Jahn-Dechent, W. (2007) Size-Dependent Cytotoxicity of Gold Nanoparticles. *Small* 3 (11), 1941–1949.

(43) Wang, Y., Cui, H., Zhou, J., Li, F., Wang, J., Chen, M., and Liu, Q. (2015) Cytotoxicity, DNA Damage, and Apoptosis Induced by Titanium Dioxide Nanoparticles in Human Non-Small Cell Lung Cancer A549 Cells. *Environ. Sci. Pollut. Res.* 22 (7), 5519–5530.

(44) Ma, Y., Guo, Y., Wu, S., Lv, Z., Zhang, Q., and Ke, Y. (2017) Titanium Dioxide Nanoparticles Induce Size-Dependent Cytotoxicity and Genomic DNA Hypomethylation in Human Respiratory Cells. *RSC Adv.* 7 (38), 23560–23572.

(45) Simon-Deckers, A., Gouget, B., Mayne-L'Hermite, M., Herlin-Boime, N., Reynaud, C., and Carrière, M. (2008) *In Vitro* Investigation of Oxide Nanoparticle and Carbon Nanotube Toxicity and Intracellular Accumulation in A549 Human Pneumocytes. *Toxicology* 253 (1–3), 137–146.

(46) Zhu, R. R., Wang, S. L., Chao, J., Shi, D. L., Zhang, R., Sun, X. Y., and Yao, S. D. (2009) Bio-Effects of Nano-TiO₂ on DNA and Cellular Ultrastructure with Different Polymorph and Size. *Mater. Sci. Eng., C* 29 (3), 691–696.

(47) Braydich-Stolle, L. K., Schaeublin, N. M., Murdock, R. C., Jiang, J., Biswas, P., Schlager, J. J., and Hussain, S. M. (2009) Crystal Structure Mediates Mode of Cell Death in TiO₂ Nanotoxicity. *J. Nanopart. Res.* 11 (6), 1361–1374.

(48) Zhang, J., Song, W., Guo, J., Zhang, J., Sun, Z., Li, L., Ding, F., and Gao, M. (2013) Cytotoxicity of Different Sized TiO₂ Nanoparticles in Mouse Macrophages. *Toxicol. Ind. Health* 29 (6), 523–533.

(49) Jiang, J., Oberdörster, G., Elder, A., Gelein, R., Mercer, P., and Biswas, P. (2008) Does Nanoparticle Activity Depend upon Size and Crystal Phase? *Nanotoxicology* 2 (1), 33–42.

(50) Jugan, M. L., Barillet, S., Simon-Deckers, A., Herlin-Boime, N., Sauvaigo, S., Douki, T., and Carrière, M. (2012) Titanium Dioxide Nanoparticles Exhibit Genotoxicity and Impair DNA Repair Activity in A549 Cells. *Nanotoxicology* 6 (5), 501–513.

(51) Wang, L., Ai, W., Zhai, Y., Li, H., Zhou, K., and Chen, H. (2015) Effects of Nano-CeO₂ with Different Nanocrystal Morphologies on Cytotoxicity in HepG2 Cells. *Int. J. Environ. Res. Public Health* 12 (9), 10806–10819.

(52) Lee, J. H., Ju, J. E., Kim, B. Il, Pak, P. J., Choi, E.-K., Lee, H.-S., and Chung, N. (2014) Rod-Shaped Iron Oxide Nanoparticles Are More Toxic than Sphere-Shaped Nanoparticles to Murine Macrophage Cells. *Environ. Toxicol. Chem.* 33 (12), 2759–2766.

(53) Gea, M., Bonetta, S., Iannarelli, L., Giovannozzi, A. M., Maurino, V., Bonetta, S., Hodoroaba, V. D., Armato, C., Rossi, A. M., and Schilirò, T. (2019) Shape-Engineered Titanium Dioxide Nanoparticles (TiO₂-NPs): Cytotoxicity and Genotoxicity in Bronchial Epithelial Cells. *Food Chem. Toxicol.* 127, 89–100.

(54) Silva, R. M., TeeSy, C., Franzl, L., Weir, A., Westerhoff, P., Evans, J. E., and Pinkerton, K. E. (2013) Biological Response to Nano-Scale Titanium Dioxide (TiO₂): Role of Particle Dose, Shape, and Retention. *J. Toxicol. Environ. Health, Part A* 76 (16), 953–972.

(55) Zhao, Y., Wang, Y., Ran, F., Cui, Y., Liu, C., Zhao, Q., Gao, Y., Wang, D., and Wang, S. (2017) A Comparison between Sphere and Rod Nanoparticles Regarding Their *In Vivo* Biological Behavior and Pharmacokinetics. *Sci. Rep.* 7 (1), 4131.

(56) Brown, S. C., Kamal, M., Nasreen, N., Baumuratov, A., Sharma, P., Antony, V. B., and Moudgil, B. M. (2007) Influence of Shape, Adhesion and Simulated Lung Mechanics on Amorphous Silica Nanoparticle Toxicity. *Adv. Powder Technol.* 18 (1), 69–79.

(57) Vold, M. J. (1954) Van Der Waals' Attraction between Anisometric Particles. *J. Colloid Sci.* 9 (5), 451–459.

(58) Yameen, B., Choi, W., Vilos, C., Swami, A., Shi, J., and Farokhzad, O. C. (2014) Insight into Nanoparticle Cellular Uptake and Intracellular Targeting. *J. Controlled Release* 190, 485–499.

(59) Meng, H., Yang, S., Li, Z., Xia, T., Chen, J., Ji, Z., Zhang, H., Wang, X., Lin, S., Huang, C., Zhou, Z. H., Zink, J. I., and Nel, A. E. (2011) Aspect Ratio Determines the Quantity of Mesoporous Silica Nanoparticle Uptake by a Small Gtpase-Dependent Macropinocytosis Mechanism. *ACS Nano* 5 (6), 4434–4447.

(60) Powers, K. W., Palazuelos, M., Moudgil, B. M., and Roberts, S. M. (2007) Characterization of the Size, Shape, and State of Dispersion of Nanoparticles for Toxicological Studies. *Nanotoxicology* 1 (1), 42–51.

(61) Magdolenova, Z., Bilaničová, D., Pojana, G., Fjellsbø, L. M., Hudecova, A., Hasplová, K., Marcomini, A., and Dusinska, M. (2012) Impact of Agglomeration and Different Dispersions of Titanium Dioxide Nanoparticles on the Human Related *In Vitro* Cytotoxicity and Genotoxicity. *J. Environ. Monit.* 14 (2), 455.

(62) Andersson, P. O., Lejon, C., Ekstrand-Hammarström, B., Akfur, C., Ahlinder, L., Bucht, A., and Österlund, L. (2011) Polymorph- and Size-Dependent Uptake and Toxicity of TiO₂ Nanoparticles in Living Lung Epithelial Cells. *Small* 7 (4), 514–523.

(63) Noël, A., Maghni, K., Cloutier, Y., Dion, C., Wilkinson, K. J., Hallé, S., Tardif, R., and Truchon, G. (2012) Effects of Inhaled Nano-TiO₂ Aerosols Showing Two Distinct Agglomeration States on Rat Lungs. *Toxicol. Lett.* 214 (2), 109–119.

(64) Forest, V., Cottier, M., and Pourchez, J. (2015) Electrostatic Interactions Favor the Binding of Positive Nanoparticles on Cells: A Reductive Theory. *Nano Today* 10 (6), 677–680.

(65) Wilhelm, C., Billotey, C., Roger, J., Pons, J. N., Bacri, J. C., and Gazeau, F. (2003) Intracellular Uptake of Anionic Superparamagnetic Nanoparticles as a Function of Their Surface Coating. *Biomaterials* 24 (6), 1001–1011.

(66) Thevenot, P., Cho, J., Wavhal, D., Timmons, R. B., and Tang, L. (2008) Surface Chemistry Influences Cancer Killing Effect of TiO₂ Nanoparticles. *Nanomedicine* 4 (3), 226–236.

(67) Lehman, S. E., Morris, A. S., Mueller, P. S., Salem, A. K., Grassian, V. H., and Larsen, S. C. (2016) Silica Nanoparticle-Generated ROS as a Predictor of Cellular Toxicity: Mechanistic Insights and Safety by Design. *Environ. Sci.: Nano* 3 (1), 56–66.

(68) Chavez, D. H., Juarez-Moreno, K., and Hirata, G. A. (2016) Aminosilane Functionalization and Cytotoxicity Effects of Uncon-

sion Nanoparticles Y₂O₃ and Gd₂O₃ Co-Doped with Yb³⁺ and Er³⁺. *Nanobiomedicine* 3, 1.

(69) Petushkov, A., Intra, J., Graham, J. B., Larsen, S. C., and Salem, A. K. (2009) Effect of Crystal Size and Surface Functionalization on the Cytotoxicity of Silicalite-1 Nanoparticles. *Chem. Res. Toxicol.* 22 (7), 1359–1368.

(70) Klein, S. G., Serchi, T., Hoffmann, L., Blömeke, B., and Gutleb, A. C. (2013) An Improved 3D Tetraculture System Mimicking the Cellular Organisation at the Alveolar Barrier to Study the Potential Toxic Effects of Particles on the Lung. *Part. Fibre Toxicol.* 10 (1), 31.

(71) Dehai, C., Bo, P., Qiang, T., Lihua, S., Fang, L., Shi, J., Jingyan, C., Yan, Y., Guangbin, W., and Zhenjun, Y. (2014) Enhanced Invasion of Lung Adenocarcinoma Cells after Co-Culture with THP-1-Derived Macrophages via the Induction of EMT by IL-6. *Immunol. Lett.* 160 (1), 1–10.

(72) Rothen-Rutishauser, B. M., Kiama, S. C., and Gehr, P. (2005) A Three-Dimensional Cellular Model of the Human Respiratory Tract to Study the Interaction with Particles. *Am. J. Respir. Cell Mol. Biol.* 32 (4), 281–289.

1. Complementary Data

We also assessed the toxicity induced by the 5 TiO₂ NPs in THP-1 macrophages differentiated from THP-1 monocytes. In parallel, we used further biological assays such as the LDH release and the MTT assay to better understand TiO₂ NP toxicity.

1.1. Cell membrane integrity-Lactate dehydrogenase release

Lactate dehydrogenase (LDH) is released by the cells to the extracellular medium when the cell membrane ruptures. LDH converts lactate to pyruvate, generating NADH from NAD⁺. The NADH interacts with the iodinitrotetrazolium chloride (INT) and subsequently INT is converted into a red color formazan (Figure 17). The amount of colored product formed is directly proportional to the LDH activity in the sample.

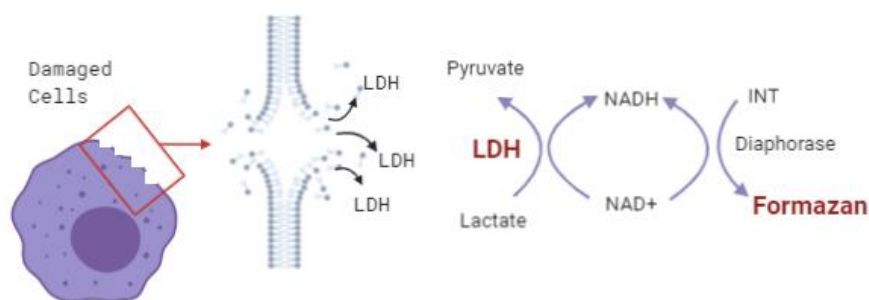


Figure 17. Principle of LDH release assay.

In order to assess cell membrane integrity after exposure to TiO₂ NPs, the release of LDH was measured in the culture medium by using a commercial kit CytoTox-96™ Homogeneous Membrane Integrity Assay (Promega, Charbonnières-les-Bains, France), following the supplier's instructions. The fluorescence was measured at 490 nm using a spectrophotometer (Multiskan RC; Thermolabsystems, Helsinki, Finland). The value of each sample was expressed as a function of the maximum LDH released by the cells (measured after cell lysis), as a percentage of cellular integrity compared to the positive control (lysed cells) as presented in Figure 18.

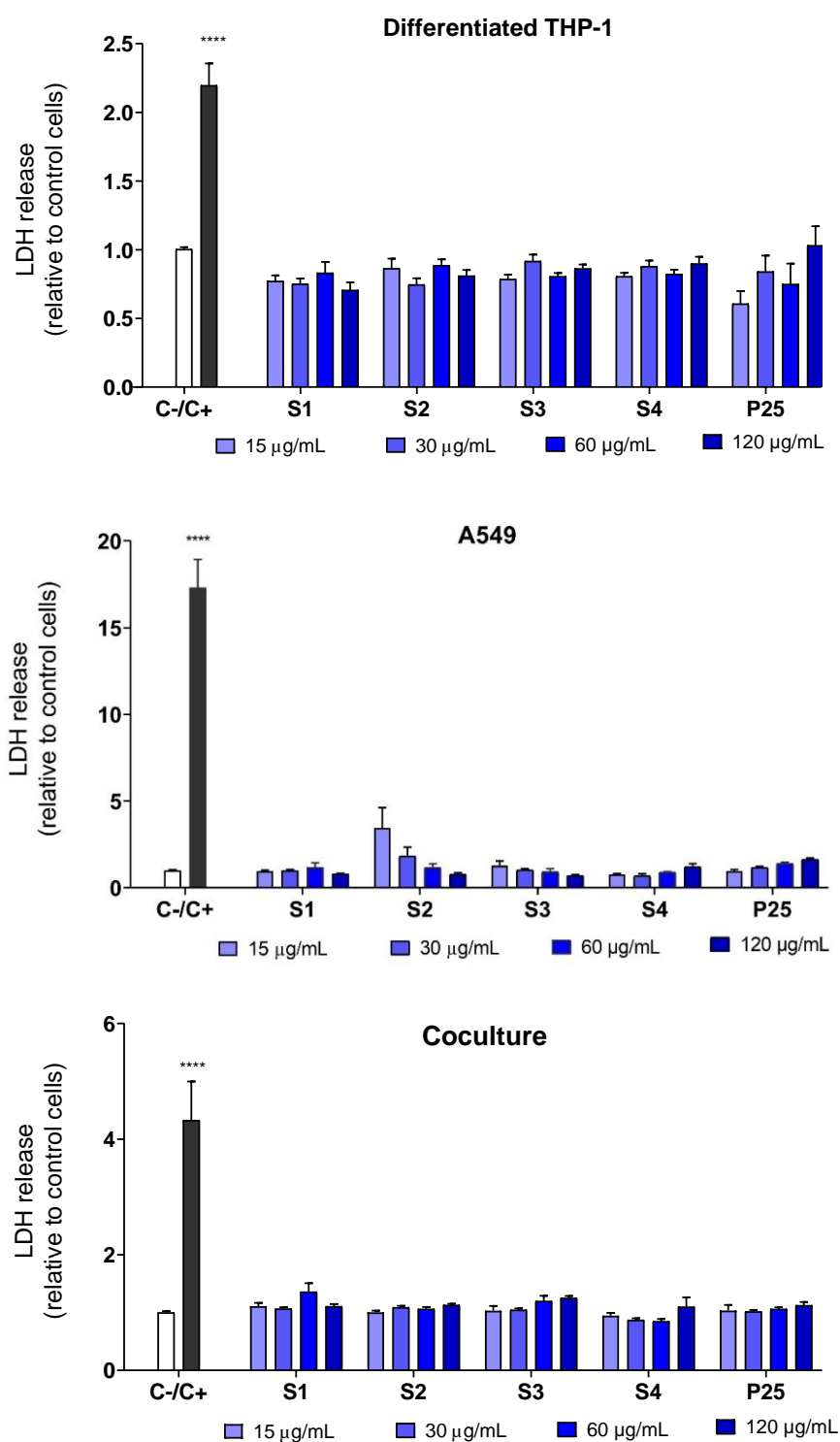


Figure 18. LDH release 24 h after cell exposure to TiO₂ NPs. Control (C-) represents unexposed cells. Lysed cells were used as positive control (C+). Values are the mean ± SEM of three independent experiments. Statistically different from control (****) $P < 0.0001$. Statistical analyses were conducted using one-way Anova analyses, followed by Dunnett's test.

Titanium dioxide NPs did not induce significant LDH release in all cell systems. This is in accordance with previous studies, which demonstrated that P25 TiO₂ NPs did not induce LDH release in THP-1 macrophages [164], A549 cells, BEAS-2B cells [169], However, other studies detected LDH increases in A549 cells especially after exposure to P25 [170] and in THP-1 cells [171].

Besides the contradictory results in the literature, our LDH results were not consistent with microscopic observations. The LDH activity was observed to lessen in TiO₂ NPs treated cells compared to the control, and this loss of activity was probably due to the interaction between NPs and LDH enzyme. The possible interaction was evaluated in *Chapter 5*. Therefore, cytotoxicity was assessed by using other methods.

1.2. Cell viability-MTT assay

The 4,5-dimethylthiazol-2-yl-2,5-diphenyltetrazolium bromide (MTT) test is a colorimetric analysis used to evaluate the metabolic activity of cells [172]. In this test, MTT (a yellow water-soluble tetrazolium salt) passes through the cell membrane and enters the cell mitochondria (Figure 19). Living cells use NAD(P)H-bound oxidoreductase enzymes to reduce the yellow MTT reagent to dark purple water-insoluble formazan while this color formation is not observed in dead cells due to their lack of metabolic activity [173,174].

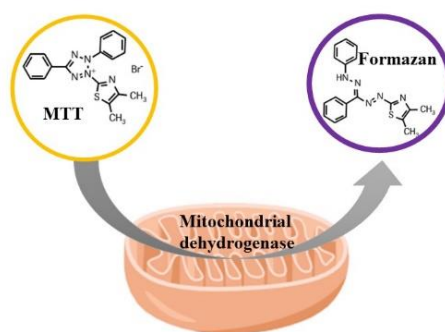


Figure 19. MTT reduction into purple formazan by mitochondrial dehydrogenase in viable cells.

Water insoluble formazan crystals formation can then be determined in DMSO by measuring the absorbance with a spectrophotometer at a specific wavelength (usually between 500 and 600 nm).

10^5 A549 cells, differentiated THP-1 cells and cocultured A549 and differentiated THP-1 at 10:1 ratio were seeded into 96 well plates. After 24 hours of seeding, cells were exposed to TiO₂ NPs at 15, 30, 60, and 120 µg/mL concentration for 24 hours. MTT (5 mg/mL stock in DPBS) was added in the volume of 20 µL/well in 200 µL of cell suspension, and the plate was incubated for 3 h at 37°C. At the end of the incubation period, the medium was carefully aspirated and 200 µL of DMSO was added to each well and mixed gently. Absorbances of cells treated with TiO₂ NPs (A_{sample}) and control cell absorbances (A_{control}) were read on a microplate reader at 570 nm (Multiskan RC; ThermoFisher, Helsinki, Finland). Viability was calculated with formula given below.

$$\text{Viability \%} = \frac{A_{\text{sample}}}{A_{\text{control}}} \times 100$$

24 hours after exposure of differentiated THP-1 cells, A549 and cocultured cells to TiO₂ NPs, cell viability was measured by MTT assay and the results are presented in Figure 20.

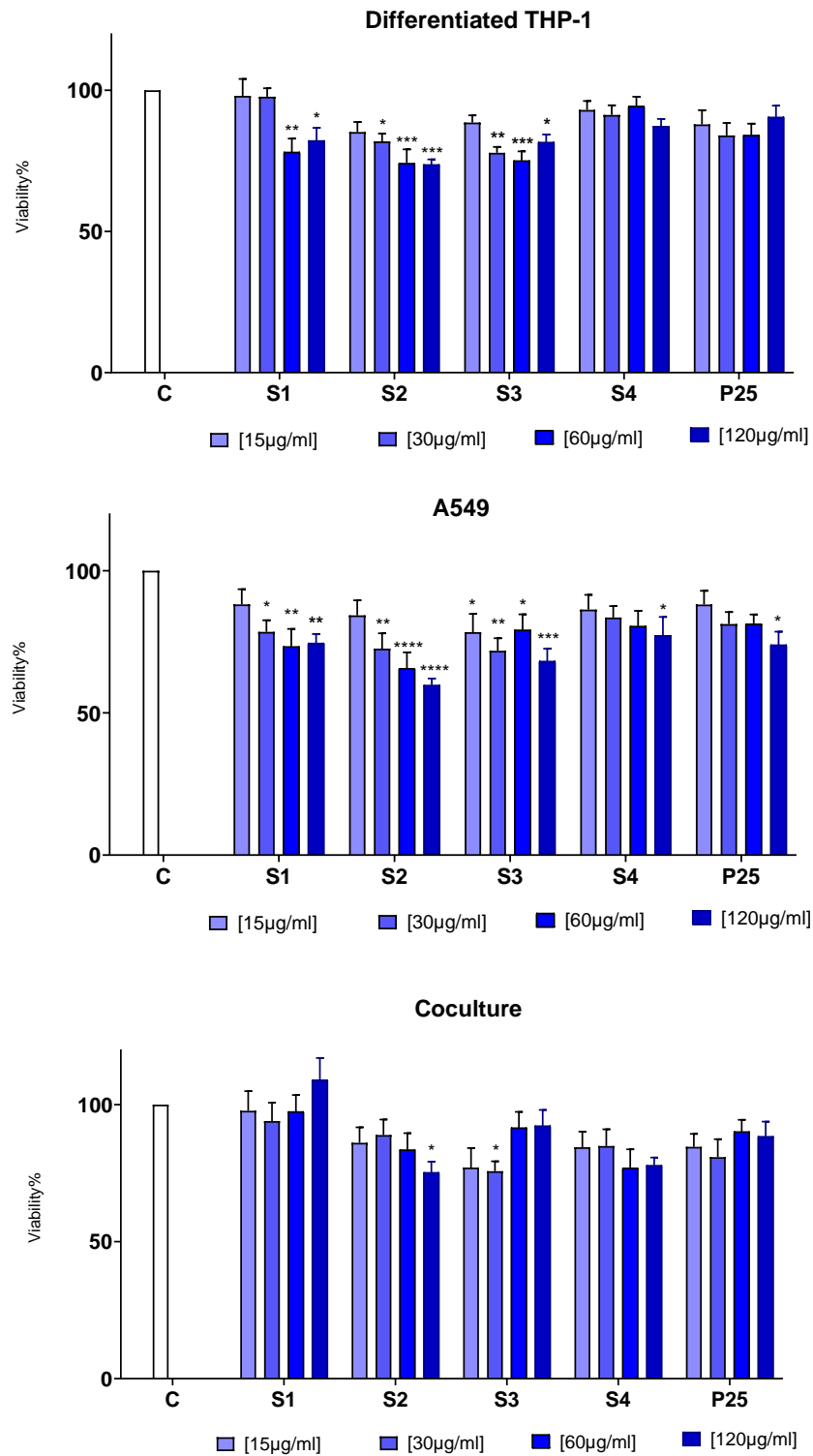


Figure 20. Cell viability after 24 h exposure to TiO₂ NPs assessed by MTT. Control (C) represents unexposed cells. Values are the mean ± SEM of three independent experiments. Statistically different from control (*) $P < 0.05$, (**) $P < 0.01$, (***) $P < 0.0001$, (****) $P < 0.0001$. Statistical analyses were conducted using one-way Anova analyses, followed by Dunnett's test.

After exposure to TiO₂ NPs, cell-type dependent cytotoxicity was observed. Slight decreases in differentiated THP-1 cell viability were detected compared to the control group (unexposed to TiO₂ NPs). TiO₂ NPs cytotoxicity was more pronounced in A549 cells than in differentiated THP-1. In coculture, lower cell viability was observed in TiO₂ NPs treated cells compared to the control group, except for S1. However, no statistically significant difference was found except for S2 at 120 µg/mL and S3 at 30 µg/mL.

Similar to our results slight but significant decreases were observed after 10, 50 and 100 µg/mL < 25 nm TiO₂ NPs exposure to A549 cells for 24 and 48 h (between 70-90% viability) [175]. 250 and 500 µg/mL 25 nm TiO₂ NPs exposure also caused significant cell viability decrease in A549 [176]. In another study, cell viability of THP-1 macrophages decreased after exposure to 10-50 µg/mL of anatase 50 nm, 100 nm TiO₂ particles [177]. However, 24 h exposure of 10, 50, 100 µg/mL P25 did not cause the decrease in cell viability of A549 and differentiated THP-1 [178], at the 0-200 µg/mL TiO₂ exposure [179] or wide range concentration (0-800 µg/mL) [180]. Even long term exposure (2 months) to 50 µg/mL TiO₂ NPs did not affect A549 cell viability [181]. The reason for these contradictory results in the literature may be due to the fact that possible interactions between NPs and MTT reagent were discussed and taken into account in some studies [175,180,181], while not in others.

There are studies reporting that commonly used cytotoxicity tests, LDH, and tetrazolium-based tests (*e.g.* MTS and MTT) are interfered by a number of different NPs [182,183]. In our study, as in the LDH experiment, the results obtained in the MTT test were not consistent with microscopic observations. For this reason, preliminary studies were conducted for the bias of MTT and LDH analysis and reported in *Chapter 5*. Because both methods might not reflect the true results of the TiO₂ NPs cytotoxicity, the cell viability was measured by the trypan blue method as reported in the *Article 1*.

1.3. Pro-inflammatory response

TNF-α production after differentiated THP-1 cells were exposed to TiO₂ NPs is shown in Figure 21.

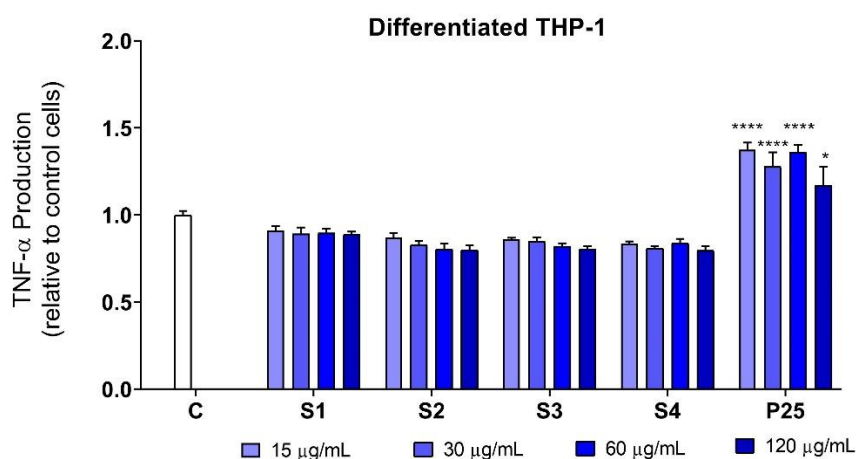


Figure 21. TNF- α production after a 24 h exposure of differentiated THP-1 to TiO₂ NPs. Control (C) represents unexposed cells. Values are the mean \pm SEM of three independent experiments. Statistically different from control (*) $P < 0.05$ (****) $P < 0.0001$. Statistical analyses were conducted using one-way Anova analyses, followed by Dunnett's test.

P25 caused a significantly increased TNF- α production compared to control group, whereas no any significant TNF- α production was observed for other samples.

Similar to our results, Morishige *et al.* showed no significant TNF- α and IL-1 β production after exposure to TiO₂ NPs (<50 μ m, <25 nm, 10 nm) in differentiated THP-1 cells with 0.5 μ M PMA for 24 h [184]. Also, 100 nm anatase TiO₂ NPs did not induce IL-1 β , IL-8, TNF- α in differentiated THP-1 cells (100 nm PMA for 72 h) [185]. 20–30 nm 2.5 mg/mL TiO₂ NPs in serum-free media also did not cause TNF- α production [186].

Although Li and Mithran (2014) showed no triggered pro-inflammatory response production upon P25 treatment [187], we found an increase in TNF- α production after P25 treatment.

In THP-1 differentiated cells, a factor contributing to the contradictory results might be the variable PMA concentrations used. Concerning PMA treatment on THP-1, the conditions for the culture should be taken into consideration to obtain a homogeneous culture expressing reliable responses. In these results, the concentration of PMA and the differentiated cell density are essentially important. The differences in stimulating reagents and treatments may result in the production of different types of cytokines at different levels.

1.4. Oxidative stress

ROS production after exposure of differentiated THP-1 cells to TiO₂ NPs is reported in Figure 22.

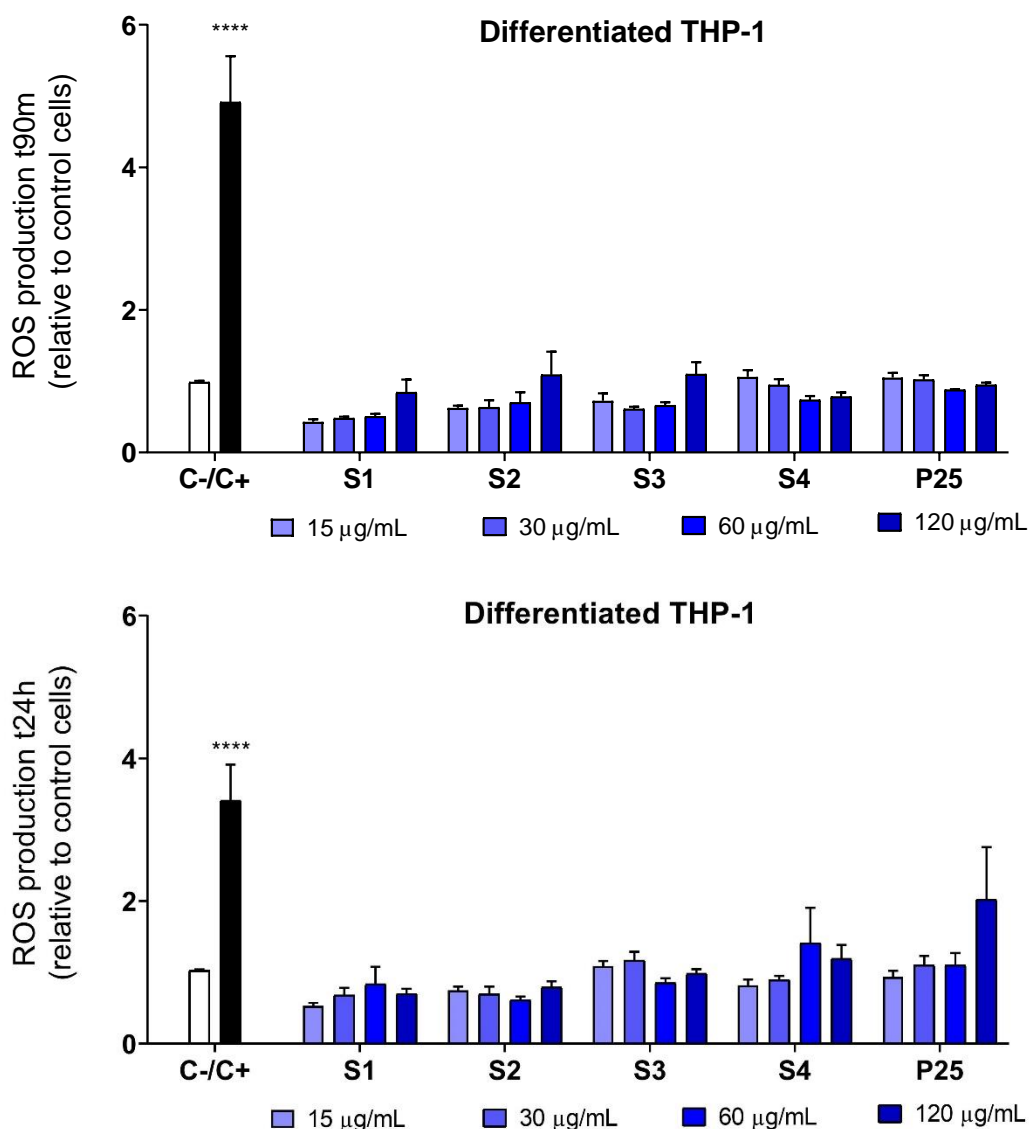


Figure 22. ROS production after 90 min and 24 hours exposure to the indicated concentrations of TiO₂ NPs in differentiated THP-1. Control (C-) represents unexposed cells, positive control (C+) cells incubated with H₂O₂. Statistically different from control (****) $P < 0.0001$. Statistical analyses were conducted using one-way Anova analyses, followed by Dunnett's test.

TiO₂ NPs did not induce significant ROS production in differentiated THP-1 compared to the control group (unexposed to TiO₂ NPs) whatever the time of analysis (90 min or 24 h). These results are not in agreement with previous studies which

reported ROS generation in differentiated THP-1 cells after 24 h exposure to 200 and 800 µg/mL TiO₂. Even at short exposure time (3h) 25-50 µg/mL of anatase 50 nm, 100 nm TiO₂ particles and P25 caused ROS production along with the pro-inflammatory induction in THP-1 macrophages [177]. It was reported that ROS were responsible for inflammation activation leading to IL-1β maturation in PMA-differentiated THP-1 macrophages, under TiO₂ nanoparticle stimulation [184,188]. Nanomaterials can induce the production of ROS, and thereby induce inflammatory pathways especially on activated macrophages. However, in our study P25 did not cause the pro-inflammatory induction, ROS generation was not observed. The reason for the absence of oxidative stress upon treatment with NPs was discussed in the *Articles 1 and 2*. There might be possible interferences between the NPs and the DCF in DCFH-DA ROS assay which could hinder the traceability chain by quenching the fluorescent signal. An unintended bias should be taken into consideration. Further studies with different methods are required for the ROS production potential of nanoparticles.

2. Conclusion

The highlights of the article '**Impact of the physicochemical features of TiO₂ NPs on their *in vitro* toxicity**' were:

- Rod, bigger, less agglomerated and positively charged particles are more toxic,
- Cocultured model seems more sensitive than A549 monocultures.

There was no correlation between microscopic observations of the cells and LDH, MTT results after TiO₂ NPs exposure. Therefore, cell viability was determined by trypan blue method and the results are reported in *Article 1*.

The possible interaction between TiO₂ NPs and MTT, LDH assays were examined in Chapter 5.

When the proinflammatory response was evaluated on differentiated THP-1 cells, a significant production of TNF-α was observed only for P25 treated cells.

In differentiated THP-1 cells, no significant ROS production was observed compared to the control.

Les points clés de l'article '**Impact des caractéristiques physicochimiques des NPs TiO₂ sur leur toxicité *in vitro***' ont été:

- Les NPs en forme de bâtonnets, de taille plus grande, moins agglomérées et chargées positivement sont plus toxiques,
- Le modèle de coculture semble plus sensible que les monocultures A549.

Il n'y avait pas de corrélation entre les observations microscopiques des cellules et les résultats des tests LDH et MTT après exposition aux NPs de TiO₂. Par conséquent, la viabilité cellulaire a été déterminée par la méthode du bleu trypan et les résultats sont rapportés dans l'*Article 1*. L'interaction possible entre les NPs de TiO₂ et les tests MTT et LDH a été examinée au Chapitre 5.

Lorsque la réponse pro-inflammatoire a été évaluée sur des cellules THP-1 différenciées, une production significative de TNF- α a été observée seulement pour les cellules exposées au P25.

Dans les cellules THP-1 différenciées, aucune production significative de ROS n'a été observée par rapport au groupe contrôle.

Chapter 3

Short Pre-irradiation of TiO₂ Nanoparticles Increases Cytotoxicity on Human Lung Coculture System

Titanium dioxide nanoparticles are semiconductor materials which are widely used in a variety of applications especially in water treatment, air purification, self-cleaning surfaces due to their photocatalytic activity. Considering the transition of TiO₂ into a photoactive state under sunlight, workers and the general population exposure to photoactivated TiO₂ by inhalation is very likely. To date, TiO₂ NPs toxicity has been extensively investigated whereas limited data is available regarding the toxicity of TiO₂ NPs that have been pre-exposed to UV light, and their impact on humans remains unknown.

After we explored the impact of physicochemical properties of TiO₂ NPs on their toxicity in *Chapter 2*, the impact of UV irradiation of TiO₂ on toxicity has been taken into account in order to improve knowledge of the mechanisms involved in the toxicity of TiO₂ NPs. The aim and originality of this study were to investigate if a short time exposure of five different TiO₂ NPs to UV light induced changes in their physicochemical properties and eventually affected their toxicity on a human lung coculture system. The ROS production induced by TiO₂ NPs in cell free conditions was assessed through a collaboration with the Department of Chemistry and “G. Scansetti” Interdepartmental Center for Studies on Asbestos and other Toxic Particulates, Università degli Studi di Torino during my 3 months doctoral mobility program.

This collaborative research led to the production of *Article 2*, submitted to *Chemical Research in Toxicology*.

Chapitre 3

Une Courte Pré-irradiation de Nanoparticules de TiO₂ Provoque une Augmentation de leur Cytotoxicité dans un Modèle de Coculture de Cellules Pulmonaires Humaines

Les nanoparticules de dioxyde de titane sont des matériaux semi-conducteurs qui sont largement utilisés dans une variété d'applications, en particulier dans le traitement de l'eau, la purification de l'air, les surfaces auto-nettoyantes en raison de leur activité photocatalytique. Compte tenu du passage du TiO₂ à un état photoactif sous la lumière du soleil, les travailleurs et la population en général sont exposés au TiO₂ photoactivé par inhalation. À ce jour, la toxicité des NPs de TiO₂ a fait l'objet de recherches approfondies alors que des données limitées sont disponibles concernant la toxicité des NPs de TiO₂ qui ont été pré-exposées à la lumière UV, et leur impact sur l'homme reste inconnu.

Après avoir exploré l'impact des propriétés physicochimiques des NPs de TiO₂ sur leur toxicité au *Chapitre 2*, l'impact de l'irradiation UV du TiO₂ sur la toxicité a été pris en compte afin d'améliorer nos connaissances des mécanismes impliqués dans la toxicité des NPs de TiO₂. L'objectif et l'originalité de cette étude étaient d'étudier si une exposition de courte durée à la lumière UV induit des changements dans les propriétés physicochimiques de cinq NPs de TiO₂ différentes et affecte finalement leur toxicité dans un modèle de coculture de cellules pulmonaires humaines.

La production de ROS induite par les NPs de TiO₂ a été testée en conditions acellulaires grâce à une collaboration avec le Département de Chimie et le "G. Scansetti" Interdepartmental Center for Studies on Asbestos and other Toxic Particulates, de l'Università degli Studi di Torino lors de ma mobilité doctorale de 3 mois.

Cette étude collaborative a conduit à la rédaction de l'*Article 2* soumis à Chemical Research in Toxicology.

Chemical Research in Toxicology

This document is confidential and is proprietary to the American Chemical Society and its authors. Do not copy or disclose without written permission. If you have received this item in error, notify the sender and delete all copies.

Short pre-irradiation of TiO₂ nanoparticles increases cytotoxicity on human lung coculture system

Journal:	<i>Chemical Research in Toxicology</i>
Manuscript ID	Draft
Manuscript Type:	Article
Date Submitted by the Author:	n/a
Complete List of Authors:	Kose, Ozge; Mines Saint-Étienne Tomatis, Maura; Università degli Studi di Torino, Dept. of Chemistry Turci, Francesco; Università degli Studi di Torino, Dept. of Chemistry Belbidia, Naila-Besma; Mines ParisTech Hochepped, Jean-François; Mines ParisTech, MAT Pourchez, Jeremie; Ecole des Mines de Saint-Etienne, center for health engineering Forest, Valerie; Mines Saint-Étienne,

SCHOLARONE™
Manuscripts

1
2
3 **Short pre-irradiation of TiO₂ nanoparticles increases cytotoxicity on human**
4
5
6 **lung coculture system**
7
8

9
10
11 Ozge Kose[†], Maura Tomatis[‡], Francesco Turci[‡], Naila-Besma Belblidia^{§,¶} Jean-François
12
13 Hochepped^{§,¶}, Jérémie Pourchez[†], Valérie Forest^{†*}
14
15

16
17
18 [†]Mines Saint-Etienne, Univ Lyon, Univ Jean Monnet, INSERM, U 1059 Sainbiose, Centre CIS,
19
20 F-42023 Saint-Etienne, France

21
22 [‡]Dipartimento di Chimica and 'G. Scansetti' Interdepartmental Center for Studies on Asbestos
23
24 and other Toxic Particulates, Università degli Studi di Torino, Torino, Italy

25
26
27 [§]Mines ParisTech, PSL Research University, MAT - Centre des matériaux, CNRS UMR 7633,
28
29 BP 87 91003 Evry, France

30
31
32 [¶]ENSTA ParisTech UCP, Institut Polytechnique Paris, 828 bd des Maréchaux, 91762 Palaiseau
33
34 cedex France

35
36
37
38
39 * **Corresponding author:** Valérie Forest:

40
41 Mines Saint-Etienne, 158 cours Fauriel, CS 62362, 42023 Saint-Etienne Cedex 2. FRANCE.

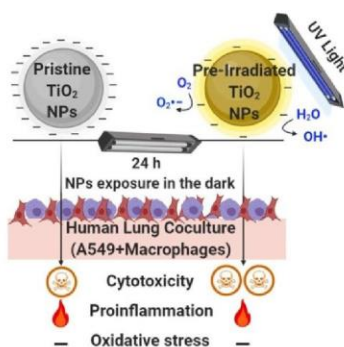
42
43 Email: vforest@emse.fr
44
45

46
47
48 **Keywords**

49
50 Titanium dioxide nanoparticles; UVA irradiation; cytotoxicity; pro-inflammatory response;
51
52 reactive oxygen species; human lung coculture
53
54
55
56
57
58
59
60

1
2
3
4
5
6
7
8
9
10
11
12
13
14
15
16
17
18
19
20
21
22
23
24
25
26
27
28
29
30
31
32
33
34
35
36
37
38
39
40
41
42
43
44
45
46
47
48
49
50
51
52
53
54
55
56
57
58
59
60

Table of Content graphic



1
2
3
4
5
6
7
8
9
10
11
12
13
14
15
16
17
18
19
20
21
22
23
24
25
26
27
28
29
30
31
32
33
34
35
36
37
38
39
40
41
42
43
44
45
46
47
48
49
50
51
52
53
54
55
56
57
58
59
60**Abstract**

Anatase titanium dioxide nanoparticles (TiO₂ NPs) are used in a large range of industrial applications mainly due to their photocatalytic properties. Before entering the lung, virtually all TiO₂ NPs are exposed to some UV light and lung toxicity of TiO₂ NPs might be influenced by photoexcitation that is known to alter TiO₂ surface properties. Although the TiO₂ NPs toxicity has been extensively investigated, limited data is available regarding the toxicity of TiO₂ NPs that have been pre-exposed to UV light, and their impact on humans remains unknown. In this study, five types of TiO₂ NPs with tailored physicochemical features were characterized and irradiated by UV for 30 min. Following irradiation, cytotoxicity, pro-inflammatory response, and oxidative stress on a human lung coculture system (A549 epithelial cells and macrophages differentiated from THP-1 cells) were assessed. The surface charge of all samples was less negative after UV irradiation of TiO₂ NPs and the average aggregate size was slightly increased. A higher cytotoxic effect was observed for pre-irradiated TiO₂ NPs compared to non-irradiated samples. Pre-irradiation of TiO₂ NPs had not a significant impact on the pro-inflammatory response and oxidative stress as shown by a similar production of IL-8, TNF- α and reactive oxygen species.

1. Introduction

Titanium dioxide nanoparticles (TiO₂ NPs), especially anatase form, are widely used in a large range of industrial applications in inks, plastic materials, ceramics, paper, foods, pharmaceutical and cosmetics due to their resistance to discoloration, high refractive index and photocatalytic activity. TiO₂ photocatalysis is a promising process and has attracted remarkable attention for the application of air and water purification¹⁻³.

Upon UV irradiation, photo-excited electrons migrate from TiO₂ bulk to surface, forming an electron/hole pair (e⁻/h⁺). In the presence of water and oxygen molecules, the electron/hole pair generates hydroxyl (OH•) or superoxide (O₂•⁻) radicals which lead to the decomposition of a variety of organic and inorganic compounds^{4,5}. This process may alter surface hydrophilicity and charge, may promote particle aggregation and enhance generation of reactive oxygen species (ROS)⁶⁻⁸. Some of these effects are transient (*e.g.*, ROS generation) and stop as soon as irradiation stops, whereas the changes in surface charge and particle aggregation persist over time⁶ and may likely affect TiO₂ NPs' toxicity potential.

While some *in vitro* studies have shown that TiO₂ NPs reduce cell viability, increase ROS production and cytokine levels and cause genotoxicity even without light⁹⁻¹¹, several recent studies have shown that toxicity of TiO₂ is higher in the presence of UV light than in the dark¹²⁻¹⁴. Furthermore, several *in vivo* studies showed that TiO₂ NPs cause pulmonary inflammation, cell damage and oxidative DNA damage¹⁵⁻¹⁷.

Sunlight reaching the Earth includes ca. 5% of UV radiation (315–400 nm, with a dose reaching the ground up to 0.1 W/cm²)¹⁸. TiO₂ NPs in the environment are expected to be exposed to UV rays and possibly modified following photoexcitation. Due to the number of applications and the consequent environmental availability of TiO₂, inhalation of pre-irradiated TiO₂ NPs is likely the most common exposure route for humans. To the best of our knowledge, only one study¹⁹ has been focused so far on the cellular effect induced by TiO₂ NPs preliminarily

1
2
3 exposed to UV light (pre-irradiated) for 24 hours and then incubated with cells in the dark. To
4
5 assess whether short time of UV light exposure induces changes in the physico-chemical
6
7 properties and eventually affects TiO₂ NPs toxicity, we evaluated: (a) the changes of
8
9 physicochemical properties caused by a short time UV irradiation on five samples differing in
10
11 size, shape and surface charge, and (b) the toxicity in human lung coculture cells, before and
12
13 after UV irradiation. To this purpose, we irradiated the samples for 30 min and we measured
14
15 surface charge, aggregate size and the ability to generate free radicals in cell-free systems.
16
17 Cytotoxicity, pro-inflammatory response (IL-8 and TNF- α release), and ROS generation were
18
19 then evaluated on a coculture of human lung epithelial cells and macrophages differentiated
20
21 from THP-1 monocytes.
22
23
24
25
26
27

28 **2. Material and Methods**

30 **2.1 Synthesis and preparation of TiO₂ nanoparticle dispersion**

31
32 In this study, we used four custom-made TiO₂ NPs with different and well-controlled properties
33
34 and one commercially available P25 sample with a purity > 99.5% (Evonik P25 CAS: 1317-
35
36 70-0, Sigma-Aldrich, Saint-Quentin-Fallavier, France). Evonik P25 TiO₂ was chosen for
37
38 analysis as a reference particle due to its well-known photocatalytic activity²⁰ and it has been
39
40 used in many tests as photocatalyst standard material by many studies^{21,22}.
41
42
43

44
45 Four TiO₂ NPs synthesis was performed using Chen *et al.*²³ method and they were named S1
46
47 to S4. Basically, titanium (IV) butoxide (CAS: 5593-70-4 reagent grade 97%, Sigma-Aldrich,
48
49 Saint-Quentin-Fallavier, France) was mixed with triethanolamine (CAS: 102-71-6, analytical
50
51 reagent 97%, VWR International, Fontenay-sous-Bois, France) in 1:2 molar ratio. The mixture
52
53 was put in Teflon lined sealed and kept at a high temperature (150°C) for 24 h in autoclave.
54
55 The pH of synthesis medium was adjusted by adding HCl or NH₄OH to tune particle size and
56
57 morphology. Finally, the solutions were centrifuged three times and washed with deionized
58
59
60

1
2
3 water. The resulting products were dried in an oven at 40°C. Surface functionalization of S2
4
5 NPs was generated by aminopropyltriethoxysilane (APTES) using Zhao *et al.*²⁴ method and
6
7 the functionalized nanoparticle labeled as S4. Their features are reported in Table 1. Stock
8
9 suspensions of all NPs (1600 µg/mL) were prepared in deionized water (Milli-Q systems,
10
11 Millipore) and sonicated with Branson Sonifier S-450 by cuphorn sonication in pulsed mode (2
12
13 s on/ 2 s off) for 10 min at 89 % amplitude. Before each experiment stock suspensions were
14
15 sonicated for 15 min in a bath sonicator and vortexed vigorously diluted in culture medium, *i.e.*
16
17 Dulbecco's Modified Eagle Medium (DMEM) containing 10% fetal bovine serum (FBS) to 15,
18
19 30, 60 and 120 µg/mL.
20
21
22

23 24 25 26 **2.2. Exposure to UV light**

27
28 The TiO₂ stock suspensions (1600 µg/mL in deionized water) were transferred into glass tubes
29
30 and irradiated by UV light provided by a 100 W UV lamp (365 nm UV light, FV-97600-15
31
32 Cole-Parmer, Paris, France) for 30 minutes. The irradiation intensity was 1 mW/cm² as
33
34 measured by a radiometer (Model PCE-UV34, PCE Instruments UK Ltd, Southampton, UK)
35
36 simulating an indoor environment^{25,26}, and maximal irradiance of occupational exposure of
37
38 UV²⁷. The stock suspensions were diluted in DMEM culture medium after the end of the UV
39
40 irradiation of TiO₂ NPs and applied to the cells. The time from the end of the UV irradiation
41
42 and the cell exposure was 15 min maximum.
43
44
45
46
47
48

49 50 **2.3. Physicochemical characterization of TiO₂ nanoparticles**

51
52 Size and shape were analyzed by transmission electron microscopy (TEM) using a FEI
53
54 TECNAI 20FST operating at 200 kV and scanning electron microscopy (SEM) at 2-3 kV on a
55
56 Zeiss Sigma 300 microscope using a secondary electron (SE) detector. Specific surface areas
57
58 were measured by Brunauer, Emmett and Teller (BET) method (ASAP 2020 Volumetric
59
60

1
2
3 Adsorption, Micrometrics, USA). Raman spectroscopy (Horiba Jobin–Yvon Xplora
4 spectrometer) and X-ray powder diffraction (XRPD, Miniflex, Rigaku, Japan) techniques were
5
6 used for the structural identification of the crystalline phases of NPs as reported in our previous
7
8 study ²⁸.

9
10
11
12 The spin trapping technique (5-5'- dimethyl-1-pyrroline-N-oxide, DMPO, as trapping agent)
13 associated to the electron spin resonance (ESR) spectroscopy (Miniscope 100 ESR
14 spectrometer, Magnettech, Germany) was used to assess the radical formation from UV
15 irradiated TiO₂ NPs in a cell free system. TiO₂ samples (120 µg/mL) were suspended in a
16 buffered solution (potassium phosphate buffer 0.25 M, pH 7.4) containing 0.04 M DMPO or
17 0.04 M DMPO and 1 M sodium formate to detect hydroxyl and carboxyl radicals, respectively.
18
19 ESR spectra were recorded on aliquot (50 µL) withdrawn after 30 min of UV irradiation. The
20 instrument settings were as follows: microwave power 10 mW; modulation 1000 mG; scan
21 range 120 G; center of field 3345 G. Blanks (negative controls) were performed with the same
22 reaction mixtures without TiO₂. All experiments were repeated at least twice.

23
24
25
26 The hydrodynamic size and surface charge of pristine and irradiated TiO₂ NPs (120 µg/mL) in
27 DI water and in DMEM were determined by using dynamic light scattering (DLS, Zetasizer
28 Nano ZS Malvern Instruments, Worcestershire, UK) and electrophoretic light scattering (ELS,
29 Zetasizer Nano ZS Malvern Instruments, Worcestershire, UK).

2.4 *In vitro* toxicity study

2.4.1 Cell culture

30
31
32
33
34
35
36
37
38
39
40
41
42
43
44
45
46
47
48
49
50
51
52
53
54
55
56
57
58
59
60
The A549 human carcinoma epithelial cell line was supplied by the American Type Culture
Collection (ATCC, CCL-185). A549 cells were grown in DMEM supplemented with 10% (v/v)
FBS (S1810; Biowest, Nuaille, France), 1% penicillin-streptomycin (VWR International,
Fontenay-sous-Bois, France) and after reaching 80% confluency cells were trypsinized, washed

1
2
3 with sterile phosphate-buffered saline (PBS) and centrifuged at 1500 g for 10 min and
4
5 subcultured. The flasks were stored at 37°C in a humidified atmosphere with 5% CO₂.
6

7
8 The THP-1 human monocytic leukemia monocyte cell line (ATCC, TIB-202™) was a generous
9
10 gift from Dr Ghislaine Lacroix from French National Institute for Industrial
11
12 Environment and Risks (INERIS, France). THP-1 was cultured in Roswell Park Memorial
13
14 Institute (RPMI) 1640 (Gibco, Life Technologies, Cergy-Pontoise, France) containing 10%
15
16 FBS and 1% penicillin-streptomycin. THP-1 cells were counted with Trypan Blue regularly
17
18 and subcultured usually twice a week. Subcultures were started with a cell concentration of 2 x
19
20 10⁵ to 4 x 10⁵ viable cells/mL and cells were maintained at a concentration between 10⁵-
21
22 10⁶ cells/mL in suspension. THP-1 cells were maintained in a humidified atmosphere
23
24 containing 5% CO₂ at 37°C. For the coculture, THP-1 cells were differentiated into mature
25
26 macrophage-like cells in 96-well plate with 30 ng/mL of phorbol myristate acetate (PMA)
27
28 (P1585, Sigma-Aldrich, Saint-Quentin-Fallavier, France) in RPMI for 24 h. After the
29
30 incubation, cell surface was rinsed two times with DPBS. Then A549 cells were added on top of
31
32 the differentiated THP-1 and the cocultured cells were cultivated for further 24 h (at a ratio of
33
34 one THP-1 to ten A549). These cocultured cells were incubated in DMEM culture media at
35
36 37°C and 5% CO₂ for 24 h in a humidified incubator before the exposure to the pristine and 30
37
38 min irradiated TiO₂ samples.
39
40
41
42
43
44
45
46

47 **2.4.2 Cell morphology**

48
49 10⁵ cells/well were seeded on 96 well plates. After 24 h exposure to the highest dose (120
50
51 µg/mL) of pristine and irradiated TiO₂ samples, the supernatant was discarded and cell surfaces
52
53 were washed with PBS. After cells were observed using optical microscopy (Leica ICC50 HD,
54
55 Leica Microsystems) at 40 x magnification and pictures were captured with the Moticam 1080
56
57 camera (Shimadzu, Japan).
58
59
60

1
2
3
4
5
6
7
8
9
10
11
12
13
14
15
16
17
18
19
20
21
22
23
24
25
26
27
28
29
30
31
32
33
34
35
36
37
38
39
40
41
42
43
44
45
46
47
48
49
50
51
52
53
54
55
56
57
58
59
60

2.4.3 Determination of cell viability

Cell viability was determined by Trypan blue exclusion assay since TiO₂ NPs have been reported to have interactions with MTT and XTT cytotoxicity assays²⁹. 1.5 x 10⁶ cells/well were plated onto 6-well microtiter plates in 1000 µL culture medium. Cells were exposed to 15, 30, 60 and 120 µg/mL of pristine and irradiated TiO₂ NPs. After incubation for 24 h at 37°C in a humidified incubator, the culture medium was removed, cells were washed with PBS and trypsinized. 20 µL cell suspensions were mixed with 80 µL Trypan blue dye to obtain 1:5 dilution and cells were counted under a microscope using Thoma cell counting chamber. Results are expressed as the mean ± standard error of the mean of three independent experiments and relative to control (unexposed) cells.

2.4.4 Pro-inflammatory response

10⁵ cells/well were seeded on 96 well plates. Cells were exposed to 15, 30, 60 and 120 µg/mL of pristine and irradiated TiO₂ NPs. After 24 h exposure, the production of the pro-inflammatory markers tumor necrosis factor alpha (TNF-α), and interleukin 8 (IL-8) were determined by sandwich enzyme-linked immunosorbent assay (Quantikine Human TNF-α, and Quantikine Human IL-8 Immunoassay; R&D Systems, Lille, France) according to the manufacturer's instructions. The optical density of each sample was determined using a microplate reader (Multiskan RC; Thermo Labsystems, Helsinki, Finland) set to 450 nm. Three independent experiments were performed, and the production of TNF-α and IL-8 was reported to that of control (unexposed) cells.

1
2
3
4
5
6
7
8
9
10
11
12
13
14
15
16
17
18
19
20
21
22
23
24
25
26
27
28
29
30
31
32
33
34
35
36
37
38
39
40
41
42
43
44
45
46
47
48
49
50
51
52
53
54
55
56
57
58
59
60

2.4.5 Determination of Reactive Oxygen Species (ROS) production

Coculture cells were seeded in 96 well black polystyrene microplates (10^5 cells/well) and were exposed to 15, 30, 60 and 120 $\mu\text{g}/\text{mL}$ pristine and irradiated TiO_2 NPs. After 90 min and 24 h exposure, the level of ROS was determined using the OxiSelect kit from Cell Bio Labs (San Diego, CA) according to the manufacturer's instructions. The assay employs the cell-permeable fluorogenic probe 2', 7'-Dichlorodihydrofluorescein diacetate (DCFH-DA). Fluorescence was detected using a Fluoroskan Ascent fluorometer (excitation: 480 nm, emission: 530 nm, Thermo Labsystems), and the generation of ROS was reported to that control (unexposed) cells.

2.5 Statistical analyses

Statistical analyses were performed using GraphPad Prism[®] (version 8.0, GraphPad Software, San Diego, CA, USA). All data were presented as the mean \pm the standard error of the mean (SEM). Differences were considered to be statistically significant when P value was < 0.05 . One-way Anova Tukey test analysis was performed for comparison between control and experimental groups and between pristine and irradiated groups.

3. Results

3.1 Physicochemical features

The toxicity-relevant physico-chemical features of the TiO_2 NPs used in this study are reported in Tables 1, 2 and Figure 1.

Table 1. Particle primary size (TEM), specific surface area (SSA, BET), particle shape (TEM, SEM), and crystal structure (XRPD) of the TiO_2 NPs. ^a minimum and maximum Feret diameters; ^b APTES coating was carried out on S2-type NPs to obtain S4 NPs.

	S1	S2	S3	S4	P25
Primary size (nm)	15	30	20 – 250 ^a	30	21
SSA (m²/g)	146	61	41	61	55
Particle Shape	Spherical	Spherical	Rod	Spherical	Spherical
Crystal structure	Anatase	Anatase	Anatase	Anatase	Anatase: Rutile (90:10)
Surface coating	No	No	No	APTES ^b	No

The radical generation through UV irradiation of different types of TiO₂ in buffer solution was explored. UV irradiation of suspension of TiO₂ in the presence of DMPO produced the DMPO-HO• and DMPO-CO₂•⁻ adducts as shown in Figure 1 a and 1 b, respectively.

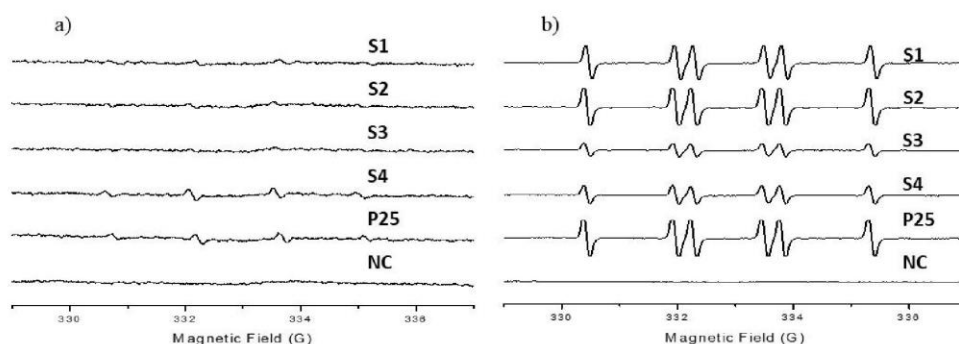


Figure 1. Generation of HO• and CO₂•⁻ radicals from suspensions of TiO₂ NPs (120 µg/mL) under irradiation with UV light. EPR spectra of (a) DMPO-HO• and (b) DMPO-CO₂•⁻ adducts. Negative Control (NC) corresponds to buffer solution without particles. The number of radicals produced is proportional to the intensity of the ESR signal.

Regarding hydroxyl radical formation, negligible traces of HO• radicals were observed at 30 min UV irradiation for S1, S2 and S3, whereas weak signals of the DMPO-HO• adduct were detected for S4 and P25. Although HO• is frequently assigned to the major reactant responsible for the photo-oxidative activity of TiO₂, the observed weak HO• signal might be due to the low

concentration of the particle suspensions. However, as illustrated in Figure 1b characteristic peaks of $\text{DMPO-CO}_2\cdot^-$ were observed in all the irradiated suspensions of TiO_2 and the intensity was higher for S1, S2, and P25 than S3 and S4. As shown in our previous study²⁸, no $\text{DMPO-HO}\cdot$ and $\text{DMPO-CO}_2\cdot^-$ signals were observed for the pristine TiO_2 samples.

To verify whether short-time UV-irradiation modifies toxicologically-relevant properties of TiO_2 , we compared the size of particle aggregates and the surface charge of pristine and irradiated TiO_2 NPs in deionized water and in 10% FBS supplemented DMEM (Table 2).

Table 2. Average hydrodynamic size^a, polydispersity index (PDI)^b and Zeta potential of pristine and UV irradiated TiO_2 NPs (120 $\mu\text{g/mL}$) in deionized water (DI H_2O) and in DMEM (10% FBS). All data are presented as mean of three independent characterizations \pm SD. ^a Dynamic light scattering (DLS) measurements are the mean of at least 3 runs each containing 20 sub-measurements.

	Pristine TiO_2 (in DI H_2O)		UV irradiated TiO_2 (in DI H_2O)		Pristine TiO_2 (in DMEM)		UV Irradiated TiO_2 (in DMEM)	
	Average hydrodynamic size ^a (PDI, nm)	Zeta Potential (mV) @pH 7.5	Average hydrodynamic size ^a (PDI, nm)	Zeta Potential (mV) @pH 7.5	Average hydrodynamic size ^a (PDI, nm)	Zeta Potential (mV) @pH 7.5	Average hydrodynamic size ^a (PDI, nm)	Zeta Potential (mV) @pH 7.5
S1	211.4 \pm 2.3 (0.145)	-13.2 \pm 4.2	321 \pm 28.3 (0.415)	-9.01 \pm 0.7	226 \pm 9.1 (0.282)	-33.8 \pm 1.8	292.1 \pm 3.5 (0.234)	-8.0 \pm 0.7
S2	969.3 \pm 39.5 (0.266)	-13.8 \pm 4.4	1531 \pm 406 (0.136)	-8.36 \pm 0.4	1094 \pm 46.4 (0.364)	-32.6 \pm 1.7	1149 \pm 38.6 (0.475)	-5.3 \pm 1.2
S3	1409 \pm 89.6 (0.114)	-15.8 \pm 4.0	1795 \pm 346.4 (0.545)	-7.04 \pm 0.8	1275 \pm 66.6 (0.179)	-33.7 \pm 3.5	1299 \pm 112.1 (0.714)	-7.5 \pm 0.6
S4	1204 \pm 59.9 (0.160)	+12.3 \pm 0.5	1231 \pm 143.8 (0.504)	-8.4 \pm 0.2	1398 \pm 54.9 (0.475)	-36.4 \pm 3.5	1433 \pm 133.1 (0.308)	-9.9 \pm 0.2
P25	256.4 \pm 136.6		410 \pm 5.1		325 \pm 4.1	-33.1 \pm	353.6 \pm 3.45	-7.7 \pm 0.7

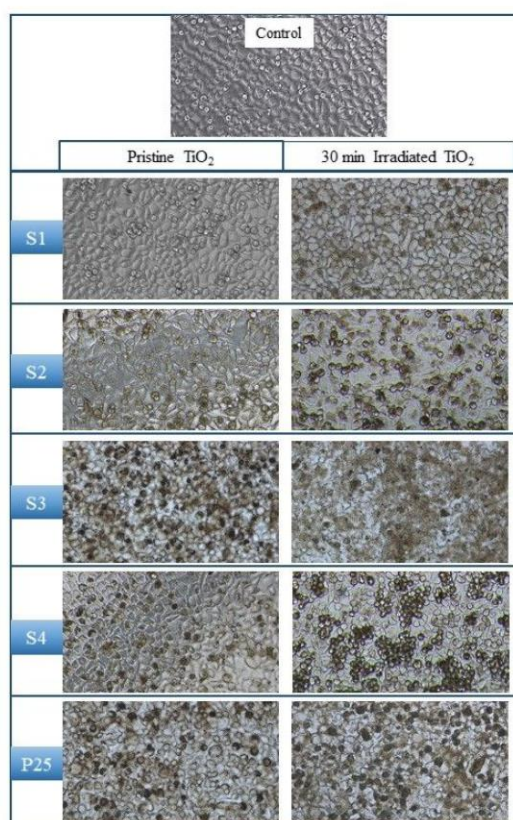
1
2
3
4
5
6
7
8
9
10
11
12
13
14
15
16
17
18
19
20
21
22
23
24
25
26
27
28
29
30
31
32
33
34
35
36
37
38
39
40
41
42
43
44
45
46
47
48
49
50
51
52
53
54
55
56
57
58
59
60

induced the TiO₂ NP surface to be less negative and the average hydrodynamic size of particles was increased indicating some further particle aggregation.

In DMEM (10% FBS), also APTES-functionalized S4 NPs acquired a negative charge at pH 7.5, likely due to adsorption of media components, as previously observed for TiO₂ NPs³⁰. UV irradiation caused a marked decrease of the negative zeta potential towards less negative values also in DMEM. Specifically, the zeta potential of pristine NPs ranged between -31 mV and -36.6 mV and decreased to -9.9 mV to -5.3 mV after irradiation.

3.5. Cell morphology

The morphology of coculture cells after 24 h exposure to the highest dose (120 µg/mL) of pristine and irradiated TiO₂ NPs were illustrated in Figure 2.



1
2
3 **Figure 2.** Microscopic images of coculture cells (A549 + macrophages differentiated from
4 THP-1 cells) exposed to 120 µg/mL pristine and 30 min irradiated TiO₂ NPs for 24 h (40 x
5 magnification). Control cells (unexposed to NPs).
6
7
8
9

10
11
12 The control (untreated) cells show the original morphology of epithelial A549 and macrophages
13 differentiated from THP-1 cells. Most of the control cells were adherent to the culture flask.
14 However after exposure to pristine and irradiated TiO₂ NPs, the cell morphology was
15 considerably changed compared to control cells. Cell shrinkage, and loss of contact with
16 adjacent cells were observed. Also, loss of cellular adhesion to the substrate was observed and
17 most of the cells detached from the surface of the culture flask and appeared floating in the
18 culture medium. The cell morphological changes induced by irradiated NPs were more
19 pronounced than those induced by pristine NPs.
20
21
22
23
24
25
26
27
28
29
30

31 32 33 **3.2. Cytotoxicity** 34

35 Cytotoxicity induced by pristine and irradiated TiO₂ NPs on coculture cells (A549 +
36 macrophages differentiated from THP-1 cells) are presented in Figure 3.
37
38
39
40
41
42
43
44
45
46
47
48
49
50
51
52
53
54
55
56
57
58
59
60

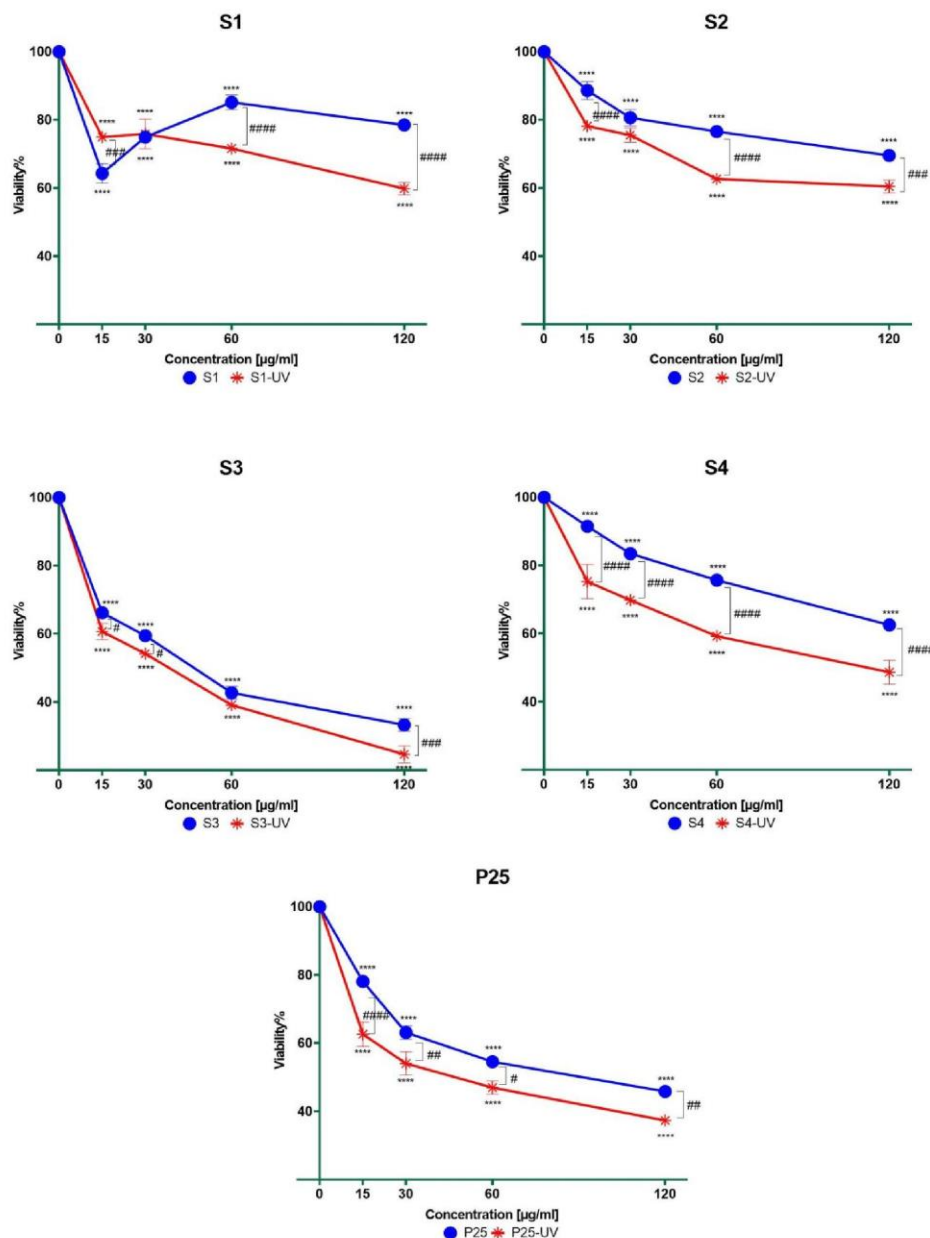


Figure 3. Cell viability assessed by Trypan blue assay 24 h after coculture cells (A549 + macrophages differentiated from THP-1 cells) were exposed to pristine and irradiated TiO₂ NPs at the indicated concentrations. Values are the mean ± SEM of three independent experiments. Statistically different from control (****) P<0.0001. Statistical difference between pristine and

1
2
3 irradiated samples (#) $P < 0.5$ (##) $P < 0.01$, (###) $P < 0.001$, (####) $P < 0.0001$. Statistical
4
5 analyses were conducted using one-way Anova analyses, followed by Tukey's multiple
6
7 comparison test.
8
9

10
11
12 Considering the exposure to pristine TiO₂ NPs, the cell viability decreased in a dose-dependent
13
14 manner in all samples except S1 compared to control. The maximal cell loss was observed for
15
16 rod shaped S3 treated cells starting from the lowest doses (15 µg/mL). At the highest
17
18 concentration (120 µg/mL), cell viability was found to be 33.3 % for S3. P25, on the other hand,
19
20 caused 45.8% cell viability at the highest concentrations, while cell viability was found to be
21
22 78.5%, 69.5% and 62.5%, for S1, S2 and S4, respectively.
23
24
25

26 Exposure to irradiated samples caused a dose-dependent decrease in cell viability compared to
27
28 the control group and showed a statistically significant difference at all the tested concentrations
29
30 ($P < 0.0001$, all). Irradiated rod shaped S3 and P25 caused the highest cytotoxic effects and this
31
32 effect was more pronounced at the highest doses (24.6% and 37% at 120 µg/mL, respectively).
33
34 The comparison of toxicities induced by pristine and irradiated TiO₂ NPs highlighted a
35
36 significant increase of cytotoxicity when all particles at all tested concentrations were pre-
37
38 exposed to UV light, and few negligible exceptions to this trend were observed. The only
39
40 relevant exception is caused by pristine S1, likely due to the agglomeration of the smallest NP
41
42 investigated in this work used at the highest doses.
43
44
45
46
47
48

49 **3.3. Pro-inflammatory response**

50
51 Since IL-8 and TNF- α are major pro-inflammatory mediators in lung epithelial cells and
52
53 macrophages respectively ³¹ we examined whether TiO₂ samples induced IL-8 and TNF- α
54
55 production in coculture (A549 + macrophages differentiated from THP-1 cells). Results are
56
57 reported in Figure 4.
58
59
60

1
2
3
4
5
6
7
8
9
10
11
12
13
14
15
16
17
18
19
20
21
22
23
24
25
26
27
28
29
30
31
32
33
34
35
36
37
38
39
40
41
42
43
44
45
46
47
48
49
50
51
52
53
54
55
56
57
58
59
60

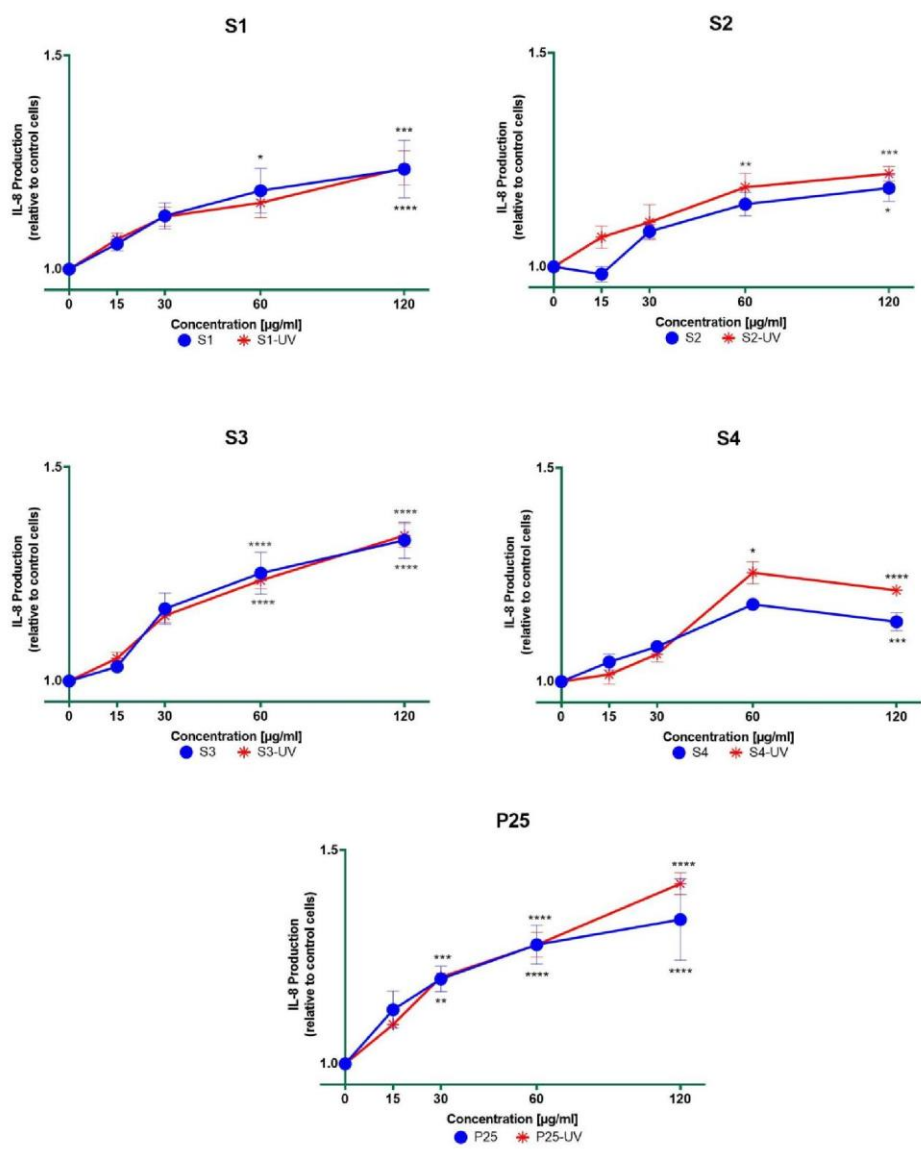
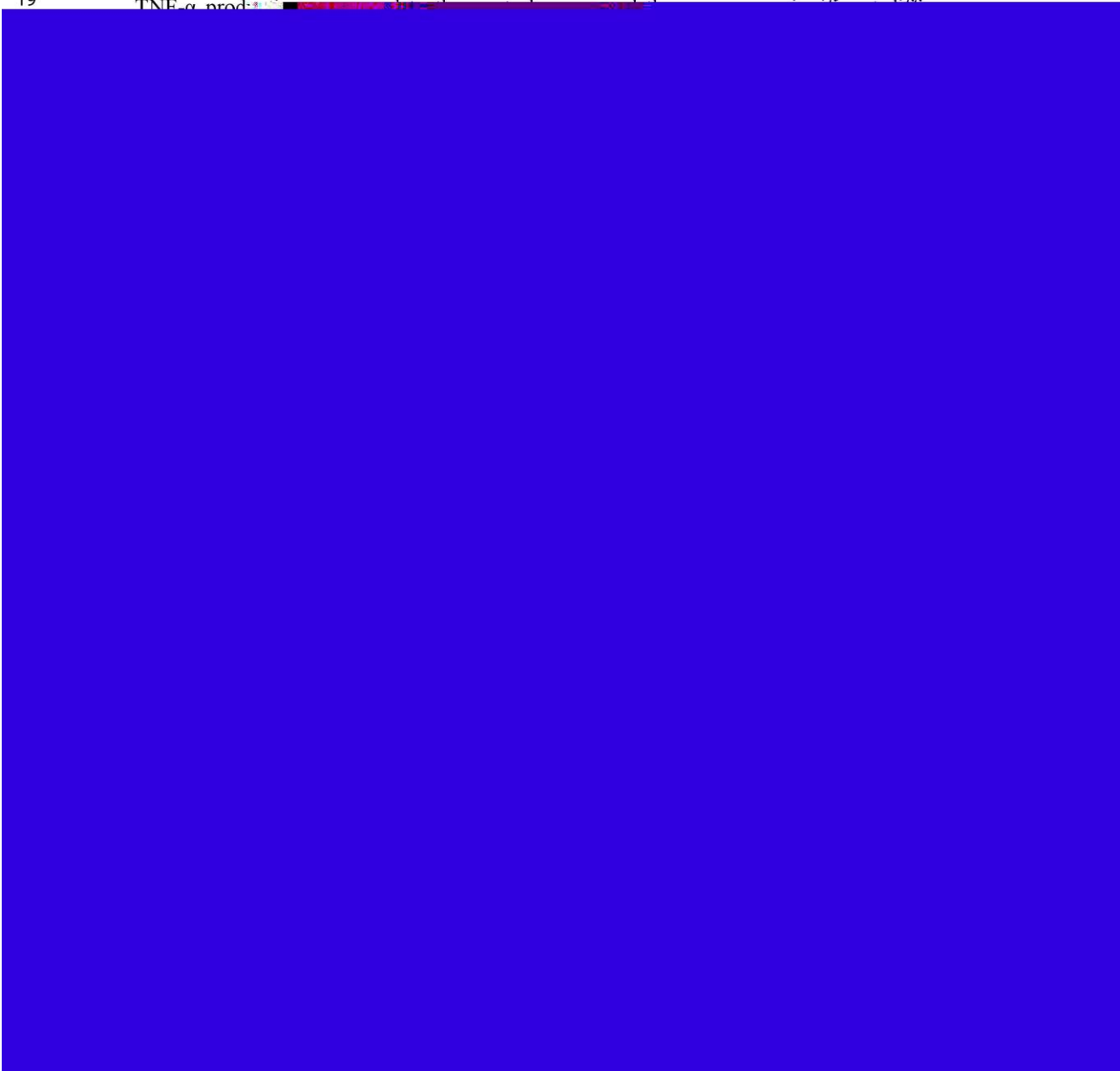


Figure 4. IL-8 production after 24 h exposure to the indicated concentrations of pristine and irradiated TiO₂ NPs in coculture cells (A549 + macrophages differentiated from THP-1 cells). Values are the mean ± SEM of three independent experiments. Statistically different from control (*) P < 0.05, (**) P < 0.01, (***) P < 0.001, (****) P < 0.0001. Statistical analyses were conducted using one-way Anova analyses, followed by Tukey's multiple comparison test.

1
2
3
4
5
6
7
8
9
10
11
12
13
14
15
16
17
18
19

Regarding IL-8 production, all pristine TiO₂ samples caused a dose-dependent increase compared to the control group. A higher production was observed significantly for S3 and P25 at 60 µg/mL (P < 0.0001) and at the highest dose (120 µg/mL, P < 0.0001). Similarly, IL-8 release from coculture was enhanced after exposure to irradiated samples whereas this increased production was almost the same as that observed for the pristine samples (no statistically significant difference). Similarly, UV irradiated or pristine TiO₂ NPs did not cause significant

TNF-α prod...



1
2
3 markedly negative surface charge of all TiO₂ NPs was less negative and shifted towards zeta
4
5 potential values ranging from -33 to -7.5 mV.
6

7
8 Long (50 h) UV irradiation of TiO₂ NPs is known to induce the generation of a large number
9
10 of bridging hydroxyl species that are characterized by a strong acidic character (pK_a 2.9). On
11
12 the contrary, terminal hydroxyl species ($\equiv\text{Ti} - \text{OH}$) are rather alkaline (pK_a = 12.7) and their
13
14 presence favours a more neutral surface charge in physiological media. We might speculate that
15
16 the short irradiation time used in this and other works ⁶ may favour these latter species, as the
17
18 former ones, more thermodynamically stable, require that water molecules replace oxygens that
19
20 are ejected during the h⁺-driven oxidation of O₂⁻ anions. An excess of terminal hydroxyl species
21
22 upon short time irradiation could be at the basis of the less negative surface charge observed
23
24 for all the irradiated TiO₂ NPs.
25
26

27
28 These results are in good agreement with a number of other studies showing the
29
30 physicochemical properties of TiO₂ have changed with UV irradiation ^{6,7,19,32}. The extent to
31
32 which these changes induces differences in their *in vitro* toxicity is shown in the present study.
33
34

35
36 *In vitro* cytotoxicity assay revealed that pristine TiO₂ NPs caused a significant reduction in cell
37
38 viability compared to the control group (Figure 3). The cytotoxic potential of TiO₂ NPs after
39
40 UV irradiation was increased compared to pristine NPs and this is consistent with observations
41
42 of cell morphology (Figure 2). In some studies, it has been shown that UV irradiated TiO₂ NPs
43
44 reduce cell viability more than non-irradiated TiO₂ NPs ^{12,14,33}, but only one study focused on
45
46 the effect of TiO₂ pre-irradiation on cell viability¹⁹. In this study ¹⁹, the effect of 24 h UV pre-
47
48 irradiated 18 nm and 105 nm anatase TiO₂ NPs and the cell viability of human liver cancer cell
49
50 line (Hep G2) was investigated. Our results share a number of similarities with Petkovic *et al.*¹⁹
51
52 findings that UV pre-irradiation caused more cell viability reduction than pristine TiO₂ NPs and
53
54 24 h pre-irradiation caused changes on particle surface charge. Remarkably, our data indicate
55
56
57
58
59
60

1
2
3 that even a 30 min short term UV irradiation is able to alter TiO₂ toxicologically relevant
4 features, such as surface charge and aggregate size, and thus modulate its cytotoxicity.
5

6
7 Regarding pro-inflammatory responses, in our study both pristine and irradiated TiO₂ NPs
8 caused significantly IL-8 production only at the high doses (60, 120 µg/mL) compared to
9 control group whereas there were no significant differences between pristine and irradiated
10 samples (less negative surface charge) showing that UV pre-irradiation had no effect on the
11 pro-inflammatory responses. The results of pristine TiO₂ NPs IL-8 production were consistent
12 with Dekali *et al.*'s findings³⁴. In this study, the inflammatory effect of the anatase TiO₂ NPs
13 (≤ 25 nm, 200-220 m²/g) was tested on the coculture (A549+THP-1) model. An increased IL-
14 8 production was detected although no significant changes were observed in the production of
15 TNF-α after TiO₂ NPs exposure. In the literature, the studies examining the pro-inflammatory
16 responses of TiO₂ and photo-active TiO₂ NPs on the coculture system are limited. This makes
17 it difficult to compare studies and draw conclusions.
18
19

20
21 Inflammation and oxidative stress are closely related processes that work interdependently³⁵.
22 Oxidative stress triggers inflammation, or if inflammation occurs first, oxidative stress
23 develops, which further exacerbates inflammation³⁶. In this study, TiO₂ NPs had an impact on
24 the pro-inflammatory responses but surprisingly pristine or irradiated TiO₂ NPs did not trigger
25 significant ROS production in coculture compared to the control group (unexposed to TiO₂
26 NPs). Especially considering the P25 used as a reference substance in this study, the effects of
27 P25 on oxidative stress are contradictory in the studies^{37,38} as assessed by the DCFH-DA assay.
28 The reason for the absence of oxidative stress upon treatment with pristine or irradiated TiO₂
29 NPs might be the possible interference by the NPs with the DCF in DCFH-DA ROS assay
30 which could hinder the traceability chain by quenching the fluorescent signal. An unintended
31 bias should be taken into consideration. Besides, considering the cell lines used in this study,
32 alveolar macrophages are also equipped with a well-advanced defence system of enzymatic and
33
34
35
36
37
38
39
40
41
42
43
44
45
46
47
48
49
50
51
52
53
54
55
56
57
58
59
60

1
2
3 non-enzymatic antioxidants, which are known scavengers of ROS ^{39,40}. Thus, radical
4 scavengers present in the cells may significantly protect them from UV irradiated or pristine
5 TiO₂ induced ROS production. This must be confirmed by a comprehensive study of oxidative
6 stress also including the assessment of anti-oxidant system induction.
7

8
9
10
11
12 Regarding photoactivity, our ESR results showed that UV irradiation of TiO₂ NPs resulted in
13 acellular production of CO₂•⁻ and much less HO• production without significant change in
14 oxidative stress, although many studies showed that the free radical generation triggered
15 cellular oxidative stress ^{12,41,42}. This may not be assumed in our study because after the particles
16 were exposed to UV irradiation, they were incubated with the cells in a dark environment (*i.e.*
17 incubator), where there was no UV light. When UV light irradiation is ceased, the rapid
18 recombination between electron–hole pairs stops the photocatalytic activity of TiO₂ ⁴³.
19

20
21
22
23
24
25
26
27
28
29
30
31
32
33
34
35
36
37
38
39
40
41
42
43
44
45
46
47
48
49
50
51
52
53
54
55
56
57
58
59
60
In line with the investigation of potential links between cytotoxic effects of irradiated TiO₂ NPs
and changes of physico-chemical properties, we showed that the irradiated NPs have less
negative surface charge compared to the pristine particles, creating more cytotoxicity. The
magnitude of the negative zeta potential decreased by UV irradiation, the reducing electrostatic
barrier could increase the chances of cell-particle interactions and result in higher toxicity. As
reported by Jeon *et al.* ⁴⁴, less negatively charged NPs are more efficiently taken up by THP-1
macrophages.

Besides, the surface charge is a parameter involved in the formation of the protein corona. For
example, one study ⁴⁵ showed that total serum protein, BSA and apolipoprotein 1 amounts
adsorbed to silica NPs decreased with an increase in negative charge density. Consequently,
proteins contained in the cell culture medium can adsorb differently at the altered NP surface
(*i.e.* there is a different corona) ⁴⁶. It is known that the protein corona has an impact on the
internalization of NPs by cells and thus potentially on the cytotoxicity induced ^{47–49}. This
assumption is supported by a slight change in the average aggregate size of the particles before

1
2
3 and after irradiation and an altered surface charge. Further study is necessary to better
4
5 understand if the protein corona may play a role and it is the topic of our current research.
6
7

8 9 10 **Conclusion**

11
12 In conclusion, the results of this study showed that irradiated TiO₂ NPs induced a higher
13
14 cytotoxic effect than the pristine TiO₂ NPs on human lung cells in relation to an altered surface
15
16 charge. Irradiated TiO₂ NPs caused a pro-inflammatory response in the same incidence as
17
18 pristine NPs therefore it cannot be claimed that UV irradiation has an effect on the pro-
19
20 inflammatory response. No impact was observed on ROS production neither in pristine nor in
21
22 irradiated TiO₂ NPs treated cells. However further investigations are needed. Since it is possible
23
24 for the TiO₂ in the environment to be photoactivated by sunlight, the risk assessment of
25
26 photoactive TiO₂ NPs should be taken into account. In this sense, the results of this study
27
28 contribute to the toxicological evaluation of TiO₂ NPs and photoactive TiO₂ NPs in human lung
29
30 cells.
31
32
33
34
35

36 37 38 **Funding**

39
40 This research did not receive any specific grant from funding agencies in the public,
41
42 commercial, or not-for-profit sectors.
43
44
45

46 47 48 **Acknowledgments**

49
50 We would like to thank Dr. Ingrid Corazzari for the kind support in physicochemical
51
52 characterization of the TiO₂ NPs. Ozge Kose acknowledges the support of the “G. Scansetti”
53
54 Center of the University of Torino for partially funding her international secondment.
55
56
57
58
59
60

1
2
3
4
5
6
7
8
9
10
11
12
13
14
15
16
17
18
19
20
21
22
23
24
25
26
27
28
29
30
31
32
33
34
35
36
37
38
39
40
41
42
43
44
45
46
47
48
49
50**References**

- (1) Ziental, D.; Czarczynska-Goslinska, B.; Mlynarczyk, D. T.; Glowacka-Sobotta, A.; Stanisz, B.; Goslinski, T.; Sobotta, L. Titanium Dioxide Nanoparticles: Prospects and Applications in Medicine. *Nanomaterials* **2020**, *10* (2), 387. <https://doi.org/10.3390/nano10020387>.
- (2) Chen, X.; Selloni, A. Introduction: Titanium Dioxide (TiO₂) Nanomaterials. *Chem. Rev.* **2014**, *114* (19), 9281–9282. <https://doi.org/10.1021/cr500422r>.
- (3) Binas, V.; Venieri, D.; Kotzias, D.; Kiriakidis, G. Modified TiO₂ Based Photocatalysts for Improved Air and Health Quality. *Journal of Materiomics*. Chinese Ceramic Society March 1, 2017, pp 3–16. <https://doi.org/10.1016/j.jmat.2016.11.002>.
- (4) Fujishima, A.; Rao, T. N.; Tryk, D. A. Titanium Dioxide Photocatalysis. *J. Photochem. Photobiol. C Photochem. Rev.* **2000**, *1* (1), 1–21. [https://doi.org/10.1016/S1389-5567\(00\)00002-2](https://doi.org/10.1016/S1389-5567(00)00002-2).
- (5) Qian, R.; Zong, H.; Schneider, J.; Zhou, G.; Zhao, T.; Li, Y.; Yang, J.; Bahnemann, D. W.; Pan, J. H. Charge Carrier Trapping, Recombination and Transfer during TiO₂ Photocatalysis: An Overview. *Catal. Today* **2019**, *335*, 78–90. <https://doi.org/10.1016/j.cattod.2018.10.053>.
- (6) Sun, J.; Guo, L. H.; Zhang, H.; Zhao, L. UV Irradiation Induced Transformation of TiO₂ Nanoparticles in Water: Aggregation and Photoreactivity. *Environ. Sci. Technol.* **2014**, *48* (20), 11962–11968. <https://doi.org/10.1021/es502360c>.
- (7) Wang, P.; Qi, N.; Ao, Y.; Hou, J.; Wang, C.; Qian, J. Effect of UV Irradiation on the

1
2
3
4
5
6
7
8
9
10
11
12
13
14
15
16
17
18
19
20
21
22
23
24
25
26
27
28
29
30
31
32
33
34
35
36
37
38
39
40
41
42
43
44
45
46
47
48
49
50
51
52
53
54
55
56
57
58
59
60

- <https://doi.org/10.1016/j.impact.2016.08.004>.
- (9) Gurr, J.-R.; Wang, A. S. S.; Chen, C.-H.; Jan, K.-Y. Ultrafine Titanium Dioxide Particles in the Absence of Photoactivation Can Induce Oxidative Damage to Human Bronchial Epithelial Cells. *Toxicology* **2005**, *213* (1–2), 66–73. <https://doi.org/10.1016/j.tox.2005.05.007>.
- (10) Jugan, M. L.; Barillet, S.; Simon-Deckers, A.; Sauvaigo, S.; Douki, T.; Herlin, N.; Carrière, M. Cytotoxic and Genotoxic Impact of TiO₂ Nanoparticles on A549 Cells. *J. Biomed. Nanotechnol.* **2011**, *7* (1), 22–23.
- (11) Jayaram, D. T.; Kumar, A.; Kippner, L. E.; Ho, P. Y.; Kemp, M. L.; Fan, Y.; Payne, C. K. TiO₂ Nanoparticles Generate Superoxide and Alter Gene Expression in Human Lung Cells. *RSC Adv.* **2019**, *9* (43), 25039–25047. <https://doi.org/10.1039/c9ra04037d>.
- (12) Uchino, T.; Tokunaga, H.; Ando, M.; Utsumi, H. Quantitative Determination of OH Radical Generation and Its Cytotoxicity Induced by TiO₂-UVA Treatment. *Toxicol. In Vitro* **2002**, *16* (5), 629–635. [https://doi.org/10.1016/s0887-2333\(02\)00041-3](https://doi.org/10.1016/s0887-2333(02)00041-3).
- (13) Wang, C.; Cao, S.; Tie, X.; Qiu, B.; Wu, A.; Zheng, Z. Induction of Cytotoxicity by Photoexcitation of TiO₂ Can Prolong Survival in Glioma-Bearing Mice. *Mol. Biol. Rep.* **2011**, *38* (1), 523–530. <https://doi.org/10.1007/s11033-010-0136-9>.
- (14) Gopalan, R. C.; Osman, I. F.; Amani, A.; De Matas, M.; Anderson, D. The Effect of Zinc Oxide and Titanium Dioxide Nanoparticles in the Comet Assay with UVA Photoactivation of Human Sperm and Lymphocytes. *Nanotoxicology* **2009**, *3* (1), 33–39. <https://doi.org/10.1080/17435390802596456>.
- (15) Warheit, D. B.; Webb, T. R.; Sayes, C. M.; Colvin, V. L.; Reed, K. L. Pulmonary Instillation Studies with Nanoscale TiO₂ Rods and Dots in Rats: Toxicity Is Not Dependent upon Particle Size and Surface Area. *Toxicol. Sci.* **2006**, *91* (1), 227–236. <https://doi.org/10.1093/toxsci/kfj140>.

- 1
2
3 (16) Nemmar, A.; Melghit, K.; Ali, B. H. The Acute Proinflammatory and Prothrombotic
4 Effects of Pulmonary Exposure to Rutile TiO₂ Nanorods in Rats. *Exp. Biol. Med.* **2008**,
5 233 (5), 610–619. <https://doi.org/10.3181/0706-RM-165>.
6
7
8
9
10 (17) Li, Y. S.; Ootsuyama, Y.; Kawasaki, Y.; Morimoto, Y.; Higashi, T.; Kawai, K. Oxidative
11 DNA Damage in the Rat Lung Induced by Intratracheal Instillation and Inhalation of
12 Nanoparticles. *J. Clin. Biochem. Nutr.* **2018**, 62 (3), 238–241.
13 <https://doi.org/10.3164/jcbrn.17-70>.
14
15
16
17 (18) Introduction to Solar Radiation [https://www.newport.com/t/introduction-to-solar-](https://www.newport.com/t/introduction-to-solar-radiation)
18 radiation (accessed Jul 20, 2020).
19
20
21
22 (19) Petković, J.; Kuzma, T.; Rade, K.; Novak, S.; Filipič, M. Pre-Irradiation of Anatase TiO
23 2 Particles with UV Enhances Their Cytotoxic and Genotoxic Potential in Human
24 Hepatoma HepG2 Cells. *J. Hazard. Mater.* **2011**, 196, 145–152.
25 <https://doi.org/10.1016/j.jhazmat.2011.09.004>.
26
27
28
29 (20) Hurum, D. C.; Agrios, A. G.; Gray, K. A.; Rajh, T.; Thurnauer, M. C. Explaining the
30 Enhanced Photocatalytic Activity of Degussa P25 Mixed-Phase TiO₂ Using EPR. *J.*
31 *Phys. Chem. B* **2003**, 107 (19), 4545–4549. <https://doi.org/10.1021/jp0273934>.
32
33
34
35 (21) Janus, M.; Morawski, A. W. New Method of Improving Photocatalytic Activity of
36 Commercial Degussa P25 for Azo Dyes Decomposition. *Applied Catalysis B:*
37 *Environmental.* Elsevier August 29, 2007, pp 118–123.
38 <https://doi.org/10.1016/j.apcatb.2007.04.003>.
39
40
41
42 (22) Du, P.; Bueno-López, A.; Verbaas, M.; Almeida, A. R.; Makkee, M.; Moulijn, J. A.;
43 Mul, G. The Effect of Surface OH-Population on the Photocatalytic Activity of Rare
44 Earth-Doped P25-TiO₂ in Methylene Blue Degradation. *J. Catal.* **2008**, 260 (1), 75–80.
45 <https://doi.org/10.1016/j.jcat.2008.09.005>.
46
47
48
49 (23) Chen, D. W.; Shi, J. E.; Yan, J. C.; Wang, Y. H.; Yan, F. C.; Shang, S. X.; Xue, J.
50
51
52
53
54
55
56
57
58
59
60

- 1
2
3 Controllable Synthesis of Titania Nanocrystals with Different Morphologies and
4 Application to the Degradation of Phenol. *Chem. Res. Chinese Univ.* **2008**, *24* (3), 362–
5 366. [https://doi.org/10.1016/S1005-9040\(08\)60076-8](https://doi.org/10.1016/S1005-9040(08)60076-8).
6
7
8
9
10 (24) Zhao, J.; Milanova, M.; Warmoeskerken, M. M. C. G.; Dutschk, V. Surface Modification
11 of TiO₂ Nanoparticles with Silane Coupling Agents. *Colloids Surfaces A Physicochem.*
12 *Eng. Asp.* **2012**, *413*, 273–279. <https://doi.org/10.1016/j.colsurfa.2011.11.033>.
13
14
15
16
17 (25) Hashimoto, K.; Irie, H.; Fujishima, A. TiO₂ Photocatalysis: A Historical Overview and
18 Future Prospects. *Jpn. J. Appl. Phys.* **2005**, *44* (12), 8269–8285.
19
20
21
22 (26) Sendra, M.; Moreno-Garrido, I.; Yeste, M. P.; Gatica, J. M.; Blasco, J. Toxicity of TiO₂,
23 in Nanoparticle or Bulk Form to Freshwater and Marine Microalgae under Visible Light
24 and UV-A Radiation. *Environ. Pollut.* **2017**, *227*, 39–48.
25
26
27
28
29
30
31 (27) Guidelines on Limits of Exposure to Ultraviolet Radiation of Wavelengths between 180
32 Nm and 400 Nm (Incoherent Optical Radiation). The International Non-Ionizing
33 Radiation Committee of the International Radiation Protection Association. *Health Phys.*
34 **1985**, *49* (2), 331–340.
35
36
37
38
39
40 (28) Kose, O.; Tomatis, M.; Leclerc, L.; Belblidia, N.-B.; Hocheplid, J.-F.; Turci, F.;
41 Pourchez, J.; Forest, V. Impact of the Physicochemical Features of TiO₂ Nanoparticles
42 on Their in Vitro Toxicity (In Press). *Chem. Res. Toxicol.* **2020**.
43
44
45
46
47
48
49 (29) Wang, S.; Yu, H.; Wickliffe, J. K. Limitation of the MTT and XTT Assays for Measuring
50 Cell Viability Due to Superoxide Formation Induced by Nano-Scale TiO₂. *Toxicol. Vittr.*
51 **2011**, *25* (8), 2147–2151. <https://doi.org/10.1016/j.tiv.2011.07.007>.
52
53
54
55
56 (30) Marucco, A.; Fenoglio, I.; Turci, F.; Bice, F. Interaction of Fibrinogen and Albumin with
57 Titanium Dioxide Nanoparticles of Different Crystalline Phases. *J. Phys. Conf. Ser.*
58
59
60

- 1
2
3 *Nanosafe 2012 Int. Conf. Safe Prod. Use Nanomater. 13–15 Novemb. 2012, Grenoble,*
4
5 *Fr.* **2013**, 429, 012014. <https://doi.org/10.1088/1742-6596/429/1/012014>.
6
7
8 (31) Kwon, O. J.; Au, B. T.; Collins, P. D.; Adcock, I. M.; Mak, J. C.; Robbins, R. R.; Chung,
9
10 K. F.; Barnes, P. J. Tumor Necrosis Factor-Induced Interleukin-8 Expression in Cultured
11
12 Human Airway Epithelial Cells. *Am. J. Physiol.* **1994**, 267 (4 Pt 1), L398-405.
13
14 <https://doi.org/10.1152/ajplung.1994.267.4.L398>.
15
16
17 (32) Mittelman, A. M.; Fortner, J. D.; Pennell, K. D. Effects of Ultraviolet Light on Silver
18
19 Nanoparticle Mobility and Dissolution. *Environ. Sci. Nano* **2015**, 2 (6), 683–691.
20
21 <https://doi.org/10.1039/c5en00145e>.
22
23
24 (33) Cho, M.; Chung, H.; Choi, W.; Yoon, J. Linear Correlation between Inactivation of E.
25
26 Coli and OH Radical Concentration in TiO₂ Photocatalytic Disinfection. *Water Res.*
27
28 **2004**, 38 (4), 1069–1077. <https://doi.org/10.1016/j.watres.2003.10.029>.
29
30
31 (34) Dekali, S.; Divetain, A.; Kortulewski, T.; Vanbaelinghem, J.; Gamez, C.; Rogerieux, F.;
32
33 Lacroix, G.; Rat, P. Cell Cooperation and Role of the P2X7 Receptor in Pulmonary
34
35 Inflammation Induced by Nanoparticles. *Nanotoxicology* **2013**, 7 (8), 1302–1314.
36
37 <https://doi.org/10.3109/17435390.2012.735269>.
38
39
40 (35) Mittal, M.; Siddiqui, M. R.; Tran, K.; Reddy, S. P.; Malik, A. B. Reactive Oxygen
41
42 Species in Inflammation and Tissue Injury. *Antioxidants and Redox Signaling*. Mary Ann
43
44 Liebert, Inc. March 1, 2014, pp 1126–1167. <https://doi.org/10.1089/ars.2012.5149>.
45
46
47 (36) Vaziri, N. D.; Rodríguez-Iturbe, B. Mechanisms of Disease: Oxidative Stress and
48
49 Inflammation in the Pathogenesis of Hypertension. *Nature Clinical Practice*
50
51 *Nephrology*. Nature Publishing Group October 14, 2006, pp 582–593.
52
53 <https://doi.org/10.1038/ncpneph0283>.
54
55
56 (37) Jugan, M. L.; Barillet, S.; Simon-Deckers, A.; Sauvaigo, S.; Douki, T.; Herlin, N.;
57
58 Carrière, M. Cytotoxic and Genotoxic Impact of TiO₂ Nanoparticles on A549 Cells. *J.*
59
60

- 1
2
3 *Biomed. Nanotechnol.* **2011**, 7 (1), 22–23. <https://doi.org/10.1166/jbn.2011.1181>.
- 4
5 (38) Simon-Deckers, A.; Gouget, B.; Mayne-L’Hermite, M.; Herlin-Boime, N.; Reynaud, C.;
6
7 Carrière, M. In Vitro Investigation of Oxide Nanoparticle and Carbon Nanotube Toxicity
8 and Intracellular Accumulation in A549 Human Pneumocytes. *Toxicology* **2008**, 253 (1–
9 3), 137–146. <https://doi.org/10.1016/J.TOX.2008.09.007>.
- 10
11 (39) Heffner, J. E.; Repine, J. E. Pulmonary Strategies of Antioxidant Defense. *Am. Rev.*
12
13 *Respir. Dis.* **1989**, 140 (2), 531–554. <https://doi.org/10.1164/ajrccm/140.2.531>.
- 14
15 (40) Kim, J. K.; Lee, W. K.; Lee, E. J.; Cho, Y. J.; Lee, K. H.; Kim, H. S.; Chung, Y.; Kim,
16
17 K. A.; Lim, Y. Mechanism of Silica- and Titanium Dioxide-Induced Cytotoxicity in
18
19 Alveolar Macrophages. *J. Toxicol. Environ. Heal. - Part A* **1999**, 58 (7), 437–450.
20
21 <https://doi.org/10.1080/009841099157160>.
- 22
23 (41) Reeves, J. F.; Davies, S. J.; Dodd, N. J. F.; Jha, A. N. Hydroxyl Radicals (•OH) Are Associated with Titanium Dioxide (TiO₂) Nanoparticle-Induced
24
25 Cytotoxicity and Oxidative DNA Damage in Fish Cells. *Mutat. Res. - Fundam. Mol.*
26
27 *Mech. Mutagen.* **2008**, 640 (1–2), 113–122.
28
29 <https://doi.org/10.1016/j.mrfmmm.2007.12.010>.
- 30
31 (42) Cai, R.; Kubota, Y.; Shuin, T.; Sakai, H.; Hashimoto, K.; Fujishima, A. *Induction of*
32
33 *Cytotoxicity by Photoexcited TiO₂ Particles*; 1992.
- 34
35 (43) Nam, Y.; Lim, J. H.; Ko, K. C.; Lee, J. Y. Photocatalytic Activity of TiO₂ Nanoparticles:
36
37 A Theoretical Aspect. *Journal of Materials Chemistry A*. Royal Society of Chemistry
38
39 2019, pp 13833–13859. <https://doi.org/10.1039/c9ta03385h>.
- 40
41 (44) Jeon, S.; Clavadetscher, J.; Lee, D.-K.; Chankeshwara, S. V.; Bradley, M.; Cho, W.-S.
42
43 Surface Charge-Dependent Cellular Uptake of Polystyrene Nanoparticles. *Nanomater.*
44
45 *(Basel, Switzerland)* **2018**, 8 (12). <https://doi.org/10.3390/nano8121028>.
- 46
47 (45) Beck, M.; Mandal, T.; Buske, C.; Lindén, M. Serum Protein Adsorption Enhances Active
48
49
50
51
52
53
54
55
56
57
58
59
60

1
2
3
4
5
6
7
8
9
10
11
12
13
14
15
16
17
18
19
20
21
22
23
24
25
26
27
28
29
30
31
32
33
34
35
36
37
38
39
40
41
42
43
44
45
46
47
48
49
50
51
52
53
54
55
56
57
58
59
60

- Leukemia Stem Cell Targeting of Mesoporous Silica Nanoparticles. *ACS Appl. Mater. Interfaces* **2017**, *9* (22), 18566–18574. <https://doi.org/10.1021/acsami.7b04742>.
- (46) Chen, D.; Ganesh, S.; Wang, W.; Amiji, M. Plasma Protein Adsorption and Biological Identity of Systemically Administered Nanoparticles. *Nanomedicine*. Future Medicine Ltd. September 1, 2017, pp 2113–2135. <https://doi.org/10.2217/nnm-2017-0178>.
- (47) Forest, V.; Pourchez, J. Preferential Binding of Positive Nanoparticles on Cell Membranes Is Due to Electrostatic Interactions: A Too Simplistic Explanation That Does Not Take into Account the Nanoparticle Protein Corona. *Materials Science and Engineering C*. Elsevier Ltd January 1, 2017, pp 889–896. <https://doi.org/10.1016/j.msec.2016.09.016>.
- (48) Lesniak, A.; Salvati, A.; Santos-Martinez, M. J.; Radomski, M. W.; Dawson, K. A.; Åberg, C. Nanoparticle Adhesion to the Cell Membrane and Its Effect on Nanoparticle Uptake Efficiency. *J. Am. Chem. Soc.* **2013**, *135* (4), 1438–1444. <https://doi.org/10.1021/ja309812z>.
- (49) Forest, V. CHAPTER 2: Biological Significance of the Nanoparticles Protein Corona. In *Issues in Toxicology*; Royal Society of Chemistry, 2019; Vol. 2019-January, pp 31–60. <https://doi.org/10.1039/9781788016308-00031>.

1. Complementary Data

Acellular ROS production induced by TiO₂ NPs after 30 min of UV irradiation is reported in *Article 2*. We also assessed the Electron Spin Resonance (ESR) intensity of the ROS signal as a function of time during 30 min irradiation of TiO₂ NPs and these results are reported here as a complementary data.

1.1. Electron spin resonance method for detection of HO• and CO₂•⁻ radicals from UV-irradiated TiO₂ nanoparticles

Electron Spin Resonance is a spectroscopic technique that detects species with unpaired electrons. This method involves the addition of a spin trap compound such as DMPO that reacts with any reactive radicals *e.g.*, hydroxyl, carboxyl radical (carbon dioxide radical anion (CO₂•⁻), etc. present, and gives rise to a radical adduct than can be subsequently identified. Typical spectra of the spin adduct DMPO-HO• and DMPO-CO₂•⁻ are given in the Figure 23 b.

To detect the DMPO-radical adducts in UV pre-irradiated samples, ESR spectra were recorded on aliquot (50 μL) withdrawn at the 5th, 10th, 20th and 30th min of UV irradiation (Figure 23 a). ESR spectra of negative control (NC) were recorded only at the 30th min of UV irradiation.

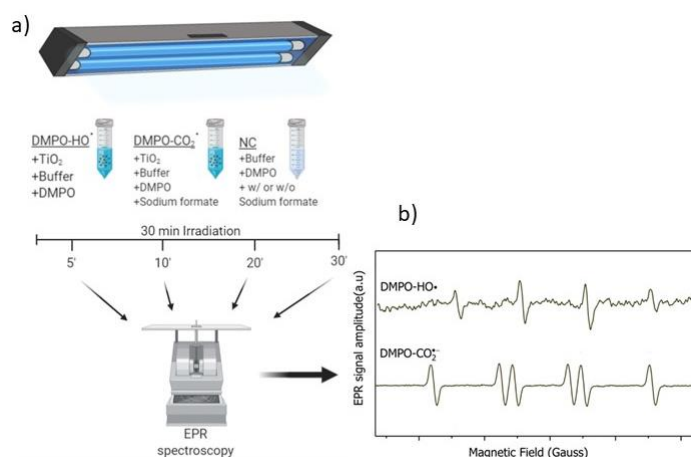


Figure 23. Detection of DMPO-HO• and the DMPO-CO₂•⁻ from UV-irradiated TiO₂ samples by ESR method (a), example of ESR spectrum of the DMPO-HO• and the DMPO-CO₂•⁻ radical adducts (b).

1.2. HO• and CO₂•⁻ radicals generation

Figures 24 and 25 show the ESR spectra of DMPO-HO• and DMPO-CO₂•⁻ adducts obtained on irradiation of TiO₂ NPs suspension.

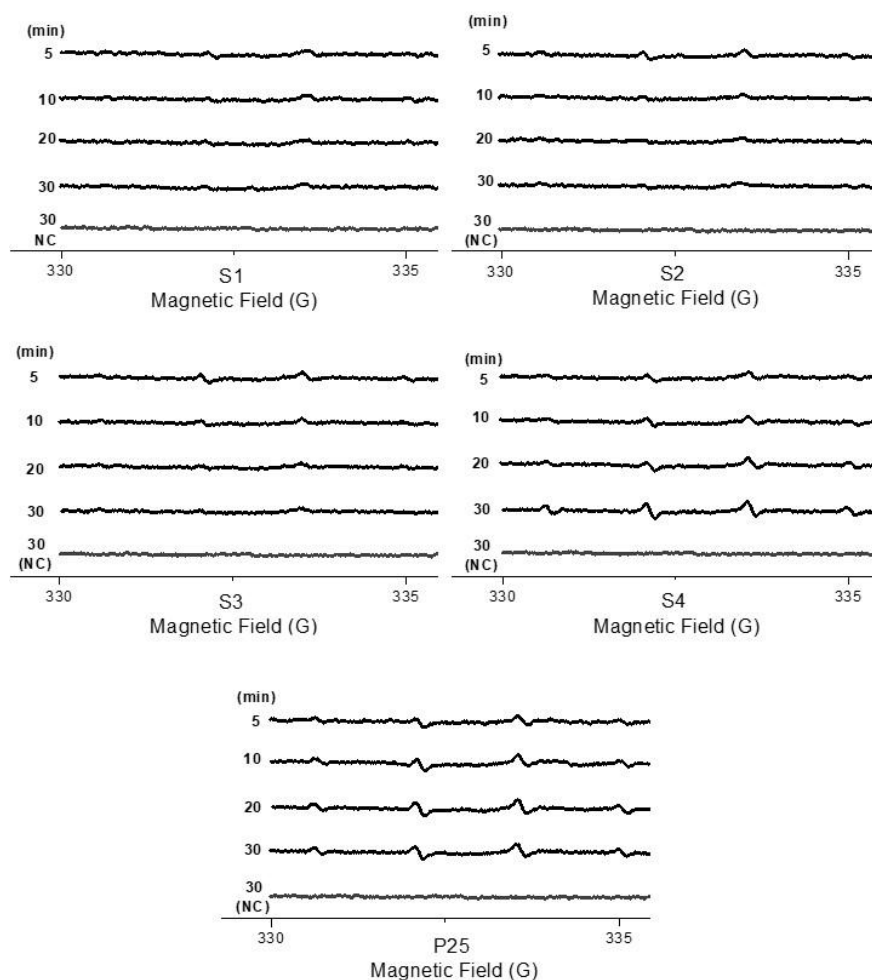


Figure 24. Generation of HO• radicals from 5, 10, 20, and 30 min UV irradiated TiO₂ NPs and 30 min UV irradiated negative control (NC-without TiO₂ NPs).

The signal intensity of DMPO-HO• formed by irradiated TiO₂ NPs did not increase during 30 minutes for S1, S2 and S3. However, S4 and P25 showed a characteristic 1:2:2:1 quartet signal and became detectable with irradiation time increase although the DMPO-HO• signals were weak. The observed weak HO• signal might be due to the low concentration of the particle suspensions. However, characteristic peaks of DMPO-CO₂•⁻ were observed in all the irradiated suspensions of TiO₂ and the intensity was increased in a time-dependent manner.

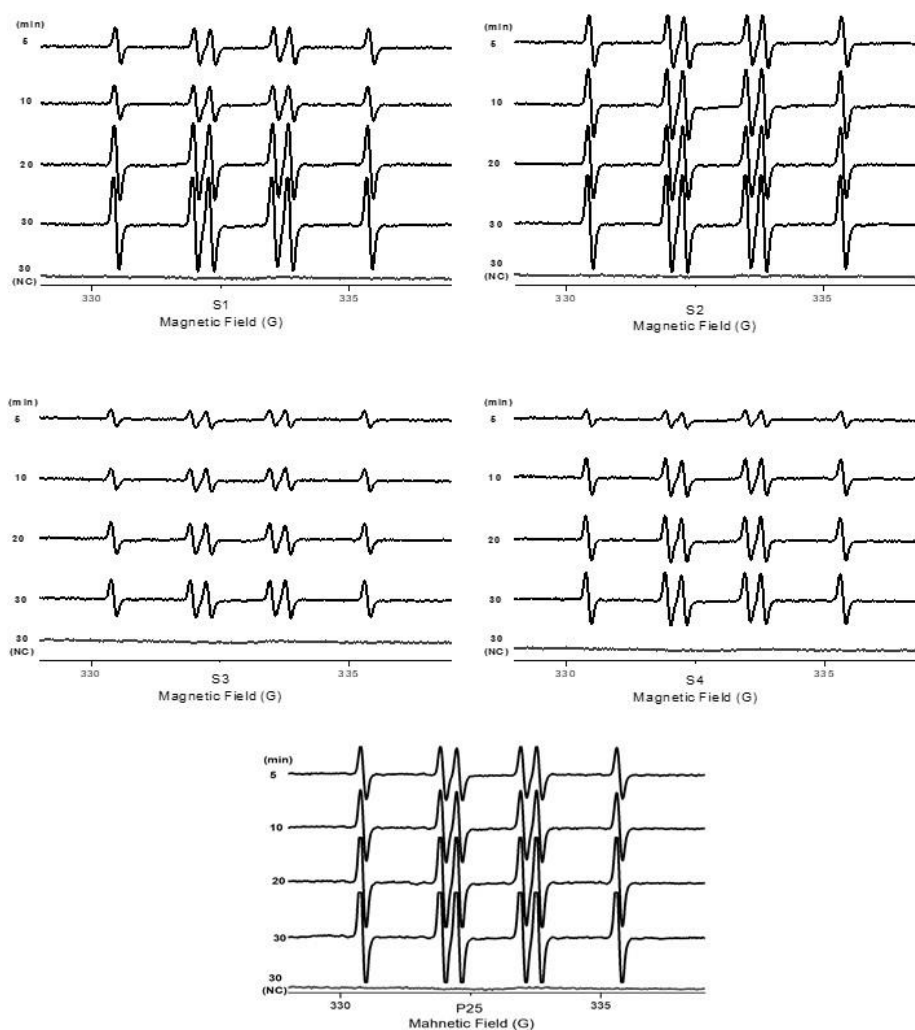


Figure 25. Generation of $\text{CO}_2\cdot^-$ radicals from 5, 10, 20, and 30 min UV irradiated TiO_2 NPs and 30 min UV irradiated negative control (NC-without TiO_2 particles).

The DMPO- $\text{CO}_2\cdot^-$ intensity was higher for S1, S2, and P25 than S3 and S4. The most prominent production of $\text{CO}_2\cdot^-$ radicals was observed with P25, followed by S2 and S1, while S3 and S4 gave the least yields.

Parameters such as crystalline structure and primary particle size affect the photocatalytic ability of TiO_2 NPs. Regarding the crystalline structure, mixed phase P25 showed greater $\text{CO}_2\cdot^-$ radical intensity in the first 5 minutes and at 30 minutes slightly higher intensity was observed than for anatase S2 (21 nm) and S1 (15 nm). This can be explained by the synergistic effect between the two phases that reduces the recombination effect, as reported earlier [189]. Also it is indicated that mixed-phase TiO_2 NPs are better photocatalysts than simple mixture of single-phase

nanoparticles due to their close-contact heterophase junctions [190]. Smaller and spherical shape TiO₂ NPs (15 nm S1, 30 nm S2 and 21 nm P25) showed greater ROS production than bigger rod shape S3 NPs. Similar to our results, P25 showed greater ROS production than bigger (108 nm) anatase TiO₂ NPs [191]. We also observed the surface charge impact: APTES coated, positively charged S4 NPs exhibited weaker signals whereas S2 NPs, their negatively charged counterparts, showed greater DMPO-CO₂•⁻ production. Overall, TiO₂ NPs enhance photocatalytic production of ROS depending on their physicochemical properties. The potential of this compound to generate larger amounts of carbon dioxide radical anion (CO₂•⁻) in suspension should be taken into account in preventing its potential oxidative damage.

2. Conclusion

The highlights of the article '**Short pre-irradiation of TiO₂ nanoparticles increases cytotoxicity on human lung coculture system**' were:

- Irradiated TiO₂ NPs caused a greater reduction in cell viability compared to the pristine TiO₂ NPs on human lung cells.
- Pristine and irradiated TiO₂ NPs caused a similar pro-inflammatory response.
- No ROS production was observed either for pristine or irradiated TiO₂ NPs treated cells.

30 min UV irradiation altered the average aggregate size and surface charge of NPs. These alterations might be responsible for the greater cell loss observed when cells were exposed to pre-irradiated TiO₂ NPs. The DMPO-HO• signal remained fairly unaffected by UV irradiation, however time-dependent changes in DMPO-CO₂•⁻ signal intensity of a suspension of TiO₂ were observed.

When the physicochemical properties of the NPs were taken into account, the NPs with smaller size, negative surface charge and spherical shape caused more intense DMPO-CO₂•⁻ signal than bigger, rod and positively charged NPs.

Les résultats marquants de l'article '**Exposure of TiO₂ NPs to UV light increases their cytotoxicity on human lung cells in relation to altered physicochemical features**' étaient :

- Les NPs de TiO₂ pré-irradiées provoquent une plus grande réduction de la viabilité cellulaire par rapport aux NPs de TiO₂ non irradiées sur les cellules pulmonaires humaines.
- Les NPs de TiO₂ pré-irradiées et non irradiées provoquent une réponse pro-inflammatoire similaire.
- Aucune production de ROS n'a été observée dans les cellules exposées aux NPs de TiO₂ pré-irradiées ou non irradiées.

Une irradiation UV de 30 min a modifié la taille moyenne des agrégats et la charge de surface des NPs. Ces changements pourraient être responsables de la diminution de viabilité observée chez les cellules exposées aux NPs de TiO₂ pré-irradiées. Le signal DMPO-HO• n'a pas été affecté par l'irradiation UV, mais des changements en fonction du temps de l'intensité du signal DMPO-CO₂•⁻ d'une suspension aqueuse de TiO₂ ont été observés.

Lorsque les propriétés physicochimiques des NPs ont été prises en compte, les NPs de plus petite taille, de charge de surface négative et de forme sphérique ont provoqué un signal DMPO-CO₂•⁻ plus intense que les bâtonnets plus gros et les NPs chargées positivement.

Chapter 4

Impact of the Physicochemical Features of Titanium Dioxide Nanoparticles on The Protein Corona Formation

After examining the toxicity of TiO₂ NPs depending on their physicochemical and photocatalytic properties in *Chapter 2* and *Chapter 3*, protein corona formation around TiO₂ NPs, which is another factor affecting toxicity, has been investigated in this chapter.

The aim of this study was to characterize the formation of the protein corona of TiO₂ NPs as a function of the main NPs physicochemical features and investigate potential relationship with the cytotoxicity NPs induce *in vitro* in human lung cells as reported in *Chapters 2* and *3*. This was the topic of the following paper published in Royal Society of Chemistry Advances.

The protein corona formation of 30 min UV irradiated TiO₂ NPs was also qualitatively /semi-quantitatively determined and reported in this chapter as complementary data.

Chapitre 4

Impact des Caractéristiques Physicochimiques de Nanoparticules de Dioxyde de Titane sur la Formation de la Corona Protéique


Après avoir examiné la toxicité des NPs de TiO₂ en fonction de leurs propriétés physicochimiques et photocatalytiques dans les chapitres 2 et 3, la formation de la corona protéique autour des NPs de TiO₂, qui est un autre facteur affectant leur toxicité, a été étudiée dans ce chapitre.

L'objectif de cette étude était de caractériser la formation de la corona protéique des NPs de TiO₂ en fonction des principales caractéristiques physicochimiques des NPs et d'étudier la relation potentielle avec la cytotoxicité que les NPs induisent *in vitro* dans les cellules pulmonaires humaines et qui est décrite aux chapitres 2 et 3. Cette étude a fait l'objet de l'article suivant publié dans Royal Society of Chemistry Advances.

La formation de la corona protéique des NPs de TiO₂ irradiées aux UV pendant 30 minutes a également été déterminée qualitativement / semi-quantitativement et est présentée dans ce chapitre en tant que données complémentaires.

Cite this: *RSC Adv.*, 2020, 10, 43950

Influence of the physicochemical features of TiO₂ nanoparticles on the formation of a protein corona and impact on cytotoxicity†

Ozge Kose, Marion Stalet, Lara Leclerc and Valérie Forest *

Due to their unique properties TiO₂ nanoparticles are widely used. The adverse effects they may elicit are usually studied in relation to their physicochemical features. However, a factor is often neglected: the influence of the protein corona formed around nanoparticles upon contact with biological media. Indeed, although it is acknowledged that it can strongly influence nanoparticle toxicity, it is not systematically considered. The aim of this study was to characterize the formation of the protein corona of TiO₂ nanoparticles as a function of the main nanoparticle properties and investigate potential relationship with the cytotoxicity nanoparticles induce *in vitro* in human lung cells. To that purpose, five TiO₂ nanoparticles differing in size, shape, agglomeration state and surface charge were incubated in cell culture media (DMEM or RPMI supplemented with 10% fetal bovine serum) and the amount and profile of adsorbed proteins on each type of nanoparticle were compared to their toxicological profile. While nanoparticle size and surface charge were found to be determinant factors for protein corona formation, no clear impact of the shape and agglomeration state was observed. Furthermore, no clear relationship was evidenced between the protein corona of the nanoparticles and the adverse effect they elicited.

Received 2nd October 2020
Accepted 24th November 2020

DOI: 10.1039/d0ra08429h

rsc.li/rsc-advances

1. Introduction

Titanium dioxide (TiO₂) nanoparticles are among the most produced and industrially used nanoparticles.¹ Because their small size confers unique properties, they are used in a wide range of application fields. They are for instance characterized by their brightness/whiteness, high refractive index, opacifying strength, resistance to discoloration, self-cleaning and antifogging property, ultraviolet block capacity, catalytic properties and antimicrobial activity.^{2–5} Many applications can take advantage of these properties, both in the industrial sector and in daily-life consumer products. Thus, TiO₂ nanoparticles can be used as pigment, catalyst, in paints, papers, inks, plastics, rubber industry, solar cells, construction material, self-cleaning roof tiles and windows, anti-fogging car mirrors, textile, as food additive (E171), in personal care products (toothpaste, cosmetics, sunscreens), in environmental or biomedical applications (photocatalytic degradation of pollutants, air and water purification, biosensing, drug delivery) and even in pharmaceuticals.^{1,2,4–6}

Initially considered as biologically inert, titanium dioxide was classified as “possibly carcinogen to humans” (Group 2B) by the International Agency for Research on Cancer (IARC).²

However, it remains a controversial issue as there is not only one type of TiO₂ nanoparticles but several depending on their physicochemical features and conclusions can hardly be generalized. Indeed, the biological impact of nanoparticles is directly influenced by their physicochemical characteristics.^{7,8} We previously assessed the cytotoxicity induced by TiO₂ nanoparticles on human lung cell lines in relation to their physicochemical features.⁹ We observed a higher toxicity with bigger sized, less agglomerated, rod-shaped, and positively charged TiO₂ nanoparticles, confirming that nanoparticle toxicity is directly correlated with their physicochemical features.

However, to fully understand this relationship, another factor has to be considered: the formation of a protein corona. Indeed, upon contact with biological media, the biomolecules they contain, and especially proteins, rapidly adsorb on the nanoparticle surface forming a crown, the so-called corona. This formation is directly influenced both by the biological environment (medium composition and factors such as temperature, pH, duration of incubation, etc.) and by the nanoparticle physicochemical features (especially, size, shape, surface charge and hydrophobicity).^{10–21} The protein corona represents the new interface between nanoparticles and biological systems and will thus have a strong impact on their interactions and the subsequent cell response. The pristine nanoparticle being “screened” by the proteins adsorbed on its surface, interactions with biological systems will be made through this protein layer and not with bare materials.²² It will

Mines Saint-Etienne, Univ Lyon, Univ Jean Monnet, INSERM, U1059 Sainbiose, Centre CIS, F-42023 Saint-Etienne Cedex 2, France. E-mail: vforest@emse.fr

† Electronic supplementary information (ESI) available. See DOI: 10.1039/d0ra08429h

consequently determine the physiological behavior of nanoparticles, triggering vast biological outcomes.^{13,23,24}

It is commonly acknowledged that the protein corona generally mitigates the cytotoxicity induced by nanoparticles^{23–28} as a consequence of a lower cell uptake.^{29–37} However, some studies have shown on the contrary that the presence of a protein corona can enhance the nanoparticle cytotoxicity.³⁸

In any way, a better characterization of the nanoparticle corona is of paramount importance to better understand the biological effects of nanoparticles. The aim of this study was to characterize the formation of the protein corona of TiO₂ nanoparticles as a function of the main nanoparticle properties and investigate potential relationship with the cytotoxicity nanoparticles induce *in vitro* in human lung cell lines. To that purpose, 5 TiO₂ nanoparticles differing in size, shape, agglomeration state and surface charge were incubated in cell culture media and the amount and profile of adsorbed proteins on each type of nanoparticle were compared to their toxicological profile.

2. Materials and methods

Our approach is summarized in Fig. 1.

The protocol used for the semi-quantitative analysis of the protein corona composition of TiO₂ nanoparticles was inspired from Docter *et al.*³⁹ but was adapted to our nanoparticles and conditions.

2.1. Nanoparticles

Five types of TiO₂ nanoparticles were used in this study. In addition to commercial P25 nanoparticles (Evonik P25 CAS:

1317-70-0, Sigma-Aldrich, France) used as a reference, four types of TiO₂ nanoparticles were synthesized with different and well-controlled physicochemical properties. They were referred to as S1 to S4 and differed in size, shape, agglomeration state and surface functionalization/charge. They were synthesized using Chen *et al.* method.⁴⁰ Basically, titanium(IV) butoxide (CAS: 5593-70-4 reagent grade 97%, Sigma-Aldrich, Saint-Quentin-Fallavier, France) was mixed with triethanolamine (CAS: 102-71-6, Analytical reagent 97%, VWR International, Fontenay-sous-Bois, France) in 1 : 2 molar ratio. The mixture was put in Teflon lined sealed autoclave and then heated at 150 °C during 24 h. The pH values of the synthesis medium were adjusted using HCl or NH₄OH to tune particle size and morphology. Finally, the solutions were washed by three centrifugations using de-ionized water and the resulting products were dried in an oven at 40 °C. Surface functionalization of S2 nanoparticles was generated by aminopropyltriethoxysilane (APTES) using Zhao *et al.* method.⁴¹ Briefly, 0.25 g of S2 nanopowder was dispersed in 25 mL de-ionized water by ultrasonication for 10 min. Then, the silane coupling agents APTES were added in the dispersion (molar ratio of 1 : 1). The mixture was sonicated until a clear solution was obtained and then refluxed at 80 °C for 4 h. After that, dispersed particles were separated from solvent by centrifugation (10 min at 1200g) followed by washing with water at least 2 times. The final functionalized samples were then prepared in de-ionized water and labeled as S4.

Stock suspensions of all nanoparticles (1600 µg mL⁻¹) were prepared in de-ionized water (MilliQ systems, Millipore, Bedford, MA, USA) and sonicated with Branson Sonifier S-450 for 10 min at 89% amplitude. Nanoparticles were then extensively characterized.⁹ The morphology and size distribution of the

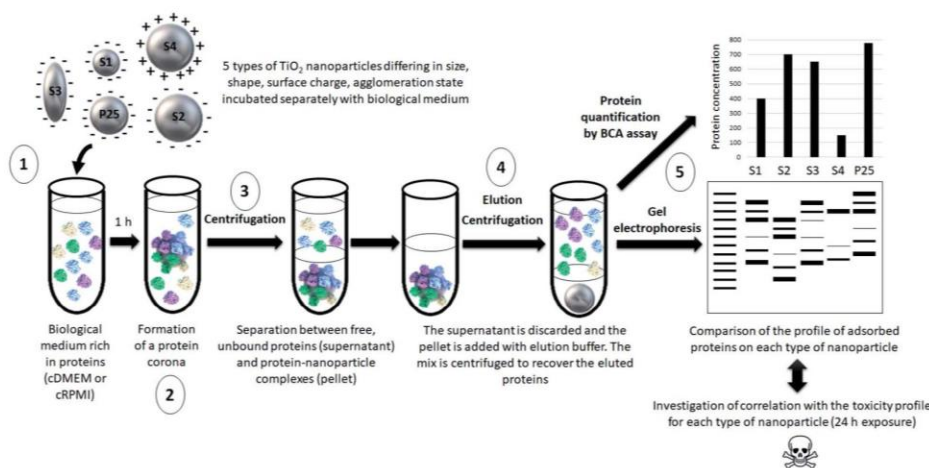


Fig. 1 Schematic representation of the main steps of our approach. (1) 5 types of nanoparticles characterized by different physicochemical features were incubated in a biological fluid (cell culture medium) for 1 h. (2) Proteins from this biological environment adsorbed at the nanoparticle surface forming the so-called protein corona. (3) The nanoparticle–protein complexes were separated from unbound proteins by centrifugation. (4) Proteins were then eluted from nanoparticles and (5) quantified by a protein assay and analyzed by gel electrophoresis. The profile of adsorbed proteins was discussed with regard to the physicochemical features of the nanoparticles and potential correlations with their previously assessed toxicity profile were investigated.

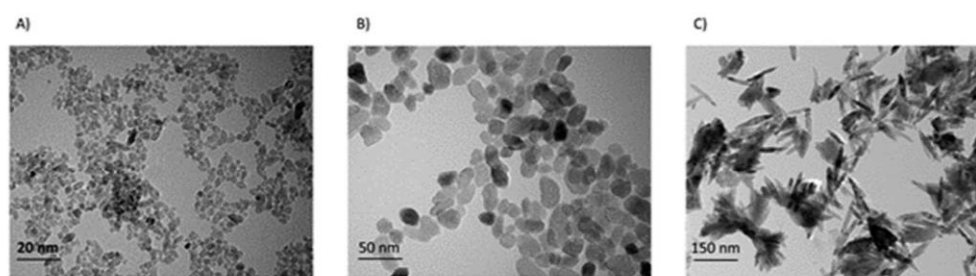


Fig. 2 Transmission electron microscope images of S1 (A), S2 (B), and S3 (C) TiO₂ nanoparticles.

Table 1 Particle primary size (TEM), specific surface area (SSA, BET), shape (TEM, SEM), and crystal structure (XRPD)

	Primary size (nm)	SSA (m ² g ⁻¹)	Particle shape	Crystal structure	Surface coating
S1	15	146	Spherical	Anatase	No
S2	30	61	Spherical	Anatase	No
S3	20–250 ^a	41	Rod	Anatase	No
S4	30	61	Spherical	Anatase	APTES ^b
P25	21	55	Spherical	Anatase: Rutile (90 : 10)	No

^a Minimum and maximum Feret diameters. ^b APTES coating was carried out on S2 nanoparticles to obtain S4 nanoparticles.

nanoparticles were analyzed by transmission electron microscopy (TEM) using a FEI TECNAI 20FST operating at 200 kV and scanning electron microscopy (SEM) at 2–3 kV on a Zeiss Sigma 300 microscope using a secondary electron detector. Fig. 2 illustrates the morphology of the nanoparticles. After each TEM image of each sample were chosen, the size distribution and the mean diameter were measured by ImageJ software.

The hydrodynamic size and the agglomeration status of the TiO₂ nanoparticles (120 µg mL⁻¹) in de-ionized water and in culture media were determined by using dynamic light scattering (DLS, Zetasizer Nano ZS Malvern Instruments, Worcestershire, UK) measurements. Surface charge of the nanoparticles was monitored using electrophoretic light scattering (ELS, Zetasizer Nano ZS Malvern Instruments, Worcestershire, UK). Specific surface areas (SSA) were measured by linearizing the physisorption isotherm of N₂ at 77 K with the classical method of Brunauer, Emmett and Teller (BET) (Volumetric Adsorption ASAP 2020, Micrometrics, USA).⁴²

Tables 1 and 2 summarize the main physicochemical features of the nanoparticles. DLS graphs can be found in ESI.†

2.2. Biological media

Two types of cell culture media were used: Dulbecco's Modified Eagle Medium (DMEM) high glucose (4.5 g L⁻¹) with stable glutamine and sodium pyruvate (cat. no. L0103-500, VWR International, France) and Roswell Park Memorial Institute (RPMI 1640) with L-glutamine (cat. no. L0500-500, Gibco, Life Technologies, France). Both media were supplemented with 10% (v/v) fetal bovine serum (FBS, cat. no. S1810-500, Biowest, France, for the reproducibility of the results, we ensured that all FBS aliquots came from the same batch) and 1% penicillin-streptomycin (VWR International, France). Once

supplemented, media were called complete and referred to as cDMEM and cRPMI respectively.

2.3. Nanoparticles/biological media contact

To ensure comparability between the results the ratio of total particle–surface area to the biological medium volume has to be kept constant for all nanoparticles. After preliminary experiments, we established that the optimal ratio was 0.1 m² mL⁻¹ in a final volume of 4 mL. Based on the nanoparticle surface specific area (SSA), we calculated for each nanoparticle type the volume of stock solution to dilute in culture medium as reported in Table 3. TiO₂ nanoparticles were incubated either in cRPMI or cDMEM for 1 h at 37 °C.

2.4. Removal of unbound proteins

Samples were centrifuged 1 h at 14 100g (Mini-centrifuge MiniSpin Plus, VWR International, Fontenay-sous-Bois, France) at room temperature to separate the nanoparticle–protein complexes from the cell culture medium. The supernatant was discarded and the pellets were washed with 1 mL PBS to remove the proteins that did not bound tightly to the nanoparticles, the tubes were sonicated (Branson Sonifier S-450, amplitude 89%, pulse 2 s and intervals 2 s). Two additional washes consisting of a 20 min centrifugation at 14 100g, room temperature were carried out. The supernatant was finally discarded and the pellet containing the nanoparticle–protein complexes was used for the next step.

2.5. Recovery of the proteins adsorbed at the surface of the nanoparticles

Proteins were eluted from the nanoparticle–protein complexes by adding 300 µL of Laemmli buffer containing 62.5 mM Tris,

Table 2 Average hydrodynamic size, polydispersity index (PDI) and zeta potential in deionized water (DI H₂O) and in culture media (cDMEM and cRPMI) after dispersion of TiO₂ nanoparticles (120 µg mL⁻¹). All data are presented as means of three independent characterizations ± standard deviation

	DI H ₂ O		cDMEM		cRPMI	
	Average hydrodynamic size ^a (nm) (PDI)	Zeta potential (mV) pH 7.5	Average hydrodynamic size ^a (nm) (PDI)	Zeta potential (mV) pH 7.5	Average hydrodynamic size ^a (nm) (PDI)	Zeta potential (mV) pH 7.5
S1	211.4 ± 2.3 (0.15)	-15.8 ± 4.0	226 ± 9.1 (0.28)	-33.8 ± 1.8	241.4 ± 3.0 (0.22)	-12.6 ± 1.6
S2	969.3 ± 39.5 (0.27)	-13.8 ± 4.4	1094 ± 46.4 (0.36)	-31.0 ± 0.3	1138 ± 35.9 (0.328)	-11.8 ± 0.6
S3	1409 ± 89.6 (0.11)	-13.2 ± 4.2	1275 ± 66.6 (0.18)	-32.0 ± 3.0	1267 ± 111.5 (0.42)	-10.9 ± 0.1
S4	1204 ± 59.9 (0.16)	+12.3 ± 0.5	1398 ± 54.9 (0.48)	-36.6 ± 4.5	1515 ± 16.01 (0.312)	-11.4 ± 0.6
P25	256.4 ± 136.6 (0.27)	-15.2 ± 5.3	325 ± 4.1 (0.26)	-28.1 ± 0.6	434.6 ± 21.1 (0.33)	-11.9 ± 0.5

^a Dynamic light scattering (DLS) measurements are the mean of at least 3 runs each containing 20 sub-measurements.

Table 3 Preparation of nanoparticle samples for cell culture media contact. The final nanoparticle–surface area ratio was 0.1 m² mL⁻¹. NP: Nanoparticle

NP type	SSA (m ² g ⁻¹)	NP stock solution concentration (µg mL ⁻¹)	NP stock volume (µL)	Cell culture medium volume (µL)	Total volume (µL)
S1	146.5	16 000	171	3829	4000
S2	61.02	16 000	410	3590	4000
S3	40.78	16 000	613	3387	4000
S4	61.02	16 000	410	3590	4000
P25	55.00	16 000	455	3545	4000

5% (vol/vol) glycerol, 2% (wt/vol) SDS. After a 5 min incubation at 95 °C, the samples were centrifuged for 15 min at 14 100g at room temperature. The supernatant containing the eluted corona proteins was transferred into an Eppendorf Protein Lobind tube and used for protein quantification and gel electrophoresis as described below.

2.6. Determination of protein concentration

The protein concentration was assessed in the supernatant using a BCA protein assay kit (Pierce, Thermo Fisher Scientific, France) according to the manufacturer's instructions. Briefly, in a microplate 25 µL of solution were transferred per well and added with 200 µL of reagents from the kit. The plate was shaken for 30 s, covered and incubated at 37 °C for 30 min. After cooling to room temperature, the absorbance at 562 nm was read with a microplate spectrophotometer (Multiskan, Thermo Fisher Scientific, France). Calculation of protein concentrations was based on the use of a standard curve established with BSA (protein standard included in the kit). Results are means of three independent experiments each performed in duplicate.

2.7. Determination of the profile of proteins adsorbed at the surface of the nanoparticles by gel electrophoresis

30 µL of sample was added with 10 µL of 4× Bolt LDS sample buffer Novex (Invitrogen, Thermo Fisher Scientific, France). The mix was heated at 70 °C for 10 min. Samples were loaded in precast polyacrylamide gels (Invitrogen Bolt Bis-Tris Plus 4–12%, 10 wells, Thermo Fisher Scientific, France). A well was

filled with 10 µL protein markers (SeeBlue Plus2 pre-stained protein standard Novex, Thermo Fisher Scientific, France). 1× running buffer was prepared by mixing 50 mL of 20× Bolt MES SDS Novex (Invitrogen, Thermo Fisher Scientific, France) with 950 mL of deionized water. The gel was run at room temperature, at 200 V constant for 22 min. It was then directly transferred into the Instant Blue staining solution (cat. no. ISB1L, Expedeon) for 1 h at room temperature with gentle shaking. A picture of the gel was taken. Three independent experiments were performed.

2.8. Nanoparticle cytotoxicity assessment

The cytotoxicity of the TiO₂ nanoparticles was previously assessed⁹ on a human lung coculture system consisting of A549 epithelial cells and THP-1 differentiated macrophages cultivated in cDMEM. After a 24 h cell exposure to 15, 30, 60 or 120 µg mL⁻¹ of nanoparticles, cytotoxicity was assessed in terms of cell viability (Trypan blue exclusion assay), pro-inflammatory response (production of the IL-8 and TNF-α cytokines assessed by commercial ELISA kits) and oxidative stress (production of reactive oxygen species, ROS detected by the cell-permeable fluorogenic probe 2',7'-dichlorodihydrofluorescein diacetate, DCFH-DA).

2.9. Statistical analysis

For protein quantification, unless otherwise stated, results are expressed as mean of 3 independent experiments, each performed in duplicate ± standard deviation (SD). Statistical

analyses were performed using GraphPad Prism® (version 8.0, GraphPad Software, San Diego, CA, USA). Statistical analyses were conducted using a one-way Anova analysis followed by a Tukey's multiple comparison test. Differences were considered statistically significant when $P < 0.05$. The amount of proteins found in the corona of S1 and S3 was compared to that of the P25 reference. The amount of proteins found in the corona of S2 was compared to that of S4, its APTES-functionalized counterpart. Finally, the protein amount was compared between protein coronas formed in cDMEM and those formed in cRPMI for each sample.

3. Results

3.1. Protein concentration

Fig. 3 reports the mean concentrations of proteins eluted from the corona of the different nanoparticles incubated either in cDMEM or cRPMI.

For both media, proteins were less abundantly found in the corona from S4 nanoparticles. S2, S3 and P25 nanoparticles exhibited similar amounts of proteins in their corona. A slightly less important protein concentration was observed in the S1 corona.

For each nanoparticle type, a similar concentration of proteins was found in the coronas formed either in cDMEM or cRPMI (no statistically significant differences).

3.2. Profile of proteins adsorbed at the surface of the nanoparticles by gel electrophoresis

Fig. 4 illustrates the protein profile of the corona of the different nanoparticle types. The picture is representative of the three experiments performed.

Both in cDMEM and cRPMI we clearly observed that the corona of S2, S3 and P25 had very similar protein profiles, S1 presented a slightly lower amount of proteins whereas S4 corona exhibited the smallest protein content. These results are

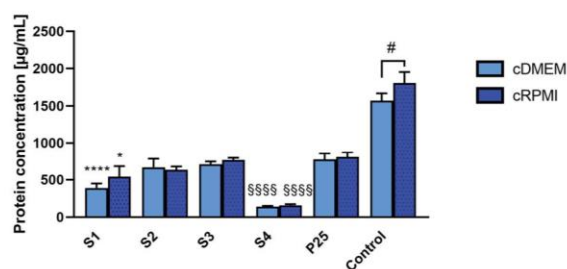


Fig. 3 Concentrations of proteins eluted from the protein corona of S1, S2, S3, S4 and P25 nanoparticles that were incubated either in cDMEM or cRPMI. Controls are cDMEM or cRPMI alone. Results are means of 3 independent experiments (except for S3 where we did not have enough nanoparticle sample to perform the last repetition so results are means of 2 independent experiments for this sample), standard deviation is also indicated. Statistically different from P25 (*) $P < 0.05$, (****) $P < 0.0001$. Statistical difference between S2 and S4 (#####) $P < 0.0001$. Statistical difference between cDMEM and cRPMI (#) $P < 0.05$.

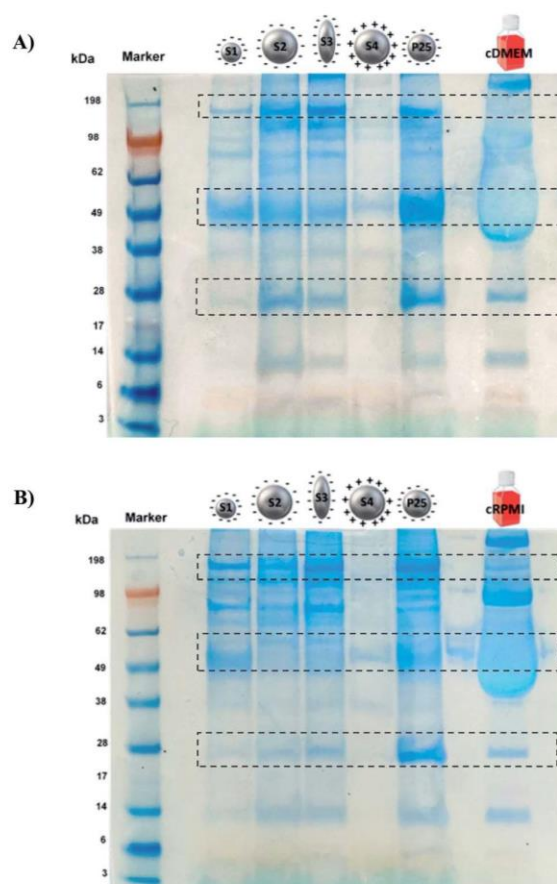


Fig. 4 SDS-PAGE of S1, S2, S3, S4 and P25 nanoparticles incubated either in cDMEM (A) or in cRPMI (B). As controls, the complete biological media alone were also run (last lane).

Table 4 Toxicity profiles observed for the studied TiO₂ nanoparticles incubated for 24 h in a lung coculture system (A549 epithelial cells/macrophages differentiated from THP-1 cells). Cytotoxicity was evaluated by assessing cell viability with Trypan blue assay. Pro-inflammatory response was assessed by the production level of the IL-8 and TNF- α pro-inflammatory cytokines. Oxidative stress was determined by the assessment of the ROS produced

	Cytotoxicity	Pro-inflammatory response	Oxidative stress
S1	+	+	–
S2	++	+	–
S3	++++	++	–
S4	++	++	–
P25	+++	++	–

in perfect agreement with those of protein quantification (Fig. 3). In qualitative terms, interestingly and as highlighted by the rectangles on Fig. 4, we could observe that some proteins largely bound to the nanoparticles were not necessarily the most abundant in the culture medium (control lane).

3.3. Nanoparticles toxicity profiles

Table 4 reports the cytotoxicity patterns of the different nanoparticle types as previously assessed.⁹

We clearly observed different patterns of toxicity depending on the nanoparticle considered in relation with its physicochemical characteristics.⁹

4. Discussion

Fig. 5 summarizes the findings of this paper as well as previous data for discussion.

4.1. Impact of the nanoparticle physicochemical features on the formation of the protein corona

It has been extensively reported in the literature that the nanoparticle physicochemical features play a key role in the formation of the protein corona, especially, size, shape, surface charge and hydrophobicity.^{19–21,43} In this study, by comparing the protein corona formation around 5 types of TiO₂ nanoparticles differing in size, shape, surface charge and agglomeration state, we aimed to shed light on the respective influence of such parameters.

By comparing S1 and P25 we could highlight the influence of nanoparticle size/SSA on the formation of the protein corona. We observed that smaller S1 nanoparticles (15 nm) showed a slightly less important amount of proteins in their corona compared to bigger P25 nanoparticles. This observation can be easily explained by the fact that when nanoparticle size varies, the curvature of the nanoparticle–protein interface is altered consequently affecting the protein adsorption at the

nanoparticle surface. Similarly, a change in nanoparticle size/SSA induces an alteration of the deflection angle between adjacent proteins, thus when the size of the nanoparticle decreases, more steric repulsion occurs between the proteins of the corona.¹² In other words, smaller nanoparticles increase the deflection angle of the proteins and have a higher curvature than bigger nanoparticles, which can strongly impact qualitatively and quantitatively the composition of the protein corona.²⁰ It has even been shown that highly curved surfaces (very small nanoparticles) can suppress protein adsorption to the point where it no longer occurs.⁴⁴ Moreover, Tenzer *et al.*¹⁸ demonstrated that even a 10 nm particle size difference significantly determined the protein corona of silica nanoparticles.

The influence of the nanoparticle shape on the formation of the protein corona was investigated by comparing rod-shaped S3 and spherical P25 nanoparticles. The amount and profile of proteins in the corona were similar, suggesting no impact of the shape. This finding is not in agreement with previous studies where nanorods were reported to adsorb more proteins than nanospheres of similar size, thanks to their small curvature.^{19,45} This discrepancy can be due to the fact that the nanoparticles used in these studies were of different chemical nature (gold and silica) and of different sizes (10 and 270 nm for nanospheres and 10–35 and 270–1100 nm for nanorods). The nanoparticle–surface area ratios used were also different (0.003 and 0.05 m² mL⁻¹). This argues for a complex picture where several parameters are concomitantly involved.

S2 and P25 nanoparticles exhibited similar pattern suggesting that nanoparticle agglomeration state does not play a major role in the formation of the protein corona.

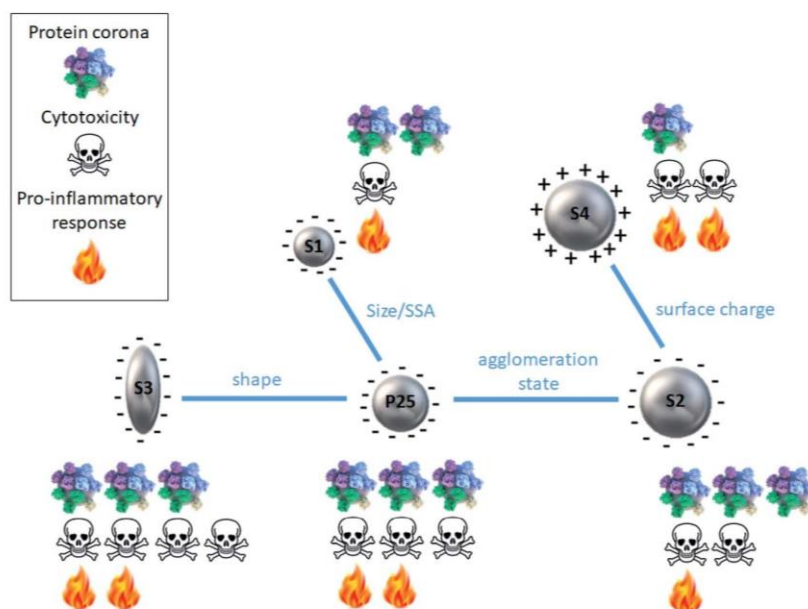


Fig. 5 Schematic summary of the protein corona and cytotoxicity profiles for each type of TiO₂ nanoparticle in relation with its physicochemical features.

On the contrary, by comparing the protein coronas of S2 and S4 (amine-functionalized form of S2) nanoparticles, we clearly observed a significant impact of the nanoparticle surface charge on the formation of a protein corona, confirming previous studies. However, it was quite surprising to observe that protein coronas were preferentially formed on negatively charged nanoparticles. Indeed, it is generally admitted that charged particles tend to adsorb more proteins than neutral nanoparticles.^{12,16,17,20} The logical explanation is that, negatively charged particles attract positively charged proteins and *vice versa*. But, proteins contained in FBS are largely negative for a pH around 8, it should thus be reasonable to expect a larger protein binding to nanoparticles which surface is positively charged. However, this simplified statement does not fit all circumstances.^{12,46,47} And our finding is consistent with those of Bewersdorff *et al.*⁴⁸ who reported that serum proteins preferably bound to negatively charged nanoparticles compared to positively charged ones. Tenzer *et al.*¹⁸ also demonstrated that, at physiological pH (7.3), proteins in general with negative charge were preferentially bound by negatively charged SiO₂ nanoparticles irrespective of their relative plasma abundance. As nanoparticle surface chemistry has been shown to deeply influence the evolution and composition of a protein corona, it could be assumed that the nature of the chemical groups used for functionalization can contribute to controversial results. In our case, we can hypothesize a smaller protein corona for positively charged S4 nanoparticle as a result of a potential steric repulsion between the serum proteins and the amine groups of the APTES.

4.2. Impact of biological media on the formation of nanoparticle corona

As it is widely acknowledged that the protein corona formation also depends upon the biological environment^{13,49–51} we compared the protein profiles obtained when TiO₂ nanoparticles were incubated in two types of standard cell culture media, DMEM and RPMI, supplemented by 10% FBS. From the protein quantification as well as the protein profiles observed on electrophoresis gels, we could conclude that the nature of the medium did not really impact the protein concentration of the corona of any nanoparticles. This finding is not in agreement with Maiorano *et al.*³⁶ who exposed various sized citrate-capped gold nanoparticles to cDMEM and cRPMI and re-

observed when nanoparticles were incubated in cDMEM compared to cRPMI. This could be due to a different protein composition of the two cell culture media resulting in the binding of proteins of various nature, differently charged on nanoparticles, making the zeta potential vary accordingly. Thus this observation is not inconsistent with a similar amount of proteins bound to nanoparticles irrespective of the biological medium (Fig. 3). Further investigations are needed, especially a qualitative characterization of the protein corona composition.

4.3. Correlation with the toxicity profile of nanoparticles

Among the numerous parameters that influence nanoparticle-cell interactions, the presence of a protein corona plays a key role. In this regard, Lesniak *et al.* showed that for identical particles and cells, under identical conditions, the nanoparticle-cell interactions and the biological outcomes could vary greatly in the presence or in the absence of a preformed corona in serum.³⁴ Because the protein corona defines the biological identity of nanoparticles and affects their biological response, it is now accepted that the types of proteins and their abundance on the nanoparticle surface encode information that predicts nanoparticle bioactivity.²⁴ And it can predict it more accurately than using models based only on the physico-chemical properties of the nanoparticles.²⁰ Usually, the protein corona has a protective role against cell uptake and nanoparticles exhibiting a protein corona are less taken up than their bare counterparts.^{30–33,35,37} The protein corona could decrease nanoparticle adhesion to the cell membrane due to the decreased surface-free energy after binding with proteins, thus decreasing particle-cell interactions and resulting in reduced uptake.^{31,33} But some studies have shown the contrary, *i.e.* the presence of the protein corona enhancing nanoparticle uptake by cells.^{52,53} These discrepancies can be explained by different cell internalization pathways: in the presence of a corona, non-specific uptake seems to be decreased whereas specific uptake seems to be promoted.^{29,33,52,54} Because of a lower cell uptake the presence of a protein corona generally reduces the cytotoxic effects of nanoparticles.^{14,25,27,29,32,34,36} Furthermore, the presence of a protein corona by masking the nanoparticle surface can mitigate its reactivity in interfacing cellular membranes and consequently prevent potential adverse effects.^{34,55} At this point it is interesting to note that the five types of

always made and can lead to misinterpretations. Finally, the presence of a protein corona can increase the safety of nanoparticles by inhibiting the generation of radical oxygen species by which several compounds exert their cytotoxic activity.⁵⁶

In this context, the characterization of a nanoparticle protein corona is of paramount importance to better understand the mechanisms underlying its toxicity. As shown by Fig. 5, we were not able to evidence a clear relationship between protein corona pattern and the toxicity elicited by the nanoparticles. For instance, S4 exhibited the smallest protein corona and a significant cytotoxic activity. While S2, S3 and P25 had similar protein corona profiles, the intensity of the adverse effects they induced ranged from low to very high.

However, we should be cautious with this result as the nanoparticle doses used for the protein corona characterization and the cytotoxicity assays were different. Indeed, to allow comparison between the protein coronas of different nanoparticles, we used a constant total particle–surface area to biological medium volume ratio. We first tried concentrations equivalent to those used for cytotoxicity assays but we did not get enough proteins for analysis, therefore we increased the doses to get exploitable results. Such concentrations allowed us to conclude on the impact of the nanoparticle physicochemical features on the formation of the protein corona as discussed before. Although lower nanoparticle doses were used for cytotoxicity assays, we were able to rank the nanoparticles with respect to their toxicity and in Fig. 5 we reasoned in terms of relative and not absolute values making the comparison still meaningful. Similarly, another parameter to consider is the incubation time of the nanoparticles in the cell culture media (1 h in the present study of the protein corona and 24 h in the cytotoxicity assessment). This difference may result in a slightly different protein corona composition as this latter is known to evolve over time. Indeed, the proteins the most abundant in the medium and with high mobility first adsorb on the nanoparticle surface but they are progressively replaced by proteins exhibiting a higher affinity.^{12,57} However, it seems to be a really fast process as Tenzer *et al.* demonstrated that an interaction between nanoparticle surface and plasma proteins is established as early as after 30 s of contact and that protein corona nature did not change over time.¹⁷ It is thus reasonable to assume that protein corona composition remains quite stable after 1 h of nanoparticle/culture medium contact and we can confidently assume that it is representative of protein corona that would be observed after 24 h.

Furthermore, several assumptions can be made to explain the absence of clear correlation between the nanoparticle protein corona and toxicity. It is mainly related to our incomplete characterization of the protein corona. Indeed, because of technical challenges, we could only study the hard corona, composed of tightly bound proteins. The soft corona, consisting of less tightly bound proteins cannot be preserved during the analysis process. However, the soft corona represents the most external layer of proteins, which is thus likely to be in contact with biological systems. The unexplored role of soft protein corona may be a determinant factor for a better understanding of nanoparticle–cell interactions. One limitation of the present

study was to consider the protein corona mainly through a quantitative aspect. In addition, we have to keep in mind that it is a preliminary study aiming to draw general patterns, to gain a first impression about the amount and composition of the corona proteins and that further investigations, including more sensitive techniques such as mass spectrometry analyses are required to refine our conclusions. Indeed, many studies evaluating the protein corona of nanoparticles by 1D or 2D gel electrophoresis are followed by mass spectrometry.^{58,59} In particular, liquid chromatography–mass spectrometry (LC-MS) could be employed to determine protein corona composition qualitatively and quantitatively.

Indeed, to draw firm conclusion further investigations on the nature of the proteins should be conducted. It cannot be excluded that some proteins present at a minor level could be responsible for major biological consequences and *vice versa*.²⁹ Finally, it should be kept in mind that protein corona formation is very sensitive to many parameters both from the nanoparticle and the biological environment and minor changes in experimental conditions can have a deep impact on the protein corona formation/composition.^{21,30} It is an interplay of different forces in a competing environment.¹²

5. Conclusions

Protein corona is a major issue for the study of the nanoparticle fate and consequences especially *in vivo* but *in vitro* studies are very useful to better understand what happens at a cellular level. In our model and experimental conditions the parameters influencing the protein corona formation are mainly nanoparticle size and surface charge, no clear impact of the shape and agglomeration state was observed. Although protein corona nature may undoubtedly influence nanoparticle cytotoxicity, no clear relationship was evidenced between the protein corona of 5 types of TiO₂ nanoparticles and the adverse effects they elicited in human lung cells. More comprehensive studies (considering qualitative/quantitative aspects, hard/soft corona) are needed to better understand the relationship between nanoparticle protein corona and toxicity.

Conflicts of interest

There are no conflicts to declare.

Funding

This research did not receive any specific grant from funding agencies in the public, commercial, or not-for-profit sectors.

References

- 1 E. Baranowska-Wójcik, D. Sz wajgier, P. Oleszczuk and A. Winiarska-Mieczan, *Biol. Trace Elem. Res.*, 2020, **193**, 118–129.
- 2 IARC Working Group on the Evaluation of Carcinogenic Risks to Humans, International Agency for Research on Cancer and World Health Organization, *Carbon black*,

- titanium dioxide, and talc, International Agency for Research on Cancer, Distributed by WHO Press, Lyon, France, Geneva, 2010.
- 3 M. Skocaj, M. Filipic, J. Petkovic and S. Novak, *Radiol. Oncol.*, 2011, **45**, 227–247.
 - 4 M. S. Waghmode, A. B. Gunjal, J. A. Mulla, N. N. Patil and N. N. Nawani, *SN Appl. Sci.*, 2019, **1**, 310.
 - 5 A. Weir, P. Westerhoff, L. Fabricius and N. von Goetz, *Environ. Sci. Technol.*, 2012, **46**, 2242–2250.
 - 6 X. Chen and A. Selloni, *Chem. Rev.*, 2014, **114**, 9281–9282.
 - 7 A. Albanese, P. S. Tang and W. C. W. Chan, *Annu. Rev. Biomed. Eng.*, 2012, **14**, 1–16.
 - 8 A. Kurtz-Chalot, J. P. Klein, J. Pourchez, D. Boudard, V. Bin, G. B. Alcantara, M. Martini, M. Cottier and V. Forest, *J. Nanopart. Res.*, 2014, **16**, 1–15.
 - 9 O. Kose, M. Tomatis, L. Leclerc, N.-B. Belblidia, J.-F. Hocheplied, F. Turci, J. Pourchez and V. Forest, *Chem. Res. Toxicol.*, 2020, **33**, 2324–2337.
 - 10 E. Casals and V. F. Puentes, *Nanomed*, 2012, **7**, 1917–1930.
 - 11 T. Cedervall, I. Lynch, S. Lindman, T. Berggård, E. Thulin, H. Nilsson, K. A. Dawson and S. Linse, *Proc. Natl. Acad. Sci. U. S. A.*, 2007, **104**, 2050–2055.
 - 12 D. Chen, S. Ganesh, W. Wang and M. Amiji, *Nanomed*, 2017, **12**, 2113–2135.
 - 13 V. Forest, in *Nanoparticle-Protein Corona*, 2019, pp. 31–60.
 - 14 M. P. Monopoli, D. Walczyk, A. Campbell, G. Elia, I. Lynch, F. B. Bombelli and K. A. Dawson, *J. Am. Chem. Soc.*, 2011, **133**, 2525–2534.
 - 15 A. E. Nel, L. Mädler, D. Velegol, T. Xia, E. M. V. Hoek, P. Somasundaran, F. Klaessig, V. Castranova and M. Thompson, *Nat. Mater.*, 2009, **8**, 543–557.
 - 16 D. E. Owens and N. A. Peppas, *Int. J. Pharm.*, 2006, **307**, 93–102.
 - 17 S. Tenzer, D. Docter, J. Kuharev, A. Musyanovych, V. Fetz, R. Hecht, F. Schlenk, D. Fischer, K. Kiouptsi, C. Reinhardt, K. Landfester, H. Schild, M. Maskos, S. K. Knauer and R. H. Stauber, *Nat. Nanotechnol.*, 2013, **8**, 772–781.
 - 18 S. Tenzer, D. Docter, S. Rosfa, A. Wlodarski, J. Kuharev, A. Rekić, S. K. Knauer, C. Bantz, T. Nawroth, C. Bier, J. Sirirattanapan, W. Mann, L. Treuel, R. Zellner, M. Maskos, H. Schild and R. H. Stauber, *ACS Nano*, 2011, **5**, 7155–7167.
 - 19 R. M. Visalakshan, L. E. G. García, M. R. Benzigar, A. Ghazaryan, J. Simon, A. Mierczynska-Vasilev, T. D. Michl, A. Vinu, V. Mailänder, S. Morsbach, K. Landfester and K. Vasilev, *Small*, 2020, 2000285.
 - 20 C. D. Walkey, J. B. Olsen, F. Song, R. Liu, H. Guo, D. W. H. Olsen, Y. Cohen, A. Emili and W. C. W. Chan, *ACS Nano*, 2014, **8**, 2439–2455.
 - 21 C. D. Walkey and W. C. W. Chan, *Chem. Soc. Rev.*, 2012, **41**, 2780–2799.
 - 22 G. Caracciolo, O. C. Farokhzad and M. Mahmoudi, *Trends Biotechnol.*, 2017, **35**, 257–264.
 - 23 G. Caracciolo, S. Palchetti, V. Colapicchioni, L. Digiacoimo, D. Pozzi, A. L. Capriotti, G. La Barbera and A. Laganà, *Langmuir*, 2015, **31**, 10764–10773.
 - 24 M. P. Monopoli, C. Åberg, A. Salvati and K. A. Dawson, *Nat. Nanotechnol.*, 2012, **7**, 779–786.
 - 25 C. Ge, J. Du, L. Zhao, L. Wang, Y. Liu, D. Li, Y. Yang, R. Zhou, Y. Zhao, Z. Chai and C. Chen, *Proc. Natl. Acad. Sci. U. S. A.*, 2011, **108**, 16968–16973.
 - 26 P. Jain, R. S. Pawar, R. S. Pandey, J. Madan, S. Pawar, P. K. Lakshmi and M. S. Sudheesh, *Biotechnol. Adv.*, 2017, **35**, 889–904.
 - 27 N. P. Mortensen, G. B. Hurst, W. Wang, C. M. Foster, P. D. Nallathamby and S. T. Retterer, *Nanoscale*, 2013, **5**, 6372–6380.
 - 28 M. Pearson, V. V. Juettner and S. Hong, *Front. Chem.*, 2014, **2**, 108.
 - 29 E. Brun and C. Sicard-Roselli, *Cancer Nanotechnol.*, 2014, **5**, 7.
 - 30 P. Chandran, J. E. Riviere and N. A. Monteiro-Riviere, *Nanotoxicology*, 2017, **11**, 507–519.
 - 31 X. Cheng, X. Tian, A. Wu, J. Li, J. Tian, Y. Chong, Z. Chai, Y. Zhao, C. Chen and C. Ge, *ACS Appl. Mater. Interfaces*, 2015, **7**, 20568–20575.
 - 32 D. Docter, C. Bantz, D. Westmeier, H. J. Galla, Q. Wang, J. C. Kirkpatrick, P. Nielsen, M. Maskos and R. H. Stauber, *Beilstein J. Nanotechnol.*, 2014, **5**, 1380–1392.
 - 33 A. Lesniak, A. Salvati, M. J. Santos-Martinez, M. W. Radomski, K. A. Dawson and C. Åberg, *J. Am. Chem. Soc.*, 2013, **135**, 1438–1444.
 - 34 A. Lesniak, F. Fenaroli, M. P. Monopoli, C. Åberg, K. A. Dawson and A. Salvati, *ACS Nano*, 2012, **6**, 5845–5857.
 - 35 A. Lesniak, A. Campbell, M. P. Monopoli, I. Lynch, A. Salvati and K. A. Dawson, *Biomaterials*, 2010, **31**, 9511–9518.
 - 36 G. Maiorano, S. Sabella, B. Sorce, V. Brunetti, M. A. Malvindi, R. Cingolani and P. P. Pompa, *ACS Nano*, 2010, **4**, 7481–7491.
 - 37 S. R. Saptarshi, A. Duschl and A. L. Lopata, *J. Nanobiotechnol.*, 2013, **11**, 26.
 - 38 Z. J. Deng, M. Liang, M. Monteiro, I. Toth and R. F. Minchin, *Nat. Nanotechnol.*, 2011, **6**, 39–44.
 - 39 D. Docter, U. Distler, W. Storck, J. Kuharev, D. Wünsch, A. Hahlbrock, S. K. Knauer, S. Tenzer and R. H. Stauber, *Nat. Protoc.*, 2014, **9**, 2030–2044.
 - 40 D. Chen, J. Shi, J. Yan, Y. Wang, F. Yan, S. Shang and J. Xue, *Chem. Res. Chin. Univ.*, 2008, **24**, 362–366.
 - 41 J. Zhao, M. Milanova, M. M. C. G. Warmoeskerken and V. Dutschk, *Colloids Surf., A*, 2012, **413**, 273–279.
 - 42 S. Brunauer, P. H. Emmett and E. Teller, *J. Am. Chem. Soc.*, 1938, **60**, 309–319.
 - 43 J. Piella, N. G. Bastús and V. Puentes, *Bioconjugate Chem.*, 2017, **28**, 88–97.
 - 44 I. Lynch and K. A. Dawson, *Nano Today*, 2008, **3**, 40–47.
 - 45 J. E. Gagner, M. D. Lopez, J. S. Dordick and R. W. Siegel, *Biomaterials*, 2011, **32**, 7241–7252.
 - 46 V. Forest, M. Cottier and J. Pourchez, *Nano Today*, 2015, **10**, 677–680.
 - 47 V. Forest and J. Pourchez, *Mater. Sci. Eng., C*, 2017, **70**, 889–896.
 - 48 T. Bewersdorff, J. Vonnemann, A. Kanik, R. Haag and A. Haase, *Int. J. Nanomed.*, 2017, **12**, 2001–2019.

- 49 C. Gräfe, A. Weidner, M. V. D. Lühe, C. Bergemann, F. H. Schacher, J. H. Clement and S. Dutz, *Int. J. Biochem. Cell Biol.*, 2016, **75**, 196–202.
- 50 V. Mirshafiee, R. Kim, M. Mahmoudi and M. L. Kraft, *Int. J. Biochem. Cell Biol.*, 2016, **75**, 188–195.
- 51 D. Pozzi, G. Caracciolo, A. L. Capriotti, C. Cavaliere, G. La Barbera, T. J. Anchordoquy and A. Laganà, *J. Proteomics*, 2015, **119**, 209–217.
- 52 Y. Qiu, Y. Liu, L. Wang, L. Xu, R. Bai, Y. Ji, X. Wu, Y. Zhao, Y. Li and C. Chen, *Biomaterials*, 2010, **31**, 7606–7619.
- 53 M. M. Yallapu, N. Chauhan, S. F. Othman, V. Khalilzad-Sharghi, M. C. Ebeling, S. Khan, M. Jaggi and S. C. Chauhan, *Biomaterials*, 2015, **46**, 1–12.
- 54 F. Zhao, Y. Zhao, Y. Liu, X. Chang, C. Chen and Y. Zhao, *Small*, 2011, **7**, 1322–1337.
- 55 C. Corbo, R. Molinaro, A. Parodi, N. E. Toledano Furman, F. Salvatore and E. Tasciotti, *Nanomed*, 2016, **11**, 81–100.
- 56 H. Yin, R. Chen, P. S. Casey, P. C. Ke, T. P. Davis and C. Chen, *RSC Adv.*, 2015, **5**, 73963–73973.
- 57 L. Vroman and A. L. Adams, *Surf. Sci.*, 1969, **16**, 438–446.
- 58 M. Wang, O. J. R. Gustafsson, E. H. Pilkington, A. Kakinen, I. Javed, A. Faridi, T. P. Davis and P. C. Ke, *J. Mater. Chem. B*, 2018, **6**, 6026–6041.
- 59 F. S. M. Tekie, M. Hajiramezanali, P. Geramifar, M. Raoufi, R. Dinarvand, M. Soleimani and F. Atyabi, *Sci. Rep.*, 2020, **10**, 9664.

1. Complementary Data

After TiO₂ NPs were exposed to UV irradiation for 30 minutes, the protein corona formation was determined.

1.1. Protein concentration of UV irradiated titanium dioxide nanoparticles

Figure 26 reports the mean concentrations of proteins eluted from the corona of the 30 min UV irradiated nanoparticles (NPs-UV) and pristine TiO₂ NPs incubated in cDMEM.

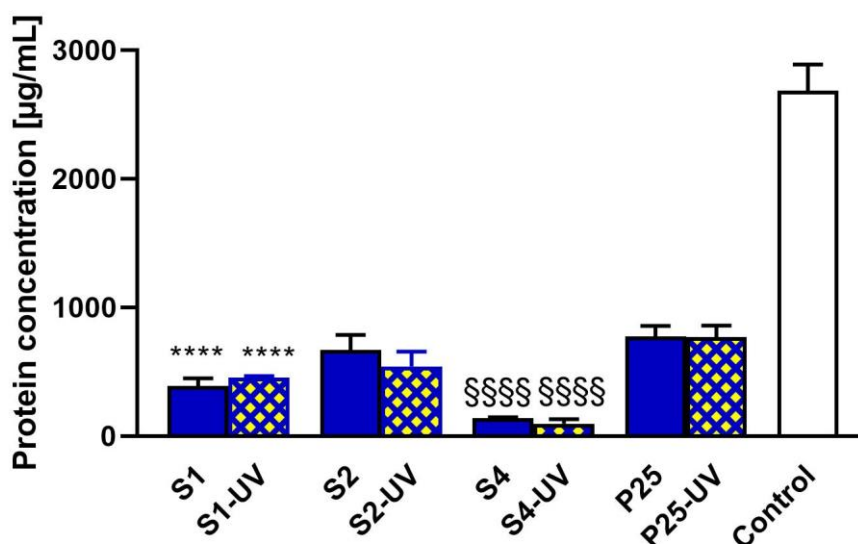


Figure 26. Concentrations of proteins eluted from the protein corona of pristine and 30 min UV irradiated NPs after incubation in cDMEM. Control is cDMEM.

Results are means of 3 independent experiments, standard deviation is also indicated. Statistically different from P25 (****) $P < 0.0001$. Statistical differences between S2 and S4 (\$\$\$\$) $P < 0.0001$. Statistical analyses were conducted using one-way Anova analyses followed by Tukey's multiple comparison test.

UV irradiated S2, S1 and P25 nanoparticles exhibited similar amounts of proteins in their corona while proteins were less abundantly found in the corona from S4 nanoparticles. For each nanoparticle type, a similar concentration of proteins was found in the coronas formed in 30 min UV irradiated or in pristine TiO₂ NPs (no statistically significant differences).

1.2. Profile of proteins adsorbed at the surface of the 30 min UV irradiated nanoparticles by gel electrophoresis

Figure 27 illustrates the protein profile of the corona of the NPs. The picture is representative of the three experiments performed.

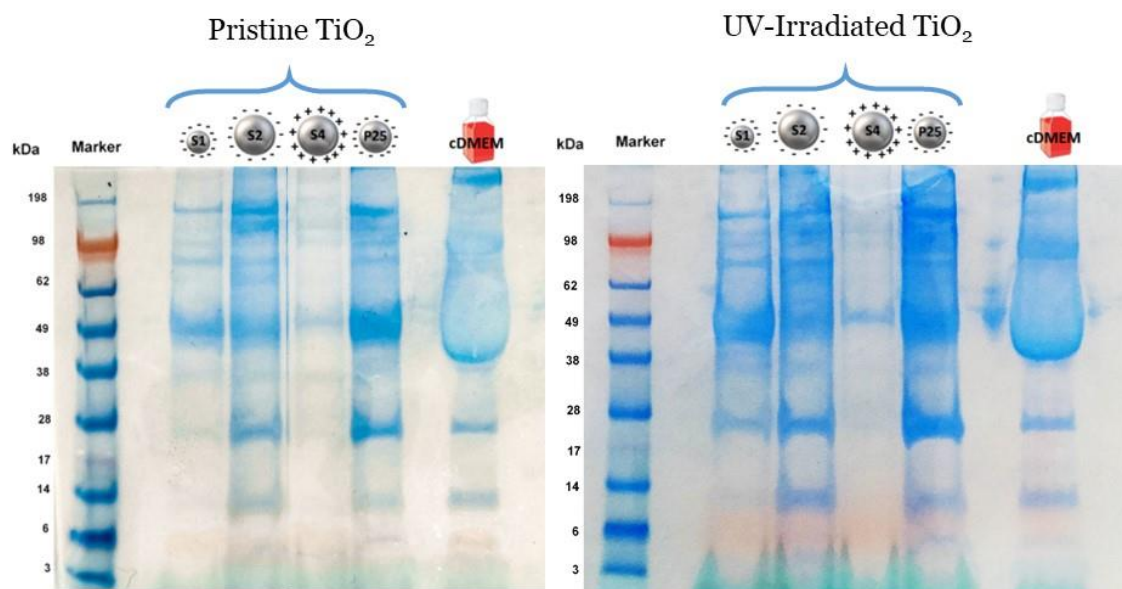


Figure 27. Electrophoresis gels for pristine and UV irradiated S1, S2, S4 and P25 NPs incubated in cDMEM. As controls, the complete biological media were also run (last lane).

Both in pristine and UV-irradiated TiO_2 NPs the corona of S2, and P25 had very similar protein profiles, S1 presented a slightly lower amount of proteins whereas S4 corona exhibited the smallest protein content. The differences were not observed between the gel profiles of pristine and UV irradiated particles. These results are in good agreement with those of protein quantification (Figure 26).

2. Conclusion

The highlights of the article '**Influence of the physicochemical features of TiO₂ nanoparticles on the formation of a protein corona and impact on cytotoxicity**' were:

- The parameters influencing the protein corona formation are mainly nanoparticle primary size and surface charge, no clear impact of the shape and agglomeration state was observed.
- Smaller NPs has slightly less important amount of proteins in their corona compared to bigger P25 nanoparticles. Protein coronas were preferentially formed on negatively charged NPs than positively charged NPs.
- No clear relationship between the protein corona and toxicity of TiO₂ NPs was observed.

30 minutes of UV radiation did not cause a remarkable change in the protein corona of the NPs compared to pristine TiO₂ NPs. Therefore, no effect of UV irradiation was observed on protein corona.

Les points clés de l'article '**Influence of the physicochemical features of TiO₂ nanoparticles on the formation of a protein corona and impact on cytotoxicity**' sont les suivants :

- les paramètres influençant la formation de la corona protéique sont principalement la taille primaire des NPs et la charge de surface, aucun impact clair de la forme et de l'état d'agglomération n'a été observé.
- Les petites NPs ont une quantité de protéines légèrement moins importante dans leur couronne que les grandes NPs de P25. Les coronas protéiques sont formées de préférence sur des NPs chargées négativement plutôt que sur des NPs chargées positivement.
- Aucune relation claire entre la corona protéique et la toxicité des NPs de TiO₂ n'a été observée.

30 minutes d'irradiation UV n'ont pas provoqué de changement remarquable dans la corona protéique des NPs par rapport aux NPs de TiO₂ non irradiées. Par conséquent, aucun effet de l'irradiation UV n'a été observé sur la corona protéique.

Chapter 5

Exploratory studies

The consistency and accuracy of the nanomaterials toxicity test results is crucial in the design, use and legal regulations of these materials.

To date, there are contradictory reports on the toxicity of various types of nanomaterials, making it difficult to predict their biological effects [192]. One of the most important factors affecting consistent toxicity results is nanomaterial interaction with the tests, leading to data artifacts and incompatible predictions of toxicity. Possible interactions include: (a) different optical properties of nanomaterials that can interfere with visible light absorption or fluorescence detection systems, (b) particles can interfere with assay compounds by chemical reactions, and (c) assay molecules can adsorb on the particle surface [182,192].

Widely used tests LDH and MTT for toxicology screening have been reported to be affected by different NPs. Through MTT assays, particle absorbance adds to the MTT absorbance and cause light absorption artifact, and particles generate formazan adding to the assay absorbance therefore leading to false results. Regarding LDH assay, particles adsorb LDH or inactivate the LDH enzyme.

The toxicity induced by the TiO₂ NPs was assessed by the LDH and MTT assays in *Chapter 2*. However, after cell exposure to TiO₂ NPs, no correlation was found between the morphological changes of the cells and the results of these two cytotoxicity assays.

To provide insight into the bias possibilities, TiO₂ NPs interaction with LDH and MTT assay components in cell free conditions were investigated in this chapter.

Chapitre 5

Etudes exploratoires

La production et l'utilisation de nanomatériaux (NMs) augmentent, et la cohérence et la fiabilité des tests de toxicité de ces matériaux sont très importantes en termes de conception, d'utilisation et de réglementation de ces matériaux.

À ce jour, il existe des rapports contradictoires sur la toxicité de divers types de nanomatériaux, ce qui rend difficile la prédiction de leurs effets biologiques [192]. L'un des facteurs les plus importants qui affectent la cohérence des résultats de toxicité est que les nanomatériaux interagissent avec les tests utilisés et entraînent des artefacts et des estimations de toxicité incohérentes. Les interactions possibles des particules sont : (a) les différentes propriétés optiques des nanomatériaux peuvent interférer avec les systèmes d'absorption de la lumière visible ou de détection de la fluorescence, (b) les particules peuvent interférer avec les composés de tests par des réactions chimiques, et (c) les molécules de tests peuvent s'adsorber sur la surface des particules [182,192].

Les tests LDH et MTT largement utilisés pour le dépistage toxicologique ont été signalés comme étant affectés par différentes NPs. Dans le test MTT, l'absorbance des particules s'ajoute à l'absorbance du MTT et provoque un artefact d'absorption de la lumière, et les particules génèrent du formazan qui s'ajoute à l'absorbance du test, ce qui entraîne des résultats erronés. En ce qui concerne le dosage de la LDH, les particules adsorbent la LDH ou inactivent l'enzyme LDH. Grâce au dosage de la LDH, en raison de la présence de particules dans le milieu de dosage pendant l'analyse spectrophotométrique, il se peut qu'il n'y ait pas d'artefact d'absorption de la lumière.

La toxicité induite par les NPs de TiO_2 a été évaluée par les tests LDH et MTT au chapitre 2. Cependant, après l'exposition des cellules aux NPs de TiO_2 , aucune corrélation n'a été trouvée entre les changements morphologiques des cellules et les résultats de ces deux essais de cytotoxicité.

Pour donner un aperçu des possibilités de biais, l'interaction des NPs de TiO_2 avec les composants des tests LDH et MTT dans les conditions acellulaires a été étudiée dans ce chapitre.

1. Titanium dioxide nanoparticles interaction with lactate dehydrogenase (cell free condition)

We hypothesized that TiO₂ NPs may either absorb or inactivate the LDH protein with both mechanisms leading to decreased absorbance in the LDH assay.

Particle interference was tested by incubating particle suspensions with LDH protein of known concentration and measuring the LDH absorbance using an LDH kit. Within this kit a LDH solution was provided as a positive control solution. This LDH was extracted from bovine heart and prepared in DMEM at 0.16 U/ μ L concentration. A solution of 0.16 U/ μ L LDH, and a mixture of 0.16 U/ μ L LDH and 120 μ g/mL TiO₂ NPs were incubated at 37°C for 24 h. At the end of incubation, the solutions were centrifuged at 115 g for 10 min, and the supernatant was collected and was mixed with the LDH assay mixture at a ratio of 1:2 and incubated at room temperature in the dark for 30 min. The reaction was stopped by the addition of 1 N HCl (1/10 of mixture volume), and the absorbance was read at 450 nm as described earlier by Forest *et al.* [193].

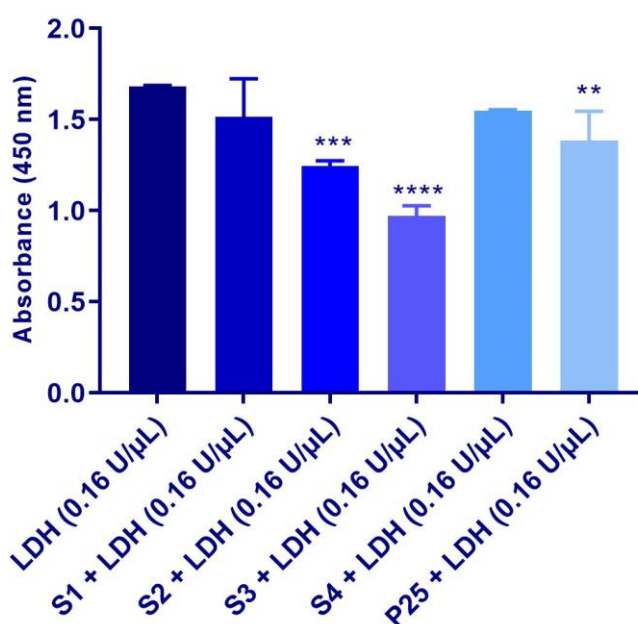


Figure 28. Absorbance at 450 nm of TiO₂ NPs (120 μ g/mL) and LDH (0.16 U/ μ L) mixture and LDH (0.16 U/ μ L) alone (cell free condition). Absorbances are the mean \pm SD of three independent experiments. Statistically different from 0.16 U/ μ L LDH standard (**) $P < 0.01$, (***) $P < 0.001$, (****) $P < 0.0001$. Statistical analyses were conducted using one-way Anova analyses, followed by Dunnett's test, compared with the value of LDH standard.

In cell free conditions, after adding 120 $\mu\text{g}/\text{mL}$ TiO_2 NPs to 0.16 $\text{U}/\mu\text{L}$ LDH solution, the decrease was observed in absorbance value compared to 0.16 $\text{U}/\mu\text{L}$ LDH control. Especially S2, S3 and P25 absorbances were significantly lower than control. These results suggest that particles inactivate or absorb the LDH enzyme, preventing LDH from being measured and resulted in lower absorbances.

Our results are in agreement with those of Zaqout *et al.* [194], they observed a decrease LDH activity induced by TiO_2 NPs in cell free conditions. Similarly, other studies showed TiO_2 NPs were able to adsorb or inactivate LDH protein [183,195,196].

Overall, these results show that TiO_2 NPs bind to LDH, and might cause false positive results in cell conditions. Particle interaction with the LDH protein needs extensive investigation, however these results show the limited utility of the LDH assay.

2. Titanium dioxide nanoparticle interaction with MTT (cell free condition)

TiO_2 nanoparticles present in the reaction mixture can influence the readout by oxidizing the assay substrate due to its photocatalytic properties [46]. The conversion of MTT into formazan by TiO_2 NPs might cause misleading cell viability results. Therefore, we examined whether TiO_2 could induce the MTT to formazan transformation under cell free conditions relevant for *in vitro* biological experiments.

The ability of TiO_2 NPs to reduce MTT to formazan was measured in the cell free conditions. 15, 30, 60, 120 $\mu\text{g}/\text{mL}$ TiO_2 suspensions in DMEM were prepared. 200 μL TiO_2 suspensions were incubated with 20 $\mu\text{g}/\text{mL}$ MTT solution at 37°C for 3 hours. DMEM without TiO_2 NPs was used as a control. At the 10th, 30th, 60th and 180th minutes within a 3 hours period incubation, the medium was carefully aspirated and 200 μL of DMSO was added to each well. Absorbance ($A_{\text{cell free}}$) measurements were made at the indicated times at 570 nm.

The absorbance of the particles in cell free conditions ($A_{\text{cell free}}$) are shown in Figure 29.

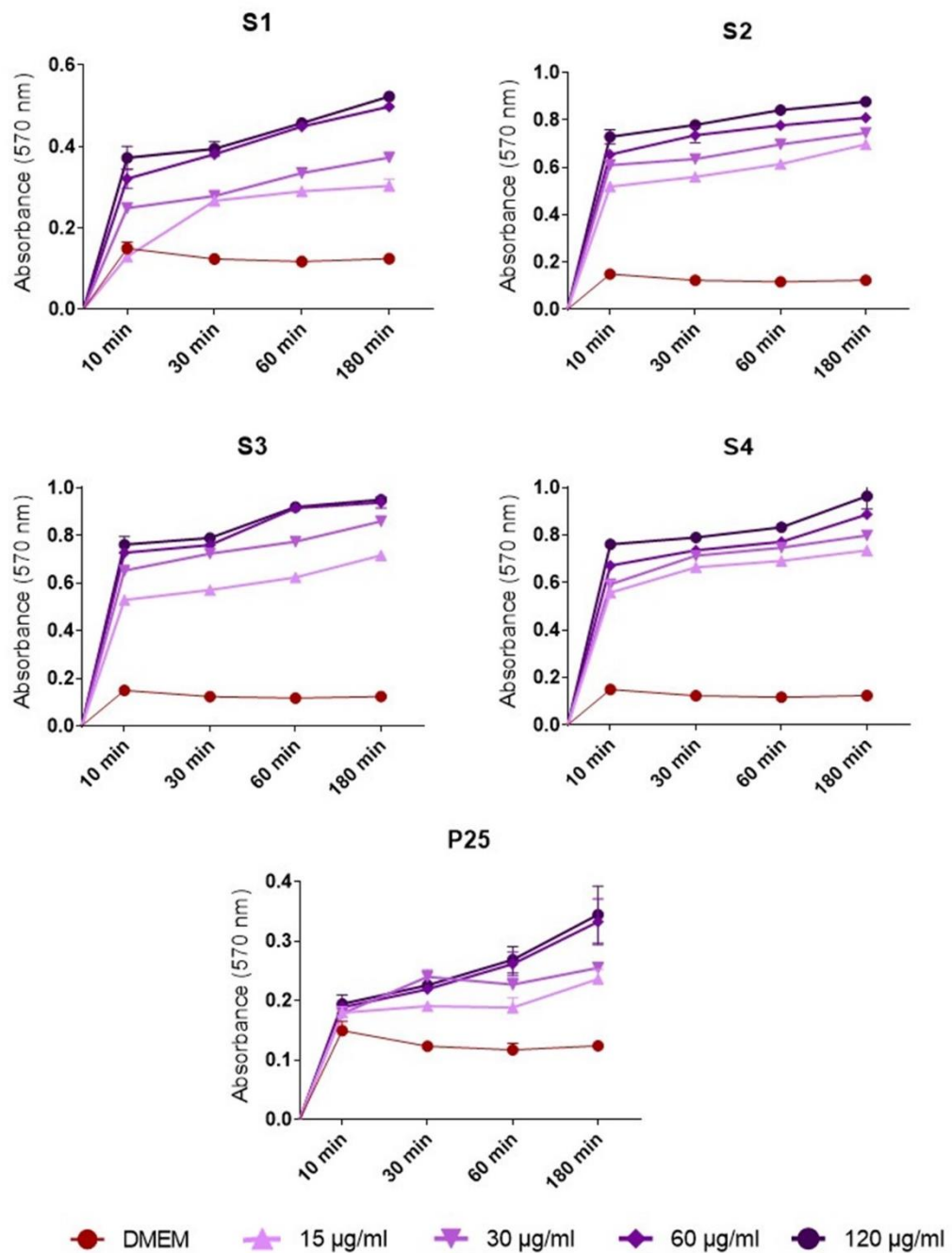


Figure 29. Absorbance measured during incubation of TiO₂ NPs with MTT. DMEM was used as a control. The absorbances were measured during 3 hours incubation at 10; 30; 60; 180 min.

S1, S2, S3, S4 and P25 at the highest concentration TiO₂ NPs increase the absorbance in cell free conditions 4.22, 7.08, 7.66, 7.78 and 2.78 times more compared to control, respectively.

This is in good agreement with studies [182,197,198] demonstrating TiO₂–MTT interactions leading to the formation of purple/blue formazan. P25-MTT incubation studies showed the concentration dependent absorbance increase compared to control (without TiO₂ NPs) in cell free conditions [197], similar to our results. TiO₂ may interfere with MTT viability tests by oxidizing the substrate MTT. Hence, redox-active nanoparticles may cause false signals in assays. This leads to critical difficulties in differentiating between true cell viability and artefacts caused by NP-assay interference. It is clear from these results that NPs have the potential to interfere with the components of the assays themselves; thus, the use of these assays in cell conditions clearly requires attention.

2.1.1. Re-evaluation of MTT results in cellular assays

The TiO₂ NPs generated formazan in cell free conditions as well as in cell conditions. Therefore, produced formazan absorbances in cell free conditions were used to correct the cell viability results obtained in Chapter 2.

In this regard, the estimated value of the viability ($V_{corrected}$) was recalculated by subtracting the mean of the absorbance of samples in cell-free conditions ($A_{cell-free}$) from the absorbance of samples observed in cell conditions (A) in accordance with Lupu *et al.* [197], with the formula given below. The corrected viability percentage is shown in Figures 30 and 31.

$$A_{corrected} = A - A_{cell\ free}$$
$$V_{corrected} = \frac{1}{N} \sum_{i=1}^N \left(\frac{A_{corrected\ sample}}{A_{corrected\ control}} \times 100 \right)$$

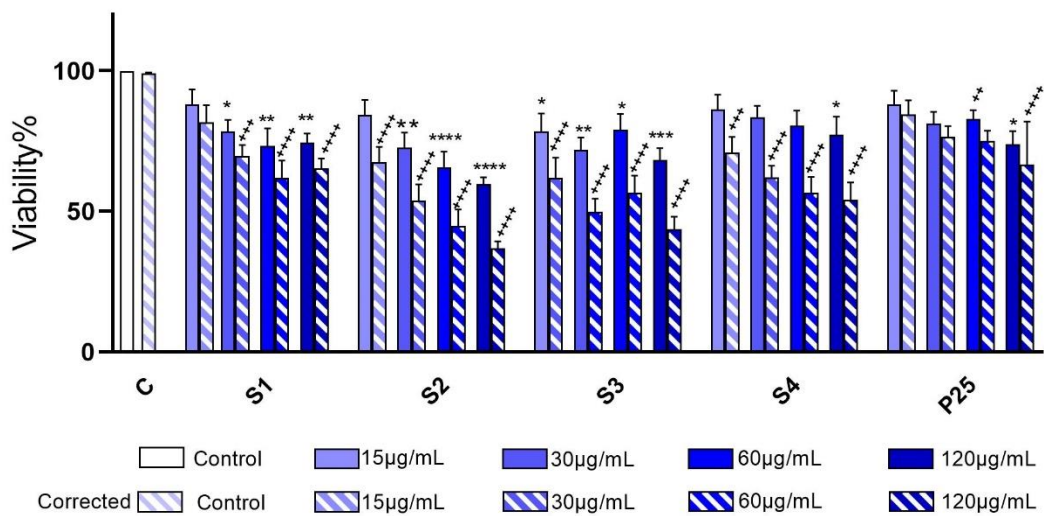


Figure 30. Corrected cell viability of A549. Control (C) represents unexposed cells. Values are the mean \pm SEM. Statistically different from control (*) $P < 0.05$, (**) $P < 0.01$, (***) $P < 0.0001$, (****) $P < 0.0001$. Statistical analyses were conducted using one-way Anova analyses, followed by Dunnett's test.

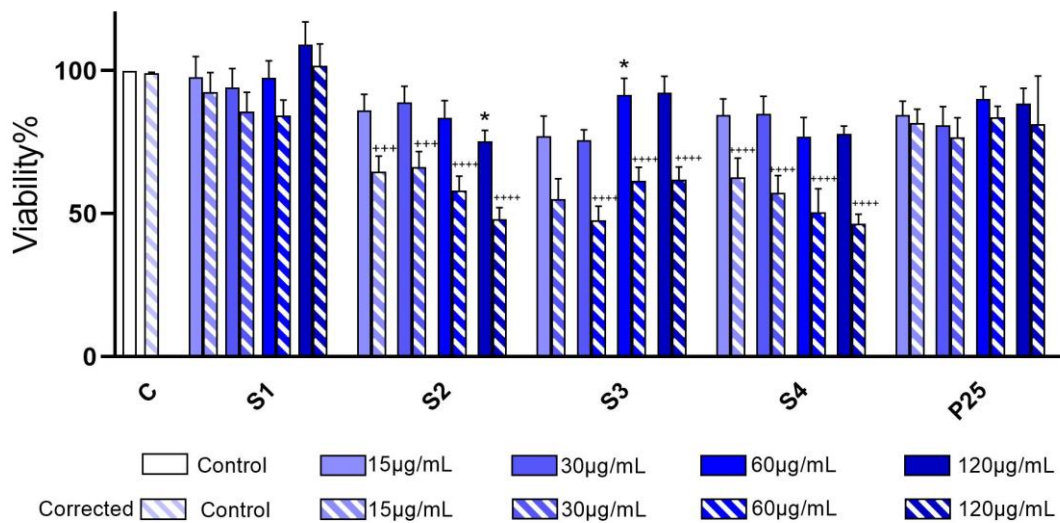


Figure 31. Corrected cell viability of cocultured cells. Control (C) represents unexposed cells. Values are the mean \pm SEM. Statistically different from control (*) $P < 0.05$, (**) $P < 0.01$, (***) $P < 0.0001$, (****) $P < 0.0001$. Statistical analyses were conducted using one-way Anova analyses, followed by Dunnett's test.

In both A549 and coculture system, the corrections led to lower viability values meaning higher toxicity. The non-corrected viability values were not significantly different with respect to control for S4 but then become so after taking into account

the artifactual formazan formation. These results are in agreement with [197] showing lower cell viability after TiO₂ induced formazan corrections. However, the corrected results are not fully consistent with results from the trypan blue assay reported in **Article 1**. This is why the correction method is not fully satisfactory.

The limit of this study is that when cells exposed to TiO₂ NPs are incubated with MTT, it is difficult to determine how much of the MTT passes through the cell membrane and is reduced to formazan by cell metabolism, and how much of it interacts with TiO₂ and is reduced to formazan. However, the obtained corrected cell viabilities represent the estimated values after cell exposure to TiO₂ NPs.

3. Conclusion

In this chapter, LDH and MTT assays which are frequently used in nanoparticle toxicity assessment were evaluated regarding their potential interactions with TiO₂ NPs. This study highlights the artifacts obtained with LDH and MTT assays in cell free conditions. Particularly, we observed nanoparticle concentration dependent interference with MTT assay. In addition, TiO₂ NPs could prevent LDH from being measured by either inactivation or adsorption of LDH.

In conclusion, potential artifacts in commonly used cytotoxicity assays should be tested prior performing cytotoxicity evaluation of nanoparticles to avoid misinterpretation of toxicity results.

Dans ce chapitre, les tests LDH et MTT qui sont fréquemment utilisés dans l'évaluation de la toxicité des nanoparticules ont été évalués en ce qui concerne leurs potentielles interactions avec les NPs de TiO₂. Cette étude met en évidence les artefacts obtenus avec les tests LDH et MTT dans des conditions sans cellule. En particulier, nous avons observé une interférence dépendante de la concentration des nanoparticules avec le test MTT. En outre, les NPs de TiO₂ pourraient empêcher la mesure de la LDH par inactivation ou adsorption de la LDH.

En conclusion, les artefacts potentiels dans les essais de cytotoxicité couramment utilisés devraient être testés avant de procéder à l'évaluation de la cytotoxicité des nanoparticules afin d'éviter toute mauvaise interprétation des résultats de toxicité.

CONCLUSIONS AND PERSPECTIVES

The main objective of this thesis work focused on the effects of various physicochemical properties on the toxicity of TiO₂ NPs toward human lung cells, in particular on the cytotoxicity, pro-inflammatory response, and oxidative stress mechanism. In this sense, 5 different TiO₂ NPs were synthesized and thoroughly characterized with the collaboration of MINES Paris Tech and University of Torino and evaluated systematically on three human lung cell system, namely monocultures of A549 human epithelial lung cells, monocultures of macrophages differentiated from THP-1 and coculture of both cell lines.

The monocyte differentiation process represents a sensitive step for correctly proceeding *in vitro* toxicity experiments. **In Chapter 1**, the process of THP-1 differentiation into the macrophages and its optimization were discussed. THP-1 cell line has been widely used to obtain macrophages in biological and toxicological researches and PMA is extensively used to stimulate their differentiation into macrophages. However, the PMA concentration, treatment durations vary widely in the literature and there is no standardized protocol. Therefore, before conducting the toxicity assays, we demonstrated the optimal conditions required for THP-1 differentiation in our laboratory. Among the different applied protocols (different treatment durations, concentration of PMA and different cell densities) the optimal conditions required for successful differentiation was selected as 30 ng/mL PMA for 24 hours incubation. Especially the concentration of PMA was carefully determined since it has been shown that higher concentrations of PMA is associated with the up-regulation of inflammatory gene expression [161,199], as compared to lower concentrations of PMA. Chapter 1 shows that the differentiation conditions must be carefully assessed within the context of the experimental question. After ensuring the suitable cell culture conditions, biological responses against TiO₂ nanoparticles were assessed in the following chapters.

The physicochemical features of TiO₂ NPs mainly determine their toxicological characteristic and establish the keystone of their fate in the biological system. To date, toxicological evaluations of TiO₂ nanoparticles have been extensively studied however what property makes a TiO₂ more or less safe has not yet fully been addressed. In this sense, **Chapter 2** and **Article 1** provide comprehensive conception on the TiO₂ nanoparticles toxicity on human lung cells depending on their physicochemical

properties. An impact on the cytotoxicity and to a lesser extent on the pro-inflammatory response depending on cell type was observed, namely: smaller, large agglomerated TiO₂ NPs were shown to be less toxic than P25 whereas rod-shaped TiO₂ NPs were found to be more toxic.

Contrarily, TiO₂ NPs, whatever their physicochemical properties, did not induce significant ROS production in A549 cell system and coculture system, which is contradictory to studies from Simon-Deckers *et al.* (2008) and Jugan *et al.* (2012) [170,200] where ROS were systematically detected whatever the size, crystalline phase, and shape of the TiO₂ NPs studied in very similar conditions to ours (same cellular model: A549 cells, exposed to various types of TiO₂ NPs, for 24 h at 100 µg/mL). Direct measurement of ROS levels with high accuracy and precision is difficult due to their short lifespan and rapid reactivity with redox state regulating components [201]. Indirect measurement of ROS by examining the oxidative damage these radicals cause to the lipids, proteins, and nucleic acids of the cells is a promising alternative approach. In this sense, it would have been interesting to study in more detail the oxidative stress and in particular the enzymatic antioxidants (SOD, CAT, GR) and non enzymatic antioxidants (GSH) levels, and total antioxidant capacity, protein carbonyl content and lipid peroxidation.

This study also highlighted the importance of selected cell systems since we detected clear differences in the cytotoxicity endpoints between the mono- and co-cultures. Biological responses vary between different *in vitro* systems, thus toxicological evaluation of nanoparticles in only one *in vitro* cell system can under or overestimate their effects, as suggested by Kasurinen *et al.* [202]. Therefore, more than one *in vitro* system should be used to complete evaluation of nanoparticle hazard assessment. It would have been interesting to estimate the uptake and localization of nanoparticles in two cell models by transmission electron microscopy and evaluate the physicochemical characteristics of nanoparticles impact on their cellular internalization.

In **Chapter 3** and **Article 2**, we further investigated whether the short time UV light exposure induced changes in the physicochemical properties of five different TiO₂ NPs and eventually affected their toxicity on human lung coculture system. We observed that 30-min UV irradiation altered the surface charges and agglomeration status of TiO₂ NPs. Pre-irradiated TiO₂ NPs (less negatively charged) induced a higher cytotoxic effect than the pristine TiO₂ NPs. In cell free conditions, TiO₂ NPs enhanced

photocatalytic production of ROS depending on their physicochemical properties: smaller primary size, negative surface charge and spherical shape caused more intense DMPO-CO₂•⁻ signal than bigger, rod and positively charged NPs. The potential of this compound to generate larger amounts of the carbon dioxide radical anion in suspension should be taken into account in preventing its potential oxidative damage. Since TiO₂ NPs in the environment are expected to be exposed to UV rays and possibly modified following photoexcitation, these results can serve as a basis for further studies as it has important implications for environmental and human health risk assessment and preventive actions to limit human exposure.

In **Chapter 4** and **Article 3**, the protein corona formation of pristine and 30 min UV irradiated TiO₂ NPs was also qualitatively/semi-quantitatively determined. The parameters influencing the protein corona formation are mainly nanoparticle primary size and surface charge, no clear impact of the shape and agglomeration state was observed. No effect of UV irradiation was observed on protein corona. When the toxicity results obtained in Chapters 2 and 3 and protein corona results were evaluated together, no clear relationship was observed between the protein corona and toxicity of TiO₂ NPs. However, in this research we obtained the preliminary results, now, mass spectrometry-based proteomic analysis might be useful to identify, quantify, and characterize the protein corona protein composition [203].

In this thesis work, TiO₂ NPs toxicity was first assessed by commonly used *in vitro* assay methods MTT and LDH as reported in Chapter 2. In **Chapter 5** particles interaction with assay compounds by chemical reactions, and assay molecules adsorption on the particle surface were investigated in LDH and MTT method in cell free conditions. LDH assays have been shown to be affected by TiO₂ NPs through the interaction of NPs with the LDH enzyme itself, causing adsorption and/or inactivation of the protein and an associated loss of activity [182,204], as shown in our study where TiO₂ NPs-LDH interaction resulted in loss of activity. Similarly, TiO₂ interfere with MTT viability tests by oxidizing the substrate MTT and TiO₂ induced the MTT to formazan transformation under cell free conditions.

As suggested by many researchers, to minimize the potential NPs-assay interactions and associated misinterpretation of results, choosing the *in vitro* test method according to the nanoparticle type and concentration is of great importance.

Therefore, the presence of NPs should be as much as possible limited in the final sample with multiple washes and/or centrifugations [182]. In nanoparticle *in vitro*

toxicity assessment, each individual formulation should be tested for compatibility with all assays used. The quality control studies provide more accurate scientific data for the establishment of regulations related to safe NPs production.

Overall, in this PhD study, the impact of physicochemical properties of TiO₂ nanoparticles on their toxicity was systematically investigated. The main conclusions of this thesis are:

- Pristine TiO₂ NPs caused cytotoxicity on human lung cells and cytotoxicity of TiO₂ NPs was dependent on their size, shape, agglomeration status and functionalization/surface charge. The effect on toxicity was higher with larger sized, less agglomerated, rod-shaped, and positively charged nanoparticles.
- Upon short-term UV irradiation, irradiated TiO₂ NPs induced a higher cytotoxic effect than the pristine TiO₂ NPs in relation to an altered surface charge.
- In acellular ROS production, the NPs with smaller size, negative surface charge and spherical shape caused more intense DMPO-CO₂•⁻ signal than bigger, rod and positively charged NPs.
- The parameters influencing the protein corona formation are mainly nanoparticle size and surface charge, no clear impact of the shape and agglomeration state was observed.

This research has raised many questions in need of further examination. Further experimental investigations are needed to evaluate the apoptosis by the formation of apoptotic bodies and altered expression of markers such as P53, P21, Bax, Bcl2 and cleaved caspase-3. As stated above, in oxidative stress, the production of reactive oxygen species and malondialdehyde and the activity of catalase and glutathione could be interesting to investigate. On the other hand, it has also been shown that nuclear factor-kappa B (NFκB) is activated in response to pro-inflammatory cytokines. Therefore, further researches should be undertaken in the evaluation of the involvement of NF-κB in TiO₂-induced inflammation.

In a context of long or chronic exposure to TiO₂ NPs, such effects can cause many pathological conditions in the lung, including cancer. In perspective, the development of non-cytotoxic TiO₂ nanoparticles under the safety-by-design approach could make it possible to control the toxicity of certain nanoparticles, but at this day, no study has

yet demonstrated this. The data obtained from this thesis contribute significantly to the toxicological profiles of these nanoparticles. Research on TiO₂ NPs need to be combined and supported with extensive toxicological studies.

CONCLUSIONS et PERSPECTIVES

L'objectif principal de ce travail de thèse était d'étudier les effets de diverses propriétés physicochimiques sur la toxicité des NPs de TiO₂ envers des cellules pulmonaires humaines, en particulier sur la cytotoxicité, la réponse pro-inflammatoire et le stress oxydatif. Pour ce faire, 5 types différents de NPs de TiO₂ ont été synthétisés et soigneusement caractérisés avec la collaboration de MINES Paris Tech et de l'Université de Turin et ont été évalués systématiquement sur 3 systèmes différents de cellules pulmonaires humaines (cellules épithéliales A549, macrophages différenciés à partir de THP-1, et cocultures de A549/THP-1 différenciées).

La différenciation des monocytes représente une étape importante pour garantir des résultats fiables et reproductibles, avant de mener des expériences de toxicité *in vitro*. Au **Chapitre 1**, la différenciation des THP-1 en macrophages et son optimisation ont été abordés, la lignée cellulaire monocyttaire humaine THP-1 a été très utilisée pour obtenir des macrophages dans les recherches biologiques et toxicologiques et le PMA est fréquemment utilisé pour stimuler leur différenciation en macrophages. Cependant, la concentration en PMA utilisée, ainsi que les durées de traitement varient considérablement dans la littérature et il n'existe pas de protocole standardisé. Par conséquent, avant de faire les essais de toxicité, nous avons déterminé les conditions optimales requises pour la différenciation des THP-1 dans notre laboratoire. Parmi les différents protocoles appliqués (différentes durées de traitement, concentrations de PMA et différentes densités cellulaires), les conditions optimales requises pour une différenciation efficace ont été sélectionnées comme suit : 30 ng/mL de PMA pour une incubation de 24 heures. La concentration de PMA a été déterminée avec soin, car il a été démontré que des concentrations plus élevées de PMA sont associées à une régulation positive de l'expression des gènes inflammatoires [161,199], par rapport à des concentrations plus faibles de PMA. Le **Chapitre 1** montre que les conditions de différenciation doivent être soigneusement évaluées dans le contexte de la question expérimentale. Après s'être assuré des conditions de culture cellulaire appropriées, des réponses biologiques envers des NPs de TiO₂ ont été évaluées dans les chapitres suivants.

Les caractéristiques physicochimiques des NPs de TiO₂ déterminent principalement leur profil toxicologique et constituent la base de leur devenir dans le système biologique. À ce jour, les évaluations toxicologiques des NPs de TiO₂ ont été largement menées, mais la question de savoir quelle propriété rend un TiO₂ plus ou moins sûr

n'a pas encore été entièrement traitée. En ce sens, le **Chapitre 2** et l'**Article 1** présentent une étude complète de la toxicité des NPs de TiO₂ sur des cellules pulmonaires humaines en fonction de leurs propriétés physicochimiques. En général, les NPs de TiO₂ provoquent une diminution de la viabilité des cellules et induisent une réponse pro-inflammatoire selon le type de cellule. L'effet sur la toxicité était plus important avec des nanoparticules de plus grande taille primaire, moins agglomérées, en forme de bâtonnet et chargées positivement. Au contraire, les NPs de TiO₂, quelles que soient leurs propriétés physicochimiques, n'ont pas induit de production significative de ROS dans le système cellulaire A549 et le système de coculture, ce qui est contradictoire avec les études de Simon-Deckers *et al.* (2008) et Jugan *et al.* (2012) [170,200] où des ROS ont été systématiquement détectés quelles que soient la taille, la phase cristalline, et la forme des NPs de TiO₂ étudiés dans des conditions très similaires des nôtres (même modèle de cellules : A549 exposées à différents types de NPs de TiO₂, pendant 24 h à 100 µg/mL). La mesure directe des niveaux de ROS avec une grande précision et exactitude est difficile en raison de leur courte durée de vie et de leur réactivité rapide avec les composants régulant l'état redox [201]. La mesure indirecte des ROS en examinant les dégradations oxydatives que ces radicaux provoquent sur les lipides, les protéines et les acides nucléiques des cellules est une approche alternative prometteuse. En ce sens, il aurait été intéressant d'étudier plus en détail le stress oxydatif et en particulier les antioxydants enzymatiques (SOD, CAT, GR), les antioxydants non enzymatiques (GSH), la capacité antioxydante totale, la teneur en carbonyle des protéines et la peroxydation des lipides.

Cette étude a également mis en évidence l'importance de certains systèmes cellulaires puisque nous avons détecté des différences nettes dans les paramètres de cytotoxicité entre les monocultures et les co-cultures. Les réponses biologiques varient entre les différents systèmes *in vitro*, de sorte que l'évaluation toxicologique des nanoparticules dans un seul système cellulaire *in vitro* peut sous-estimer ou surestimer leurs effets, comme le suggèrent Kasurinen *et al.* [202]. Par conséquent, plus d'un système *in vitro* devrait être utilisé pour réaliser l'évaluation du danger des nanoparticules. Il aurait été intéressant d'estimer l'absorption et la localisation des nanoparticules dans deux modèles cellulaires par microscopie électronique à transmission et d'évaluer les caractéristiques physicochimiques de l'impact des nanoparticules sur leur internalisation cellulaire.

Dans le **Chapitre 3** et l'**Article 2**, nous avons étudié si l'exposition de courte durée à la lumière UV provoquait des changements dans les propriétés physicochimiques de

cinq types différents de NPs de TiO₂ et affectait finalement leur toxicité sur le système de coculture de cellules pulmonaires humaines. Nous avons observé qu'une irradiation UV de 30 minutes modifiait les charges de surface et le degré d'agglomération des NPs de TiO₂. Les NPs de TiO₂ pré-irradiées (moins chargées négativement) ont provoqué un effet cytotoxique plus important que les NPs de TiO₂ non irradiées. En milieu acellulaire, les NPs de TiO₂ induisaient une production de ROS variable en fonction de leurs propriétés physicochimiques : une taille primaire plus petite, une charge de surface négative et une forme sphérique provoquaient un signal DMPO-CO₂•⁻ plus intense que celui observé pour les NPs plus grandes, en bâtonnets et chargées positivement. Le potentiel de ce composé à générer de plus grandes quantités de l'anion radical du CO₂•⁻ en suspension doit être pris en compte dans la prévention de son risque de lésions oxydatives. Étant donné que les NPs de TiO₂ présentes dans l'environnement devraient être exposés aux radiations UV et éventuellement modifiées à la suite d'une photoexcitation, ces résultats peuvent servir de base à des études ultérieures car ils ont des implications importantes pour l'évaluation des risques pour l'environnement et la santé humaine et pour les actions préventives visant à limiter l'exposition humaine.

Au **Chapitre 4** et à l'**Article 3**, la formation de la couronne protéique des NPs de TiO₂ non irradiées et irradiées aux UV pendant 30 minutes a également été déterminée de qualitative/semi-quantitative. Les paramètres influençant la formation de la couronne protéique sont principalement la taille primaire des nanoparticules et la charge de surface, aucun impact clair de la forme et de l'état d'agglomération n'a été observé. Aucun effet de l'irradiation UV n'a été observé sur la couronne protéique. Lorsque les résultats de toxicité obtenus dans les chapitres 2 et 3 et les résultats de la couronne protéique ont été évalués ensemble, aucune relation claire n'a été observée entre la couronne protéique et la toxicité des NPs de TiO₂. Cependant, dans cette recherche, nous avons obtenu les résultats préliminaires, une analyse protéomique basée sur la spectrométrie de masse pourrait être utile pour identifier, quantifier et caractériser la composition de la couronne protéique [203].

Dans ce travail de thèse, la toxicité des NPs de TiO₂ a d'abord été évaluée par des tests classiques (MTT et LDH) comme indiqué au chapitre 2. Au **Chapitre 5**, l'interaction des particules avec les composés de ces tests soit par réaction chimique soit par adsorption des réactifs du test à la surface des particules a été étudiée pour les méthodes LDH et MTT dans des conditions sans cellules. Il a été démontré que les dosages de la LDH sont affectés par les NPs de TiO₂ par interaction des NPs avec

l'enzyme LDH elle-même, provoquant l'adsorption et/ou l'inactivation de la protéine et une diminution d'activité associée [182,204], comme le montre notre étude où l'interaction NPs de TiO₂-LDH a entraîné une diminution d'activité. De même, le TiO₂ interfère avec les tests de viabilité du MTT en oxydant le substrat MTT et le TiO₂ a induit la transformation du MTT en formazan dans des conditions sans cellule.

Comme le suggèrent de nombreux chercheurs, pour réduire les interactions potentielles entre les tests de NPs et les erreurs d'interprétation des résultats qui en découlent, il est très important de choisir la méthode de test *in vitro* en fonction du type et de la concentration de nanoparticules.

Par conséquent, la présence de NPs doit être limitée autant que possible dans l'échantillon final par des lavages et/ou des centrifugations multiples [182]. Dans l'évaluation de la toxicité *in vitro* des nanoparticules, chaque formulation individuelle doit être testée pour vérifier sa compatibilité avec tous les tests utilisés. Les études de contrôle de la qualité fournissent des données scientifiques plus précises pour l'établissement de réglementations relatives à la production sûre de NPs.

Dans l'ensemble, dans cette étude de doctorat, l'impact des propriétés physicochimiques des NPs de TiO₂ sur leur toxicité a été systématiquement étudié. Les principales conclusions de cette thèse sont les suivantes :

- Les NPs de TiO₂ ont causé une cytotoxicité sur des cellules pulmonaires humaines et la cytotoxicité des NPs de TiO₂ était dépendante de leur taille, forme, état d'agglomération et fonctionnalisation/charge de surface. L'effet sur la toxicité était plus important avec des nanoparticules de plus grande taille primaire, moins agglomérées, en forme de bâtonnet et chargées positivement.
- Lors d'une irradiation UV de courte durée, les NPs de TiO₂ irradiées ont induit un effet cytotoxique plus important que les NPs de TiO₂ non irradiées en lien avec une charge de surface modifiée.
- Dans la production de ROS acellulaire, les NPs de taille plus petite, de charge de surface négative et de forme sphérique ont provoqué un signal DMPO-CO₂•⁻ plus intense que les NPs plus grandes, en forme de bâtonnet et chargées positivement.

- Les paramètres influençant la formation de la couronne protéique sont principalement la taille primaire des nanoparticules et la charge de surface, aucun impact clair de la forme et de l'état d'agglomération n'a été observé.

Cette recherche a soulevé de nombreuses questions nécessitant des recherches plus avancées. Des recherches expérimentales supplémentaires sont nécessaires pour évaluer l'apoptose par la formation de structures apoptotiques et la modification de l'expression de marqueurs comme P53, P21, Bax, Bcl2 et la caspase-3. Comme indiqué ci-dessus, en cas de stress oxydatif, la production d'espèces réactives de l'oxygène et de malondialdéhyde et l'activité de la catalase et du glutathion pourraient être intéressantes à étudier. D'autre part, il a également été démontré que le facteur nucléaire-kappa B (NFκB) est activé en réponse à des cytokines pro-inflammatoires. Par conséquent, des recherches approfondies devraient être entreprises pour évaluer l'implication du NF-κB dans l'inflammation induite par le TiO₂.

Dans un contexte d'exposition longue ou chronique aux NPs de TiO₂, de tels effets peuvent provoquer de nombreux problèmes pathologiques dans les poumons, y compris le cancer. En perspective, le développement de nanoparticules de TiO₂ non cytotoxiques dans le cadre de l'approche "safety-by-design" pourrait permettre de contrôler la toxicité de certaines nanoparticules, mais à ce jour, aucune étude ne l'a encore démontré. Les données obtenues dans le cadre de cette thèse contribuent de manière significative à l'établissement des profils toxicologiques de ces nanoparticules. La recherche sur les NPs de TiO₂ doit être combinée et soutenue par des études toxicologiques approfondies.

REFERENCES

- [1] EU, Definition - Nanomaterials - Environment - European Commission, (n.d.). https://ec.europa.eu/environment/chemicals/nanotech/faq/definition_en.htm (accessed March 24, 2020).
- [2] ANSES, CLH REPORT FOR TITANIUM DIOXIDE CLH report Proposal for Harmonised Classification and Labelling Based on Regulation (EC) No 1272/2008 (CLP Regulation), Annex VI, Part 2, 2016.
- [3] A.J. Haider, R.H. Al-Anbari, G.R. Kadhim, C.T. Salame, Exploring potential Environmental applications of TiO₂ Nanoparticles, in: Energy Procedia, Elsevier Ltd, 2017: pp. 332–345. <https://doi.org/10.1016/j.egypro.2017.07.117>.
- [4] I. Khan, K. Saeed, I. Khan, Nanoparticles: Properties, applications and toxicities, Arab. J. Chem. 12 (2019) 908–931. <https://doi.org/10.1016/j.arabjc.2017.05.011>.
- [5] K.P. Lee, H.J. Trochimowicz, C.F. Reinhardt, Pulmonary response of rats exposed to titanium dioxide (TiO₂) by inhalation for two years, Toxicol. Appl. Pharmacol. 79 (1985) 179–192. [https://doi.org/10.1016/0041-008X\(85\)90339-4](https://doi.org/10.1016/0041-008X(85)90339-4).
- [6] U. Heinrich, R. Fuhst, S. Rittinghausen, O. Creutzenberg, B. Bellmann, W. Koch, K. Levsen, Chronic inhalation exposure of wistar rats and two different strains of mice to diesel engine exhaust, carbon black, and titanium dioxide, Inhal. Toxicol. 7 (1995) 533–556. <https://doi.org/10.3109/08958379509015211>.
- [7] IARC, IARC Monographs on the Evaluation of Carcinogenic Risks to Humans Carbon Black, Titanium Dioxide, and Talc, IARC. 93 (2006) 193–412. <https://doi.org/10.1136/jcp.48.7.691-a>.
- [8] Arrêté du 17 avril 2019 portant suspension de la mise sur le marché des denrées contenant l’additif E 171 (dioxyde de titane - TiO₂) - Légifrance, (n.d.). <https://www.legifrance.gouv.fr/jorf/id/JORFTEXT000038410047/> (accessed December 11, 2020).
- [9] Titanium dioxide | Anses - Agence nationale de sécurité sanitaire de l’alimentation, de l’environnement et du travail, (n.d.). <https://www.anses.fr/en/content/titanium-dioxide> (accessed December 11, 2020).
- [10] A. Kraegelo, B. Suarez-Merino, T. Sluijters, C. Micheletti, Implementation of safe-by-design for nanomaterial development and safe innovation: Why we need a comprehensive approach, Nanomaterials. 8 (2018). <https://doi.org/10.3390/nano8040239>.
- [11] C. Buzea, I.I. Pacheco, K. Robbie, Nanomaterials and nanoparticles: Sources and toxicity, Biointerphases. 2 (2007) MR17–MR71. <https://doi.org/10.1116/1.2815690>.
- [12] M. Geiser, B. Rothen-Rutishauser, N. Kapp, S. Schürch, W. Kreyling, H. Schulz, M. Semmler, V. Im Hof, J. Heyder, P. Gehr, Ultrafine particles cross cellular membranes by nonphagocytic mechanisms in lungs and in cultured cells, Environ. Health Perspect. 113 (2005) 1555–1560.

<https://doi.org/10.1289/ehp.8006>.

- [13] I.F. Osman, B.K. Jacob, D. Anderson, Effect of nanoparticles on human cells from healthy individuals and patients with respiratory diseases, *J. Biomed. Nanotechnol.* 7 (2011) 26–27. <https://doi.org/10.1166/jbn.2011.1183>.
- [14] M.H. Ahn, C.M. Kang, C.S. Park, S.J. Park, T. Rhim, P.O. Yoon, H.S. Chang, S.H. Kim, H. Kyono, K.C. Kim, Titanium dioxide particle - Induced goblet cell hyperplasia: Association with mast cells and IL-13, *Respir. Res.* 6 (2005). <https://doi.org/10.1186/1465-9921-6-34>.
- [15] France bans Titanium Dioxide in food products by January 2020, 2019.
- [16] ISO/TS 80004-1:2015(en), Nanotechnologies — Vocabulary — Part 1: Core terms, (n.d.). <https://www.iso.org/obp/ui/#iso:std:iso:ts:80004:-1:ed-2:vi:en> (accessed March 24, 2020).
- [17] M.A. Gato, S. Naseem, M.Y. Arfat, A.M. Dar, K. Qasim, S. Zubair, Physicochemical properties of nanomaterials: implication in associated toxic manifestations., *Biomed Res. Int.* 2014 (2014) 498420. <https://doi.org/10.1155/2014/498420>.
- [18] A review on the classification, characterisation, synthesis of nanoparticles and their application - NASA/ADS, (n.d.). <https://ui.adsabs.harvard.edu/abs/2017MS%26E..263c2019E/abstract> (accessed April 7, 2020).
- [19] J.N. Tiwari, R.N. Tiwari, K.S. Kim, Zero-dimensional, one-dimensional, two-dimensional and three-dimensional nanostructured materials for advanced electrochemical energy devices, *Prog. Mater. Sci.* 57 (2012) 724–803. <https://doi.org/10.1016/j.pmatsci.2011.08.003>.
- [20] K.S. Ibrahim, Carbon nanotubes-properties and applications: a review, *Carbon Lett.* 14 (2013) 131–144. <https://doi.org/10.5714/cl.2013.14.3.131>.
- [21] E. Baranowska-Wójcik, D. Sz wajgier, P. Oleszczuk, A. Winiarska-Mieczan, Effects of Titanium Dioxide Nanoparticles Exposure on Human Health—a Review, *Biol. Trace Elem. Res.* 193 (2020) 118–129. <https://doi.org/10.1007/s12011-019-01706-6>.
- [22] M. Koelsch, S. Cassaignon, J.F. Guillemoles, J.P. Jolivet, Comparison of optical and electrochemical properties of anatase and brookite TiO₂ synthesized by the sol-gel method, in: *Thin Solid Films*, Elsevier, 2002: pp. 312–319. [https://doi.org/10.1016/S0040-6090\(01\)01509-7](https://doi.org/10.1016/S0040-6090(01)01509-7).
- [23] S. Di Mo, W.Y. Ching, Electronic and optical properties of three phases of titanium dioxide: Rutile, anatase, and brookite, *Phys. Rev. B.* 51 (1995) 13023–13032. <https://doi.org/10.1103/PhysRevB.51.13023>.
- [24] A. Fujishima, T.N. Rao, D.A. Tryk, Titanium dioxide photocatalysis, *J. Photochem. Photobiol. C Photochem. Rev.* 1 (2000) 1–21. [https://doi.org/10.1016/S1389-5567\(00\)00002-2](https://doi.org/10.1016/S1389-5567(00)00002-2).
- [25] Y. Nam, J.H. Lim, K.C. Ko, J.Y. Lee, Photocatalytic activity of TiO₂ nanoparticles: A theoretical aspect, *J. Mater. Chem. A.* 7 (2019) 13833–13859. <https://doi.org/10.1039/c9ta03385h>.
- [26] R. Qian, H. Zong, J. Schneider, G. Zhou, T. Zhao, Y. Li, J. Yang, D.W. Bahnemann, J.H. Pan, Charge carrier trapping, recombination and transfer during TiO₂ photocatalysis: An overview, *Catal. Today.* 335 (2019) 78–90.

<https://doi.org/10.1016/j.cattod.2018.10.053>.

- [27] P. Wang, N. Qi, Y. Ao, J. Hou, C. Wang, J. Qian, Effect of UV irradiation on the aggregation of TiO₂ in an aquatic environment: Influence of humic acid and pH, *Environ. Pollut.* 212 (2016) 178–187. <https://doi.org/10.1016/j.envpol.2016.01.030>.
- [28] H. Zhang, J. Sun, L.H. Guo, UV irradiation mediated aggregation of TiO₂ nanoparticles in simulated aquatic system, *NanoImpact.* 3–4 (2016) 75–80. <https://doi.org/10.1016/j.impact.2016.08.004>.
- [29] K. Hashimoto, H. Irie, A. Fujishima, TiO₂ Photocatalysis: A Historical Overview and Future Prospects, *Jpn. J. Appl. Phys.* 44 (2005) 8269–8285.
- [30] J. Sun, L.H. Guo, H. Zhang, L. Zhao, UV irradiation induced transformation of TiO₂ nanoparticles in water: Aggregation and photoreactivity, *Environ. Sci. Technol.* 48 (2014) 11962–11968. <https://doi.org/10.1021/es502360c>.
- [31] T. Watanabe, A. Nakajima, R. Wang, M. Minabe, S. Koizumi, A. Fujishima, K. Hashimoto, Photocatalytic activity and photoinduced hydrophilicity of titanium dioxide coated glass, *Thin Solid Films.* 351 (1999) 260–263. [https://doi.org/10.1016/S0040-6090\(99\)00205-9](https://doi.org/10.1016/S0040-6090(99)00205-9).
- [32] D. Ziental, B. Czarczynska-Goslinska, D.T. Mlynarczyk, A. Glowacka-Sobotta, B. Stanis, T. Goslinski, L. Sobotta, Titanium Dioxide Nanoparticles: Prospects and Applications in Medicine, *Nanomaterials.* 10 (2020) 387. <https://doi.org/10.3390/nano10020387>.
- [33] S. Wagner, A. Gondikas, E. Neubauer, T. Hofmann, F. von der Kammer, Spot the Difference: Engineered and Natural Nanoparticles in the Environment-Release, Behavior, and Fate, *Angew. Chemie Int. Ed.* 53 (2014) n/a-n/a. <https://doi.org/10.1002/anie.201405050>.
- [34] M. Bundschuh, J. Filser, S. Lüderwald, M.S. McKee, G. Metreveli, G.E. Schaumann, R. Schulz, S. Wagner, Nanoparticles in the environment: where do we come from, where do we go to?, *Environ. Sci. Eur.* 30 (2018). <https://doi.org/10.1186/s12302-018-0132-6>.
- [35] T.Y. Sun, N.A. Bornhöft, K. Hungerbühler, B. Nowack, Dynamic Probabilistic Modelling of Environmental Emissions of Engineered Nanomaterials Supplementary Information, n.d.
- [36] C.J. Tsai, C.Y. Huang, S.C. Chen, C.E. Ho, C.H. Huang, C.W. Chen, C.P. Chang, S.J. Tsai, M.J. Ellenbecker, Exposure assessment of nano-sized and respirable particles at different workplaces, *J. Nanoparticle Res.* 13 (2011) 4161–4172. <https://doi.org/10.1007/s11051-011-0361-8>.
- [37] M. Methner, L. Hodson, A. Dames, C. Geraci, Nanoparticle emission assessment technique (NEAT) for the identification and measurement of potential inhalation exposure to engineered nanomaterials—part b: Results from 12 field studies, *J. Occup. Environ. Hyg.* 7 (2010) 163–176. <https://doi.org/10.1080/15459620903508066>.
- [38] S. Plitzko, Workplace exposure to engineered nanoparticles, *Inhal. Toxicol.* 21 (2009) 25–29. <https://doi.org/10.1080/08958370902962317>.
- [39] Y. Ding, T.A.J. Kuhlbusch, M. Van Tongeren, A.S. Jiménez, I. Tuinman, R. Chen, I.L. Alvarez, U. Mikolajczyk, C. Nickel, J. Meyer, H. Kaminski, W. Wohlleben, B. Stahlmecke, S. Clavaguera, M. Riediker, Airborne engineered

- nanomaterials in the workplace—a review of release and worker exposure during nanomaterial production and handling processes, *J. Hazard. Mater.* 322 (2017) 17–28. <https://doi.org/10.1016/j.jhazmat.2016.04.075>.
- [40] C.H. Huang, C.Y. Tai, C.Y.U. Huang, C.J. Tsai, C.W. Chen, C.P. Chang, T.S. Shih, Measurements of respirable dust and nanoparticle concentrations in a titanium dioxide pigment production factory, *J. Environ. Sci. Heal. - Part A Toxic/Hazardous Subst. Environ. Eng.* 45 (2010) 1227–1233. <https://doi.org/10.1080/10934529.2010.493792>.
- [41] T.Y. Sun, N.A. Bornhöft, K. Hungerbühler, B. Nowack, Dynamic Probabilistic Modeling of Environmental Emissions of Engineered Nanomaterials, *Environ. Sci. Technol.* 50 (2016) 4701–4711. <https://doi.org/10.1021/acs.est.5b05828>.
- [42] N.A. Bornhöft, T.Y. Sun, L.M. Hilty, B. Nowack, A dynamic probabilistic material flow modeling method, *Environ. Model. Softw.* 76 (2016) 69–80. <https://doi.org/10.1016/j.envsoft.2015.11.012>.
- [43] NIOSH, Occupational Exposure to Titanium Dioxide, *Dep. Heal. Hum. Serv. Centers Dis. Control Prev. Natl. Inst. Occup. Saf. Heal.* (2011). www.cdc.gov/niosh. (accessed February 13, 2020).
- [44] A.M. Świdwińska-Gajewska, S. Czerczak, Titanium dioxide nanoparticles: Occupational exposure limits, *Med. Pr.* 65 (2014) 407–418. <https://doi.org/10.13075/mp.5893.2014.046>.
- [45] P. Oberbek, P. Kozikowski, K. Czarnecka, P. Sobiech, S. Jakubiak, T. Jankowski, Inhalation exposure to various nanoparticles in work environment—contextual information and results of measurements, *J. Nanoparticle Res.* 21 (2019) 222. <https://doi.org/10.1007/s11051-019-4651-x>.
- [46] Titanium dioxide in nanoparticle form: ANSES defines a toxicity reference value (TRV) for chronic inhalation exposure | Anses - Agence nationale de sécurité sanitaire de l'alimentation, de l'environnement et du travail, (n.d.). <https://www.anses.fr/en/content/titanium-dioxide-nanoparticle-form-anses-defines-toxicity-reference-value-trv-chronic> (accessed December 3, 2020).
- [47] Literature review on the safety of titanium dioxide and zinc oxide nanoparticles in sunscreens | Therapeutic Goods Administration (TGA), (n.d.). <https://www.tga.gov.au/literature-review-safety-titanium-dioxide-and-zinc-oxide-nanoparticles-sunscreens> (accessed September 21, 2020).
- [48] C.S. Yah, S.E. Iyuke, G.S. Simate, A review of nanoparticles toxicity and their routes of exposures, *Iran. J. Pharm. Sci.* 8 (2012) 299–314.
- [49] R.A. Yokel, R.C. MacPhail, Engineered nanomaterials: Exposures, hazards, and risk prevention, *J. Occup. Med. Toxicol.* 6 (2011) 7. <https://doi.org/10.1186/1745-6673-6-7>.
- [50] P. Muralidharan, M. Malapit, E. Mallory, D. Hayes, H.M. Mansour, Inhalable nanoparticulate powders for respiratory delivery, *Nanomedicine Nanotechnology, Biol. Med.* 11 (2015) 1189–1199. <https://doi.org/10.1016/j.nano.2015.01.007>.
- [51] M.A. Kling, A Review of Respiratory System Anatomy, Physiology, and Disease in the Mouse, Rat, Hamster, and Gerbil, *Vet. Clin. North Am. Exot. Anim. Pract.* 14 (2011) 287–337. <https://doi.org/10.1016/j.cvex.2011.03.007>.
- [52] R.O. Williams, T.C. Carvalho, J.I. Peters, Influence of particle size on regional

- lung deposition - What evidence is there?, *Int. J. Pharm.* 406 (2011) 1–10. <https://doi.org/10.1016/j.ijpharm.2010.12.040>.
- [53] B. Asgharian, O.T. Price, Deposition of Ultrafine (NANO) Particles in the Human Lung, *Inhal. Toxicol.* 19 (2007) 1045–1054. <https://doi.org/10.1080/08958370701626501>.
- [54] G. Oberdorster, J. Ferin, B.E. Lehnert, Correlation between particle size, in vivo particle persistence, and lung injury, in: *Environ. Health Perspect.*, 1994: pp. 173–179. <https://doi.org/10.2307/3432080>.
- [55] M. Ellender, A. Hodgson, K.L. Wood, J.C. Moody, Effect of bronchopulmonary lavage on lung retention and clearance of particulate material in hamsters, in: *Environ. Health Perspect.*, *Environ Health Perspect*, 1992: pp. 209–213. <https://doi.org/10.1289/ehp.9297209>.
- [56] G. Oberdorster, J. Ferin, B.E. Lehnert, Correlation between particle size, in vivo particle persistence, and lung injury, in: *Environ. Health Perspect.*, Public Health Services, US Dept of Health and Human Services, 1994: pp. 173–179. <https://doi.org/10.1289/ehp.102-1567252>.
- [57] W.G. Kreyling, U. Holzwarth, N. Haberl, J. Kozempel, A. Wenk, S. Hirn, C. Schleh, M. Schäffler, J. Lipka, M. Semmler-Behnke, N. Gibson, Quantitative biokinetics of titanium dioxide nanoparticles after intratracheal instillation in rats: Part 3, *Nanotoxicology.* 11 (2017) 454–464. <https://doi.org/10.1080/17435390.2017.1306894>.
- [58] M. Geiser, W.G. Kreyling, Deposition and biokinetics of inhaled nanoparticles, *Part. Fibre Toxicol.* 7 (2010) 1–17. <https://doi.org/10.1186/1743-8977-7-2>.
- [59] R.G. Crystal, S.H. Randell, J.F. Engelhardt, J. Voynow, M.E. Sunday, Airway epithelial cells: Current concepts and challenges, in: *Proc. Am. Thorac. Soc.*, American Thoracic Society, 2008: pp. 772–777. <https://doi.org/10.1513/pats.200805-041HR>.
- [60] D.A. Knight, S.T. Holgate, The airway epithelium: Structural and functional properties in health and disease, *Respirology.* 8 (2003) 432–446. <https://doi.org/10.1046/j.1440-1843.2003.00493.x>.
- [61] L.E. Ostrowski, W.D. Bennett, Cilia and Mucociliary Clearance, in: *Encycl. Respir. Med. Four-Volume Set*, Elsevier Inc., 2006: pp. 466–470. <https://doi.org/10.1016/B0-12-370879-6/00079-X>.
- [62] G.J. Doherty, H.T. McMahon, Mechanisms of Endocytosis, *Annu. Rev. Biochem.* 78 (2009) 857–902. <https://doi.org/10.1146/annurev.biochem.78.081307.110540>.
- [63] A. Aderem, D.M. Underhill, Mechanisms of phagocytosis in macrophages, *Annu. Rev. Immunol.* 17 (1999) 593–623. <https://doi.org/10.1146/annurev.immunol.17.1.593>.
- [64] J. Monks, D. Rosner, F.J. Geske, L. Lehman, L. Hanson, M.C. Neville, V.A. Fadok, Epithelial cells as phagocytes: Apoptotic epithelial cells are engulfed by mammary alveolar epithelial cells and repress inflammatory mediator release, *Cell Death Differ.* 12 (2005) 107–114. <https://doi.org/10.1038/sj.cdd.4401517>.
- [65] T. Cedervall, I. Lynch, S. Lindman, T. Berggård, E. Thulin, H. Nilsson, K.A. Dawson, S. Linse, Understanding the nanoparticle-protein corona using methods to quantify exchange rates and affinities of proteins for nanoparticles,

- Proc. Natl. Acad. Sci. U. S. A. 104 (2007) 2050–2055. <https://doi.org/10.1073/pnas.0608582104>.
- [66] V. Forest, M. Cottier, J. Pourchez, Electrostatic interactions favor the binding of positive nanoparticles on cells: A reductive theory, *Nano Today*. 10 (2015) 677–680. <https://doi.org/10.1016/J.NANTOD.2015.07.002>.
- [67] M.P. Monopoli, D. Walczyk, A. Campbell, G. Elia, I. Lynch, F. Baldelli Bombelli, K.A. Dawson, Physical-Chemical aspects of protein corona: Relevance to in vitro and in vivo biological impacts of nanoparticles, *J. Am. Chem. Soc.* 133 (2011) 2525–2534. <https://doi.org/10.1021/ja107583h>.
- [68] P. Foroozandeh, A.A. Aziz, Merging Worlds of Nanomaterials and Biological Environment: Factors Governing Protein Corona Formation on Nanoparticles and Its Biological Consequences, *Nanoscale Res. Lett.* 10 (2015) 221. <https://doi.org/10.1186/s11671-015-0922-3>.
- [69] T. Cedervall, I. Lynch, S. Lindman, T. Berggård, E. Thulin, H. Nilsson, K.A. Dawson, S. Linse, Understanding the nanoparticle-protein corona using methods to quantify exchange rates and affinities of proteins for nanoparticles, *Proc. Natl. Acad. Sci. U. S. A.* 104 (2007) 2050–2055. <https://doi.org/10.1073/pnas.0608582104>.
- [70] A.C.G. Weiss, K. Krüger, Q.A. Besford, M. Schlenk, K. Kempe, S. Förster, F. Caruso, In Situ Characterization of Protein Corona Formation on Silica Microparticles Using Confocal Laser Scanning Microscopy Combined with Microfluidics, *ACS Appl. Mater. Interfaces*. 11 (2019) 2459–2469. <https://doi.org/10.1021/acsami.8b14307>.
- [71] D. Walczyk, F.B. Bombelli, M.P. Monopoli, I. Lynch, K.A. Dawson, What the cell “sees” in bionanoscience, *J. Am. Chem. Soc.* 132 (2010) 5761–5768. <https://doi.org/10.1021/ja910675v>.
- [72] M. Lundqvist, J. Stigler, T. Cedervall, T. Berggård, M.B. Flanagan, I. Lynch, G. Elia, K. Dawson, The evolution of the protein corona around nanoparticles: A test study, *ACS Nano*. 5 (2011) 7503–7509. <https://doi.org/10.1021/nn202458g>.
- [73] V. Forest, CHAPTER 2: Biological Significance of the Nanoparticles Protein Corona, in: *Issues Toxicol.*, Royal Society of Chemistry, 2019: pp. 31–60. <https://doi.org/10.1039/9781788016308-00031>.
- [74] C. Corbo, R. Molinaro, A. Parodi, N.E. Toledano Furman, F. Salvatore, E. Tasciotti, The impact of nanoparticle protein corona on cytotoxicity, immunotoxicity and target drug delivery, *Nanomedicine*. 11 (2016) 81–100. <https://doi.org/10.2217/nnm.15.188>.
- [75] B. Halliwell, J.M.C. Gutteridge, *Free Radicals in Biology and Medicine*, Oxford University Press, 2015. <https://doi.org/10.1093/acprof:oso/9780198717478.001.0001>.
- [76] E. Castellucci Estevam, M.J. Nasim, L. Faulstich, M. Hakenesch, T. Burkholz, C. Jacob, A Historical Perspective on Oxidative Stress and Intracellular Redox Control, in: *Humana Press, Cham*, 2015: pp. 3–20. https://doi.org/10.1007/978-3-319-19096-9_1.
- [77] H. Sies, On the history of oxidative stress: Concept and some aspects of current development, *Curr. Opin. Toxicol.* 7 (2018) 122–126. <https://doi.org/10.1016/J.COTOX.2018.01.002>.

- [78] J.M.C. Gutteridge, Biological origin of free radicals, and mechanisms of antioxidant protection, *Chem. Biol. Interact.* 91 (1994) 133–140. [https://doi.org/10.1016/0009-2797\(94\)90033-7](https://doi.org/10.1016/0009-2797(94)90033-7).
- [79] L. Gonzalez, D. Lison, M. Kirsch-Volders, Genotoxicity of engineered nanomaterials: A critical review, *Nanotoxicology.* 2 (2008) 252–273. <https://doi.org/10.1080/17435390802464986>.
- [80] P.P. Fu, Q. Xia, H.M. Hwang, P.C. Ray, H. Yu, Mechanisms of nanotoxicity: Generation of reactive oxygen species, *J. Food Drug Anal.* 22 (2014) 64–75. <https://doi.org/10.1016/j.jfda.2014.01.005>.
- [81] M.R. Hoffmann, S.T. Martin, W. Choi, D.W. Bahnemann, Environmental Applications of Semiconductor Photocatalysis, *Chem. Rev.* 95 (1995) 69–96. <https://doi.org/10.1021/cr00033a004>.
- [82] A. Manke, L. Wang, Y. Rojanasakul, Mechanisms of nanoparticle-induced oxidative stress and toxicity, *Biomed Res. Int.* 2013 (2013). <https://doi.org/10.1155/2013/942916>.
- [83] P.D. Dwivedi, A. Tripathi, K.M. Ansari, R. Shanker, M. Das, Impact of nanoparticles on the immune system, *J. Biomed. Nanotechnol.* 7 (2011) 193–194. <https://doi.org/10.1166/jbn.2011.1264>.
- [84] M. Elsabahy, K.L. Wooley, Cytokines as biomarkers of nanoparticle immunotoxicity, *Chem. Soc. Rev.* 42 (2013) 5552–5576. <https://doi.org/10.1039/c3cs60064e>.
- [85] D.F. Moyano, Y. Liu, D. Peer, V.M. Rotello, Modulation of Immune Response Using Engineered Nanoparticle Surfaces, *Small.* 12 (2016) 76–82. <https://doi.org/10.1002/sml.201502273>.
- [86] K.W. Powers, M. Palazuelos, B.M. Moudgil, S.M. Roberts, Characterization of the size, shape, and state of dispersion of nanoparticles for toxicological studies, *Nanotoxicology.* 1 (2007) 42–51. <https://doi.org/10.1080/17435390701314902>.
- [87] Arnida, A. Malugin, H. Ghandehari, Cellular uptake and toxicity of gold nanoparticles in prostate cancer cells: a comparative study of rods and spheres, *J. Appl. Toxicol.* 30 (2009) n/a-n/a. <https://doi.org/10.1002/jat.1486>.
- [88] K.C. Chitra, C. Latchoumycandane, P.P. Mathur, Induction of oxidative stress by bisphenol A in the epididymal sperm of rats., *Toxicology.* 185 (2003) 119–27. <http://www.ncbi.nlm.nih.gov/pubmed/12505450> (accessed June 19, 2019).
- [89] K. Huang, H. Ma, J. Liu, S. Huo, A. Kumar, T. Wei, X. Zhang, S. Jin, Y. Gan, P.C. Wang, S. He, X. Zhang, X.J. Liang, Size-dependent localization and penetration of ultrasmall gold nanoparticles in cancer cells, multicellular spheroids, and tumors in vivo, *ACS Nano.* 6 (2012) 4483–4493. <https://doi.org/10.1021/nn301282m>.
- [90] A. Elbakry, E.-C. Wurster, A. Zaky, R. Liebl, E. Schindler, P. Bauer-Kreisel, T. Blunk, R. Rachel, A. Goepferich, M. Breunig, Layer-by-Layer Coated Gold Nanoparticles: Size-Dependent Delivery of DNA into Cells, *Small.* 8 (2012) 3847–3856. <https://doi.org/10.1002/sml.201201112>.
- [91] F. Lu, S.-H. Wu, Y. Hung, C.-Y. Mou, Size Effect on Cell Uptake in Well-Suspended, Uniform Mesoporous Silica Nanoparticles, *Small.* 5 (2009) 1408–

1413. <https://doi.org/10.1002/sml.200900005>.
- [92] J.A. Varela, M.G. Bexiga, C. Åberg, J.C. Simpson, K.A. Dawson, Quantifying size-dependent interactions between fluorescently labeled polystyrene nanoparticles and mammalian cells, *J. Nanobiotechnology*. 10 (2012) 39. <https://doi.org/10.1186/1477-3155-10-39>.
- [93] J. Huang, L. Bu, J. Xie, K. Chen, Z. Cheng, X. Li, X. Chen, Effects of nanoparticle size on cellular uptake and liver MRI with polyvinylpyrrolidone-coated iron oxide nanoparticles, *ACS Nano*. 4 (2010) 7151–7160. <https://doi.org/10.1021/nn101643u>.
- [94] J. Huang, L. Bu, J. Xie, K. Chen, Z. Cheng, X. Li, X. Chen, Effects of nanoparticle size on cellular uptake and liver MRI with polyvinylpyrrolidone-coated iron oxide nanoparticles, *ACS Nano*. 4 (2010) 7151–7160. <https://doi.org/10.1021/nn101643u>.
- [95] Q. Sun, T. Ishii, K. Kanehira, T. Sato, A. Taniguchi, Uniform TiO₂ nanoparticles induce apoptosis in epithelial cell lines in a size-dependent manner, *Biomater. Sci*. 5 (2017) 1014–1021. <https://doi.org/10.1039/c6bm00946h>.
- [96] J. Rejman, V. Oberle, I.S. Zuhorn, D. Hoekstra, Size-dependent internalization of particles via the pathways of clathrin- and caveolae-mediated endocytosis, *Biochem. J*. 377 (2004) 159–169. <https://doi.org/10.1042/BJ20031253>.
- [97] L. Shang, K. Nienhaus, G.U. Nienhaus, Engineered nanoparticles interacting with cells: Size matters, *J. Nanobiotechnology*. 12 (2014) 5. <https://doi.org/10.1186/1477-3155-12-5>.
- [98] Y. Hou, K. Cai, J. Li, X. Chen, M. Lai, Y. Hu, Z. Luo, X. Ding, D. Xu, Effects of titanium nanoparticles on adhesion, migration, proliferation, and differentiation of mesenchymal stem cells, *Int. J. Nanomedicine*. 8 (2013) 3619–3630. <https://doi.org/10.2147/IJN.S38992>.
- [99] J. Lovrić, H.S. Bazzi, Y. Cuie, G.R.A. Fortin, F.M. Winnik, D. Maysinger, Differences in subcellular distribution and toxicity of green and red emitting CdTe quantum dots, *J. Mol. Med*. 83 (2005) 377–385. <https://doi.org/10.1007/s00109-004-0629-x>.
- [100] R. Coradeghini, S. Gioria, C.P. García, P. Nativo, F. Franchini, D. Gilliland, J. Ponti, F. Rossi, Size-dependent toxicity and cell interaction mechanisms of gold nanoparticles on mouse fibroblasts, *Toxicol. Lett*. 217 (2013) 205–216. <https://doi.org/10.1016/j.toxlet.2012.11.022>.
- [101] H. Yen, S. Hsu, C. Tsai, Cytotoxicity and Immunological Response of Gold and Silver Nanoparticles of Different Sizes, *Small*. 5 (2009) 1553–1561. <https://doi.org/10.1002/sml.200900126>.
- [102] S. Schübbe, C. Schumann, C. Cavelius, M. Koch, T. Müller, A. Kraegeloh, Size-dependent localization and quantitative evaluation of the intracellular migration of silica nanoparticles in Caco-2 cells, *Chem. Mater*. 24 (2012) 914–923. <https://doi.org/10.1021/cm2018532>.
- [103] J. Park, D.H. Lim, H.J. Lim, T. Kwon, J.S. Choi, S. Jeong, I.H. Choi, J. Cheon, Size dependent macrophage responses and toxicological effects of Ag nanoparticles, *Chem. Commun*. 47 (2011) 4382–4384. <https://doi.org/10.1039/c1cc10357a>.
- [104] Y. Pan, S. Neuss, A. Leifert, M. Fischler, F. Wen, U. Simon, G. Schmid, W.

- Brandau, W. Jahnen-Dechent, Size-Dependent Cytotoxicity of Gold Nanoparticles, *Small*. 3 (2007) 1941–1949. <https://doi.org/10.1002/smll.200700378>.
- [105] J. Zhang, W. Song, J. Guo, J. Zhang, Z. Sun, L. Li, F. Ding, M. Gao, Cytotoxicity of different sized TiO₂nanoparticles in mouse macrophages, *Toxicol. Ind. Health*. 29 (2013) 523–533. <https://doi.org/10.1177/0748233712442708>.
- [106] A. Verma, F. Stellacci, Effect of surface properties on nanoparticle-cell interactions, *Small*. 6 (2010) 12–21. <https://doi.org/10.1002/smll.200901158>.
- [107] B.D. Chithrani, A.A. Ghazani, W.C.W. Chan, Determining the size and shape dependence of gold nanoparticle uptake into mammalian cells, *Nano Lett.* 6 (2006) 662–668. <https://doi.org/10.1021/nl052396o>.
- [108] J.A. Champion, S. Mitragotri, Role of target geometry in phagocytosis., *Proc. Natl. Acad. Sci. U. S. A.* 103 (2006) 4930–4. <https://doi.org/10.1073/pnas.0600997103>.
- [109] S. Behzadi, V. Serpooshan, W. Tao, M.A. Hamaly, M.Y. Alkawareek, E.C. Dreaden, D. Brown, A.M. Alkilany, O.C. Farokhzad, M. Mahmoudi, Cellular uptake of nanoparticles: Journey inside the cell, *Chem. Soc. Rev.* 46 (2017) 4218–4244. <https://doi.org/10.1039/c6cs00636a>.
- [110] I.-L. Hsiao, Y.-J. Huang, Effects of various physicochemical characteristics on the toxicities of ZnO and TiO₂ nanoparticles toward human lung epithelial cells, *Sci. Total Environ.* 409 (2011) 1219–1228. <https://doi.org/10.1016/j.scitotenv.2010.12.033>.
- [111] K. Donaldson, The inhalation toxicology of p-aramid fibrils, *Crit. Rev. Toxicol.* 39 (2009) 487–500. <https://doi.org/10.1080/10408440902911861>.
- [112] K.P. Steckiewicz, E. Barcinska, A. Malankowska, A. Zauszkiewicz–Pawlak, G. Nowaczyk, A. Zaleska-Medynska, I. Inkielewicz-Stepniak, Impact of gold nanoparticles shape on their cytotoxicity against human osteoblast and osteosarcoma in in vitro model. Evaluation of the safety of use and anti-cancer potential, *J. Mater. Sci. Mater. Med.* 30 (2019) 1–15. <https://doi.org/10.1007/s10856-019-6221-2>.
- [113] C.M. Goodman, C.D. McCusker, T. Yilmaz, V.M. Rotello, Toxicity of gold nanoparticles functionalized with cationic and anionic side chains, *Bioconjug. Chem.* 15 (2004) 897–900. <https://doi.org/10.1021/bc049951i>.
- [114] V. Forest, J. Pourchez, Preferential binding of positive nanoparticles on cell membranes is due to electrostatic interactions: A too simplistic explanation that does not take into account the nanoparticle protein corona, *Mater. Sci. Eng. C*. 70 (2017) 889–896. <https://doi.org/10.1016/j.msec.2016.09.016>.
- [115] Y. Li, N. Gu, Thermodynamics of charged nanoparticle adsorption on charge-neutral membranes: A simulation study, *J. Phys. Chem. B*. 114 (2010) 2749–2754. <https://doi.org/10.1021/jp904550b>.
- [116] J. Lin, H. Zhang, Z. Chen, Y. Zheng, Penetration of lipid membranes by gold nanoparticles: Insights into cellular uptake, cytotoxicity, and their relationship, *ACS Nano*. 4 (2010) 5421–5429. <https://doi.org/10.1021/nn1010792>.
- [117] E.J. Park, K. Park, Oxidative stress and pro-inflammatory responses induced by silica nanoparticles in vivo and in vitro, *Toxicol. Lett.* 184 (2009) 18–25. <https://doi.org/10.1016/j.toxlet.2008.10.012>.

- [118] F. Wang, F. Gao, M. Lan, H. Yuan, Y. Huang, J. Liu, Oxidative stress contributes to silica nanoparticle-induced cytotoxicity in human embryonic kidney cells, *Toxicol. Vitro.* 23 (2009) 808–815. <https://doi.org/10.1016/j.tiv.2009.04.009>.
- [119] W. Lin, Y. wern Huang, X.D. Zhou, Y. Ma, In vitro toxicity of silica nanoparticles in human lung cancer cells, *Toxicol. Appl. Pharmacol.* 217 (2006) 252–259. <https://doi.org/10.1016/j.taap.2006.10.004>.
- [120] K.M. Waters, L.M. Masiello, R.C. Zangar, B.J. Tarasevich, N.J. Karin, R.D. Quesenberry, S. Bandyopadhyay, J.G. Teeguarden, J.G. Pounds, B.D. Thrall, Macrophage responses to silica nanoparticles are highly conserved across particle sizes., *Toxicol. Sci.* 107 (2009) 553–69. <https://doi.org/10.1093/toxsci/kfn250>.
- [121] B.L. Baisch, N.M. Corson, P. Wade-Mercer, R. Gelein, A.J. Kennell, G. Oberdörster, A. Elder, Equivalent titanium dioxide nanoparticle deposition by intratracheal instillation and whole body inhalation: The effect of dose rate on acute respiratory tract inflammation, *Part. Fibre Toxicol.* 11 (2014) 5. <https://doi.org/10.1186/1743-8977-11-5>.
- [122] J. Wang, Y. Fan, Lung injury induced by TiO₂ nanoparticles depends on their structural features: Size, shape, crystal phases, and surface coating, *Int. J. Mol. Sci.* 15 (2014) 22258–22278. <https://doi.org/10.3390/ijms151222258>.
- [123] R.M. Silva, C. TeeSy, L. Franzi, A. Weir, P. Westerhoff, J.E. Evans, K.E. Pinkerton, Biological Response to Nano-Scale Titanium Dioxide (TiO₂): Role of Particle Dose, Shape, and Retention, *J. Toxicol. Environ. Heal. Part A.* 76 (2013) 953–972. <https://doi.org/10.1080/15287394.2013.826567>.
- [124] H. Shi, R. Magaye, V. Castranova, J. Zhao, Titanium dioxide nanoparticles: A review of current toxicological data, *Part. Fibre Toxicol.* 10 (2013).
- [125] A. Noël, M. Charbonneau, Y. Cloutier, R. Tardif, G. Truchon, Rat pulmonary responses to inhaled nano-TiO₂: Effect of primary particle size and agglomeration state, *Part. Fibre Toxicol.* 10 (2013) 48. <https://doi.org/10.1186/1743-8977-10-48>.
- [126] A. Noël, K. Maghni, Y. Cloutier, C. Dion, K.J. Wilkinson, S. Hallé, R. Tardif, G. Truchon, Effects of inhaled nano-TiO₂ aerosols showing two distinct agglomeration states on rat lungs, *Toxicol. Lett.* 214 (2012) 109–119. <https://doi.org/10.1016/J.TOXLET.2012.08.019>.
- [127] G. Oberdörster, J.N. Finkelstein, C. Johnston, R. Gelein, C. Cox, R. Baggs, A.C.P. Elder, Acute Pulmonary Effects of Ultrafine Particles in Rats and Mice, 2000.
- [128] Y. Li, J. Li, J. Yin, W. Li, C. Kang, Q. Huang, Q. Li, Systematic influence induced by 3 nm titanium dioxide following intratracheal instillation of mice, in: *J. Nanosci. Nanotechnol.*, *J Nanosci Nanotechnol*, 2010: pp. 8544–8549. <https://doi.org/10.1166/jnn.2010.2690>.
- [129] G. Oberdorster, J. Ferin, B.E. Lehnert², Correlation between Particle Size, In Vivo Particle Persistence, and Lung Injury, n.d.
- [130] D.B. Warheit, T.R. Webb, C.M. Sayes, V.L. Colvin, K.L. Reed, Pulmonary Instillation Studies with Nanoscale TiO₂ Rods and Dots in Rats: Toxicity Is not Dependent upon Particle Size and Surface Area, *Toxicol. Sci.* 91 (2006) 227–236. <https://doi.org/10.1093/toxsci/kfj140>.

- [131] M. Roursgaard, K.A. Jensen, S.S. Poulsen, N.E. V. Jensen, L.K. Poulsen, M. Hammer, G.D. Nielsen, S.T. Larsen, Acute and subchronic airway inflammation after intratracheal instillation of quartz and titanium dioxide agglomerates in mice, *ScientificWorldJournal*. 11 (2011) 801–825. <https://doi.org/10.1100/tsw.2011.67>.
- [132] E. Bermudez, J.B. Mangum, B. Asgharian, B.A. Wong, E.E. Reverdy, D.B. Janszen, P.M. Hext, D.B. Warheit, J.I. Everitt, Long-Term Pulmonary Responses of Three Laboratory Rodent Species to Subchronic Inhalation of Pigmentary Titanium Dioxide Particles, *Toxicol. Sci.* 70 (2002) 86–97. <https://doi.org/10.1093/toxsci/70.1.86>.
- [133] G. Oberdorster, J. Ferin, B.E. Lehnert, Correlation between Particle Size, In Vivo Particle Persistence, and Lung Injury, *Environ. Health Perspect.* 102 (1994) 173. <https://doi.org/10.2307/3432080>.
- [134] E. Bermudez, J.B. Mangum, B.A. Wong, B. Asgharian, P.M. Hext, D.B. Warheit, J.I. Everitt, Pulmonary Responses of Mice, Rats, and Hamsters to Subchronic Inhalation of Ultrafine Titanium Dioxide Particles, (2004) 27709. <https://doi.org/10.1093/toxsci/kfh019>.
- [135] IARC, IARC, Monogr. Eval. Carcinog. Risks to Humans. 98 (2010) 9–38. <https://monographs.iarc.fr/wp-content/uploads/2018/06/mono98.pdf> (accessed May 22, 2019).
- [136] J. Ferin, G. Oberdörster, D.P. Penney, Pulmonary retention of ultrafine and fine particles in rats., *Am. J. Respir. Cell Mol. Biol.* 6 (1992) 535–542. <https://doi.org/10.1165/ajrcmb/6.5.535>.
- [137] G. Oberdorster, J. Ferin, R. Gelein, S.C. Soderholm, J. Finkelstein, Role of the alveolar macrophage in lung injury: Studies with ultrafine particles, in: *Environ. Health Perspect.*, *Environ Health Perspect*, 1992: pp. 193–199. <https://doi.org/10.1289/ehp.97-1519541>.
- [138] I. Gosens, J.A. Post, L.J.J. de la Fonteyne, E.H.J.M. Jansen, J.W. Geus, F.R. Cassee, W.H. de Jong, Impact of agglomeration state of nano- and submicron sized gold particles on pulmonary inflammation, *Part. Fibre Toxicol.* 7 (2010) 37. <https://doi.org/10.1186/1743-8977-7-37>.
- [139] O. Schmid, T. Stoeger, Surface area is the biologically most effective dose metric for acute nanoparticle toxicity in the lung, *J. Aerosol Sci.* 99 (2016) 133–143. <https://doi.org/10.1016/j.jaerosci.2015.12.006>.
- [140] N. Kobayashi, M. Naya, S. Endoh, J. Maru, K. Yamamoto, J. Nakanishi, Comparative pulmonary toxicity study of nano-TiO₂ particles of different sizes and agglomerations in rats: Different short- and long-term post-instillation results, *Toxicology*. 264 (2009) 110–118. <https://doi.org/10.1016/j.tox.2009.08.002>.
- [141] G. Oberdörster, J. Ferin, B.E. Lehnert, Correlation between particle size, in vivo particle persistence, and lung injury., *Environ. Health Perspect.* 102 (1994) 173–179. <https://doi.org/10.1289/ehp.102-1567252>.
- [142] C. Uboldi, P. Urbán, D. Gilliland, E. Bajak, E. Valsami-Jones, J. Ponti, F. Rossi, Role of the crystalline form of titanium dioxide nanoparticles: Rutile, and not anatase, induces toxic effects in Balb/3T3 mouse fibroblasts, *Toxicol. Vitr.* 31 (2016) 137–145. <https://doi.org/10.1016/j.tiv.2015.11.005>.
- [143] A.S. Morris, A. Adamcakova-Dodd, S.E. Lehman, A. Wongrakpanich, P.S.

- Thorne, S.C. Larsen, A.K. Salem, Amine modification of nonporous silica nanoparticles reduces inflammatory response following intratracheal instillation in murine lungs, *Toxicol. Lett.* 241 (2016) 207–215. <https://doi.org/10.1016/j.toxlet.2015.11.006>.
- [144] S. Lanone, F. Rogerieux, J. Geys, A. Dupont, E. Maillot-Marechal, J. Boczkowski, G. Lacroix, P. Hoet, Comparative toxicity of 24 manufactured nanoparticles in human alveolar epithelial and macrophage cell lines, (2009). <https://doi.org/10.1186/1743-8977-6-14>.
- [145] D. Gandamalla, H. Lingabathula, N. Yellu, Nano titanium exposure induces dose- and size-dependent cytotoxicity on human epithelial lung and colon cells, *Drug Chem. Toxicol.* 42 (2019) 24–34. <https://doi.org/10.1080/01480545.2018.1452930>.
- [146] P.O. Andersson, C. Lejon, B. Ekstrand-Hammarström, C. Akfur, L. Ahlinder, A. Bucht, L. Österlund, Polymorph- and Size-Dependent Uptake and Toxicity of TiO₂ Nanoparticles in Living Lung Epithelial Cells, *Small.* 7 (2011) 514–523. <https://doi.org/10.1002/sml.201001832>.
- [147] Y. Ma, Y. Guo, S. Wu, Z. Lv, Q. Zhang, Y. Ke, Titanium dioxide nanoparticles induce size-dependent cytotoxicity and genomic DNA hypomethylation in human respiratory cells, *RSC Adv.* 7 (2017) 23560–23572. <https://doi.org/10.1039/c6ra28272e>.
- [148] S. Hussain, S. Boland, A. Baeza-Squiban, R. Hamel, L.C.J. Thomassen, J.A. Martens, M.A. Billon-Galland, J. Fleury-Feith, F. Moisan, J.C. Pairon, F. Marano, Oxidative stress and proinflammatory effects of carbon black and titanium dioxide nanoparticles: Role of particle surface area and internalized amount, *Toxicology.* 260 (2009) 142–149. <https://doi.org/10.1016/j.tox.2009.04.001>.
- [149] J.-R. Gurr, A.S.S. Wang, C.-H. Chen, K.-Y. Jan, Ultrafine titanium dioxide particles in the absence of photoactivation can induce oxidative damage to human bronchial epithelial cells, *Toxicology.* 213 (2005) 66–73. <https://doi.org/10.1016/j.tox.2005.05.007>.
- [150] L.K. Braydich-Stolle, N.M. Schaeublin, R.C. Murdock, J. Jiang, P. Biswas, J.J. Schlager, S.M. Hussain, Crystal structure mediates mode of cell death in TiO₂ nanotoxicity, *J. Nanoparticle Res.* 11 (2009) 1361–1374. <https://doi.org/10.1007/s11051-008-9523-8>.
- [151] C.M. Sayes, R. Wahi, P.A. Kurian, Y. Liu, J.L. West, K.D. Ausman, D.B. Warheit, V.L. Colvin, Correlating Nanoscale Titania Structure with Toxicity: A Cytotoxicity and Inflammatory Response Study with Human Dermal Fibroblasts and Human Lung Epithelial Cells, *Toxicol. Sci.* 92 (2006) 174–185. <https://doi.org/10.1093/toxsci/kfj197>.
- [152] B. Ekstrand-Hammarström, C.M. Akfur, P.O. Andersson, C. Lejon, L. Österlund, A. Bucht, Human primary bronchial epithelial cells respond differently to titanium dioxide nanoparticles than the lung epithelial cell lines A549 and BEAS-2B, *Nanotoxicology.* 6 (2012) 623–634. <https://doi.org/10.3109/17435390.2011.598245>.
- [153] M. Hanot-Roy, E. Tubeuf, A. Guilbert, A. Bado-Nilles, P. Vigneron, B. Trouiller, A. Braun, G. Lacroix, Oxidative stress pathways involved in cytotoxicity and genotoxicity of titanium dioxide (TiO₂) nanoparticles on cells constitutive of alveolo-capillary barrier in vitro, *Toxicol. Vitr.* 33 (2016) 125–135.

<https://doi.org/10.1016/j.tiv.2016.01.013>.

- [154] F. Rosário, M.J. Bessa, F. Brandão, C. Costa, C.B. Lopes, A.C. Estrada, D.S. Tavares, J.P. Teixeira, A.T. Reis, Unravelling the Potential Cytotoxic Effects of Metal Oxide Nanoparticles and Metal(Loid) Mixtures on A549 Human Cell Line, *Nanomaterials*. 10 (2020) 447. <https://doi.org/10.3390/nano10030447>.
- [155] Y. Wang, H. Cui, J. Zhou, F. Li, J. Wang, M. Chen, Q. Liu, Cytotoxicity, DNA damage, and apoptosis induced by titanium dioxide nanoparticles in human non-small cell lung cancer A549 cells, *Environ. Sci. Pollut. Res.* 22 (2015) 5519–5530. <https://doi.org/10.1007/s11356-014-3717-7>.
- [156] T. Brzicova, E. Javorkova, K. Vrbova, A. Zajicova, V. Holan, D. Pinkas, V. Philimonenko, J. Sikorova, J. Klema, J. Topinka, P. Rossner, Molecular responses in THP-1 macrophage-like cells exposed to diverse nanoparticles, *Nanomaterials*. 9 (2019) 687. <https://doi.org/10.3390/nano9050687>.
- [157] W.L. Poon, H. Alenius, J. Ndika, V. Fortino, V. Kolhinen, A. Meščeriakovas, M. Wang, D. Greco, A. Lähde, J. Jokiniemi, J.C.Y. Lee, H. El-Nezami, P. Karisola, Nano-sized zinc oxide and silver, but not titanium dioxide, induce innate and adaptive immunity and antiviral response in differentiated THP-1 cells, *Nanotoxicology*. 11 (2017) 936–951. <https://doi.org/10.1080/17435390.2017.1382600>.
- [158] T. Xia, M. Kovochich, J. Brant, M. Hotze, J. Sempf, T. Oberley, C. Sioutas, J.I. Yeh, M.R. Wiesner, A.E. Nel, Comparison of the abilities of ambient and manufactured nanoparticles to induce cellular toxicity according to an oxidative stress paradigm, *Nano Lett.* 6 (2006) 1794–1807. <https://doi.org/10.1021/nl061025k>.
- [159] S. Tsuchiya, M. Yamabe, Y. Yamaguchi, Y. Kobayashi, T. Konno, K. Tada, Establishment and characterization of a human acute monocytic leukemia cell line (THP-1), *Int. J. Cancer*. 26 (1980) 171–176. <https://doi.org/10.1002/ijc.2910260208>.
- [160] M. Daigneault, J.A. Preston, H.M. Marriott, M.K.B. Whyte, D.H. Dockrell, The identification of markers of macrophage differentiation in PMA-stimulated THP-1 cells and monocyte-derived macrophages, *PLoS One*. 5 (2010). <https://doi.org/10.1371/journal.pone.0008668>.
- [161] M.E. Lund, J. To, B.A. O'Brien, S. Donnelly, The choice of phorbol 12-myristate 13-acetate differentiation protocol influences the response of THP-1 macrophages to a pro-inflammatory stimulus, *J. Immunol. Methods*. 430 (2016) 64–70. <https://doi.org/10.1016/j.jim.2016.01.012>.
- [162] E.K. Park, H.S. Jung, H.I. Yang, M.C. Yoo, C. Kim, K.S. Kim, Optimized THP-1 differentiation is required for the detection of responses to weak stimuli, *Inflamm. Res.* 56 (2007) 45–50. <https://doi.org/10.1007/s00011-007-6115-5>.
- [163] K. Traore, M.A. Trush, M. George, E.W. Spannhake, W. Anderson, A. Asseffa, Signal transduction of phorbol 12-myristate 13-acetate (PMA)-induced growth inhibition of human monocytic leukemia THP-1 cells is reactive oxygen dependent, *Leuk. Res.* 29 (2005) 863–879. <https://doi.org/10.1016/j.leukres.2004.12.011>.
- [164] T. Xia, R.F. Hamilton, J.C. Bonner, E.D. Crandall, A. Elder, F. Fazlollahi, T.A. Girtsman, K. Kim, S. Mitra, S.A. Ntim, G. Orr, M. Tagmount, A.J. Taylor, D. Telesca, A. Tolic, C.D. Vulpe, A.J. Walker, X. Wang, F.A. Witzmann, N. Wu, Y. Xie, J.I. Zink, A. Nel, A. Holian, Interlaboratory evaluation of in vitro

- cytotoxicity and inflammatory responses to engineered nanomaterials: The NIEHS Nano go consortium, *Environ. Health Perspect.* 121 (2013) 683–690. <https://doi.org/10.1289/ehp.1306561>.
- [165] Y.A. Hayman, L.R. Sadofsky, J.D. Williamson, S.P. Hart, A.H. Morice, The effects of exogenous lipid on THP-1 cells: An in vitro model of airway aspiration?, *ERS Monogr.* 3 (2017). <https://doi.org/10.1183/23120541.00026-2016>.
- [166] S.M. Pinto, H. Kim, Y. Subbannayya, M. Giambelluca, K. Bösl, R.K. Kandasamy, Dose-dependent phorbol 12-myristate-13-acetate-mediated monocyte-to-macrophage differentiation induces unique proteomic signatures in THP-1 cells, *BioRxiv.* (2020) 2020.02.27.968016. <https://doi.org/10.1101/2020.02.27.968016>.
- [167] T. Starr, T.J. Bauler, P. Malik-Kale, O. Steele-Mortimer, The phorbol 12-myristate-13-acetate differentiation protocol is critical to the interaction of THP-1 macrophages with *Salmonella Typhimurium*, *PLoS One.* 13 (2018). <https://doi.org/10.1371/journal.pone.0193601>.
- [168] H. Schwende, E. Fitzke, P. Ambs, P. Dieter, Differences in the state of differentiation of THP-1 cells induced by phorbol ester and 1,25-dihydroxyvitamin D₃, *J. Leukoc. Biol.* 59 (1996) 555–561. <https://doi.org/10.1002/jlb.59.4.555>.
- [169] M. Gea, S. Bonetta, L. Iannarelli, A.M. Giovannozzi, V. Maurino, S. Bonetta, V.D. Hodoroaba, C. Armato, A.M. Rossi, T. Schilirò, Shape-engineered titanium dioxide nanoparticles (TiO₂ -NPs): cytotoxicity and genotoxicity in bronchial epithelial cells, *Food Chem. Toxicol.* 127 (2019) 89–100. <https://doi.org/10.1016/j.fct.2019.02.043>.
- [170] A. Simon-Deckers, B. Gouget, M. Mayne-L’Hermite, N. Herlin-Boime, C. Reynaud, M. Carrière, In vitro investigation of oxide nanoparticle and carbon nanotube toxicity and intracellular accumulation in A549 human pneumocytes, *Toxicology.* 253 (2008) 137–146. <https://doi.org/10.1016/J.TOX.2008.09.007>.
- [171] S.C. Tilton, N.J. Karin, A. Tolic, Y. Xie, X. Lai, R.F. Hamilton, K.M. Waters, A. Holian, F.A. Witzmann, G. Orr, Three human cell types respond to multi-walled carbon nanotubes and titanium dioxide nanobelts with cell-specific transcriptomic and proteomic expression patterns, *Nanotoxicology.* 8 (2014) 533–548. <https://doi.org/10.3109/17435390.2013.803624>.
- [172] T. Mosmann, Rapid colorimetric assay for cellular growth and survival: application to proliferation and cytotoxicity assays., *J. Immunol. Methods.* 65 (1983) 55–63. <http://www.ncbi.nlm.nih.gov/pubmed/6606682> (accessed June 3, 2019).
- [173] J.C. Stockert, R.W. Horobin, L.L. Colombo, A. Blázquez-Castro, Tetrazolium salts and formazan products in Cell Biology: Viability assessment, fluorescence imaging, and labeling perspectives, *Acta Histochem.* 120 (2018) 159–167. <https://doi.org/10.1016/j.acthis.2018.02.005>.
- [174] T. Bernas, J. Dobrucki, Mitochondrial and nonmitochondrial reduction of MTT: Interaction of MTT with TMRE, JC-1, and NAO mitochondrial fluorescent probes, *Cytometry.* 47 (2002) 236–242. <https://doi.org/10.1002/cyto.10080>.
- [175] R.K. Srivastava, Q. Rahman, M.P. Kashyap, A.K. Singh, G. Jain, S. Jahan, M.

- Lohani, M. Lantow, A.B. Pant, Nano-titanium dioxide induces genotoxicity and apoptosis in human lung cancer cell line, A549., *Hum. Exp. Toxicol.* 32 (2013) 153–66. <https://doi.org/10.1177/0960327112462725>.
- [176] S. Aueviriyavit, D. Phummiratch, K. Kulthong, R. Maniratanachote, Titanium dioxide nanoparticles-mediated in vitro cytotoxicity does not induce Hsp70 and Grp78 expression in human bronchial epithelial A549 cells, *Biol. Trace Elem. Res.* 149 (2012) 123–132. <https://doi.org/10.1007/s12011-012-9403-z>.
- [177] S. Tada-Oikawa, G. Ichihara, H. Fukatsu, Y. Shimanuki, N. Tanaka, E. Watanabe, Y. Suzuki, M. Murakami, K. Izuoka, J. Chang, W. Wu, Y. Yamada, S. Ichihara, Titanium Dioxide Particle Type and Concentration Influence the Inflammatory Response in Caco-2 Cells, *Int. J. Mol. Sci.* 17 (2016) 576. <https://doi.org/10.3390/ijms17040576>.
- [178] A. Lankoff, W.J. Sandberg, A. Wegierek-Ciuk, H. Lisowska, M. Refsnes, B. Sartowska, P.E. Schwarze, S. Meczynska-Wielgosz, M. Wojewodzka, M. Kruszewski, The effect of agglomeration state of silver and titanium dioxide nanoparticles on cellular response of HepG2, A549 and THP-1 cells, *Toxicol. Lett.* 208 (2012) 197–213. <https://doi.org/10.1016/j.toxlet.2011.11.006>.
- [179] K. Kansara, P. Patel, D. Shah, R.K. Shukla, S. Singh, A. Kumar, A. Dhawan, TiO₂ nanoparticles induce DNA double strand breaks and cell cycle arrest in human alveolar cells, *Environ. Mol. Mutagen.* 56 (2015) 204–217. <https://doi.org/10.1002/em.21925>.
- [180] M. Hanot-Roy, E. Tubeuf, A. Guilbert, A. Bado-Nilles, P. Vigneron, B. Trouiller, A. Braun, G. Lacroix, Oxidative stress pathways involved in cytotoxicity and genotoxicity of titanium dioxide (TiO₂) nanoparticles on cells constitutive of alveolo-capillary barrier in vitro, *Toxicol. Vitro.* 33 (2016) 125–135. <https://doi.org/10.1016/j.tiv.2016.01.013>.
- [181] L. Armand, A. Tarantini, D. Beal, M. Biola-Clier, L. Bobyk, S. Sorieul, K. Pernet-Gallay, C. Marie-Desvergne, I. Lynch, N. Herlin-Boime, M. Carriere, Long-term exposure of A549 cells to titanium dioxide nanoparticles induces DNA damage and sensitizes cells towards genotoxic agents, *Nanotoxicology.* 10 (2016) 913–923. <https://doi.org/10.3109/17435390.2016.1141338>.
- [182] K.J. Ong, T.J. MacCormack, R.J. Clark, J.D. Ede, V.A. Ortega, L.C. Felix, M.K.M. Dang, G. Ma, H. Fenniri, J.G.C. Veinot, G.G. Goss, Widespread nanoparticle-assay interference: Implications for nanotoxicity testing, *PLoS One.* 9 (2014) 90650. <https://doi.org/10.1371/journal.pone.0090650>.
- [183] A. Kroll, M.H. Pillukat, D. Hahn, J. Schnekenburger, Current in vitro methods in nanoparticle risk assessment: Limitations and challenges, *Eur. J. Pharm. Biopharm.* 72 (2009) 370–377. <https://doi.org/10.1016/J.EJPB.2008.08.009>.
- [184] T. Morishige, Y. Yoshioka, A. Tanabe, X. Yao, S. ichi Tsunoda, Y. Tsutsumi, Y. Mukai, N. Okada, S. Nakagawa, Titanium dioxide induces different levels of IL-1 β production dependent on its particle characteristics through caspase-1 activation mediated by reactive oxygen species and cathepsin B, *Biochem. Biophys. Res. Commun.* 392 (2010) 160–165. <https://doi.org/10.1016/j.bbrc.2009.12.178>.
- [185] T. Brzicova, E. Javorkova, K. Vrbova, A. Zajicova, V. Holan, D. Pinkas, V. Philimonenko, J. Sikorova, J. Klema, J. Topinka, P. Rossner, Molecular responses in THP-1 macrophage-like cells exposed to diverse nanoparticles, *Nanomaterials.* 9 (2019). <https://doi.org/10.3390/nano9050687>.

- [186] L. Müller, M. Riediker, P. Wick, M. Mohr, P. Gehr, B. Rothen-Rutishauser, Oxidative stress and inflammation response after nanoparticle exposure: Differences between human lung cell monocultures and an advanced three-dimensional model of the human epithelial airways, *J. R. Soc. Interface.* 7 (2010). <https://doi.org/10.1098/rsif.2009.0161.focus>.
- [187] T. Xia, R.F. Hamilton, J.C. Bonner, E.D. Crandall, A. Elder, F. Fazlollahi, T.A. Girtsman, K. Kim, S. Mitra, S.A. Ntim, G. Orr, M. Tagmount, A.J. Taylor, D. Telesca, A. Tolic, C.D. Vulpe, A.J. Walker, X. Wang, F.A. Witzmann, N. Wu, Y. Xie, J.I. Zink, A. Nel, A. Holian, A. Holian, Interlaboratory Evaluation of *in Vitro* Cytotoxicity and Inflammatory Responses to Engineered Nanomaterials: The NIEHS Nano GO Consortium, *Environ. Health Perspect.* 121 (2013) 683–690. <https://doi.org/10.1289/ehp.1306561>.
- [188] A.S. Yazdi, G. Guarda, N. Riteau, S.K. Drexler, A. Tardivel, I. Coullin, J. Tschopp, Nanoparticles activate the NLR pyrin domain containing 3 (Nlrp3) inflammasome and cause pulmonary inflammation through release of IL-1 α and IL-1 β , *Proc. Natl. Acad. Sci. U. S. A.* 107 (2010) 19449–19454. <https://doi.org/10.1073/pnas.1008155107>.
- [189] G. Odling, N. Robertson, Why is Anatase a Better Photocatalyst than Rutile? The Importance of Free Hydroxyl Radicals, *ChemSusChem.* 8 (2015) 1838–1840. <https://doi.org/10.1002/cssc.201500298>.
- [190] V. Likodimos, A. Chrysi, M. Calamiotou, C. Fernández-Rodríguez, J.M. Doña-Rodríguez, D.D. Dionysiou, P. Falaras, Microstructure and charge trapping assessment in highly reactive mixed phase TiO₂ photocatalysts, *Appl. Catal. B Environ.* 192 (2016) 242–252. <https://doi.org/10.1016/j.apcatb.2016.03.068>.
- [191] Y. Tang, R. Cai, D. Cao, X. Kong, Y. Lu, Photocatalytic production of hydroxyl radicals by commercial TiO₂ nanoparticles and phototoxic hazard identification, *Toxicology.* 406–407 (2018) 1–8. <https://doi.org/10.1016/j.tox.2018.05.010>.
- [192] N.A. Monteiro-Riviere, A.O. Inman, L.W. Zhang, Limitations and relative utility of screening assays to assess engineered nanoparticle toxicity in a human cell line, *Toxicol. Appl. Pharmacol.* 234 (2009) 222–235. <https://doi.org/10.1016/j.taap.2008.09.030>.
- [193] V. Forest, A. Figarol, D. Boudard, M. Cottier, P. Grosseau, J. Pourchez, Adsorption of lactate dehydrogenase enzyme on carbon nanotubes: how to get accurate results about the cytotoxicity of these nanomaterials, (n.d.). <https://doi.org/10.1021/acs.langmuir.5b00631i>.
- [194] M.S.K. Zaqout, T. Sumizawa, H. Igisu, D. Wilson, T. Myojo, S. Ueno, Binding of titanium dioxide nanoparticles to lactate dehydrogenase, *Environ. Health Prev. Med.* 17 (2012) 341–345. <https://doi.org/10.1007/s12199-011-0245-7>.
- [195] A.L. Holder, R. Goth-Goldstein, D. Lucas, C.P. Koshland, Particle-induced artifacts in the MTT and LDH viability assays, *Chem. Res. Toxicol.* (2012). <https://doi.org/10.1021/tx3001708>.
- [196] Y. Duan, N. Li, C. Liu, H. Liu, Y. Cui, H. Wang, F. Hong, Interaction between nanoparticulate anatase TiO₂ and lactate dehydrogenase, *Biol. Trace Elem. Res.* 136 (2010) 302–313. <https://doi.org/10.1007/s12011-009-8548-x>.
- [197] A.R. Lupu, T. Popescu, The noncellular reduction of MTT tetrazolium salt by TiO₂ nanoparticles and its implications for cytotoxicity assays, *Toxicol. Vitr.* 27 (2013) 1445–1450. <https://doi.org/10.1016/j.tiv.2013.03.006>.

- [198] S. Wang, H. Yu, J.K. Wickliffe, Limitation of the MTT and XTT assays for measuring cell viability due to superoxide formation induced by nano-scale TiO₂, *Toxicol. Vitro.* 25 (2011) 2147–2151. <https://doi.org/10.1016/j.tiv.2011.07.007>.
- [199] M. Cooke, V. Casado-Medrano, J. Ann, J. Lee, P.M. Blumberg, M.C. Abba, M.G. Kazanietz, Differential Regulation of Gene Expression in Lung Cancer Cells by Diacylglycerol-Lactones and a Phorbol Ester Via Selective Activation of Protein Kinase C Isozymes, *Sci. Rep.* 9 (2019) 1–15. <https://doi.org/10.1038/s41598-019-42581-4>.
- [200] M.-L. Jugan, S. Barillet, A. Simon-Deckers, N. Herlin-Boime, S. Sauvaigo, T. Douki, M. Carriere, Titanium dioxide nanoparticles exhibit genotoxicity and impair DNA repair activity in A549 cells, *Nanotoxicology.* 6 (2012) 501–513. <https://doi.org/10.3109/17435390.2011.587903>.
- [201] M. Katerji, M. Filippova, P. Duerksen-Hughes, Approaches and methods to measure oxidative stress in clinical samples: Research applications in the cancer field, *Oxid. Med. Cell. Longev.* 2019 (2019). <https://doi.org/10.1155/2019/1279250>.
- [202] S. Kasurinen, M.S. Happonen, T.J. Rönkkö, J. Orasche, J. Jokiniemi, M. Kortelainen, J. Tissari, R. Zimmermann, M.R. Hirvonen, P.I. Jalava, Differences between co-cultures and monocultures in testing the toxicity of particulate matter derived from log wood and pellet combustion, *PLoS One.* 13 (2018). <https://doi.org/10.1371/journal.pone.0192453>.
- [203] C. Carrillo-Carrion, M. Carril, W.J. Parak, Techniques for the experimental investigation of the protein corona, *Curr. Opin. Biotechnol.* 46 (2017) 106–113. <https://doi.org/10.1016/j.copbio.2017.02.009>.
- [204] A.L. Holder, R. Goth-Goldstein, D. Lucas, C.P. Koshland, Particle-induced artifacts in the MTT and LDH viability assays, *Chem. Res. Toxicol.* 25 (2012) 1885–1892. <https://doi.org/10.1021/tx3001708>.

NNT : 2020LYSEM022

Özge KÖSE

IN VITRO TOXICITY OF TITANIUM DIOXIDE NANOPARTICLES ON HUMAN LUNG CELLS
- IMPACT OF THE PHYSICOCHEMICAL FEATURES

Speciality: Process Engineering

Keywords: Titanium dioxide nanoparticles; cytotoxicity; pro-inflammatory response; reactive oxygen species; human lung cells.

Abstract :

With the growing development of nanoscience and nanotechnology, concerns on the potential health effect of nanoparticles have increased. Titanium dioxide nanoparticles (TiO₂ NPs) are widely used in a wide variety of industrial applications, mainly because of their unique properties such as their small size, high refractive index, or photocatalytic properties.

Although there are growing researches on TiO₂ toxicity, studies examining the impact of TiO₂ NPs physicochemical properties on their toxicity are limited. Therefore, the main aims of this thesis were: (i) to evaluate the toxicity of TiO₂ NPs in human lung cells as a function of their main physicochemical properties, (ii) to evaluate if a short time exposure to UV light induced changes in the physicochemical properties of TiO₂ NPs and eventually affected their toxicity.

For these purposes, 4 custom made and one commercial TiO₂ NPs which differ in size/SSA, shape, agglomeration, and surface functionalization/charge (APTES) were used.

In the first stage of the study, the influence of the physicochemical properties of TiO₂ NPs on their toxicity was evaluated on 3 different human lung cell systems (A549 epithelial cells, macrophages differentiated from THP-1, and A549/differentiated THP-1 cocultures). In general, TiO₂ NPs caused a decrease in cell viability and induced a pro-inflammatory response depending on the cell type. The effect on toxicity was higher with larger sized, less agglomerated, rod-shaped, and positively charged nanoparticles.

In the second stage of the study, we evaluated if a short time exposure of TiO₂ NPs to UV light induced changes in their physicochemical properties and their toxicity. Irradiated TiO₂ NPs induced a higher cytotoxic effect than the pristine TiO₂ NPs in relation to an altered surface charge.

After examining the toxicity of TiO₂ NPs depending on their physicochemical and photocatalytic properties, protein corona composition, which is another factor affecting toxicity, was investigated. The parameters influencing the protein corona composition are mainly nanoparticle primary size and surface charge, no clear impact of the shape and agglomeration state was observed. No effect of UV irradiation was observed on the formation of the protein corona.

Overall, the impact of the TiO₂ NPs physicochemical properties on their toxicity was observed and the toxicity was more pronounced after UV irradiation of NPs. Besides another main finding of this study was that the co-culture model seemed more sensitive to the adverse effects of TiO₂ NPs than the monoculture model.

This study improves our understanding of the hazards and risks that five different types of pristine TiO₂ NPs and their UV irradiated counterparts could pose to public health. It can serve as a basis for a safer by design approach to mitigate the toxicity of this material.

NNT : 2020LYSEM022

Özge KÖSE

TOXICITE *IN VITRO* DE NANOPARTICULES DE DIOXYDE DE TITANE SUR DES CELLULES PULMONAIRES HUMAINES - IMPACT DES CARACTERISTIQUES PHYSICOCHIMIQUES

Spécialité: Génie des Procédés

Mots-clés: Nanoparticules de dioxyde de titane; cytotoxicité; réponse pro-inflammatoire; espèces réactives de l'oxygène; cellules pulmonaires humaines.

Résumé :

Avec le développement rapide des nanosciences et des nanotechnologies, les préoccupations concernant les effets potentiels des nanoparticules sur la santé se sont renforcées. Les nanoparticules de dioxyde de titane (NPs de TiO₂) sont largement utilisées dans une grande variété d'applications industrielles, principalement en raison de caractéristiques remarquables telles que leur taille, leur indice de réfraction ou leurs propriétés photocatalytiques.

Bien que les recherches sur la toxicité du TiO₂ soient de plus en plus nombreuses, les études examinant l'impact des propriétés physicochimiques des NPs de TiO₂ sur leur toxicité sont limitées. Par conséquent, les principaux objectifs de cette thèse étaient d'évaluer : (i) la toxicité des NPs de TiO₂ sur des cellules pulmonaires humaines en lien avec leurs principales propriétés physicochimiques, (ii) l'impact de l'exposition de courte durée des NPs de TiO₂ à la lumière UV sur leurs propriétés physicochimiques et leur toxicité.

Pour atteindre cet objectif, quatre types de NPs de TiO₂ ont été synthétisés à façon et un TiO₂ commercial a été utilisé. Ces cinq types de NPs de TiO₂ diffèrent par leur taille/surface spécifique, leur forme, leur agglomération et leur fonctionnalisation/charge de surface (APTES).

Dans la première étape de l'étude, l'effet des propriétés physicochimiques des NPs de TiO₂ sur leur toxicité a été évalué sur 3 systèmes différents de cellules pulmonaires humaines (cellules épithéliales A549, macrophages différenciés à partir de THP-1, et cocultures de A549/THP-1 différenciées). En général, les NPs de TiO₂ provoquent une diminution de la viabilité des cellules et induisent une réponse pro-inflammatoire selon le type de cellule. L'effet sur la toxicité était plus important avec des nanoparticules de plus grande taille primaire, moins agglomérées, en forme de bâtonnet et chargées positivement.

Lors de la deuxième étape de l'étude, nous avons évalué si une exposition de courte durée des NPs de TiO₂ aux rayons UV induisait des changements dans leurs propriétés physicochimiques et leur toxicité. Les NPs de TiO₂ irradiées ont induit un effet cytotoxique plus élevé que les NPs de TiO₂ non irradiées en lien avec une charge de surface modifiée.

Après avoir examiné la toxicité des NPs de TiO₂ en fonction de leurs propriétés physicochimiques et photocatalytiques, la formation de la corona protéique, qui est un autre facteur affectant la toxicité, a été étudiée. Les paramètres influençant la formation de la "protein corona" sont principalement la taille primaire des nanoparticules et la charge de surface, aucun impact clair de la forme et de l'état d'agglomération n'a été observé. Aucun effet de l'irradiation UV n'a été observé sur la formation de la couronne protéique.

Dans l'ensemble, l'impact des propriétés physicochimiques des NPs de TiO₂ sur leur toxicité a été observé et la toxicité est plus prononcée après l'irradiation UV des NPs. Une autre conclusion importante de cette étude est que le modèle de co-culture semble plus sensible aux effets indésirables des NPs de TiO₂ que le modèle de monoculture.

Cette étude contribue à améliorer notre compréhension des dangers et des risques que cinq types différents de NPs de TiO₂ et leurs homologues irradiées aux UV peuvent présenter pour la santé publique. Elle peut servir de base à une approche "safer by design" pour atténuer la toxicité de ces nanoparticules.